Datashare 81

Atlas of fields and discoveries, central Mississippi Canyon, Atwater Valley, northwestern Lloyd Ridge, and western DeSoto Canyon protraction areas, northern deep-water Gulf of Mexico

Paul Weimer, Eric Zimmerman, Stephen P. J. Cossey, Harrison Hirsh, Brandon Snyder, Mike Leibovitz, Kris Schwendeman, Brian Hankins, Benjamin Herber, Daniel Bettinger, James Adson, William S. Gutterman, Travis J. Payeur, Renaud Bouroullec, John G. Roesink, Joseph Nicolette, Todd G. Lapinski, and Aaron A. van den Berg

AAPG Bulletin, v. 101, no. 7 (July 2017), pp. 995–1002

Merganser Field, Figure 5

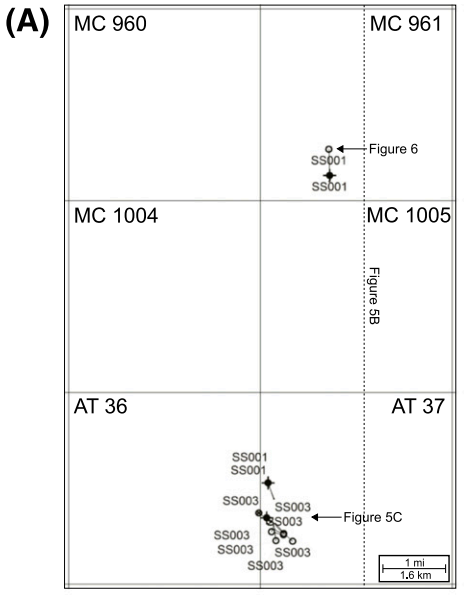

Field Name	Merganser (Figure 5)
Block Numbers	AT 037, 036
Partners	Operator: Anadarko
	Enterprise Products Partners (80%)
	Helix Energy Solutions (20%)
Discovery Date	February 2002
Production Start Date	August 2007
Production Facility	Subsea tie-back to Independence Hub in MC 920
Water Depth (feet)	7,946
Development Status	abandoned-2010
Number of Wells	2
Number of Reservoirs	1
Age	middle Miocene
Sedimentary deposit	channel fill
Trap	three-way closure against salt flank
Liquids Recoverable Reserves (MMbbl)	0
Gas Recoverable Reserves (BCF)	160
Recovery Efficiency (percent)	100
Porosity (percent)	27
Initial Reservoir Temperature Range (°F)	145
Gas Specific Gravity Range (at 60 and 15,025 PSI)	0.56
Sulfur Content (percent)	0
Viscosity (centipoise)	0.03
Upper Seal	shale
Lateral Seal	shale
Reservoir Intervals (Subsea true vertical depth-feet)	16,700-20,000
Source Of Information	M. Morris, pers. comm., 2009
	Cossey and Associates Inc.

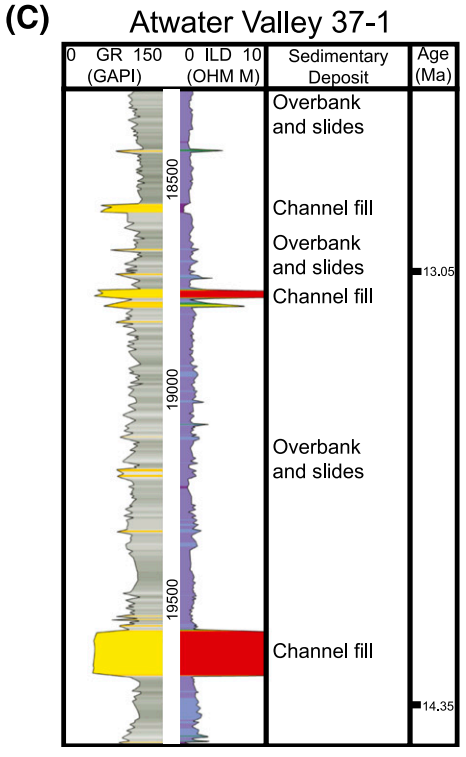

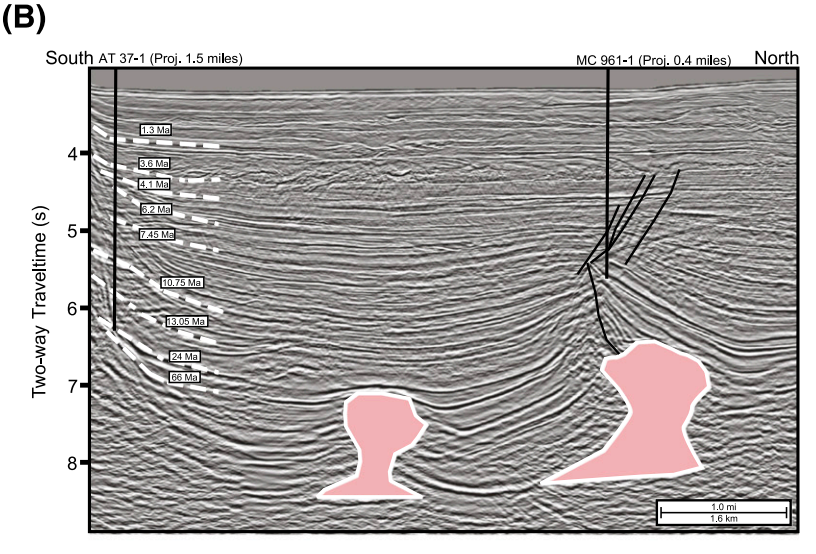

Figure 5. Atwater Valley (AT) Merganser 37 field. (A) Location map of AT Merganser 37 and Mississippi Canyon (MC) 961 Q fields. (B) Seismic profile. Reprinted with permission of Schlumberger. (C) Gamma-ray (GR) and resistivity log. See Figure 4 for the regional setting of the field. ILD = deep induction.

Q Field, Figure 6

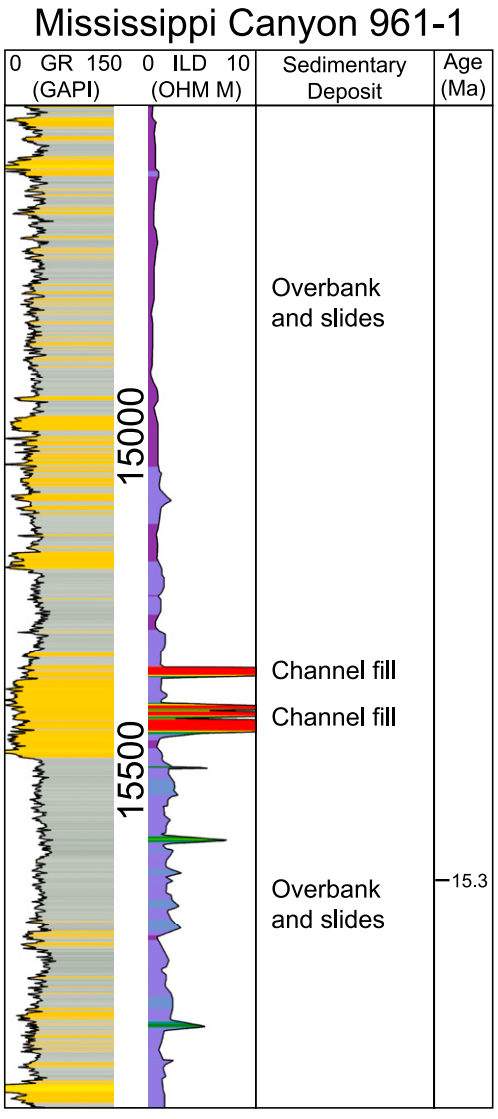

Field Name	Q (Figure 6)
Block Numbers	MC 961, 960, MC 1004, 1005
Partners	Statoil (50.00%), Eni (50.00%)
Discovery Date	May 2005
Production Start Date	October 2007
Production Facility	Subsea tie-back to Independence Hub in MC 920
Water Depth (feet)	7,973
Development Status	abandoned-2010
Number of Wells	1
Number of Reservoirs	1
Age	middle Miocene
Sedimentary deposit	channelized sheets
Trap	three-way closure against fault
Liquids Recoverable Reserves (MMbbl)	0
Gas Recoverable Reserves (BCF)	73
Initial Production (BOPD), (MCFGPD)	100,000 MCFPD
Porosity (percent)	low 30's
Permeability (mD)	up to 1000
Upper Seal	shale
Lateral Seal	shale
Reservoir Intervals (Subsea true vertical depth-feet)	15,350-15,450
Source Of Information	Cossey and Associates Inc.

Figure 6. Mississippi Canyon 961 Q field. Gamma-ray (GR) and resistivity log. See Figure 5A for location map and Figure 5B for seismic profile across the field. See Figure 4 for the regional setting of the field. ILD = deep induction.

Vortex Field, Figure 7

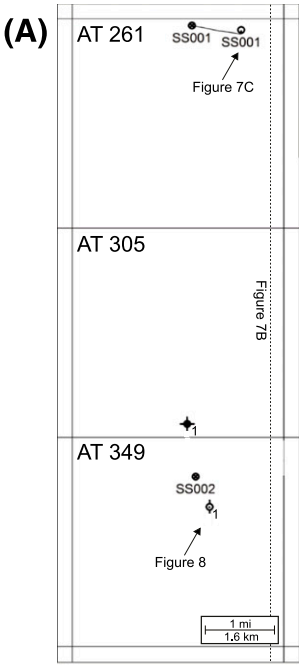

Field Name	Vortex (Figure 7)
Block Numbers	AT 261, 217, LL 177, 221
Partners	Anadarko (100.00%)
Discovery Date	December 2002
Production Start Date	July 2007
Production Facility	Subsea tie-back to Independence Hub in MC 920
Water Depth (feet)	8,392
Development Status	abandoned-2011
Number of Wells	1
Number of Reservoirs	1
Age	middle to late Miocene
Sedimentary deposit	channel fill
Trap	four-way closure (compactional drape)
Liquids Recoverable Reserves (MMbbl)	0
Gas Recoverable Reserves (BCF)	125
Recovery Efficiency (percent)	100
Initial Reservoir Temperature Range (°F)	145
Gas Specific Gravity Range (at 60 and 15.025 PSI)	0.56
Sulfur Content (percent)	0
Viscosity (centipoise)	0.03
Upper Seal	shale
Lateral Seal	shale
Reservoir Intervals (Subsea true vertical depth-feet)	15,500-16,900
Source Of Information	M. Morris, pers. comm., 2009
	Cossey and Associates Inc.

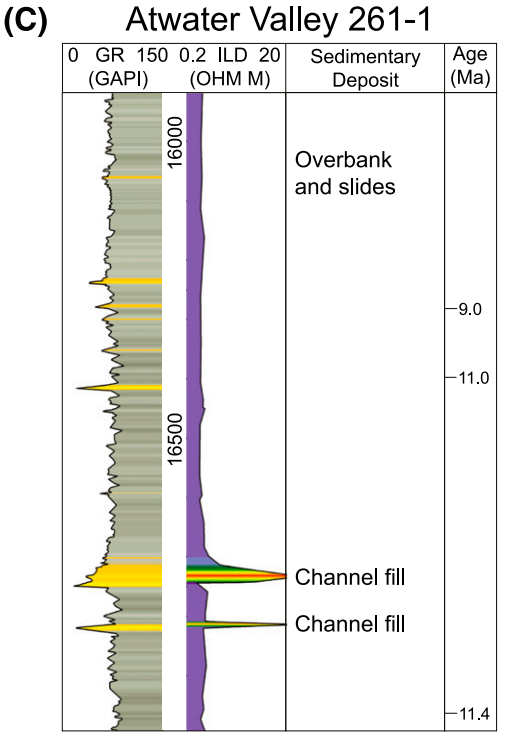

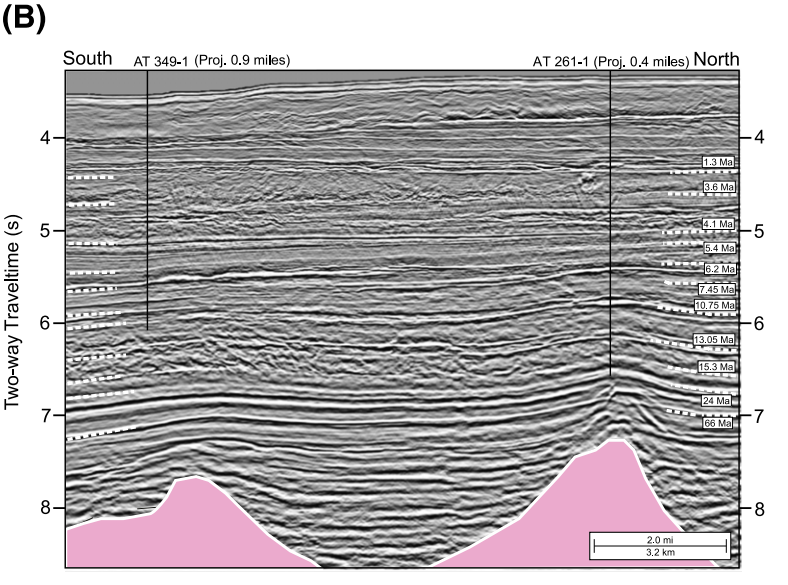

Figure 7. Atwater Valley (AT) 261 Vortex field. (A) Location map of AT 261 Vortex field and AT 349/Lloyd Ridge 309 Jubilee fields. (B) Seismic profile. Reprinted with permission of Schlumberger. (C) Gamma-ray (GR) and resistivity log. See Figure 4 for the regional setting of the field. ILD = deep induction.

Jubilee Field, Figure 8

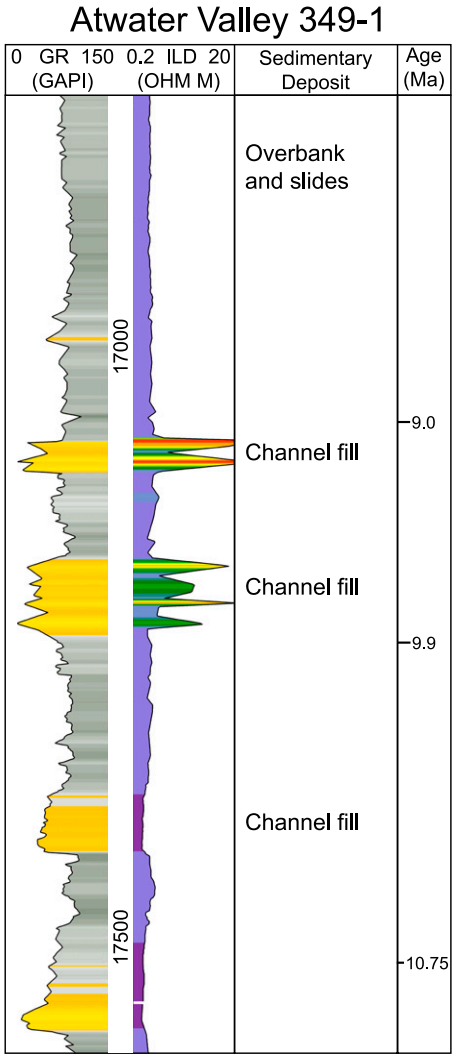

Field Name	Jubilee (Figure 8)
Block Numbers	AT 349, AT305, LL265, LL309
Partners	Anadarko (100.00%)
Discovery Date	April 2003
Production Start Date	July 2007
Production Facility	Subsea tie-back to Independence Hub in MC 920
Water Depth (feet)	8,851
Development Status	abandoned-2010
Number of Wells	2
Number of Reservoirs	2
Age	late Miocene
Sedimentary deposit	channel fill
Trap	four-way closure (compactional drape)
Liquids Recoverable Reserves (MMbbl)	0
Gas Recoverable Reserves (BCF)	350
Recovery Efficiency (percent)	100
Initial Reservoir Temperature Range (°F)	145
Gas Specific Gravity Range (at 60 and 15.025 PSI)	0.56
Sulfur Content (percent)	0
Viscosity (centipoise)	0.03
Upper Seal	shale
Lateral Seal	shale
Reservoir Intervals (Subsea true vertical depth-feet)	17,000-17,250
Source Of Information	M. Morris, pers. comm., 2009
	Cossey and Associates Inc.

Figure 8. Atwater Valley 349/Lloyd Ridge 309 Jubilee field. Gamma-ray (GR) and resistivity log. See Figure 7A for location map and Figure 7B for seismic profile across the field. See Figure 4 for the regional setting of the field. ILD = deep induction.

Bass Lite Field, Figure 9

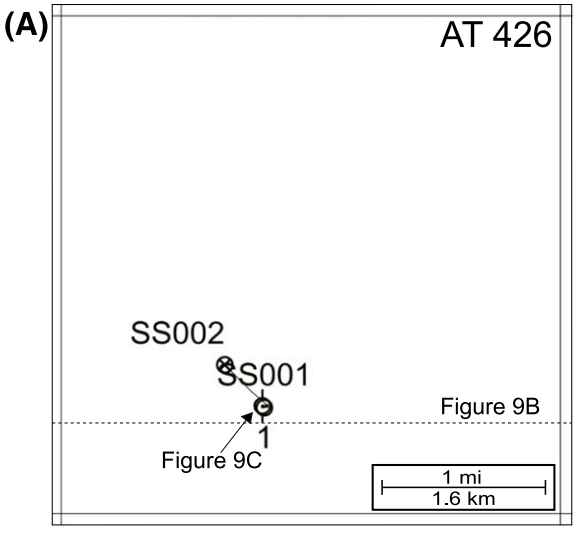

Field Name	Bass Lite (Figure 9)
Block Numbers	AT426, AT380, AT381, AT425
Partners	Bennu (61.25%), Helix Energy Solutions (17.50%),
	Deep Gulf Energy (15.00%), Eni (6.25%)
Discovery Date	February 2001
Production Start Date	February 2008
Production Facility	Subsea tie-back to Devil's Tower MC 773
Water Depth (feet)	6,692
Development Status	producing
Field Size (acres)	1,000
Number of Wells	2
Number of Reservoirs	1
Drive Mechanism	depletion-water
Age	late Pleistocene
Sedimentary deposit	thin bed levees
Trap	three-way closure against fault-salt-stratigraphic
Liquids Recoverable Reserves (MMbbl)	0
Gas Recoverable Reserves (BCF)	178
Initial Production (BOPD), (MCFGPD)	111 MMCFGPD
Porosity (percent)	32-36
Permeability (mD)	10-1,000
Water Saturation Range (percent)	30-40
Initial Reservoir Temperature Range (°F)	108
Initial Reservoir Pressure Range (PSI)	6,650
Gas Column (feet)	800
Upper Seal	shale
Lateral Seal	shale
Reservoir Intervals (Subsea true vertical depth-feet)	12,900-13,500
Source Of Information	Cossey and Associates Inc.
	P. Wieg, pers. comm., 2010
	S. Burt, pers. comm., 2010

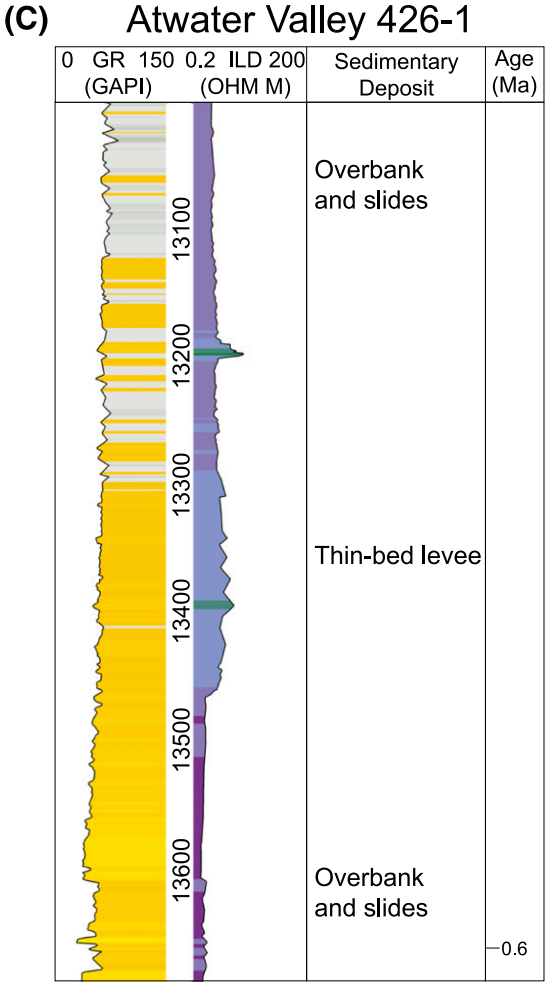

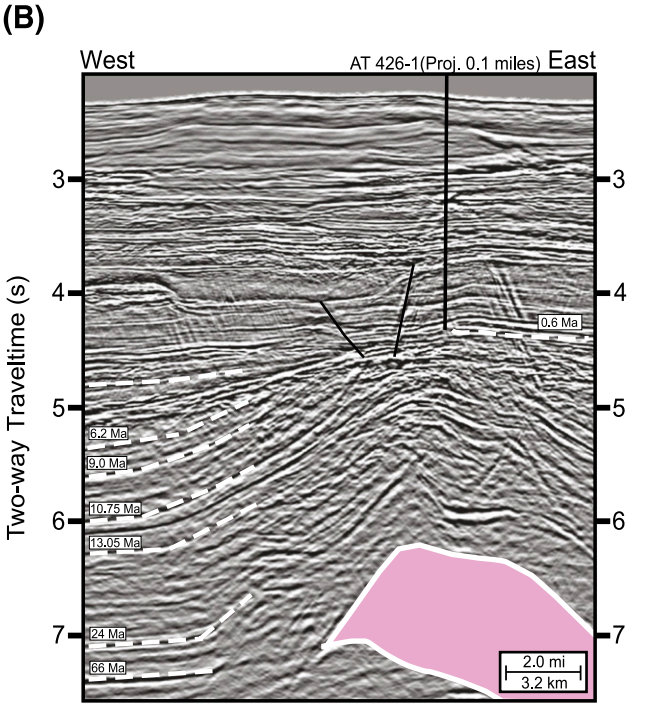

Figure 9. Atwater Valley (AT) 426 Bass Lite field. (A) Location map. (B) Seismic profile. Reprinted with permission of Schlumberger. (C) Gamma-ray (GR) and resistivity log. See Figure 4 for the regional setting of the field. ILD = deep induction.

Neptune Field, Figure 10

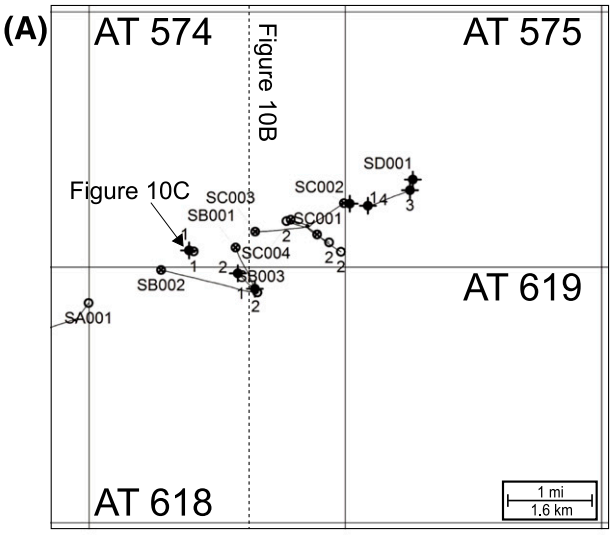

Field Name	Neptune (Figure 10)
Block Numbers	AT 574, AT 573, AT 575, AT 617, AT 618
Partners	BHP Billiton (35.00%), Marathon (30.00%),
	Woodside Petroleum (20.00%),
	Repsol (15.00%)
Discovery Date	September 1995
Production Start Date	July 2008
Production Facility	Subsea tie-back to Neptune TLP in Green Canyon 613
Water Depth (feet)	6,287
Development Status	producing
Field Size (acres)	3,600
Number of Wells	10
Number of Reservoirs	3
Age	early to middle Miocene
Sedimentary deposit	channel fill, mass-transport complex
Trap	four-way closure (contractional anticline)
Liquids Recoverable Reserves (MMbbl)	104.3
Gas Recoverable Reserves (BCF)	89.3
Initial Production (BOPD), (MCFGPD)	50,000
Gas Oil Ratio	900
Porosity (percent)	27.8
Permeability (mD)	114-648
Initial Reservoir Temperature Range (°F)	165
Initial Reservoir Pressure Range (PSI)	11,000
API Oil Gravity	21.8
Oil Column (feet)	1,200
Upper Seal	shale
Lateral Seal	shale
Reservoir Intervals (Subsea true vertical depth-feet)	16,500-18,500
Source Of Information	Purnel et al., 1997
	Cossey and Associates Inc.
	Haak et al., 2014
	Newberry, 2014

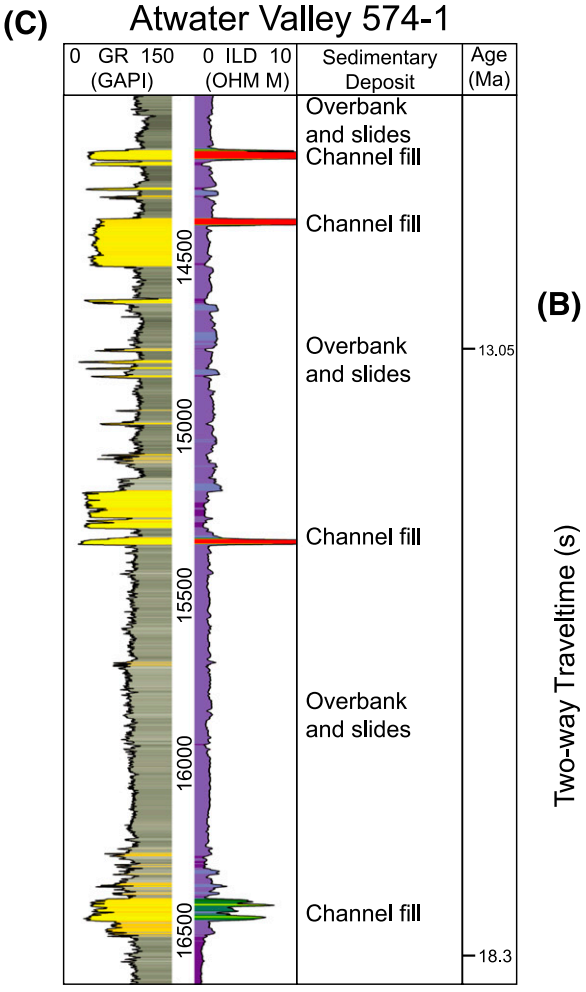

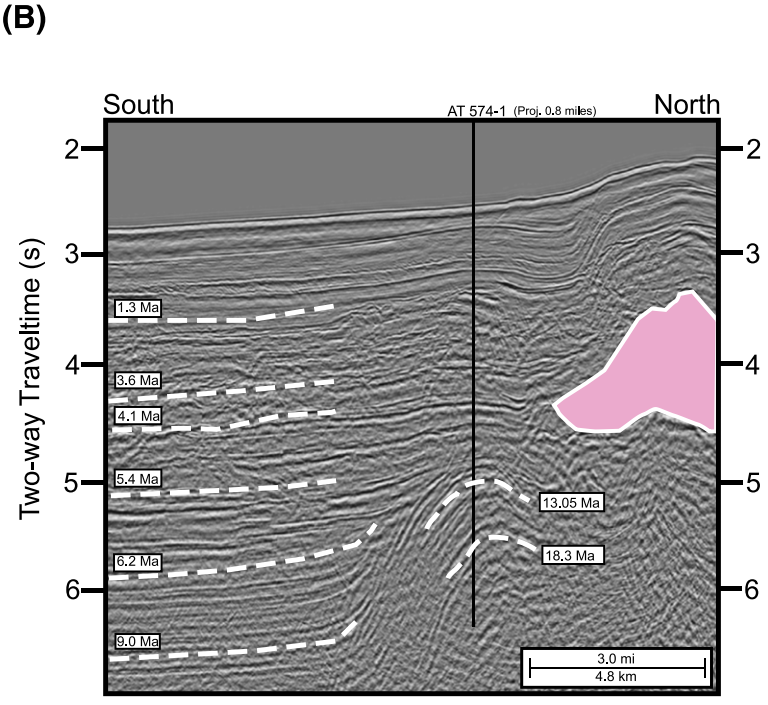

Figure 10. Atwater Valley (AT) 574–575 Neptune field. (A) Location map. (B) Seismic profile. Reprinted with permission of Schlumberger. (C) Gamma-ray (GR) and resistivity log. See Figure 4 for the regional setting of the field. ILD = deep induction.

Dalamatian North Field, Figure 11

(A)

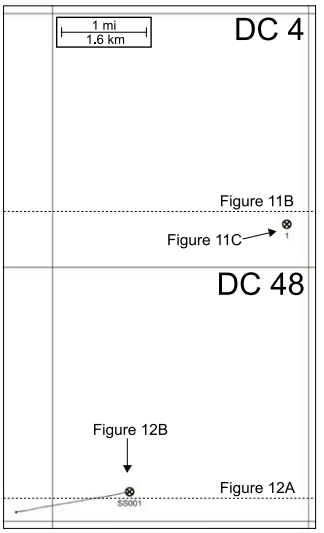

Field Name	Dalamatian North (Figure 11)
Block Numbers	DC 004
Partners	Murphy (70%), Ecopetrol (30%)
Discovery Date	2008
Production Start Date	April 2014
Production Facility	Subsea tie-back to Petronius in Viosca Knoll 786
Water Depth (feet)	5,449
Development Status	producing
Number of Wells	1
Number of Reservoirs	1
Age	late Miocene
Sedimentary deposit	channel fill-levee
Trap	stratigraphic
Gas Recoverable Reserves (BCF)	
Initial Production (BOPD), (MCFGPD)	10,324 BOPD, 8,072 MCFGPD
Gas Oil Ratio	782
Porosity (percent)	30-32
API Oil Gravity	32.8
Pay Thickness (feet)	123 (gross)
Upper Seal	shale
Lateral Seal	shale
Reservoir Intervals (Subsea true vertical depth-feet)	12,524-12,647
Source Of Information	D. Huffman, pers. comm., 2015

(C)

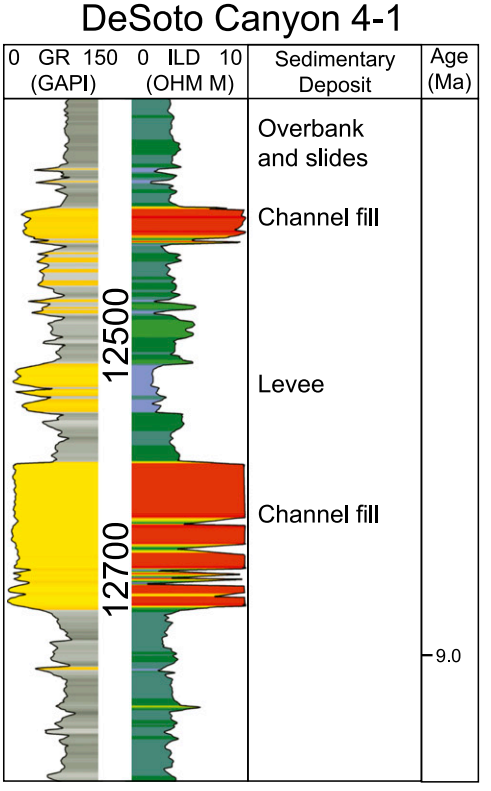

(B)

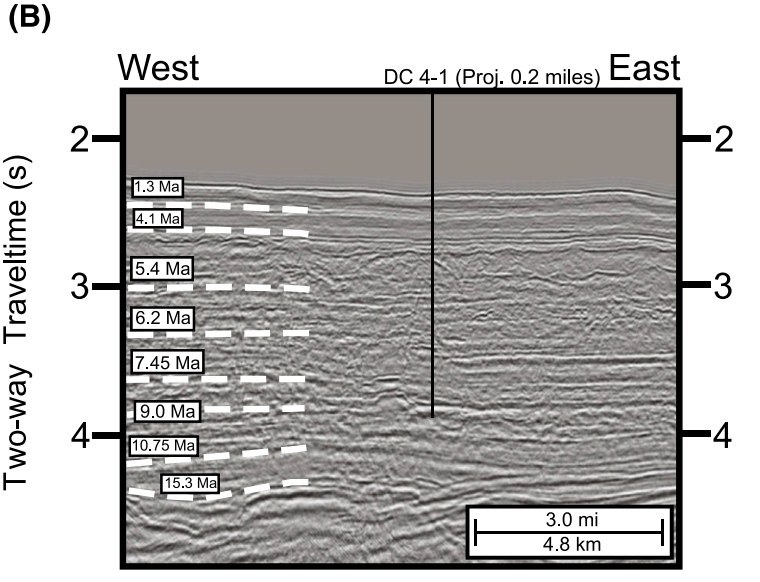

Figure 11. DeSoto Canyon (DC) 4 Dalmatian North Field. (A) Location map. (B) Seismic profile across the DC 4 Dalmatian North Field. Reprinted with permission of Schlumberger. See Figure 4 for the regional setting of the field.

Dalmatian Field, Figure 12

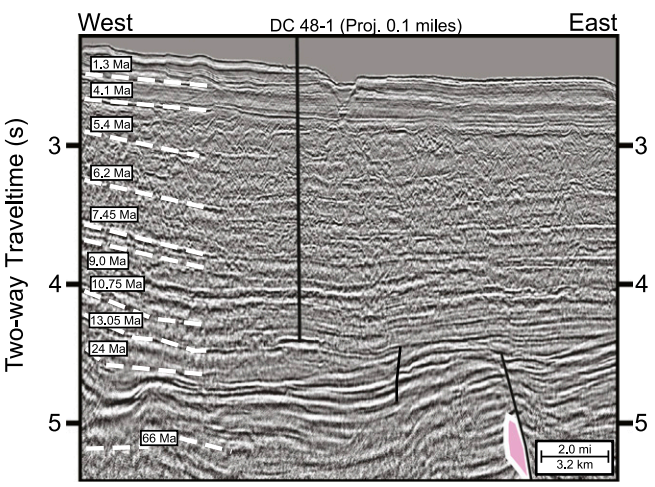

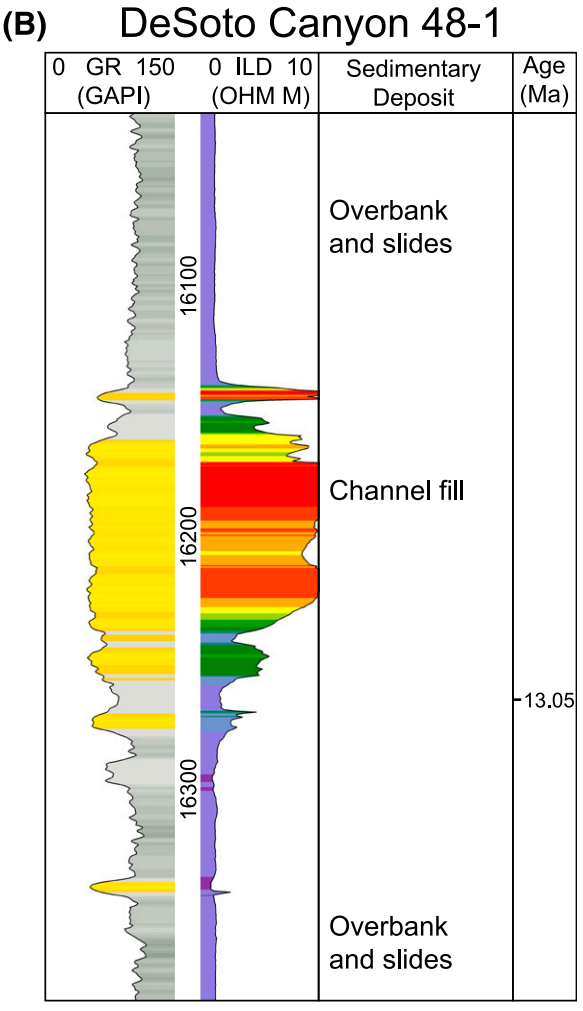

Field Name	Dalmatian (Figure 12)
Block Numbers	DC 048
Partners	Murphy (70%), Ecopetrol (30%)
Discovery Date	2008
Production Start Date	April 2014
Production Facility	Subsea tie-back to Petronius Viosca Knoll 786
Water Depth (feet)	5,876
Development Status	producing
Number of Wells	1
Number of Reservoirs	1
Age	middle Miocene
Sedimentary deposit	channel fill-levee
Trap	stratigraphic
Liquids Recoverable Reserves (MMbbl)	0.003
Gas Recoverable Reserves (BCF)	16.3
Initial Production (BOPD), (MCFGPD)	40 BOPD, 62,284 MCFGPD
Gas Oil Ratio	155-710
Porosity (percent)	30
API Oil Gravity	24.3
Pay Thickness (feet)	66 (gross)
Upper Seal	shale
Lateral Seal	shale
Reservoir Intervals (Subsea true vertical depth-feet)	12,652-12,718
Source Of Information	Herron et al., 2014
	L. Czerniakowski, pers. comm., 2010
	D. Huffman, pers. comm., 2015

Figure 12. DeSoto Canyon (DC) 48 Dalmatian field. (A) Seismic profile. Reprinted with permission of Schlumberger. (B) Gamma-ray (GR) and resistivity log. See Figure 11A for location of seismic and well, and Figure 4 for the regional setting of the field. ILD = deep induction.

Dalmatian South Field, Figure 13

(A)

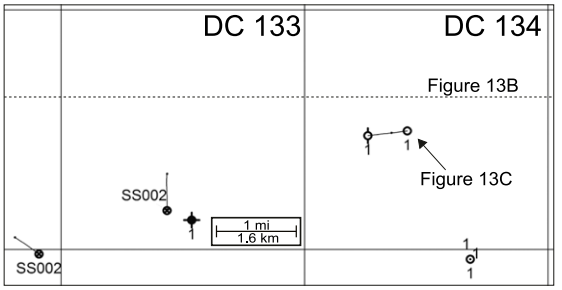

Field Name	Dalmatian South (Figure 13)
Block Numbers	DC 134
Partners	Murphy (70%), Ecopetrol (30%)
Discovery Date	November 2012
Production Start Date	Early 2016
Production Facility	Subsea tie-back to Petronius Viosca Knoll 786
Water Depth (feet)	6394
Development Status	producing
Number of Wells	1
Number of Reservoirs	2
Age	late Miocene
Sedimentary deposit	Channel-fill
Trap	stratigraphic
Upper Seal	shale
Lateral Seal	shale

(C)

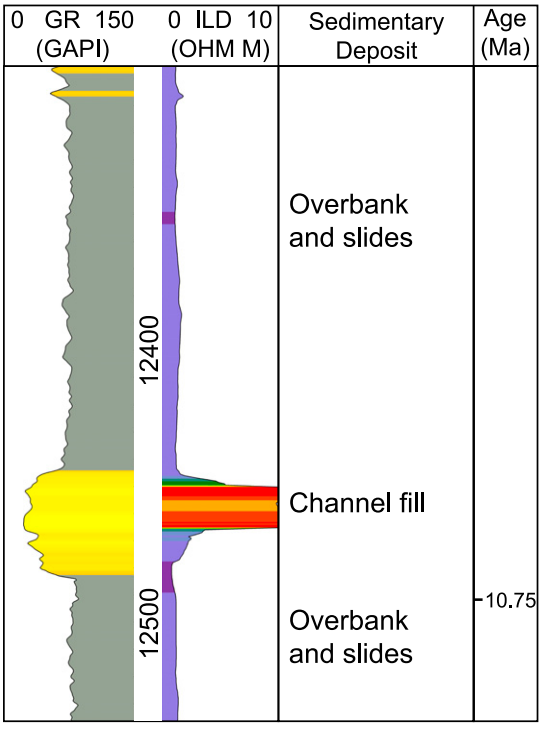

(B)

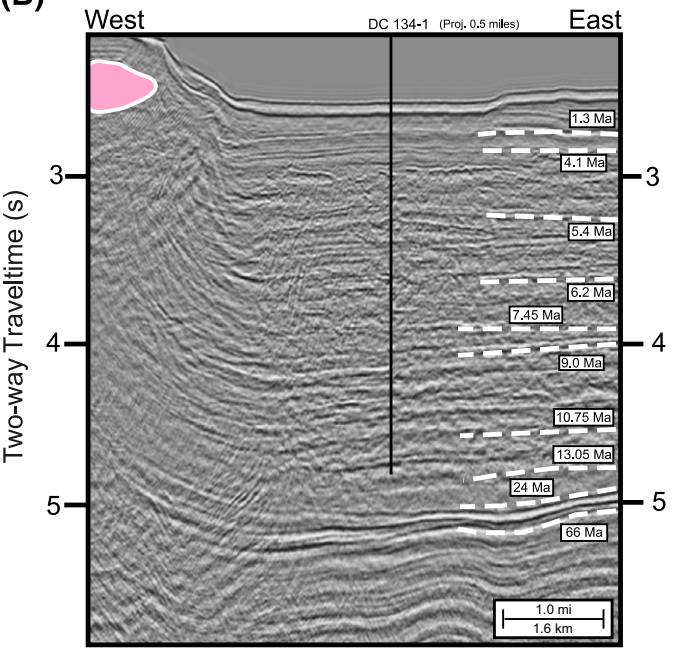

Figure 13. DeSoto Canyon (DC) 134 Dalmatian South Field. (A) Location map. (B) Seismic profile. Reprinted with permission of Schlumberger. (C) Gamma-ray and resistivity log. See Figure 4 for the regional setting of the field. ILD = deep induction.

Vicksburg Field, Figure 14

(A)

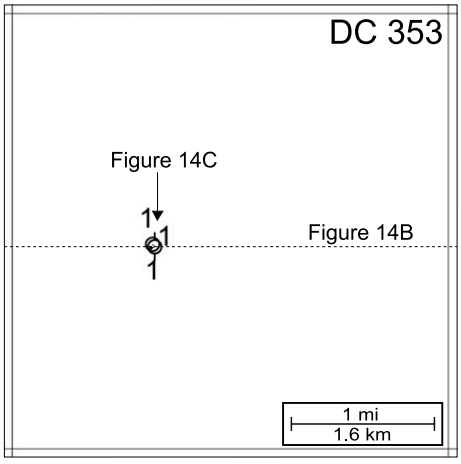

Field Name	Vicksburg (Figure 14)
Block Numbers	DC 353
Partners	Shell (75%), Nexen (25.00%)
Discovery Date	October 2007
Production Start Date	2020 (Projected)
Production Facility	Subsea-tieback to Appomattox Hub in MC 437
Water Depth (feet)	7,457
Development Status	under evaluation
Number of Wells	1
Number of Reservoirs	1
Age	Late Jurassic
Sedimentary deposit	eolian
Trap	three-way closure against fault
Liquids Recoverable Reserves (MMbbl)	90
Gas Recoverable Reserves (BCF)	200
Upper Seal	shale
Lateral Seal	shale

(C)

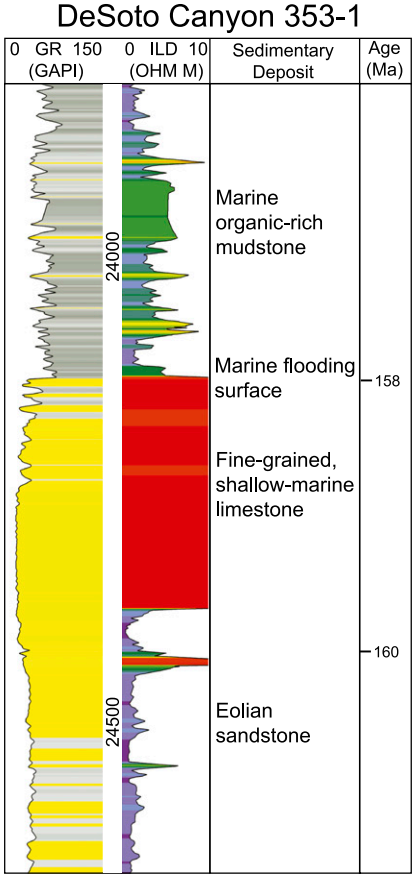

(B)

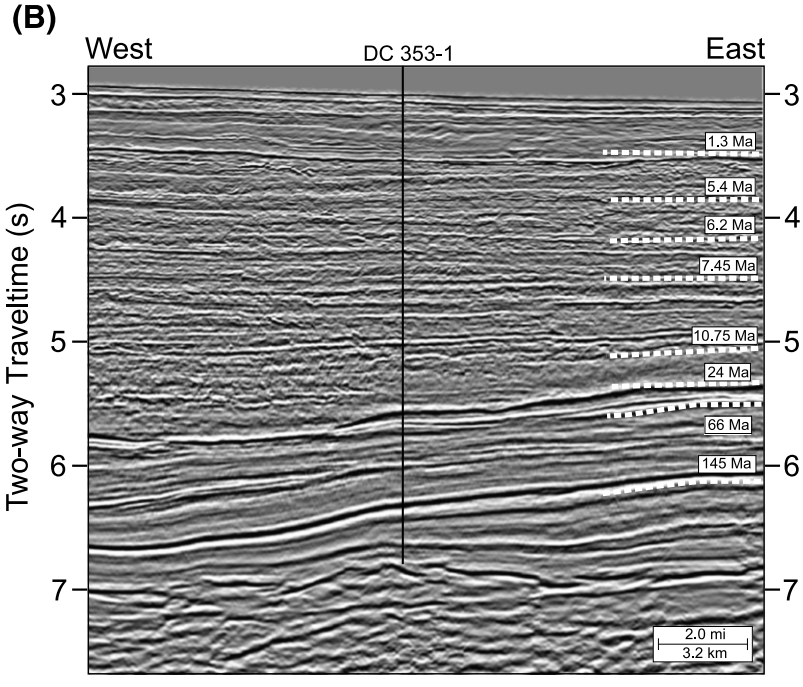

Figure 14. DeSoto Canyon (DC) 353 Vicksburg field. (A) Location map. (B) Seismic profile. Reprinted with permission of Schlumberger. (C) Gamma-ray (GR) and resistivity log. See Figure 4 for the regional setting of the field. ILD = deep induction.

San Jacinto Field, Figure 15

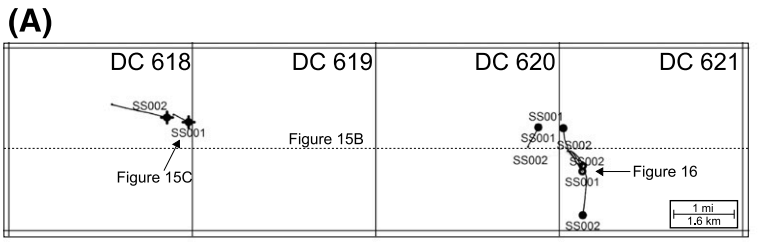

Field Name	San Jacinto (Figure 15)
Block Numbers	DC 618, DC 619
Partners	Eni (53.33%), Statoil (26.67%),
	Anadarko (20.00%)
Discovery Date	May 2004
Production Start Date	November 2007
Production Facility	Subsea tie-back to Independence Hub in MC 920
Water Depth (feet)	7,851
Development Status	abandoned-2015
Number of Wells	2
Number of Reservoirs	3
Age	middle to late Miocene
Sedimentary deposit	channel fill
Trap	four-way closure (compactional drape)
Liquids Recoverable Reserves (MMbbl)	0
Gas Recoverable Reserves (BCF)	160.02
Recovery Efficiency (percent)	100
Initial Reservoir Temperature Range (°F)	127-149
Initial Reservoir Pressure Range (PSI)	7590-7708
Gas Specific Gravity Range (at 60 and 15.025 PSI)	0.56
Sulfur Content (percent)	0
Pay Thickness (feet)	106 (net)
Upper Seal	shale
Lateral Seal	shale
Source Of Information	M. Morris, pers comm., 2009
	Vercher and Blakeley, 2007

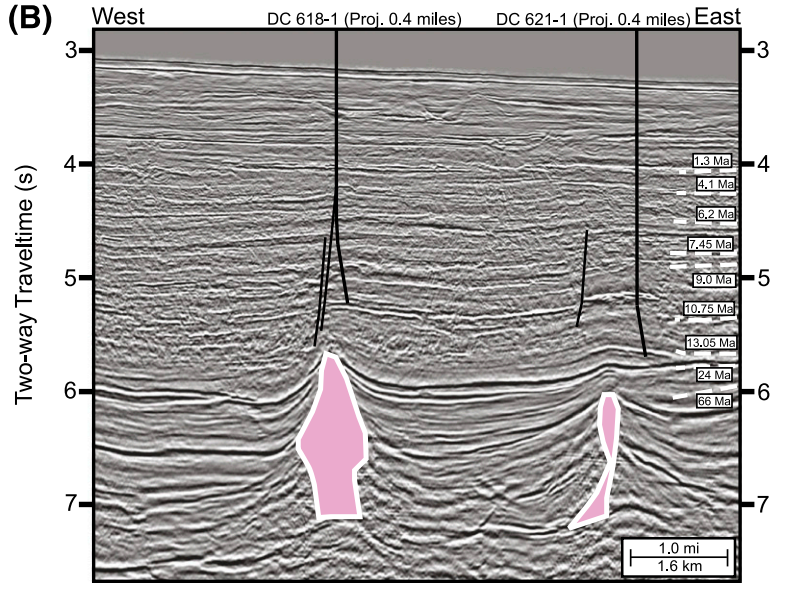

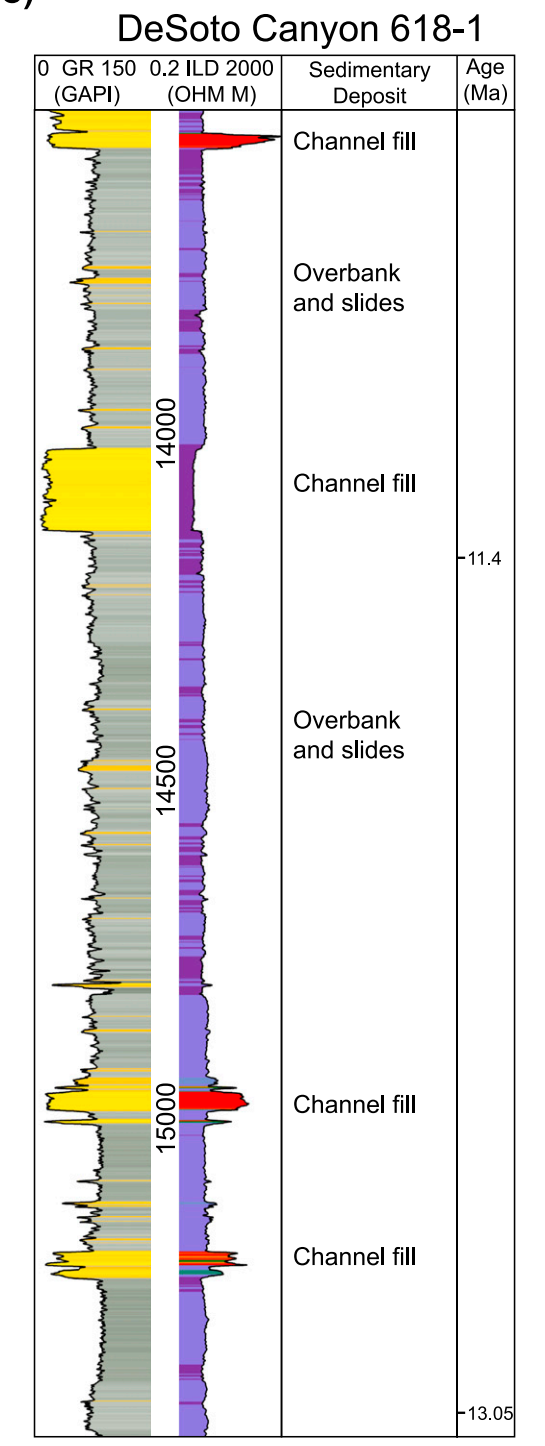

Figure 15. DeSoto Canyon (DC) 618 San Jacinto field. (A) Location map of DC 618 San Jacinto and DC 621 Spiderman fields. (B) Seismic profile. Reprinted with permission of Schlumberger. (C) Gamma-ray (GR) and resistivity log. See Figure 4 for the regional setting of the field. ILD = deep induction.

Spiderman Field, Figure 16

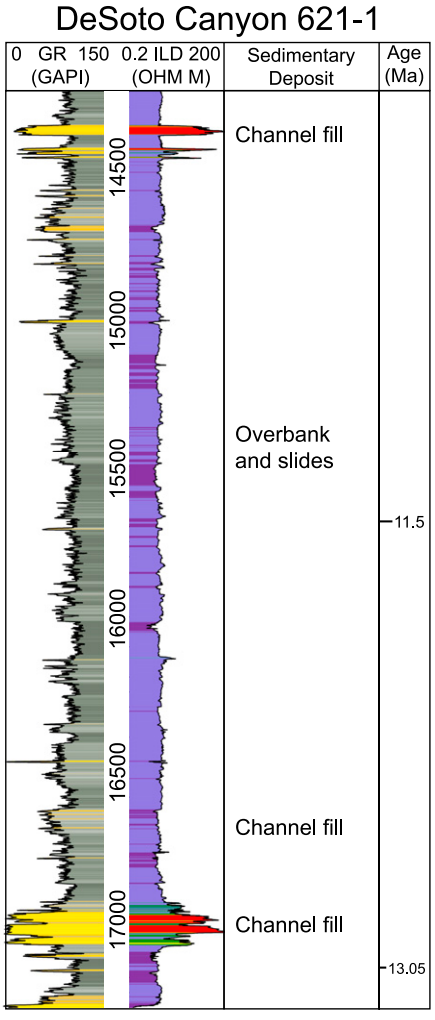

Field Name	Spiderman (Figure 16)
Block Numbers	DC 621, DC620, DC664
Partners	Anadarko (45,00%), Eni (36,67%),
	Statoil (18,33%)
Discovery Date	November 2003
Production Start Date	November 2007
Production Facility	Subsea tie-back to Independence Hub in MC 920
Water Depth (feet)	8,910
Development Status	abandoned-2015
Number of Wells	3
Number of Reservoirs	4
Age	middle Miocene
Sedimentary deposit	channel fill
Trap	three-way closure against fault
Gas Recoverable Reserves (BCF)	300
Recovery Efficiency (percent)	100
Porosity (percent)	26
Permeability (mD)	50-5000
Water Saturation Range (percent)	10-14
Initial Reservoir Temperature Range (°F)	129-155
Initial Reservoir Pressure Range (PSI)	7500-8630
Gas Specific Gravity Range (at 60 and 15,025 PSI)	0,56
Sulfur Content (percent)	0
Pay Thickness (feet)	136 (net)
Upper Seal	shale
Lateral Seal	shale
Source Of Information	Greene and O'Neil, 2005
	Vercher and Blakeley, 2007
	M. Morris, pers comm., 2009

Figure 16. DeSoto Canyon 621 Spiderman field. Gamma-ray (GR) and resistivity log. Location of well is shown in Figure 15A. See Figure 15A for location map and Figure 15B for seismic profile. See Figure 4 for the regional setting of the field. ILD = deep induction.

Mondo Northwest Field, Figure 17

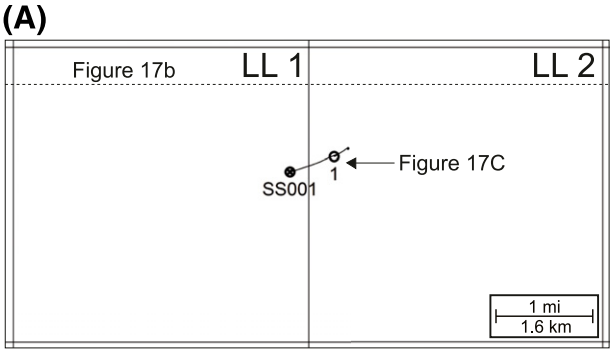

Field Name	Mondo Northwest (Figure 17)
Block Numbers	LL 001, LL 002
Partners	Anadarko (50.00%), Murphy Oil (50.00%)
Discovery Date	January 2005
Production Start Date	July 2007
Production Facility	Subsea tie-back to Independence Hub in MC 920
Water Depth (feet)	8,412
Development Status	abandoned-2015
Number of Wells	1
Number of Reservoirs	3
Age	late Miocene
Sedimentary deposit	channel fill
Trap	four-way closure fault bounded
Liquids Recoverable Reserves (MMbbl)	0
Recovery Efficiency (percent)	100
Initial Reservoir Temperature Range (°F)	145
Gas Specific Gravity Range (at 60 and 15.025 PSI)	0.56
Sulfur Content (percent)	0
Viscosity (centipoise)	0.03
Upper Seal	shale
Lateral Seal	shale
Reservoir Intervals (Subsea true vertical depth-feet)	14,900-15,600
Source Of Information	Cossey and Associates Inc.

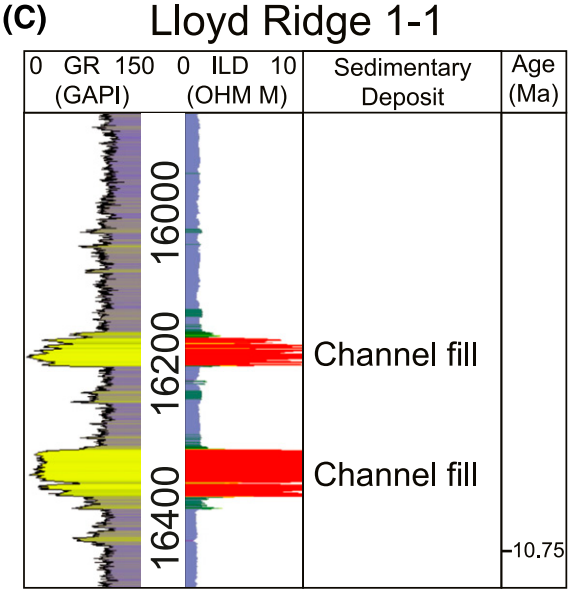

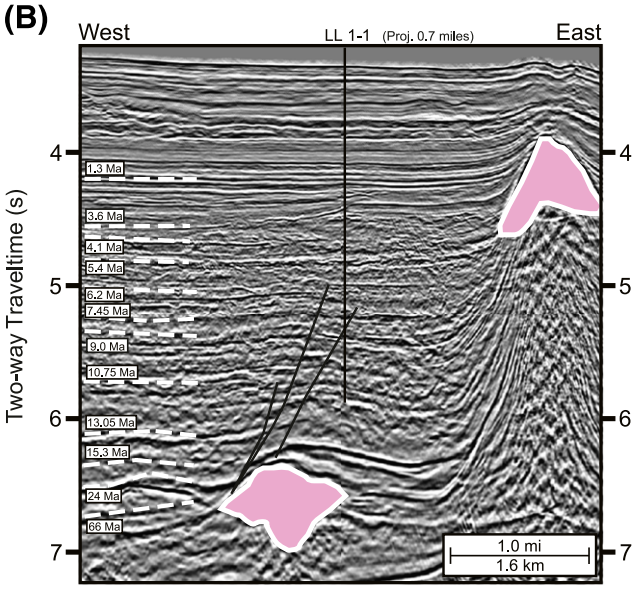

Figure 17. Lloyd Ridge (LL) 1 Mondo Northwest field. (A) Location map. (B) Seismic profile. (C) Gamma-ray (GR) and resistivity log. See Figure 4 for the regional setting of the field. ILD = deep induction.

Atlas Northwest Field, Figure 18

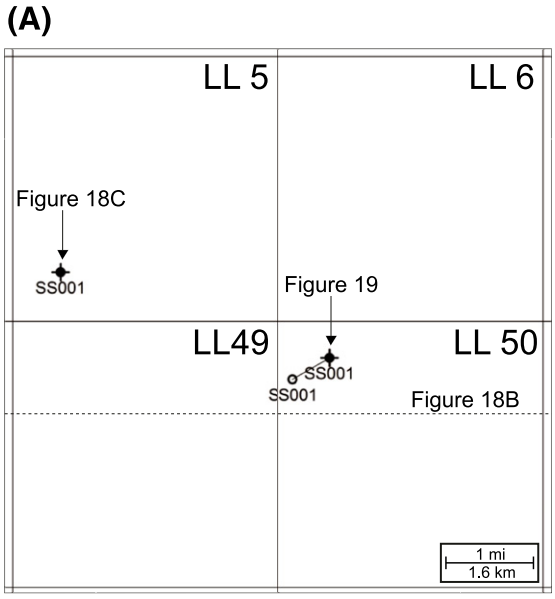

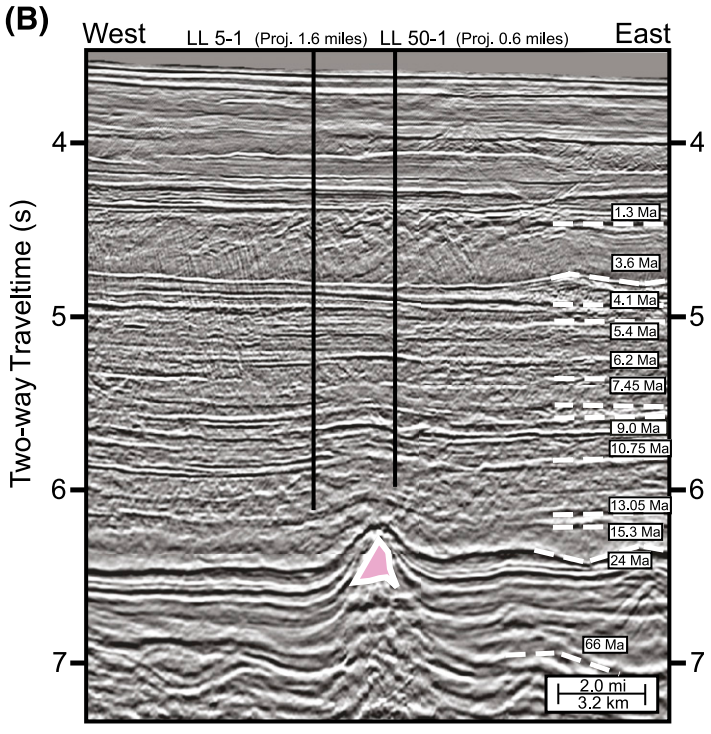

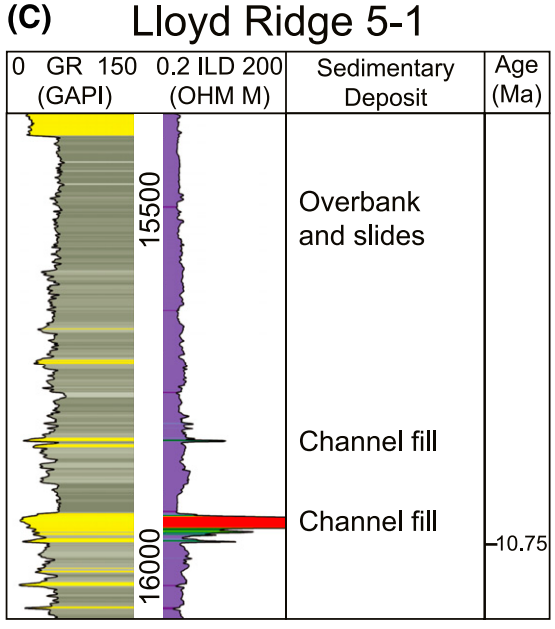

Field Name	Atlas Northwest (Figure 18)
Block Numbers	LL 005
Partners	Anadarko (100.00%)
Discovery Date	June 2003
Production Start Date	July 2007
Production Facility	Subsea tie-back to Independence Hub in MC 920
Water Depth (feet)	8861
Development Status	abandoned-2009
Number of Wells	1
Number of Reservoirs	1
Age	late Miocene
Sedimentary deposit	channel fill
Trap	four-way closure (compactional drape)
Liquids Recoverable Reserves (MMbbl)	0
Recovery Efficiency (percent)	100
Porosity (percent)	25
Initial Reservoir Temperature Range (°F)	145
Gas Specific Gravity Range (at 60 and 15.025 PSI)	0.56
Sulfur Content (percent)	0
Viscosity (centipoise)	0.03
Upper Seal	shale
Lateral Seal	shale
Source Of Information	M. Miller, pers. comm., 2009

Figure 18. Lloyd Ridge (LL) 5 Atlas Northwest field. (A) Location map of Lloyd Ridge 50 Atlas and Atlas NW 5 fields. (B) Seismic profile. Reprinted with permission of Schlumberger. (C) Gamma-ray (GR) and resistivity log. See Figure 4 for the regional setting of the field. ILD = deep induction.

Atlas Field, Figure 19

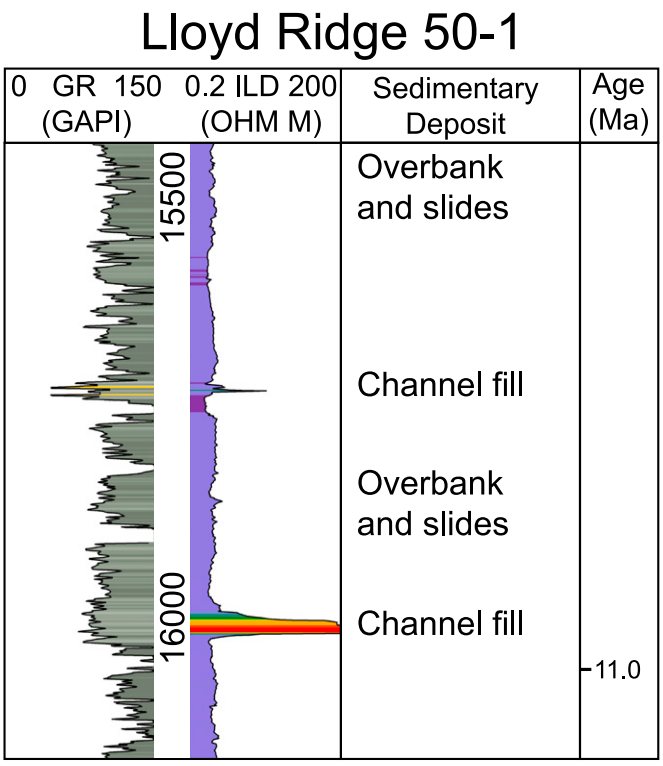

Field Name	Atlas (Figure 19)
Block Numbers	LL 050, LL 005, LL 049
Partners	Anadarko (100.00%)
Discovery Date	February 2003
Production Start Date	July 2007
Production Facility	Subsea tie-back to Independence Hub in MC 920
Water Depth (feet)	9,000
Development Status	abandoned-2009
Number of Wells	1
Number of Reservoirs	2
Age	late Miocene
Sedimentary deposit	channel fill
Trap	four-way closure (compactional drape)
Liquids Recoverable Reserves (MMbbl)	0
Recovery Efficiency (percent)	100
Porosity (percent)	24
Initial Reservoir Temperature Range (°F)	145
Gas Specific Gravity Range (at 60 and 15.025 PSI)	0.56
Sulfur Content (percent)	0
Viscosity (centipoise)	0.03
Upper Seal	shale
Lateral Seal	shale
Reservoir Intervals (Subsea true vertical depth-feet)	15,700-17,000
Source Of Information	M. Miller, pers. comm., 2009

Figure 19. Lloyd Ridge Atlas 50 field. Gamma-ray (GR) and resistivity log. See Figure 18A for location map and Figure 18B for seismic profile. See Figure 4 for the regional setting of the field. ILD = deep induction.

Cheyenne Field, Figure 20

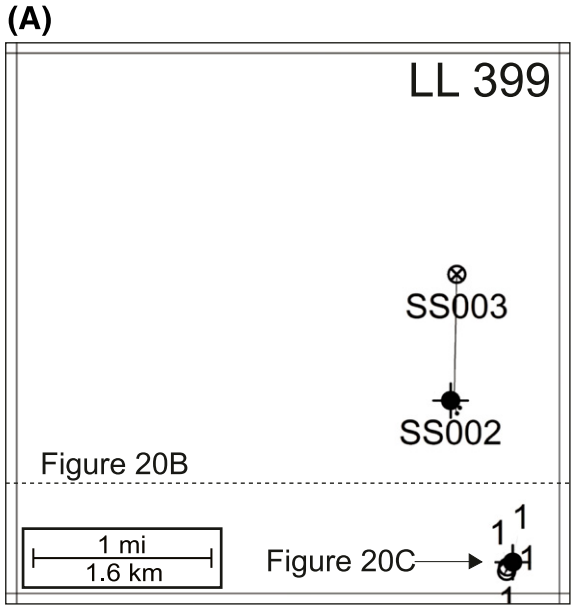

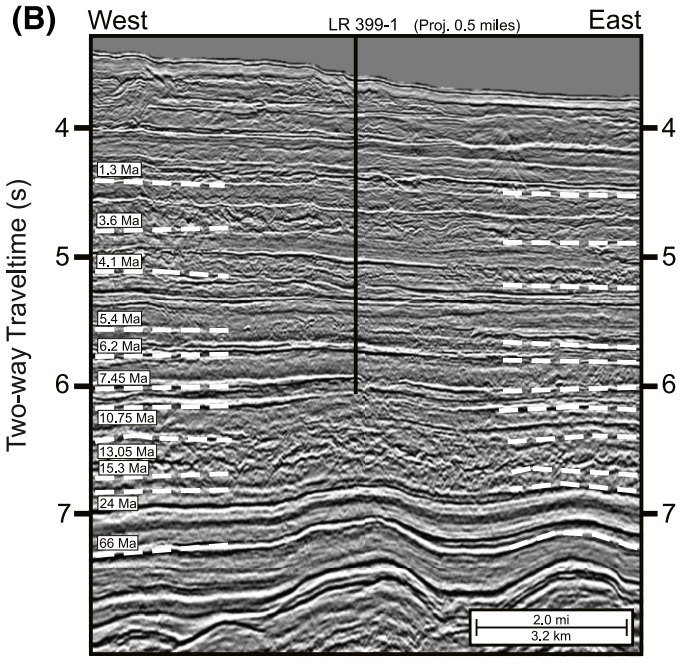

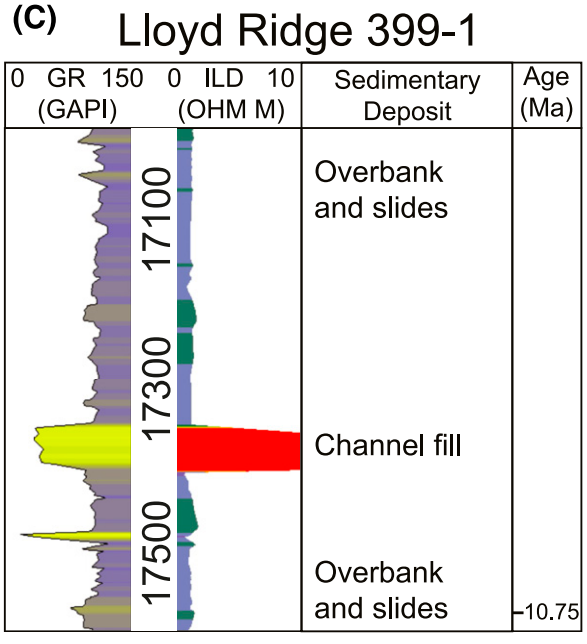

Field Name	Cheyenne (Figure 20)
Block Numbers	LL 399
Partners	Anadarko (100.00%)
Discovery Date	January 2005
Production Start Date	June 2008
Production Facility	Subsea tie-back to Independence Hub in MC 920
Water Depth (feet)	9,039
Development Status	abandoned-2011
Number of Wells	2
Number of Reservoirs	1
Age	late Miocene
Sedimentary deposit	channel fill
Trap	four-way closure (compactional drape)
Liquids Recoverable Reserves (MMbbl)	0
Gas Recoverable Reserves (BCF)	189.95
Recovery Efficiency (percent)	100
Porosity (percent)	28
Initial Reservoir Temperature Range (°F)	145
Gas Specific Gravity Range (at 60 and 15,025 PSI)	0.56
Sulfur Content (percent)	0
Viscosity (centipoise)	0.03
Upper Seal	shale
Lateral Seal	shale
Reservoir Intervals (Subsea true vertical depth-feet)	17,300-17,500
Source Of Information	M. Miller, pers. comm., 2009
	Cossey and Associates Inc.

Figure 20. Lloyd Ridge (LL) 399 Cheyenne field. (A) Location map of LL 399. (B) Seismic profile. Reprinted with permission of Schlumberger. (C) Gamma-ray (GR) and resistivity log. See Figure 4 for the regional setting of the field. ILD = deep induction.

Otis Field, Figure 21

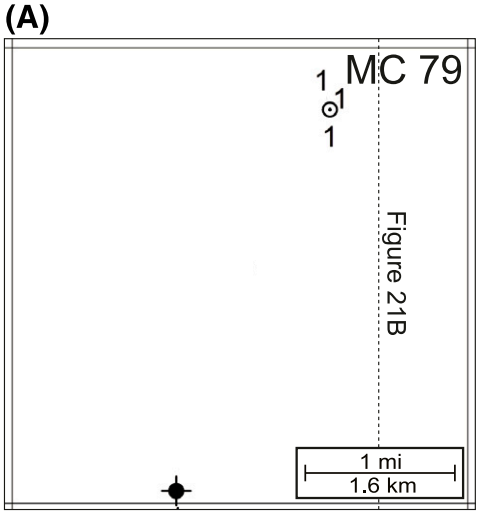

Field Name	Otis (Figure 21)
Block Numbers	MC 79
Partners	LLOG (70%) Ridgewood (30%)
Discovery Date	October 2014
Production Start Date	April 2016
Production Facility	Subsea tie-back to Delta House MC 254
Water Depth (feet)	3950
Development Status	producing
Number of Wells	1
Number of Reservoirs	1
Drive Mechanism	water drive
Age	late Miocene
Sedimentary deposit	sheet
Trap	three-way closure against fault
Porosity (percent)	32
Permeability (mD)	800
Water Saturation Range (percent)	25-30
Sulfur Content (percent)	0
Pay Thickness (feet)	73 (gross)
Upper Seal	shale
Lateral Seal	shale
Source Of Information	Fowler et al., 2015

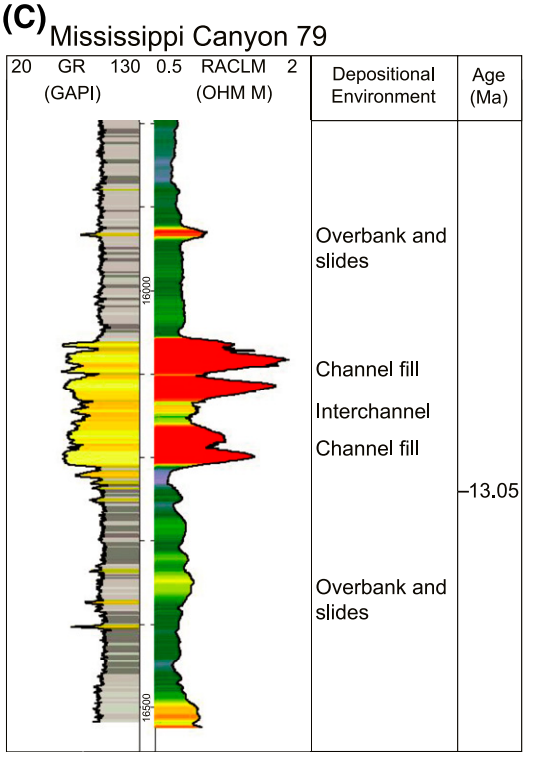

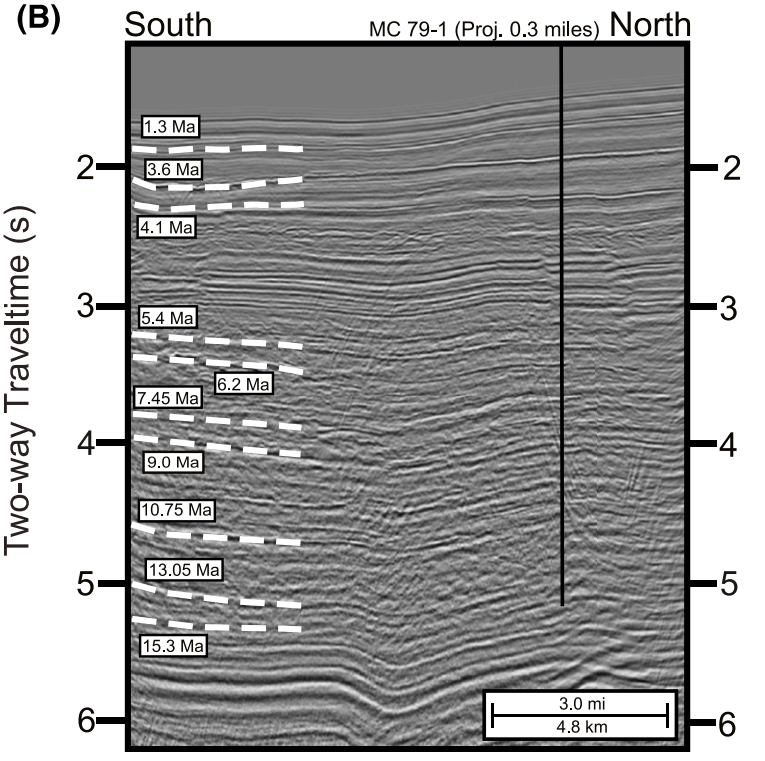

Figure 21. Mississippi Canyon (MC) 79 Otis field. (A) Location map. (B) Seismic profile. Reprinted with permission of Schlumberger. (C) Gamma-ray (GR) and resistivity log. See Figure 4 for the regional setting of the field. RACLM = attenuated resistivity.

King Field, Figure 22

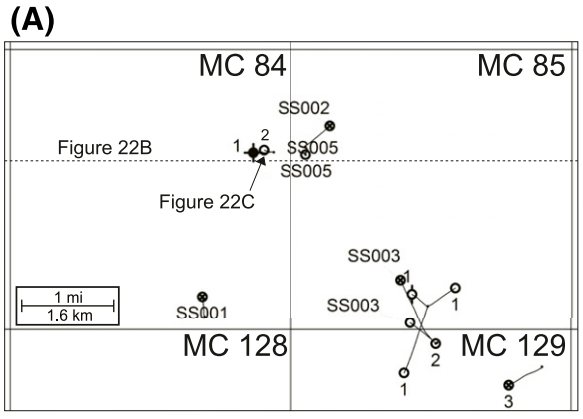

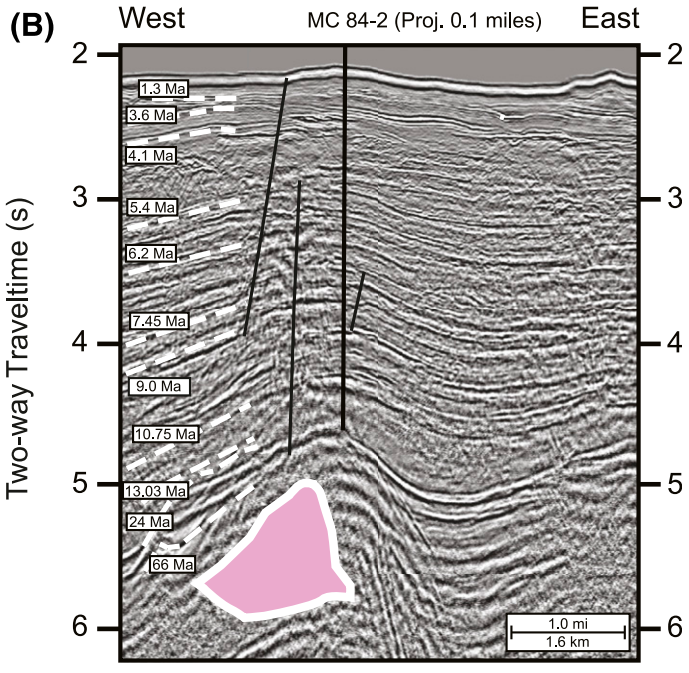

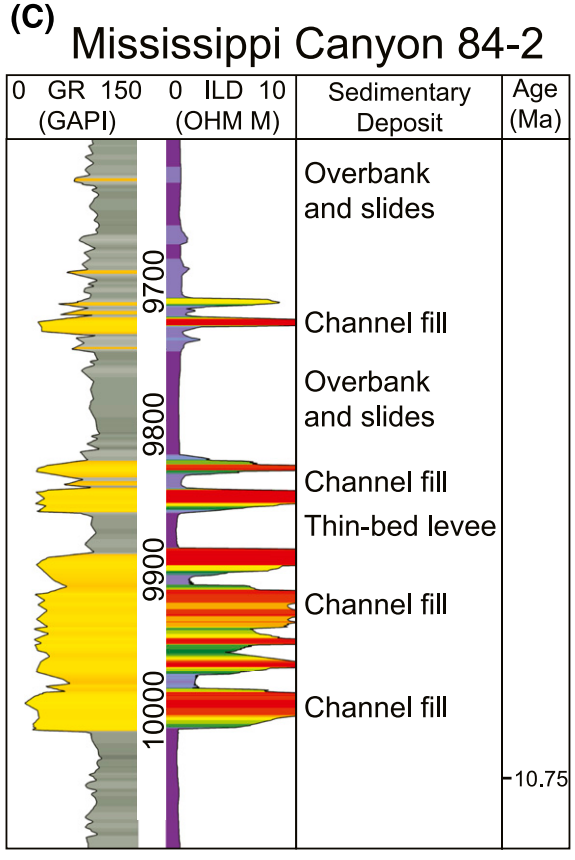

Field Name	King (Figure 22)
Block Numbers	MC 84
Partners	Anadarko (100%)
Discovery Date	January 1993
Production Start Date	June 2002
Production Facility	Subsea tie-back to Marlin TLP Viosca Knoll 915
Water Depth (feet)	5,940
Development Status	producing
Number of Wells	2
Number of Reservoirs	1
Drive Mechanism	water-partial gas
Age	late Miocene
Sedimentary deposit	amalgamated channel fill
Trap	three-way closure against fault
Liquids Recoverable Reserves (MMbbl)	93.15
Gas Recoverable Reserves (BCF)	106.17
Initial Production (BOPD), (MCFGPD)	28,000 BOPD
Gas Oil Ratio	1,100
Porosity (percent)	28-33
Permeability (mD)	149-1,602
Water Saturation Range (percent)	16-31
Initial Reservoir Temperature Range (°F)	120-160
Initial Reservoir Pressure Range (PSI)	5,900-7,000
API Oil Gravity	33.8
Gas Specific Gravity Range (at 60 and 15.025 PSI)	0.6
Sulfur Content (percent)	0.02
Pay Thickness (feet)	30-50 (gross)
Oil Column (feet)	1,400-2,000
Upper Seal	shale
Lateral Seal	shale
Reservoir Intervals (Subsea true vertical depth-feet)	11,300-11,450
Source Of Information	Wagner et al., 1994
	Haddad et al., 2003
	Li et al., 2005
	Cossey and Associates Inc.

Figure 22. Mississippi Canyon (MC) 84 King–King West field. (A) Location map. (B) Seismic profile. Reprinted with permission of Schlumberger. (C) Gamma-ray (GR) and resistivity log. See Figure 4 for the regional setting of the field. ILD = deep induction.

Horn Mountain Field, Figure 23

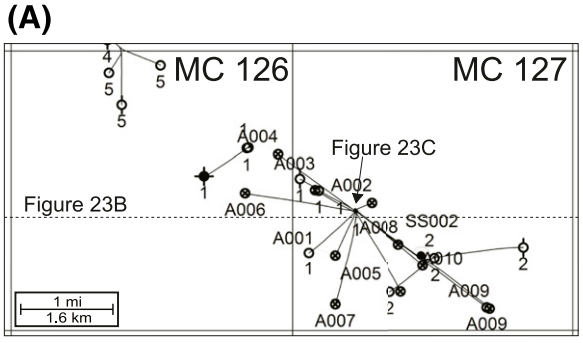

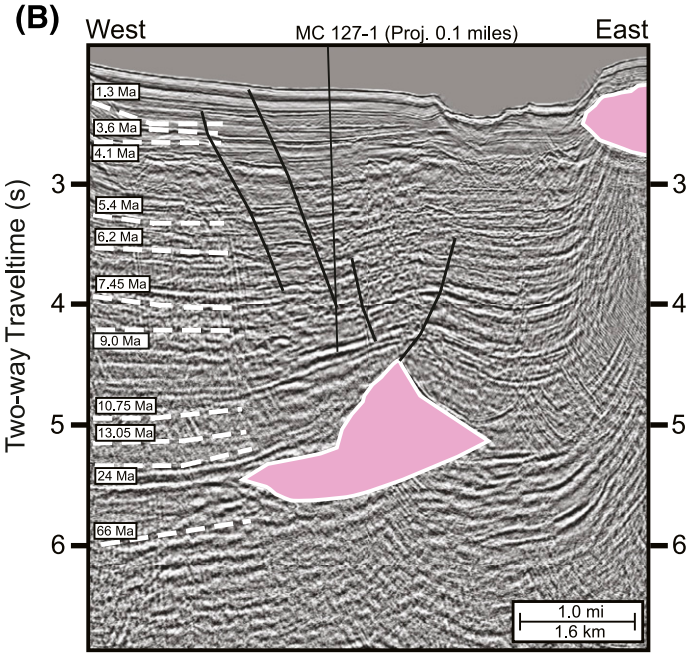

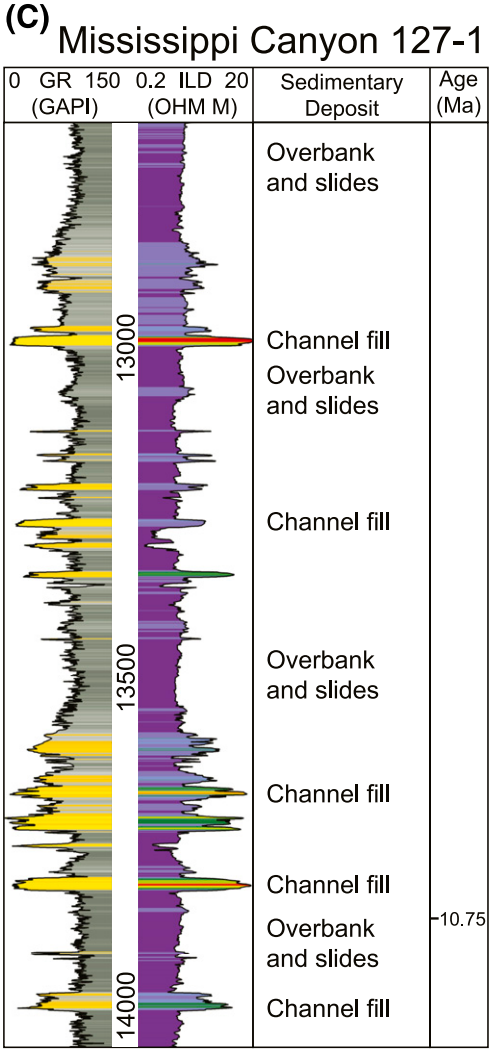

Field Name	Horn Mountain (Figure 23)
Block Numbers	MC 126, MC 127
Partners	Anadarko (100%)
Discovery Date	August 1999
Production Start Date	November 2002
Production Facility	Subsea tie-back to SPAR Platform in MC 127
Water Depth (feet)	5,399
Development Status	producing
Field Size (acres)	5,000
Number of Wells	10 development wells (8 producers, 2 injection)
Number of Reservoirs	2
Drive Mechanism	water and compaction
Age	late Miocene
Sedimentary deposit	channel fill- levees
Trap	three-way closure against fault-stratigraphic
Liquids Recoverable Reserves (MMbbl)	123
Gas Recoverable Reserves (BCF)	129
Initial Production (BOPD), (MCFGPD)	65,000 BOPD, 68 MCFGPD
Gas Oil Ratio	630-1400
Recovery Efficiency (percent)	46
Porosity (percent)	24-28
Permeability (mD)	500-2,500
Water Saturation Range (percent)	15-25
Initial Reservoir Pressure Range (PSI)	6,800-7,200
API Oil Gravity	31-36
Sulfur Content (percent)	0.25-0.28
Pay Thickness (feet)	25-45 (gross)
Oil Column (feet)	2,500
Upper Seal	shale-fault
Lateral Seal	shale
Reservoir Intervals (Subsea true vertical depth-feet)	12,500-14,400
Source Of Information	van Gestel et al., 2012
	Mikov et al., 2007
	Cossey and Associates Inc.

Figure 23. Mississippi Canyon (MC) 126–127 Horn Mountain field. (A) Location map. (B) Seismic profile. Reprinted with permission of Schlumberger. (C) Gamma-ray (GR) and resistivity log. See Figure 4 for the regional setting of the field. ILD = deep induction.

MC 161 Field, Figure 24

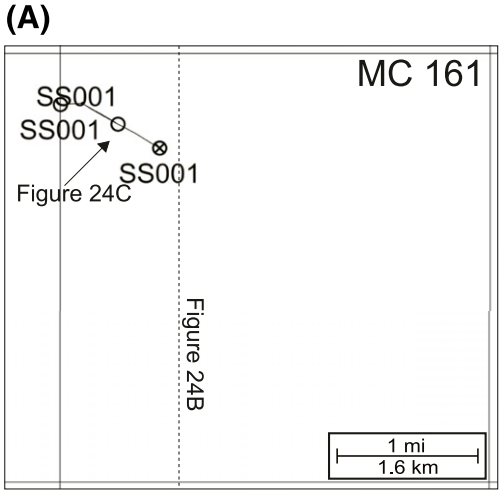

Field Name	MC 161 (Figue 24)
Block Numbers	MC 161
Partners	Stone 50%, Tana 50%
Discovery Date	August 2005
Production Start Date	2008
Production Facility	Subsea tieback to Pompano Viosca Knoll 989
Water Depth (feet)	2924
Development Status	producing
Number of Wells	1
Number of Reservoirs	1
Drive Mechanism	mixed
Age	early Pliocene
Sedimentary deposit	Channel fill
Trap	stratigraphic
Gas Recoverable Reserves (BCF)	20 bcf
Initial Production (BOPD), (MCFGPD)	10.65 Mmcfd
Porosity (percent)	28
Initial Reservoir Temperature Range (°F)	153
Upper Seal	shale
Lateral Seal	shale
Source Of Information	Peter Hetherington (pers. comm, 2015)

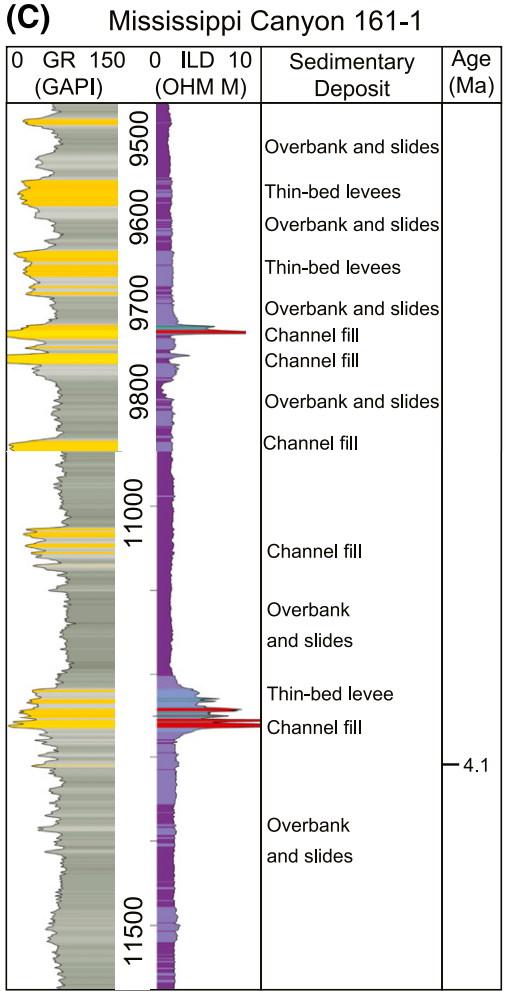

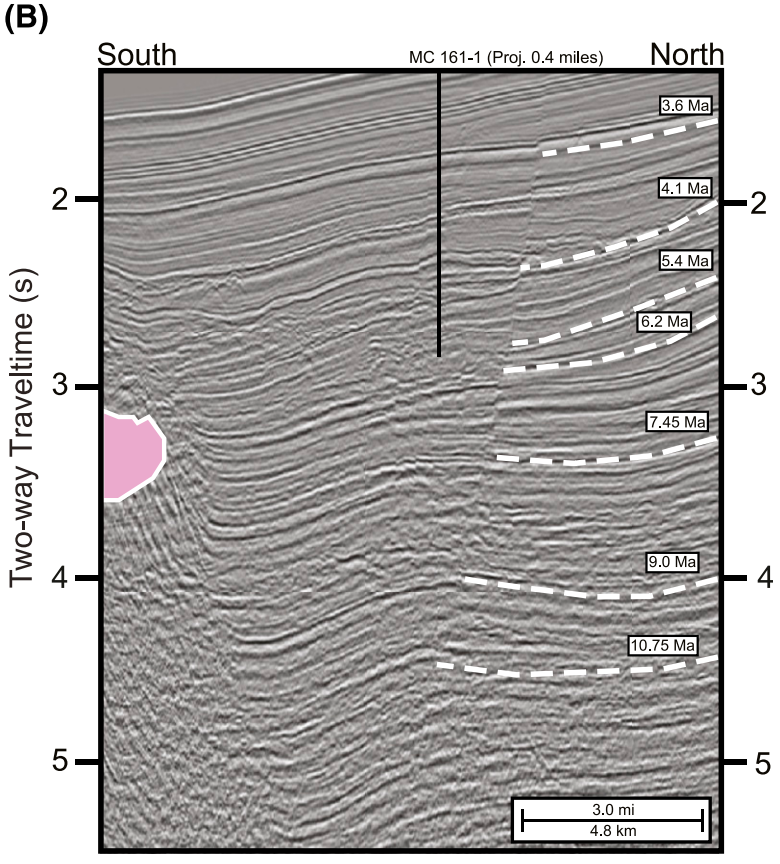

Figure 24. Mississippi Canyon (MC) 161 field. (A) Location map. (B) Seismic profile. Reprinted with permission of Schlumberger. (C) Gamma-ray (GR) and resistivity log. See Figure 4 for the regional setting of the field. ILD = deep induction.

Mandy Field, Figure 25

(A)

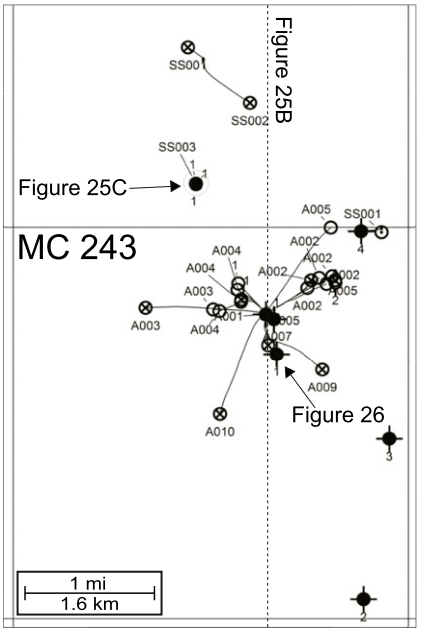

Field Name	Mandy (Figure 25)
Block Numbers	MC 199
Partners	LLOG (100%)
Discovery Date	February 2010
Production Start Date	2012
Production Facility	Subsea tie-back to Matterhorn TLP in MC 243
Water Depth (feet)	2467
Development Status	producing
Field Size (acres)	1,000-1,500
Number of Wells	3
Number of Reservoirs	1 in 3 fault blocks
Drive Mechanism	partial water
Age	middle Miocene
Sedimentary deposit	channel fill
Trap	three-way closure against fault-stratigraphic
Liquids Recoverable Reserves (MMbbl)	15
Gas Recoverable Reserves (BCF)	15
Initial Production (BOPD), (MCFGPD)	8,000 BOPD
Gas Oil Ratio	900
Recovery Efficiency (percent)	35
Porosity (percent)	30
Permeability (mD)	500-600
Water Saturation Range (percent)	30
API Oil Gravity	30
Sulfur Content (percent)	0
Pay Thickness (feet)	100-150 (gross)
Oil Column (feet)	300-500
Upper Seal	shale
Lateral Seal	shale

(B)

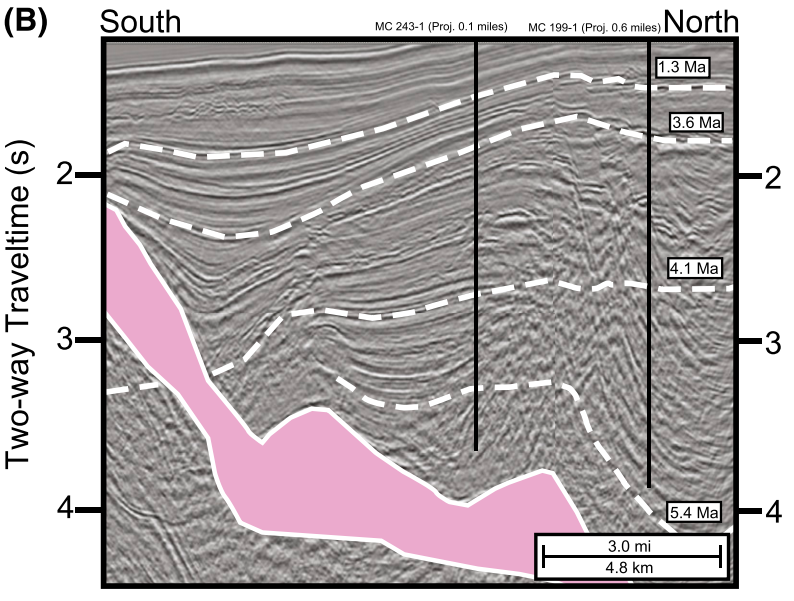

(C) Mississippi Canyon 199-1

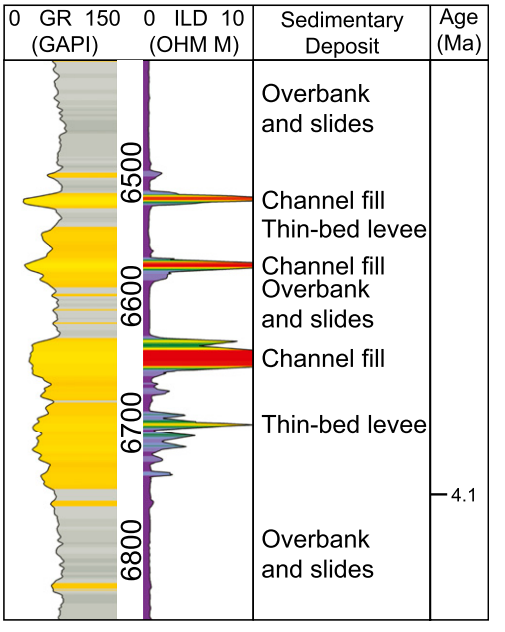

Figure 25. Mississippi Canyon (MC) 199 Mandy field. (A) Location map of MC 199 Mandy field and MC 243 Matterhorn. (B) Seismic profile. Reprinted with permission of Schlumberger. (C) Gamma-ray (GR) and resistivity log. See Figure 4 for the regional setting of the field. ILD = deep induction.

Matterhorn Field, Figure 26

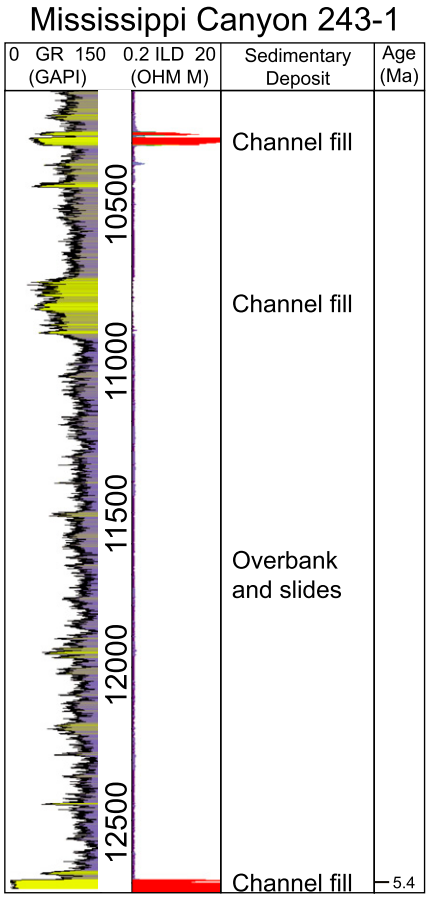

Field Name	Matterhorn (Figure 26)
Block Numbers	MC 243
Partners	W&T Offshore (100%)
Discovery Date	July 1999
Production Start Date	November 2003
Production Facility	Subsea tie-back to Matterhorn TLP in MC 243
Water Depth (feet)	2,868
Development Status	producing
Number of Wells	7 producers, 1 injector
Number of Reservoirs	5
Age	early Pliocene
Sedimentary deposit	channel fill
Trap	three-way closure against salt flank
Liquids Recoverable Reserves (MMbbl)	50.34
Gas Recoverable Reserves (BCF)	78.11
API Oil Gravity	43.8
Sulfur Content (percent)	0.005
Pay Thickness (feet)	370 (net)
Upper Seal	shale
Lateral Seal	shale
Reservoir Intervals (Subsea true vertical depth-feet)	6,300-8,100
Source Of Information	Cossey and Associates Inc.

Figure 26. Mississippi Canyon 243 Matterhorn field. Gamma-ray (GR) and resistivity log. See Figure 25A for location map and Figure 25B for seismic profile. See Figure 4 for the regional setting of the field. ILD = deep induction.

Mica Field, Figure 27

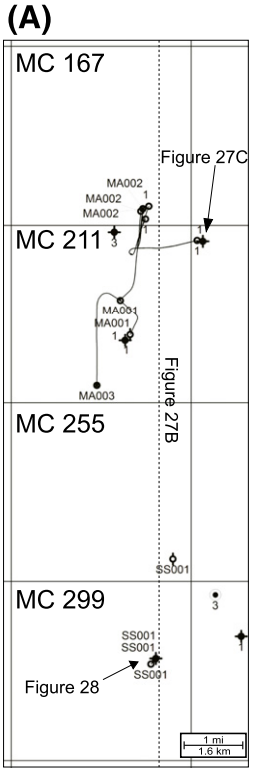

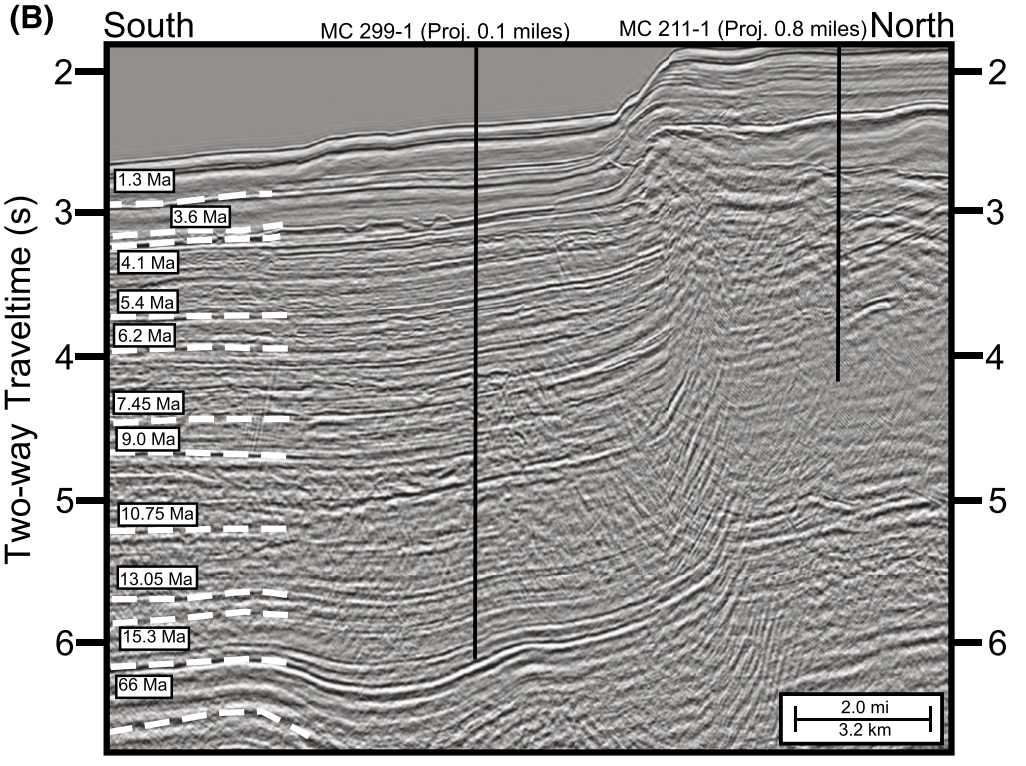

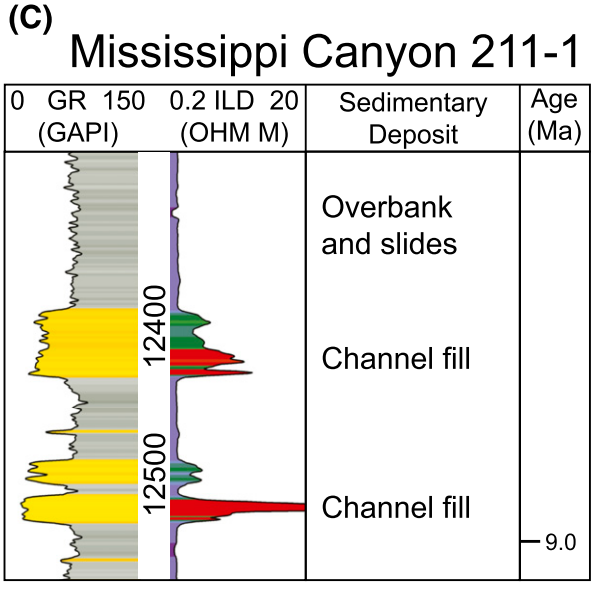

Field Name	Mica (Figure 27)
Block Numbers	MC 211, MC 167
Partners	ExxonMobil (50.00%), Stone (50.00%)
Discovery Date	April 1990
Production Start Date	August 2001
Production Facility	Subsea tie-back to Viosca Knoll 989 Platform
Water Depth (feet)	4,376
Development Status	producing
Number of Wells	4
Number of Reservoirs	3
Drive Mechanism	combination
Age	late Miocene
Sedimentary deposit	channel fill-levee
Trap	four-way closure against faults with stratigraphic component
Liquids Recoverable Reserves (MMbbl)	9.07
Gas Recoverable Reserves (BCF)	288.75
Initial Production (BOPD), (MCFGPD)	13,000 BOPD, 140 MCFGPD
Gas Oil Ratio	1,000-8,000
Porosity (percent)	29-36
Permeability (mD)	18-2,996
Water Saturation Range (percent)	15-64
Initial Reservoir Temperature Range (°F)	110-131
Initial Reservoir Pressure Range (PSI)	6,000-7,500
API Oil Gravity	32-44
Gas Specific Gravity Range (at 60 and 15.025 PSI)	0.68
Pay Thickness (feet)	30-125 (gross)
Upper Seal	shale
Lateral Seal	shale
Reservoir Intervals (Subsea true vertical depth-feet)	10,700-12,600
Source Of Information	Ballard, 2006
	Cossey and Associates Inc.
	P. Wieg, pers. comm., 2010

Figure 27. Mississippi Canyon (MC) 211–167 Mica field. (A) Location map of MC 211 Mica and MC 299 17 Hands fields. (B) Seismic profile. Reprinted with permission of Schlumberger. (C) Gamma-ray (GR) and resistivity log. See Figure 4 for the regional setting of the field. ILD = deep induction.

Seventeen Hands Field, Figure 28

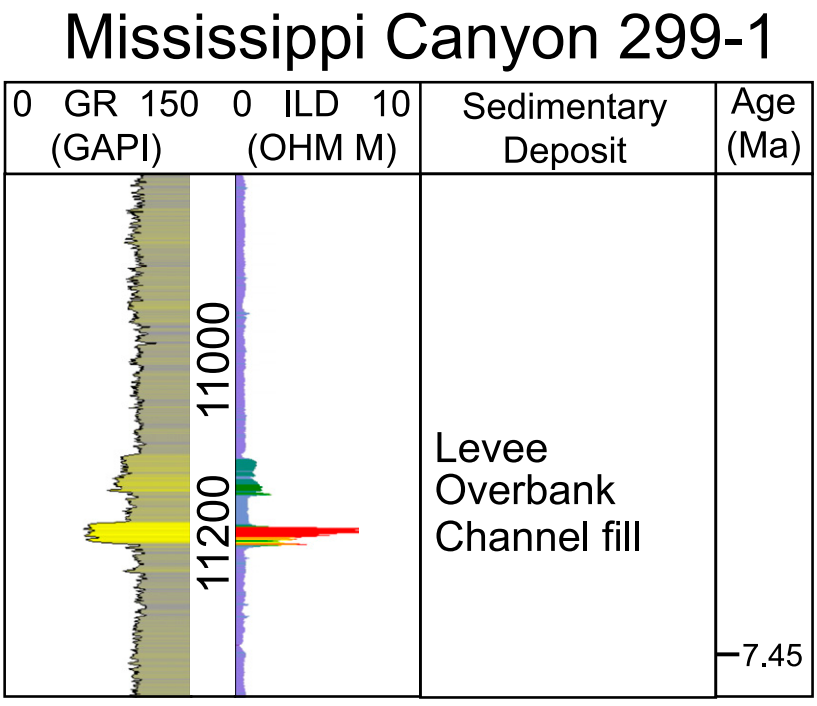

Field Name	Seventeen Hands (Figure 28)
Block Numbers	MC 299
Partners	Eni (37.50%), Murphy Oil (37.50%)
	Statoil (25.00%)
Discovery Date	2000
Production Start Date	March 2006
Production Facility	Subsea tie-back to Gemini (MC 292)
Water Depth (feet)	5,400
Development Status	abandoned-2011
Number of Wells	1
Number of Reservoirs	1
Age	late Miocene
Sedimentary deposit	channel fill
Trap	stratigraphic
Liquids Recoverable Reserves (MMbbl)	0.17 MMbl
Gas Recoverable Reserves (BCF)	75
Porosity (percent)	Low 30's
Permeability (mD)	up to 1000
Oil Column (feet)	~ 200
Upper Seal	shale
Lateral Seal	shale
Source Of Information	Ballard, 2006
	Cossey and Associates Inc.

Figure 28. Mississippi Canyon 299 17 Hands field. Gamma-ray (GR) and resistivity log. See Figure 27A for location map and Figure 27B for seismic profile. See Figure 4 for the regional setting of the field. ILD = deep induction.

King's Peak Field, Figure 29

(A)

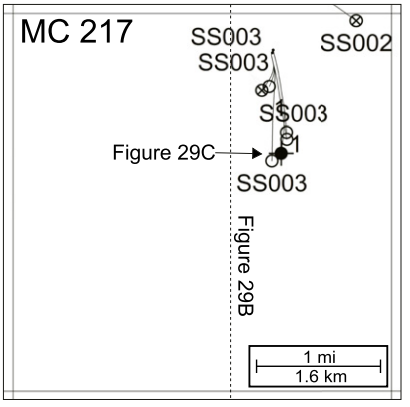

Field Name	King's Peak (Figure 29)
Block Numbers	MC 217, MC 173, DC 133, DC 177
Partners	Bennu (55.00%), Marubeni (45.00%)
Discovery Date	March 1993
Production Start Date	September 2002
Production Facility	Subsea tie-back to Main Pass 261 (Canyon Express)
Water Depth (feet)	6,237
Development Status	abandoned-2013
Number of Wells	4
Age	late Miocene
Sedimentary deposit	channel fill- thin bed levee
Trap	stratigraphic
Liquids Recoverable Reserves (MMbbl)	0.2
Gas Recoverable Reserves (BCF)	168.05
Upper Seal	shale
Lateral Seal	shale
Reservoir Intervals (Subsea true vertical depth-feet)	11,200-11,300
Source Of Information	Cossey and Associates Inc.

(C)

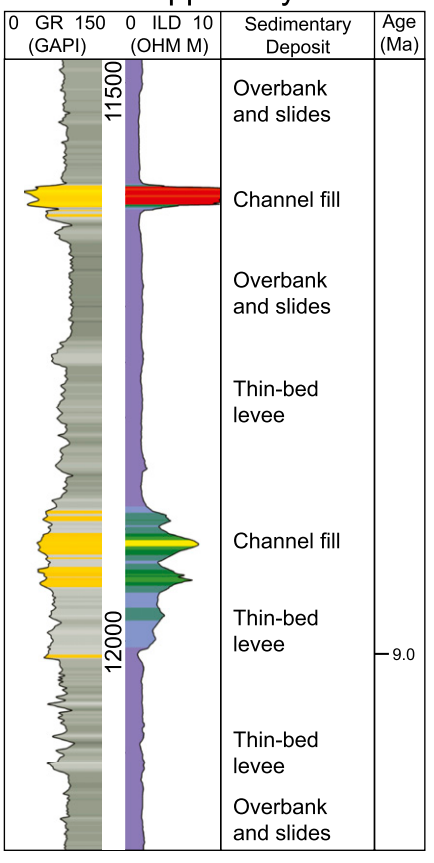

(B)

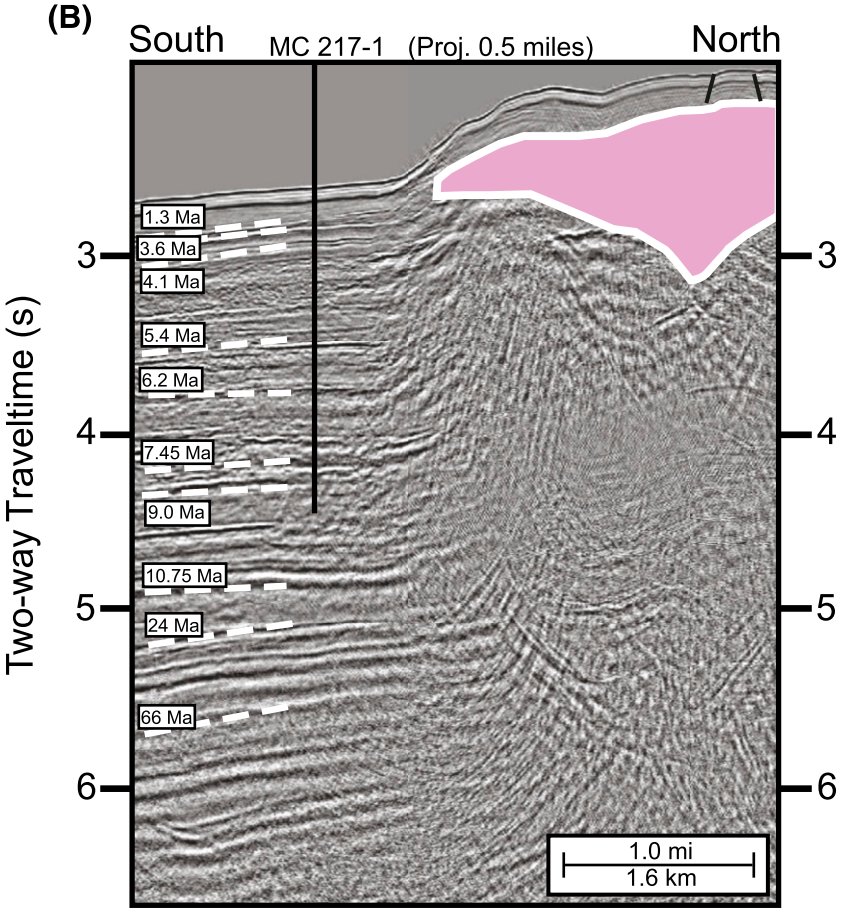

Figure 29. Mississippi Canyon (MC) 217 Kings Peak field. (A) Location map. (B) Seismic profile. Reprinted with permission of Schlumberger. (C) Gamma-ray (GR) and resistivity log. See Figure 4 for the regional setting of the field. ILD = deep induction.

Gemini-Raton-Raton South Field, Figure 30

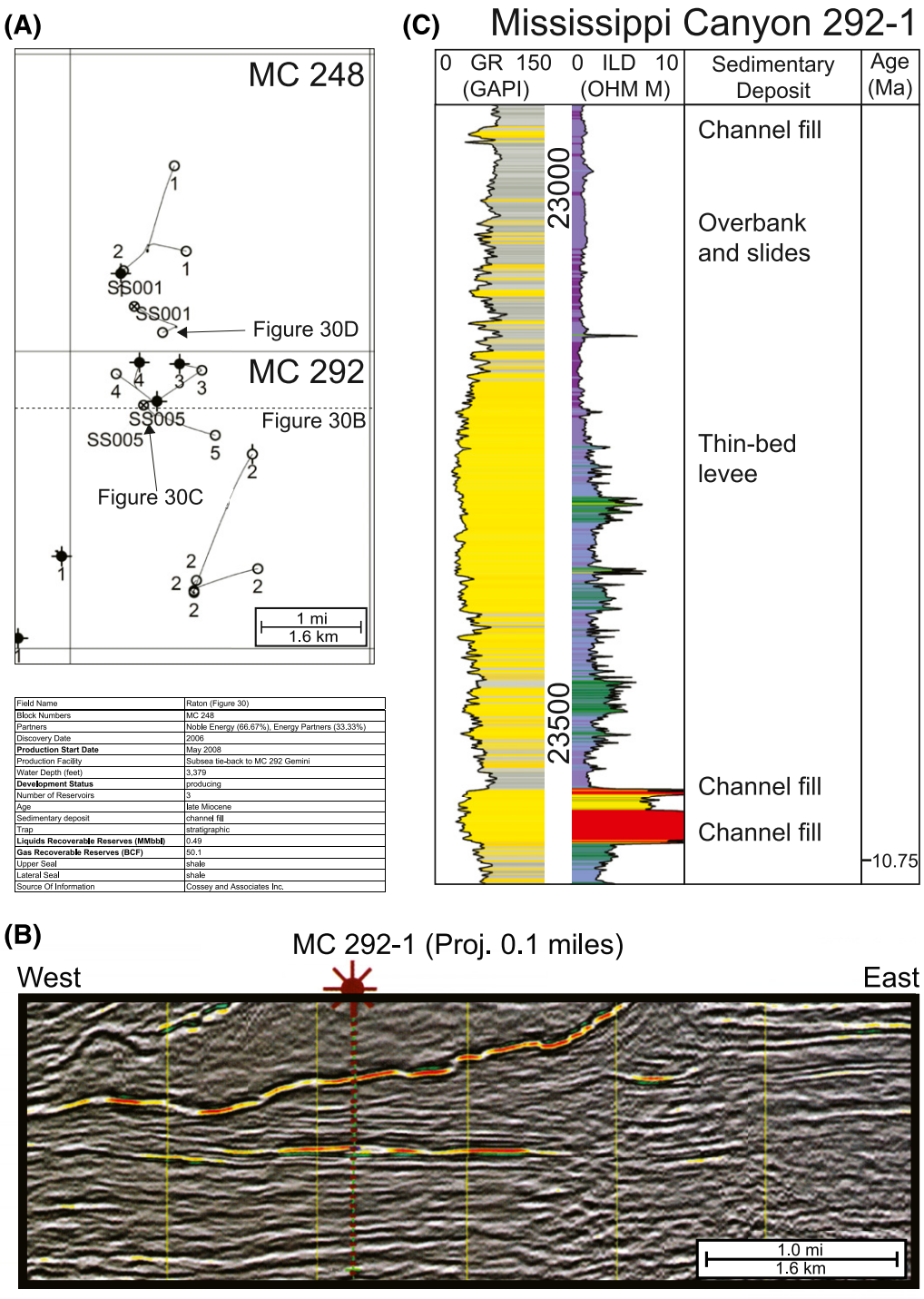

Field Name	Raton (Figure 30)
Block Numbers	MC 248
Partners	Noble Energy (66.67%), Energy Partners (33.33%)
Discovery Date	2006
Production Start Date	May 2008
Production Facility	Subsea tie-back to MC 292 Gemini
Water Depth (feet)	3,379
Development Status	producing
Number of Reservoirs	3
Age	late Miocene
Sedimentary deposit	channel fill
Trap	stratigraphic
Liquids Recoverable Reserves (MMbbl)	0.49
Gas Recoverable Reserves (BCF)	50.1
Upper Seal	shale
Lateral Seal	shale
Source Of Information	Cossey and Associates Inc.

Figure 30. Mississippi Canyon (MC) 248 Raton, MC 292 Raton South, and MC 292 Gemini fields. Note: The Gemini field was discovered and developed first and was then sold to Noble, who developed the Raton and Raton South fields. The three reservoirs are stratigraphically trapped and offset of one another. (A) Location map. (B) Seismic profile across the MC 292 Gemini field. After Abriel (2008). Reprinted with permission of Society of Exploration Geophysicists. (C) Gamma-ray (GR) and resistivity log from the MC 292 well (Gemini). (D) The GR and resistivity log from the MC 248-1 well (Raton). See Figure 4 for the regional setting of the field. ILD = deep induction.

Gemini-Raton-Raton South Field, Figure 30

Field Name	Gemini (Figure 30)
Block Numbers	MC 292
Partners	Noble 62.22%, Energy Partners 21.11%,
	Stephens Production 16.67%
Discovery Date	1995
Production Start Date	June 1999
Production Facility	SPAR
Water Depth (feet)	3,488
Development Status	abandoned 2009
Number of Wells	3
Number of Reservoirs	1
Drive Mechanism	retrograde gas
Age	late Miocene
Sedimentary deposit	channel fill, thin bed levees
Trap	stratigraphic
Liquids Recoverable Reserves (MMbbl)	1.5
Gas Recoverable Reserves (BCF)	120
Initial Production (BOPD), (MCFGPD)	150 mmcfpd
Recovery Efficiency (percent)	65
Porosity (percent)	22-30
Permeability (mD)	10-1,000
Water Saturation Range (percent)	46
Initial Reservoir Temperature Range (°F)	146
Initial Reservoir Pressure Range (PSI)	5,990
API Oil Gravity	58.2 (12-52)
Gas Specific Gravity Range (at 60 and 15.025 PSI)	0.594
Pay Thickness (feet)	100 (gross)
Upper Seal	shale
Lateral Seal	shale
Reservoir Intervals (Subsea true vertical depth-feet)	11,000-18,000
Source Of Information	Abriel, 2008
	Cossey and Associates Inc.

Field Name	Raton South (Figure 30)
Block Numbers	MC 292
Partners	Noble Energy (78.87%), Stephens (21.13%)
Discovery Date	January 2007
Production Start Date	February 2012
Production Facility	Subsea tie-back to MC 292 Gemini
Water Depth (feet)	3,405
Development Status	producing
Age	late Miocene
Sedimentary deposit	channel fill- levee
Trap	stratigraphic
Liquids Recoverable Reserves (MMbbl)	7
Gas Recoverable Reserves (BCF)	10
Upper Seal	shale
Lateral Seal	shale

(D)

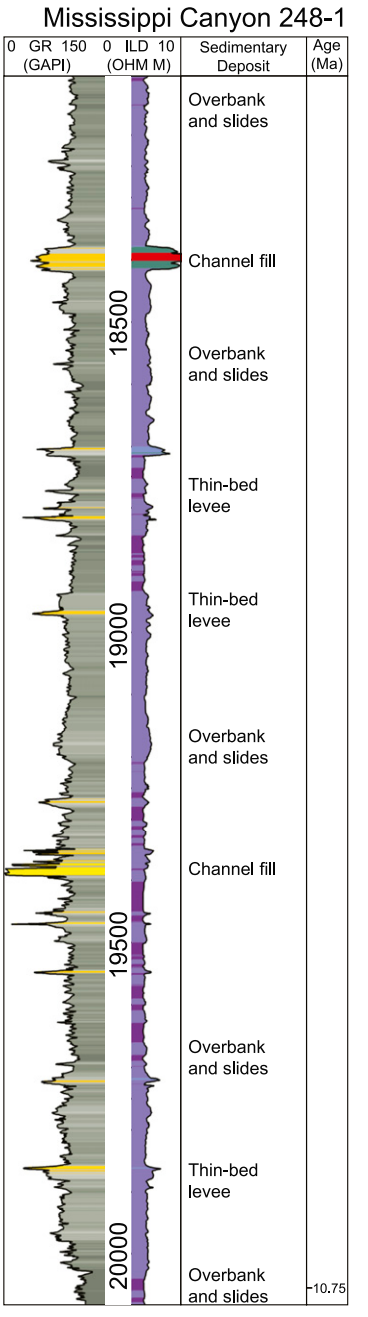

Figure 30. Continued.

Rigel Field, Figure 31

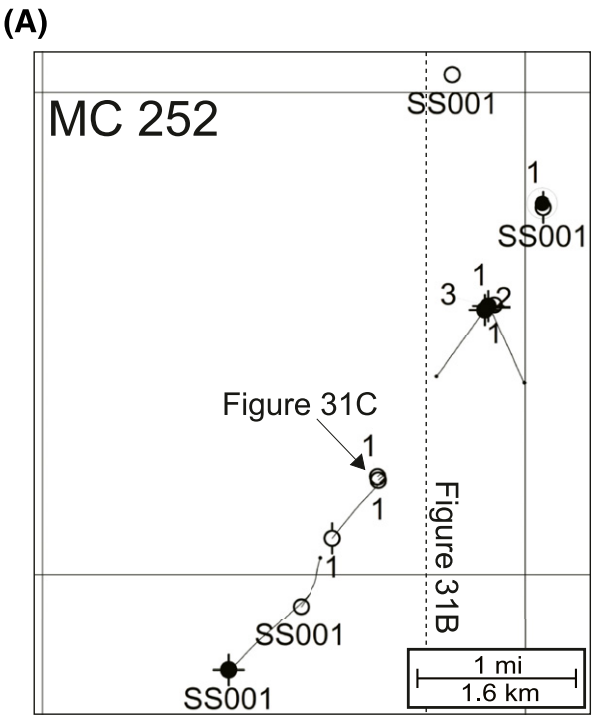

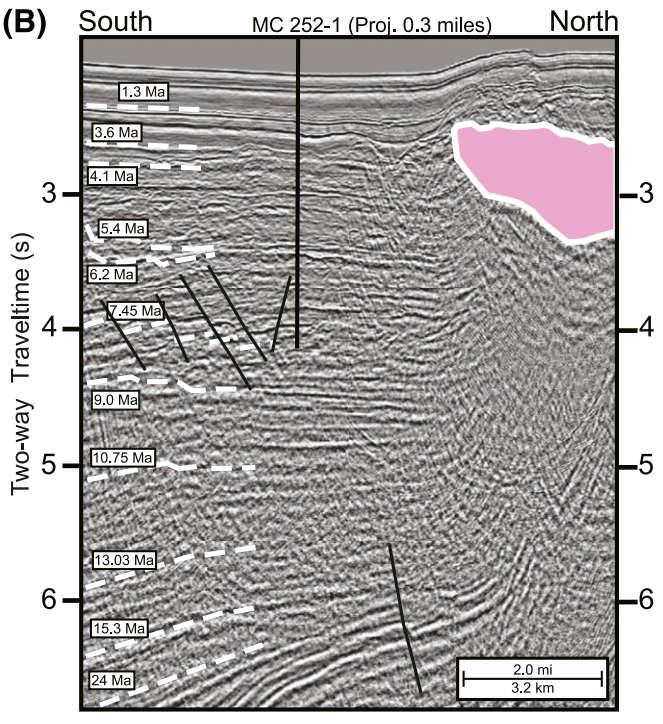

Field Name	Rigel (Figure 31)
Block Numbers	MC 252, MC 292
Partners	Eni (52.50%), Newfield Exploration (25.00%),
	Apache (22.50%)
Discovery Date	2003
Production Start Date	March 2006
Production Facility	Subsea tie-back to MC 292 Gemini
Water Depth (feet)	5229
Development Status	abandoned-2011
Number of Wells	1
Number of Reservoirs	1
Age	late Miocene
Sedimentary deposit	channel fill- levee
Trap	stratigraphic (weak structural component)
Liquids Recoverable Reserves (MMbbl)	0.057
Gas Recoverable Reserves (BCF)	74.8
Initial Production (BOPD), (MCFGPD)	10 BOPD, 32,000 MCFGPD
Gas Oil Ratio	0-320
Porosity (percent)	30-32
API Oil Gravity	42.9
Pay Thickness (feet)	135 (net)
Upper Seal	shale
Lateral Seal	shale
Reservoir Intervals (Subsea true vertical depth-feet)	11,065-11,200
Source Of Information	Cossey and Associates Inc.
	P. Wieg, pers. comm., 2010
	D. Huffman, pers. comm., 2015

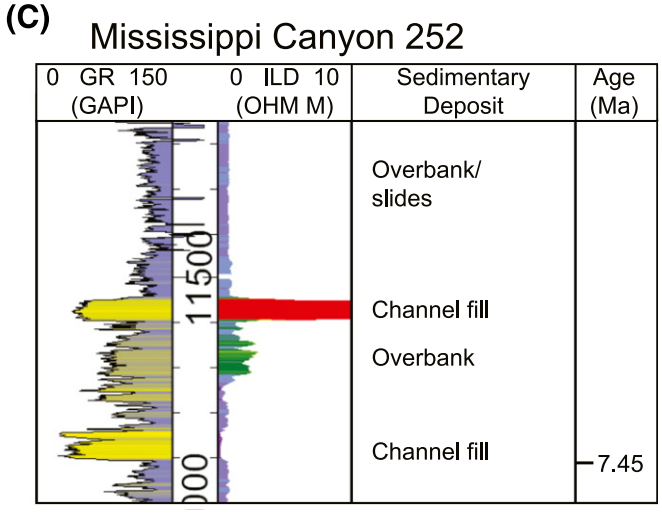

Figure 31. Mississippi Canyon (MC) 252 Rigel field. (A) Location map. (B) Seismic profile. (C) Gamma-ray (GR) and resistivity log. See Figure 4 for the regional setting of the field. ILD = deep induction.

Neidermeyer Field, Figure 32

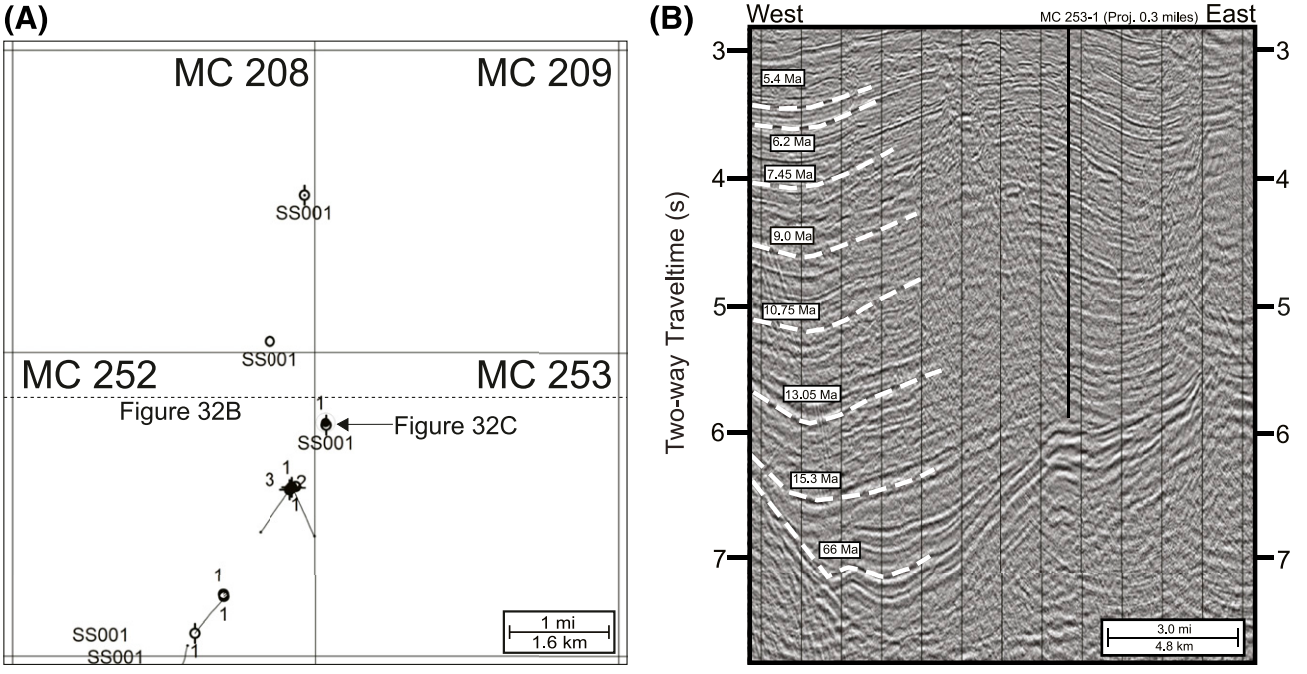

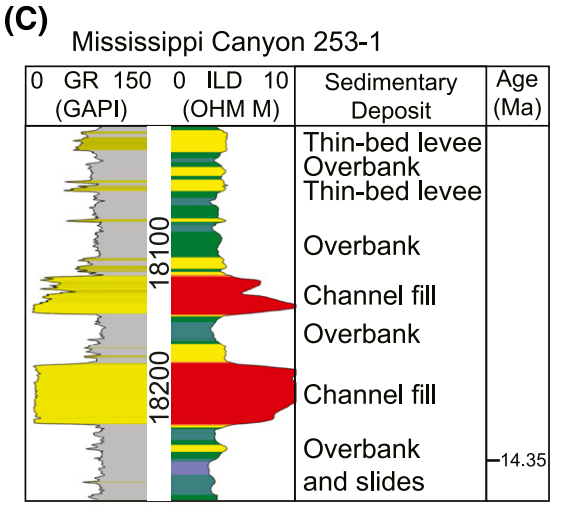

Field Name	Neidermeyer (Figure 32)
Block Numbers	MC 253, MC 209, MC 210
Partners	LLOG (52.792%) , Crux1 (16.156%), Red Willow (10.125%)
	Calypso (10.125%), ILX Prosp (10.802%),
Discovery Date	December 2012
Production Start Date	April 2015
Production Facility	Subsea tie-back to Delta House in MC 254
Water Depth (feet)	4992
Development Status	producing
Number of Wells	1
Number of Reservoirs	1
Age	middle Miocene
Sedimentary deposit	channel fill-levee
Trap	four-way closure (extensional anticline-turtle)
Initial Production (BOPD), (MCFGPD)	8,000 BOPD
Sulfur Content (percent)	0
Upper Seal	shale
Lateral Seal	shale
Source Of Information	D. Huffman, pers. comm., 2015

Figure 32. Mississippi Canyon (MC) 253 Neidermeyer field. (A) Location map. (B) Seismic profile. Reprinted with permission of Schlumberger. (C) Gamma-ray (GR) and resistivity log. See Figure 4 for the regional setting of the field. ILD = deep induction.

Marmalard Field, Figure 33

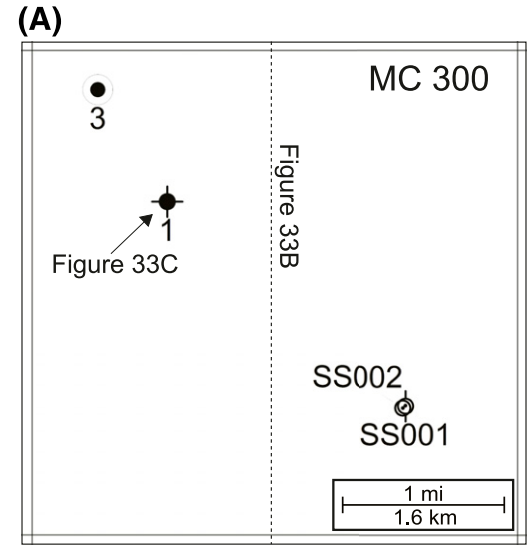

Field Name	Marmalard (Figure 33)
Block Numbers	MC 300, MC 255, MC 256
Partners	LLOG (27 %), Ridgewood Energy (23.5%), Red Willow (20.25 %),
	Deep Gulf Energy (11.7%), Calypso Exploration (10.25%), Crux (7.3%)
Discovery Date	May 2012
Production Start Date	April 2015
Production Facility	Subsea tie-back to Delta House Floating Production Unit in MC 254
Water Depth (feet)	6,148
Development Status	producing
Field Size (acres)	8,000-10,000
Number of Wells	4
Number of Reservoirs	5
Drive Mechanism	combination mostly water
Age	latest middle to early Miocene
Sedimentary deposit	channel fil
Trap	four-way closure (extensional anticline with stratigraphic component)
Initial Production (BOPD), (MCFGPD)	8,000-10,000 BOPD per well
Gas Oil Ratio	2,000
Porosity (percent)	28
Permeability (mD)	300-900
Water Saturation Range (percent)	25
API Oil Gravity	32-35
Sulfur Content (percent)	0
Pay Thickness (feet)	50-1 0 (gross)
Upper Seal	shale
Lateral Seal	shale
Reservoir Intervals (Subsea true vertical depth-feet)	17,000

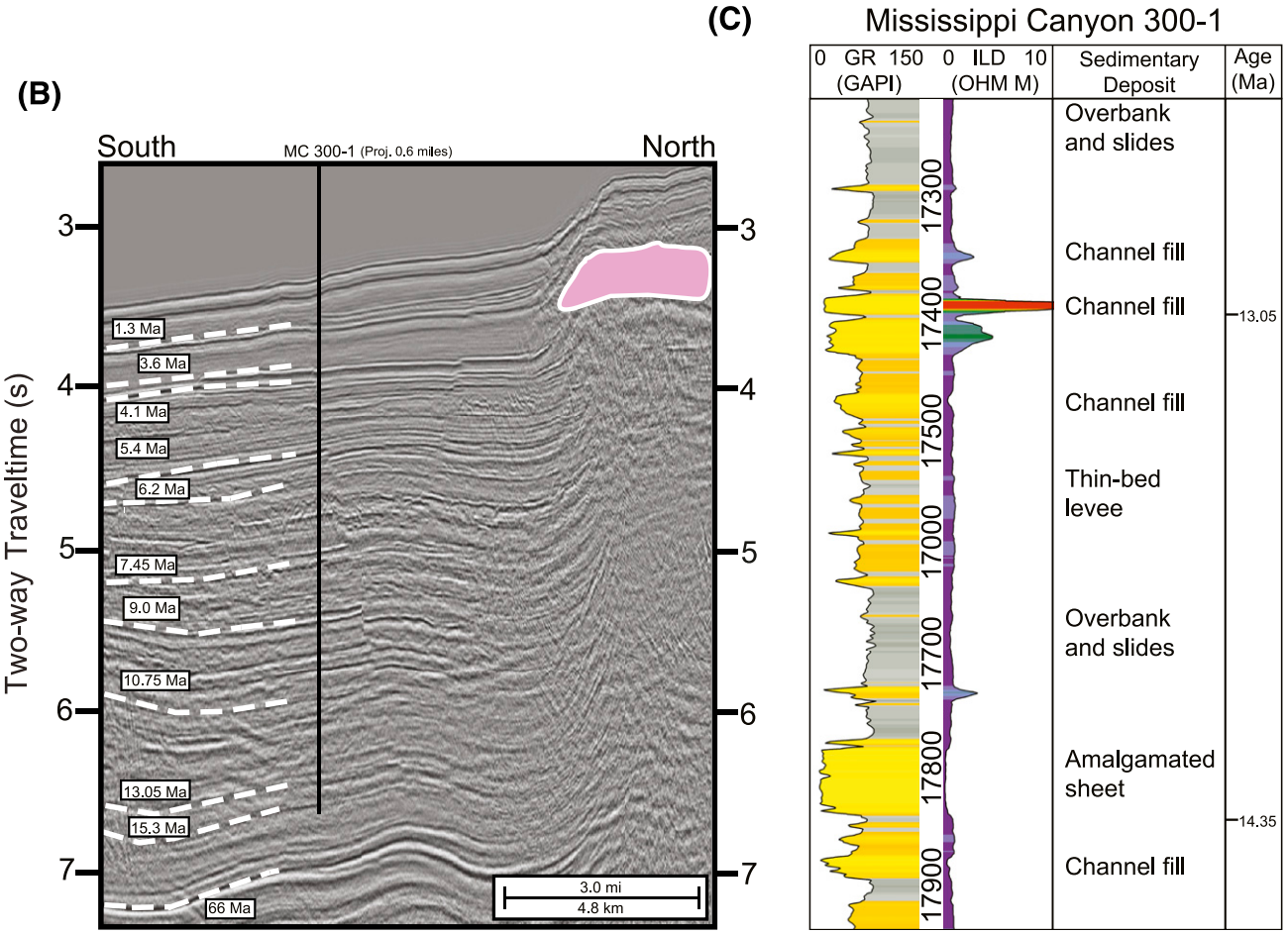

Figure 33. Mississippi Canyon (MC) 300 Marmalard field. (A) Location map. (B) Seismic profile. Reprinted with permission of Schlumberger. (C) Gamma-ray (GR) and resistivity log. See Figure 4 for the regional setting of the field. ILD = deep induction.

Aconcagua Field, Figure 34

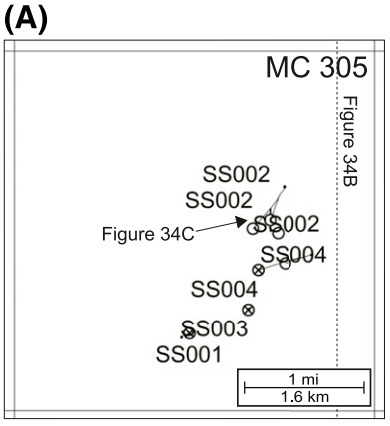

Field Name	Aconcagua (Figure 34)
Block Numbers	MC 305
Partners	Bennu (50.00%), Marubeni (37.50%)
	Nippon Oil Corporation (12.50%)
Discovery Date	January 1999
Production Start Date	September 2002
Production Facility	Subsea tie-back to Main Pass 261(Canyon Expess)
Water Depth (feet)	7,096
Development Status	abandoned-2013
Number of Wells	4
Number of Reservoirs	4
Age	late Miocene
Sedimentary deposit	channel fill
Trap	three-way closure against faults
Liquids Recoverable Reserves (MMbbl)	0.24
Gas Recoverable Reserves (BCF)	218.45
Porosity (percent)	31-33
Permeability (mD)	1,246
Initial Reservoir Temperature Range (°F)	175
Initial Reservoir Pressure Range (PSI)	6,490-6,550
API Oil Gravity	41.8 avg, (35-53 range)
Gas Specific Gravity Range (at 60 and 15.025 PSI)	0.56
Sulfur Content (percent)	1.5
Upper Seal	shale
Lateral Seal	shale
Reservoir Intervals (Subsea true vertical depth-feet)	11,200-14,000
Source Of Information	Geyelin et al., 2003
	Hare et al., 2003
	Nielsen et al., 2005
	Cossey and Associates Inc.
	Keller, 2015

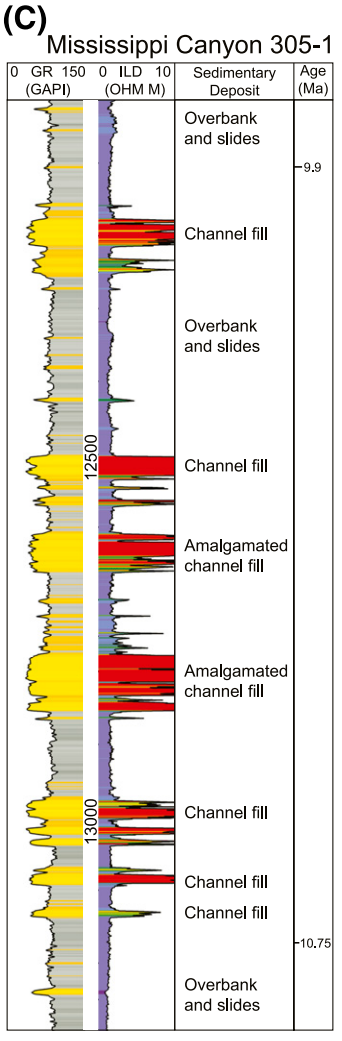

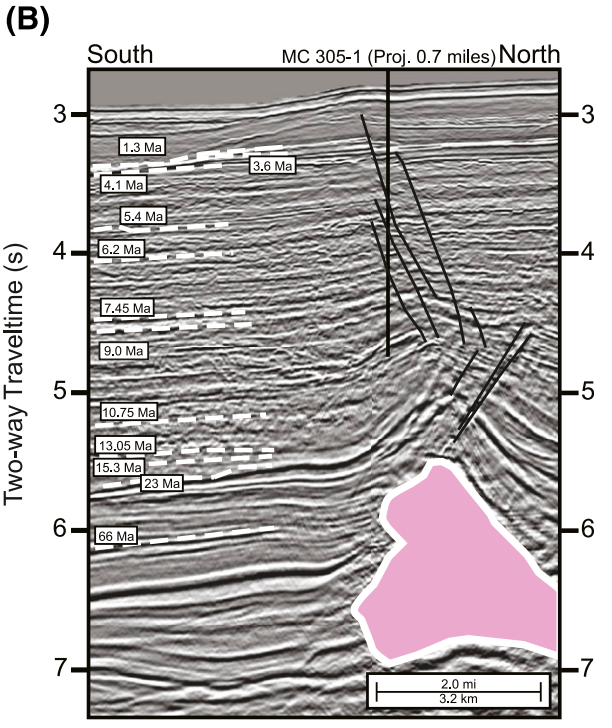

Figure 34. Mississippi Canyon (MC) 305 Aconcagua field. (A) Location map. (B) Seismic profile. Reprinted with permission of Schlumberger. (C) Gamma-ray (GR) and resistivity log. See Figure 4 for the regional setting of the field. ILD = deep induction.

Camden Hills Field, Figure 35

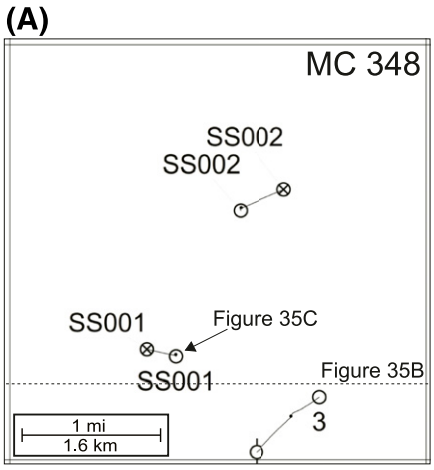

Field Name	Camden Hills (Figure 35)
Block Numbers	MC 348
Partners	Bennu (66.70%), Marubeni (33.30%)
Discovery Date	August 1999
Production Start Date	September 2002
Production Facility	Subsea tie-back to Main Pass 261(Canyon Express)
Water Depth (feet)	7,933
Development Status	abandoned-2010
Number of Wells	2
Age	middle Miocene
Sedimentary deposit	channel fill
Trap	stratigraphic
Liquids Recoverable Reserves (MMbbl)	0.15
Gas Recoverable Reserves (BCF)	120.56
Initial Reservoir Temperature Range (°F)	165
Initial Reservoir Pressure Range (PSI)	7,060-7,460
API Oil Gravity	49
Gas Specific Gravity Range (at 60 and 15.025 PSI)	0.56
Pay Thickness (feet)	203 (gross)
Upper Seal	shale
Lateral Seal	shale
Reservoir Intervals (Subsea true vertical depth-feet)	13,800-14,400
Source Of Information	Edman et al., 2001
	Wells et al., 2011
	Cossey and Associates Inc.

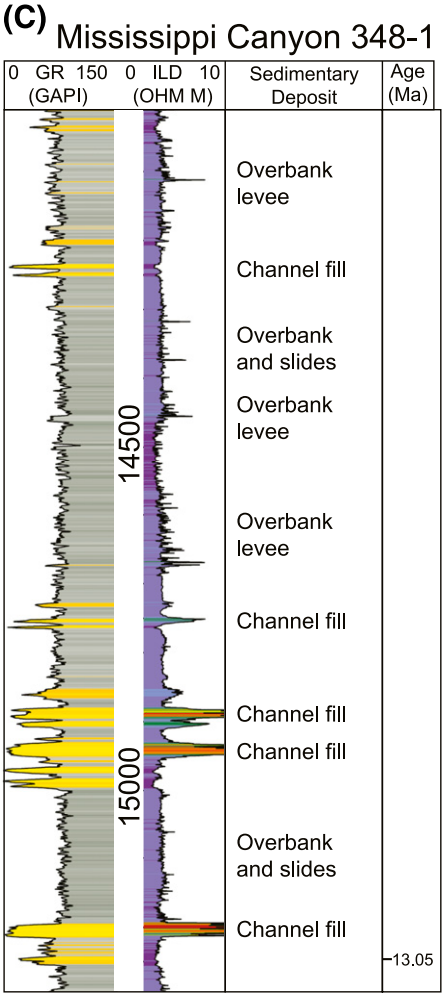

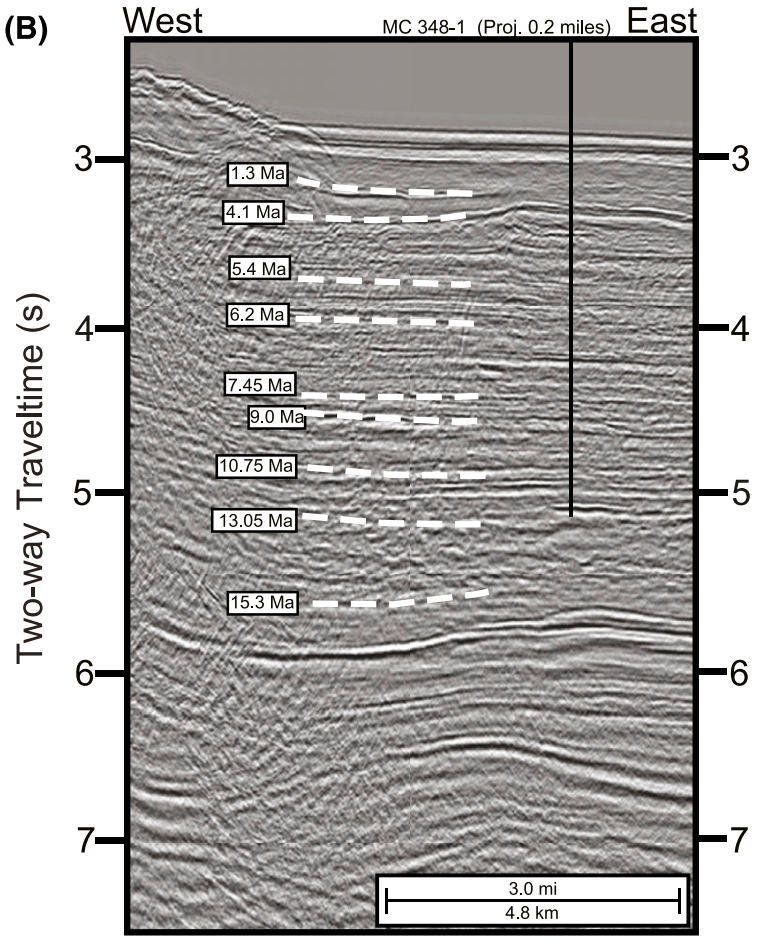

Figure 35. Mississippi Canyon (MC) 348 Camden Hills field. (A) Location map. (B) Seismic profile. Reprinted with permission of Schlumberger. (C) Gamma-ray (GR) and resistivity log. See Figure 4 for the regional setting of the field. ILD = deep induction.

Kepler Field, Figure 36

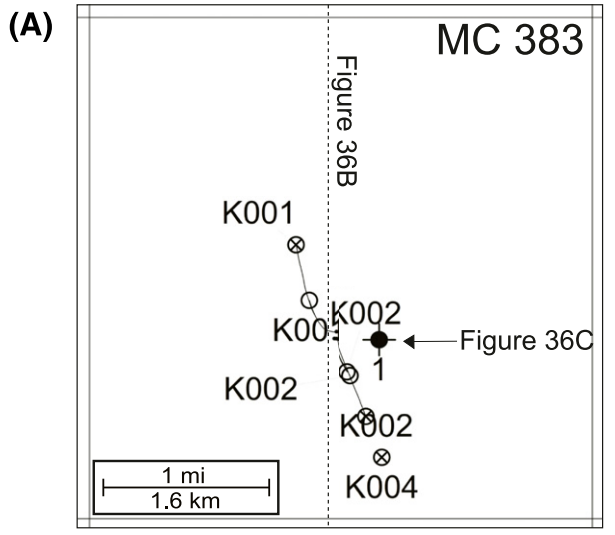

Field Name	Kepler (Figure 36)
Block Numbers	MC 383
Partners	BP (50.00%), Shell (50.00%)
Discovery Date	December 1987
Production Start Date	April 2004
Production Facility	Subsea tie-back to Na Kika in MC 474
Water Depth (feet)	5,834
Development Status	producing
Field Size (acres)	2,200
Number of Wells	2
Number of Reservoirs	3
Drive Mechanism	partial gas
Age	late Miocene
Sedimentary deposit	channel fill-sheet
Trap	stratigraphic
Liquids Recoverable Reserves (MMbbl)	50
Gas Recoverable Reserves (BCF)	60
Gas Oil Ratio	1,200
Porosity (percent)	34-35
Permeability (mD)	2000-3000
Water Saturation Range (percent)	17-19
Initial Reservoir Temperature Range (°F)	117-130
API Oil Gravity	29
Viscosity (centipoise)	1.1
Pay Thickness (feet)	50 (gross)
Upper Seal	shale
Lateral Seal	shale
Reservoir Intervals (Subsea true vertical depth-feet)	12,130-12,180 , 12,020-12,070
Source Of Information	Rajasingam and Freckelton, 2004
	Schott et al., 2007
	Cossey and Associates Inc.

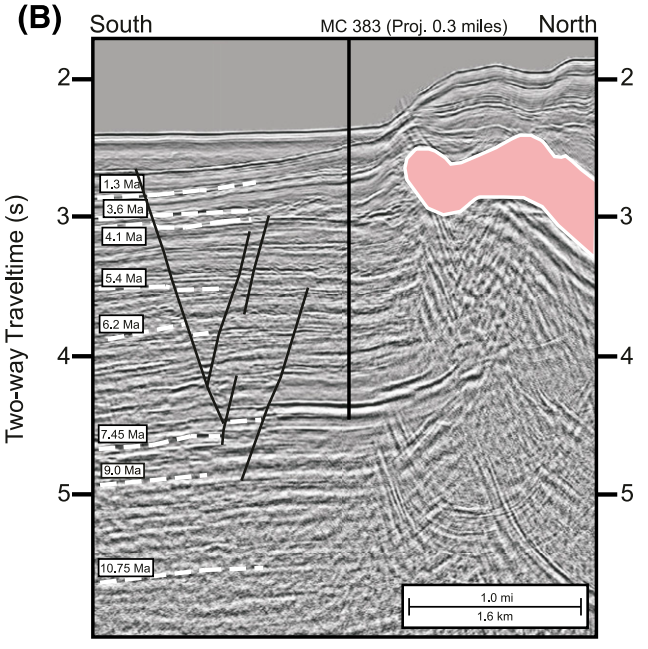

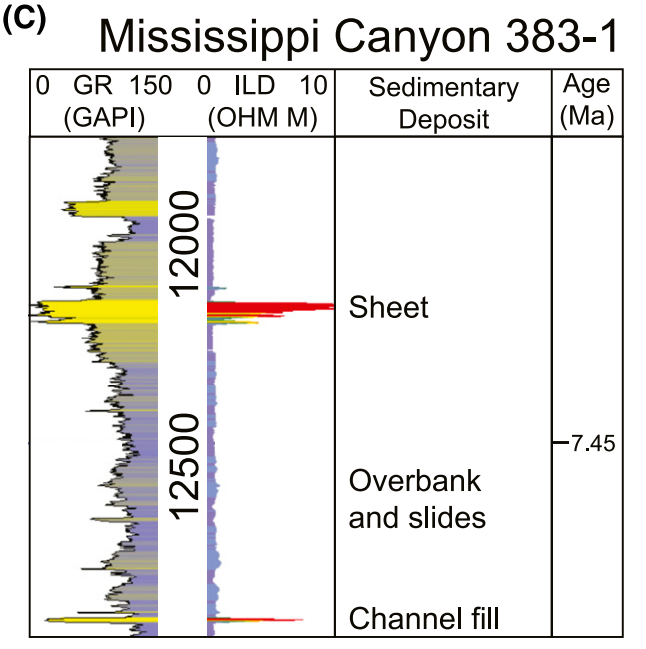

Figure 36. Mississippi Canyon (MC) 383 Kepler field. (A) Location map. (B) Seismic profile. Reprinted with permission of Schlumberger. (C) Gamma-ray (GR) and resistivity log. See Figure 4 for the regional setting of the field. ILD = deep induction.

Appomattox Field, Figure 37

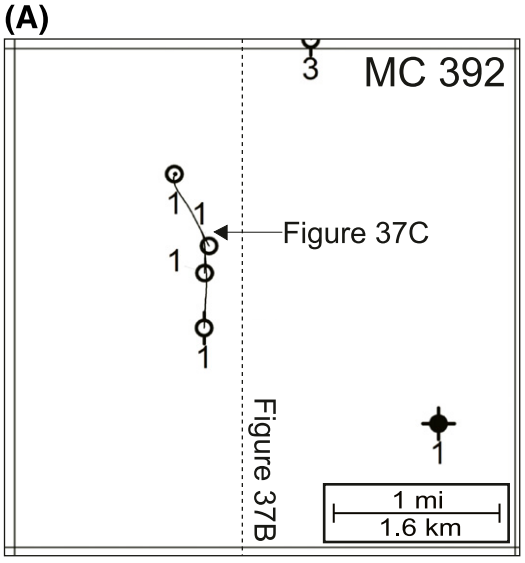

Field Name	Appomattox (Figure 37)
Block Numbers	MC 391, MC 392
Partners	Shell (80%) , Nexen (20%)
Discovery Date	December 2009
Production Start Date	2020 (Projected)
Production Facility	Subsea-tieback to Appomattox Hub in MC 437
Water Depth (feet)	7,333
Development Status	under evaluation
Number of Wells	1
Number of Reservoirs	2
Age	Late Jurassic
Sedimentary deposit	eolian
Trap	three-way closure against fault
Liquids Recoverable Reserves (MMbbl)	120-370
Gas Recoverable Reserves (BCF)	512
Gas Oil Ratio	1,250
Pay Thickness (feet)	530 (net)
Upper Seal	shale
Lateral Seal	shale
Reservoir Intervals (Subsea true vertical depth-feet)	27,775

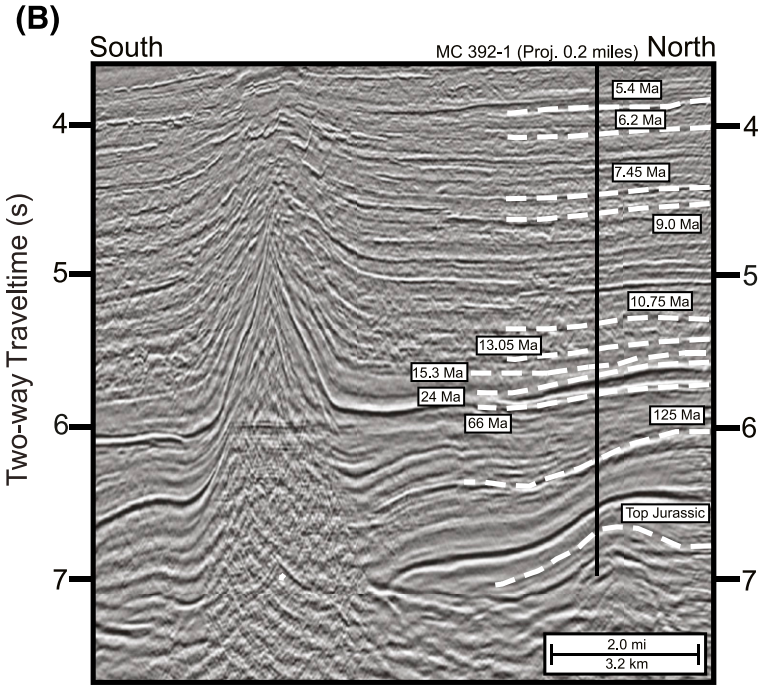

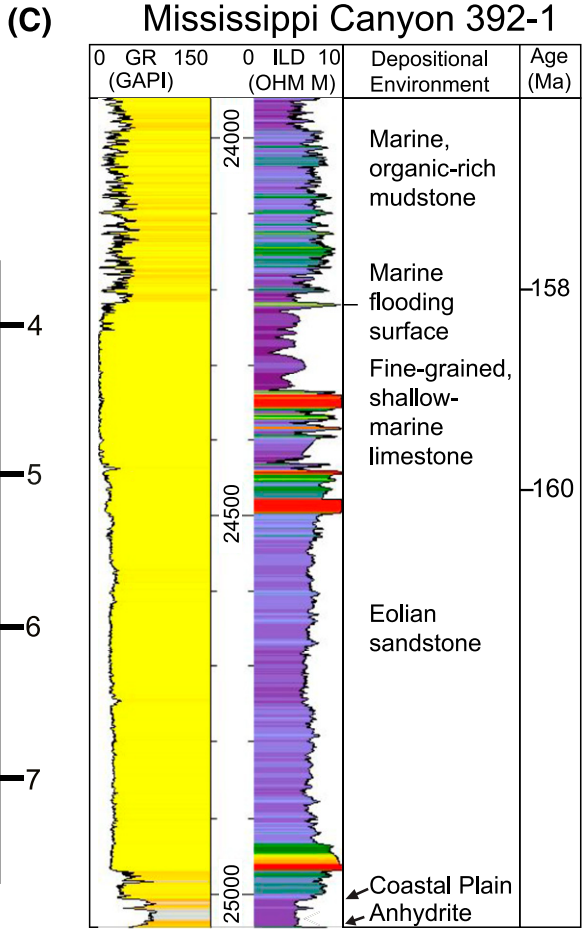

Figure 37. Mississippi Canyon (MC) 392 Appomattox field. (A) Location map of MC 392 Appomattox field. (B) Seismic profile. Reprinted with permission of Schlumberger. (C) Gamma-ray (GR) and resistivity log. See Figure 4 for the regional setting of the field. ILD = deep induction.

La Femme Field, Figure 38

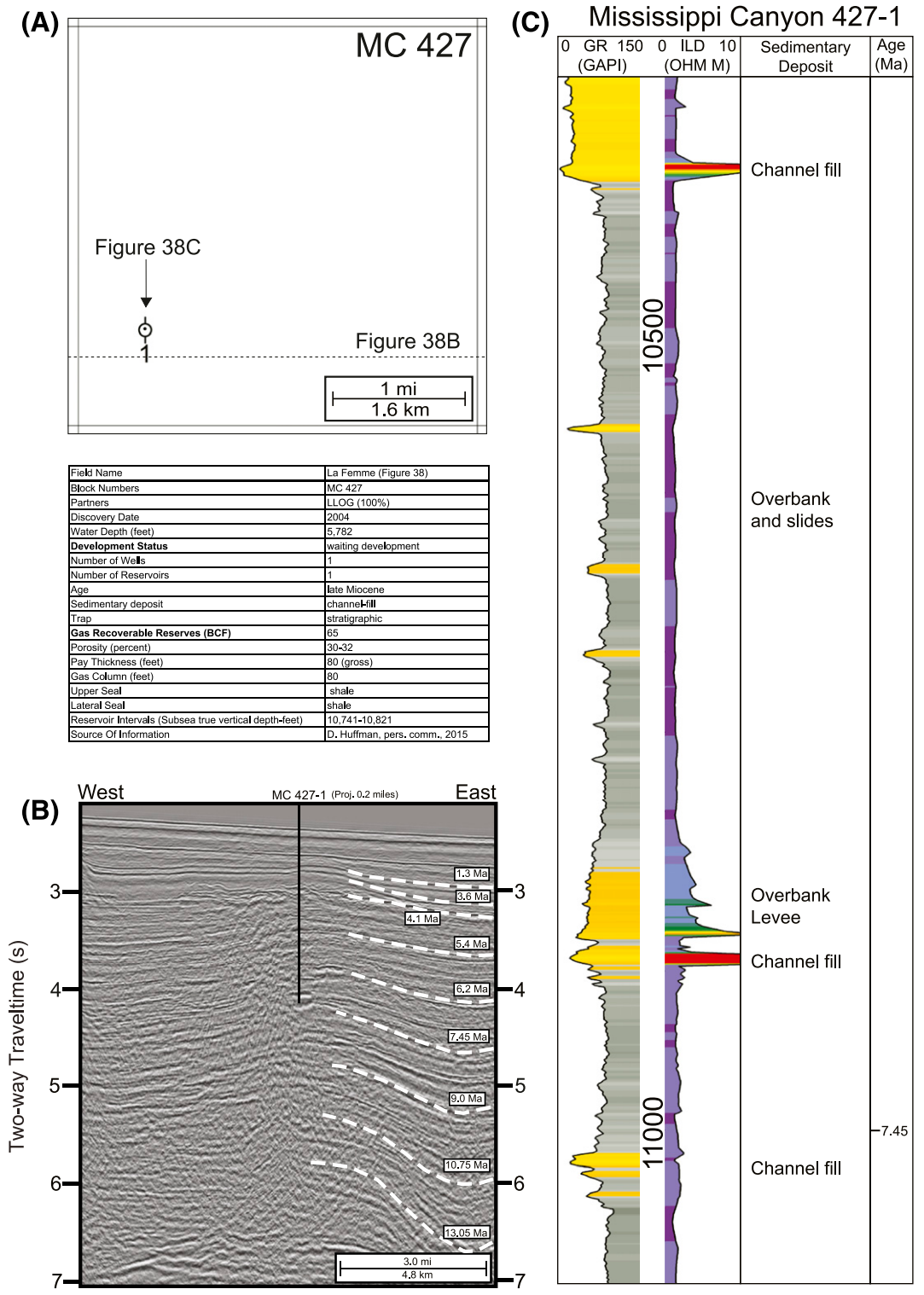

Field Name	La Femme (Figure 38)
Block Numbers	MC 427
Partners	LLOG (100%)
Discovery Date	2004
Water Depth (feet)	5,782
Development Status	waiting development
Number of Wells	1
Number of Reservoirs	1
Age	late Miocene
Sedimentary deposit	channel-fill
Trap	stratigraphic
Gas Recoverable Reserves (BCF)	65
Porosity (percent)	30-32
Pay Thickness (feet)	80 (gross)
Gas Column (feet)	80
Upper Seal	shale
Lateral Seal	shale
Reservoir Intervals (Subsea true vertical depth-feet)	10,741-10,821
Source Of Information	D. Huffman, pers. comm., 2015

Figure 38. Mississippi Canyon (MC) 427 La Femme field. (A) Location map. (B) Seismic profile. Reprinted with permission of Schlumberger. (C) Gamma-ray (GR) and resistivity log. See Figure 4 for the regional setting of the field. ILD = deep induction.

Ariel Field, Figure 39

(A)

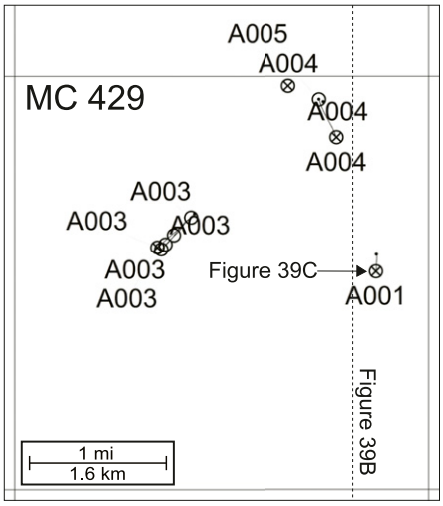

Field Name	Ariel (Figure 39)
Block Numbers	MC 429
Partners	BP (50.00%), Shell (50.00%)
Discovery Date	June 1995
Production Start Date	November 2003
Production Facility	Subsea tie-back to Na Kika in MC 474
Water Depth (feet)	6,171
Development Status	producing
Number of Wells	5
Number of Reservoirs	4
Age	late Miocene
Sedimentary deposit	channel fill- levee
Trap	three-way closure against fault-stratigraphic
Liquids Recoverable Reserves (MMbbl)	80
Gas Recoverable Reserves (BCF)	115
Gas Oil Ratio	800
Initial Reservoir Pressure Range (PSI)	7,380
API Oil Gravity	27.9
Upper Seal	shale
Lateral Seal	shale
Reservoir Intervals (Subsea true vertical depth-feet)	12,000-12,900
Source Of Information	Rajasingam and Freckelton, 2004
	Cossey and Associates Inc.
	Salunke and Hamman, 2015

(B)

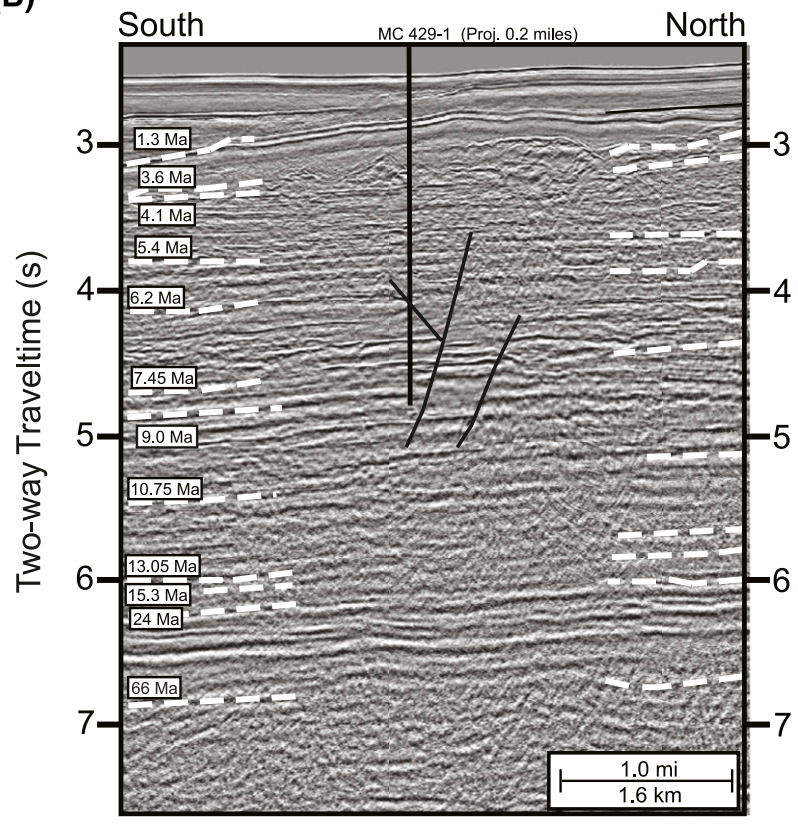

(C)

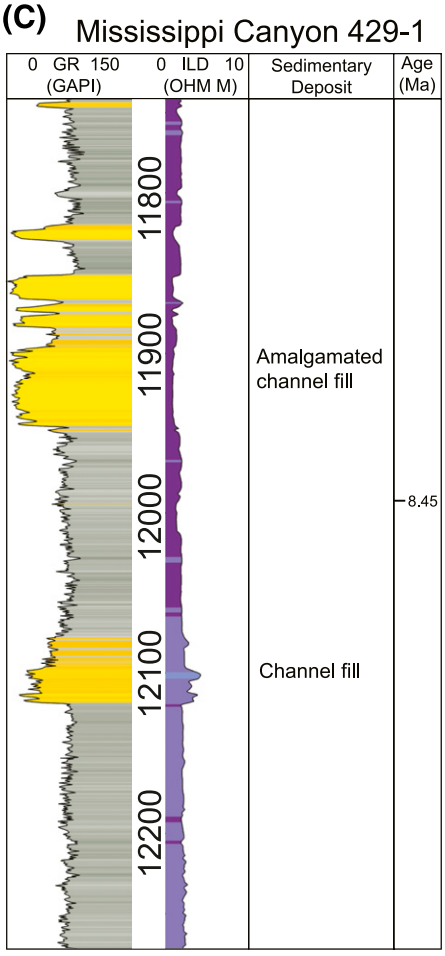

Figure 39. Mississippi Canyon (MC) 429 Ariel field. (A) Location map. (B) Seismic profile. Reprinted with permission of Schlumberger. (C) Gamma-ray (GR) and resistivity log. See Figure 4 for the regional setting of the field. ILD = deep induction.

Son of Bluto 2 Field, Figure 40

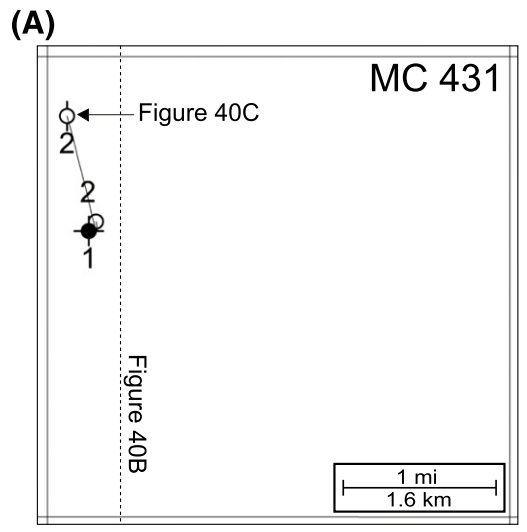

Field Name	Son of Bluto 2 (Figure 40)
Block Numbers	MC 431
Partners	LLOG (27 %), Ridgewood Energy (23.5%), Red Willow (20.25 %),
	Deep Gulf (11.825%), Calypso (10.125), Cruz (7.3%)
Discovery Date	March 2012
Production Start Date	July 2015
Production Facility	Subsea tie-back to Delta House in MC 254
Water Depth (feet)	6461
Development Status	producing
Field Size (acres)	2,000
Number of Wells	5
Number of Reservoirs	2
Drive Mechanism	water
Age	late Miocene
Sedimentary deposit	channel fill
Trap	stratigraphic
Gas Oil Ratio	1,200
Porosity (percent)	28
Permeability (mD)	800
Sulfur Content (percent)	0
Pay Thickness (feet)	40 (Net)
Oil Column (feet)	800-1,000
Upper Seal	shale
Lateral Seal	shale
Source Of Information	Zimmerman et al., 2015

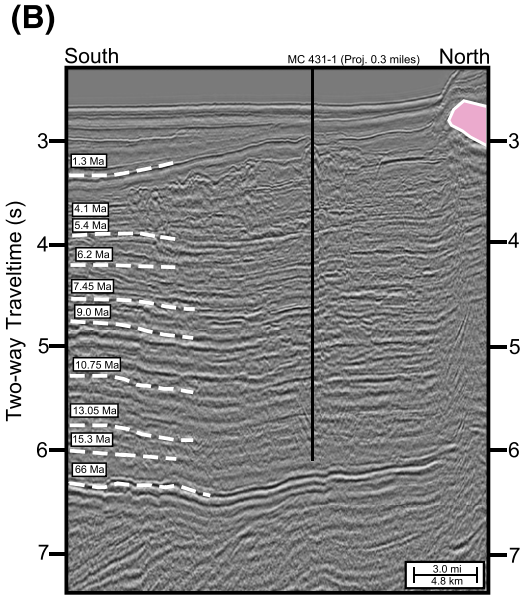

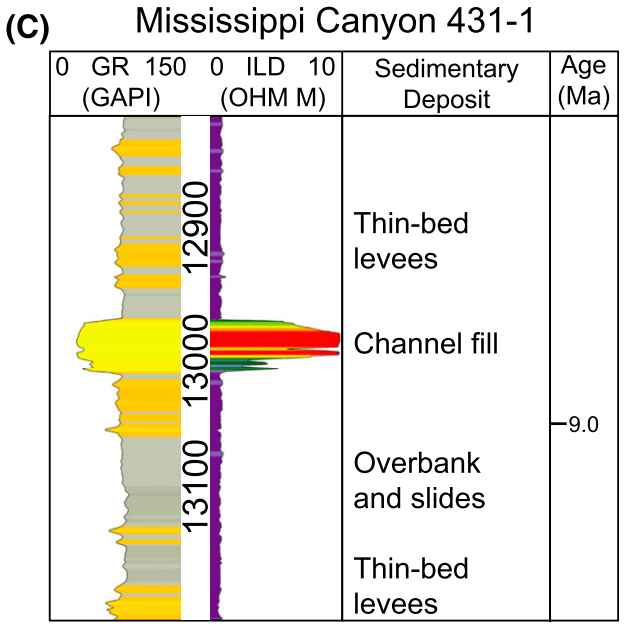

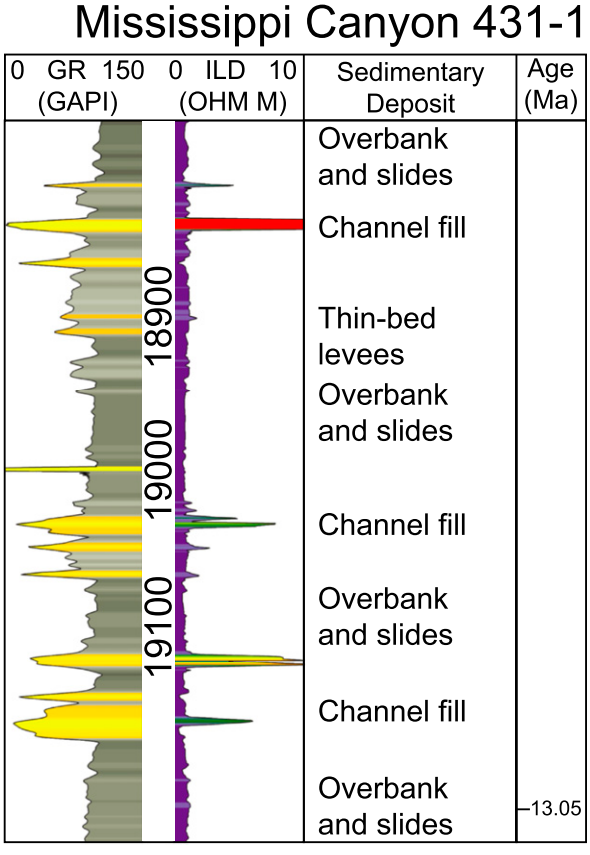

Figure 40. Mississippi Canyon (MC) 431 Son of Bluto II field. (A) Location map. (B) Seismic profile. Reprinted with permission of Schlumberger. (C) Gamma-ray (GR) and resistivity log. See Figure 4 for the regional setting of the field. ILD = deep induction.

Appaloosa Field, Figure 41

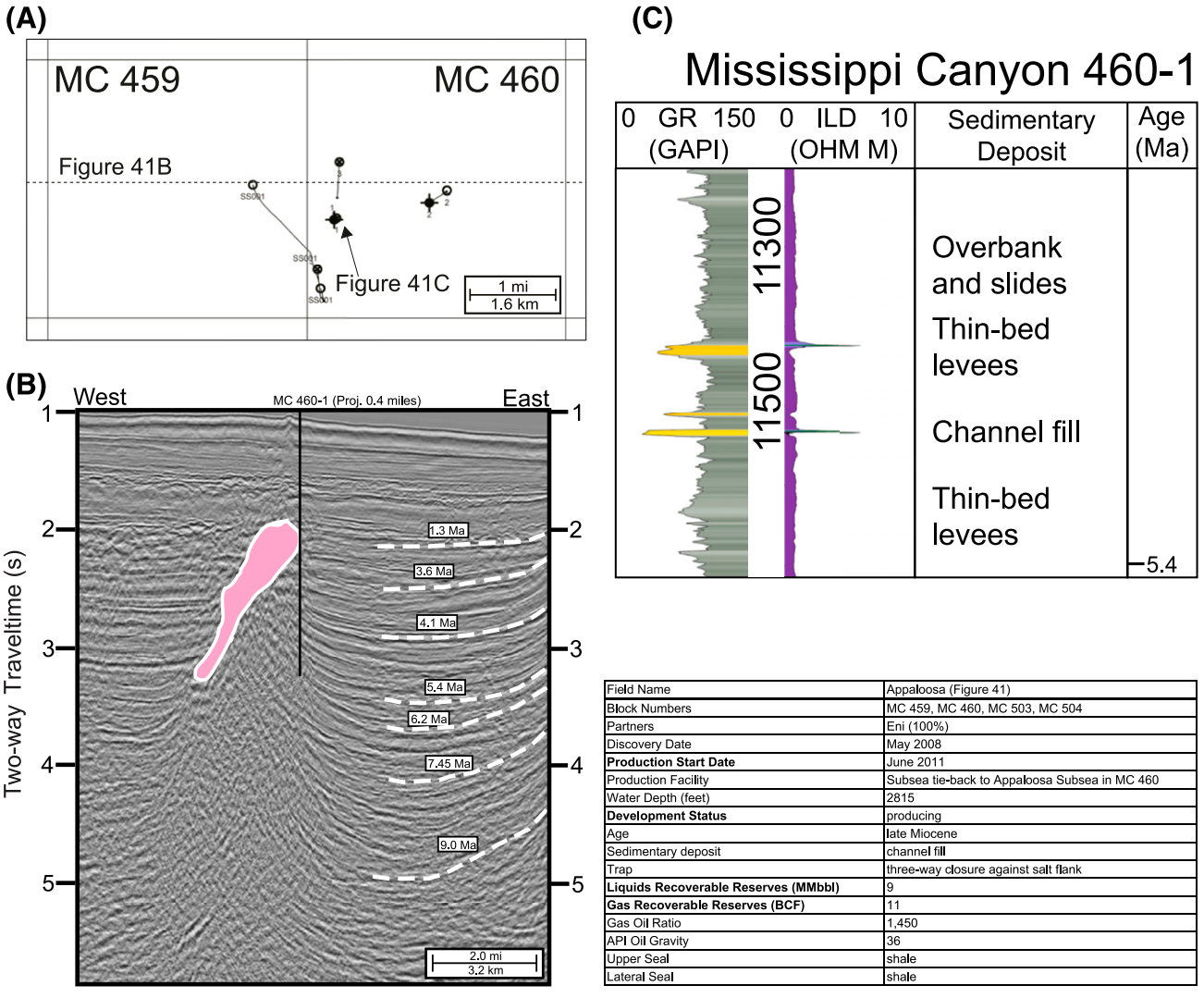

Field Name	Appaloosa (Figure 41)
Block Numbers	MC 459, MC 460, MC 503, MC 504
Partners	Eni (100%)
Discovery Date	May 2008
Production Start Date	June 2011
Production Facility	Subsea tie-back to Appaloosa Subsea in MC 460
Water Depth (feet)	2815
Development Status	producing
Age	late Miocene
Sedimentary deposit	channel fill
Trap	three-way closure against salt flank
Liquids Recoverable Reserves (MMbbl)	9
Gas Recoverable Reserves (BCF)	11
Gas Oil Ratio	1,450
API Oil Gravity	36
Upper Seal	shale
Lateral Seal	shale

Figure 41. Mississippi Canyon (MC) 460 Appaloosa field. (A) Location map. (B) Seismic profile. Reprinted with permission of Schlumberger. (C) Gamma-ray (GR) and resistivity log. See Figure 4 for the regional setting of the field. ILD = deep induction.

Longhorn-Longhorn North Field, Figure 42

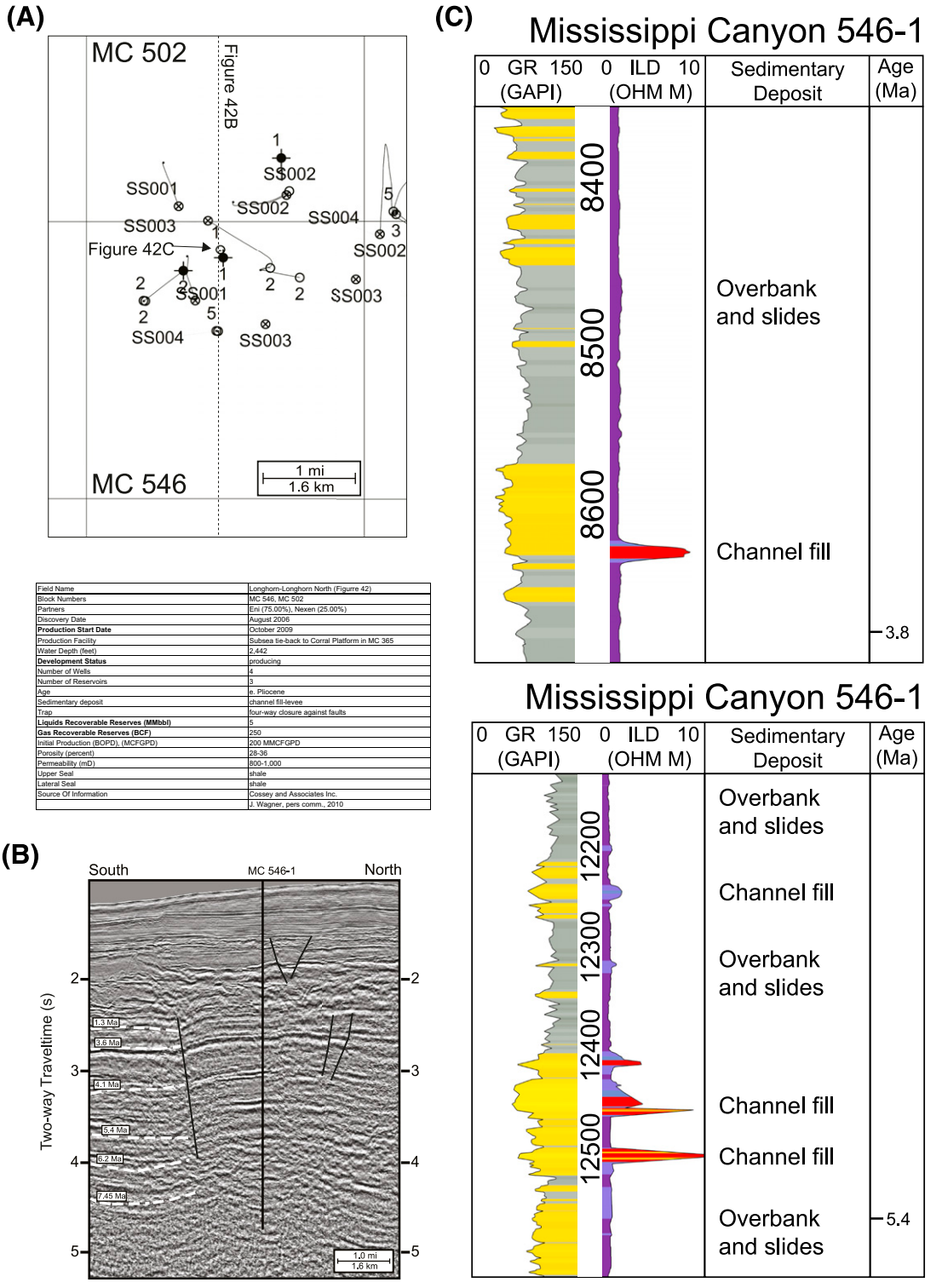

Field Name	Longhorn-Longhorn North (Figurre 42)
Block Numbers	MC 546, MC 502
Partners	Eni (75.00%), Nexen (25.00%)
Discovery Date	August 2006
Production Start Date	October 2009
Production Facility	Subsea tie-back to Corral Platform in MC 365
Water Depth (feet)	2,442
Development Status	producing
Number of Wells	4
Number of Reservoirs	3
Age	e. Pliocene
Sedimentary deposit	channel fill-levee
Trap	four-way closure against faults
Liquids Recoverable Reserves (MMbbl)	5
Gas Recoverable Reserves (BCF)	250
Initial Production (BOPD), (MCFGPD)	200 MMCFGPD
Porosity (percent)	28-36
Permeability (mD)	800-1,000
Upper Seal	shale
Lateral Seal	shale
Source Of Information	Cossey and Associates Inc.
	J. Wagner, pers comm., 2010

Figure 42. Mississippi Canyon (MC) 502 Longhorn North and 546 Longhorn field. (A) Location map. (B) Seismic profile. Reprinted with permission of Schlumberger. (C) Gamma-ray (GR) and resistivity log. See Figure 4 for the regional setting of the field. ILD = deep induction.

Who Dat Field, Figure 43

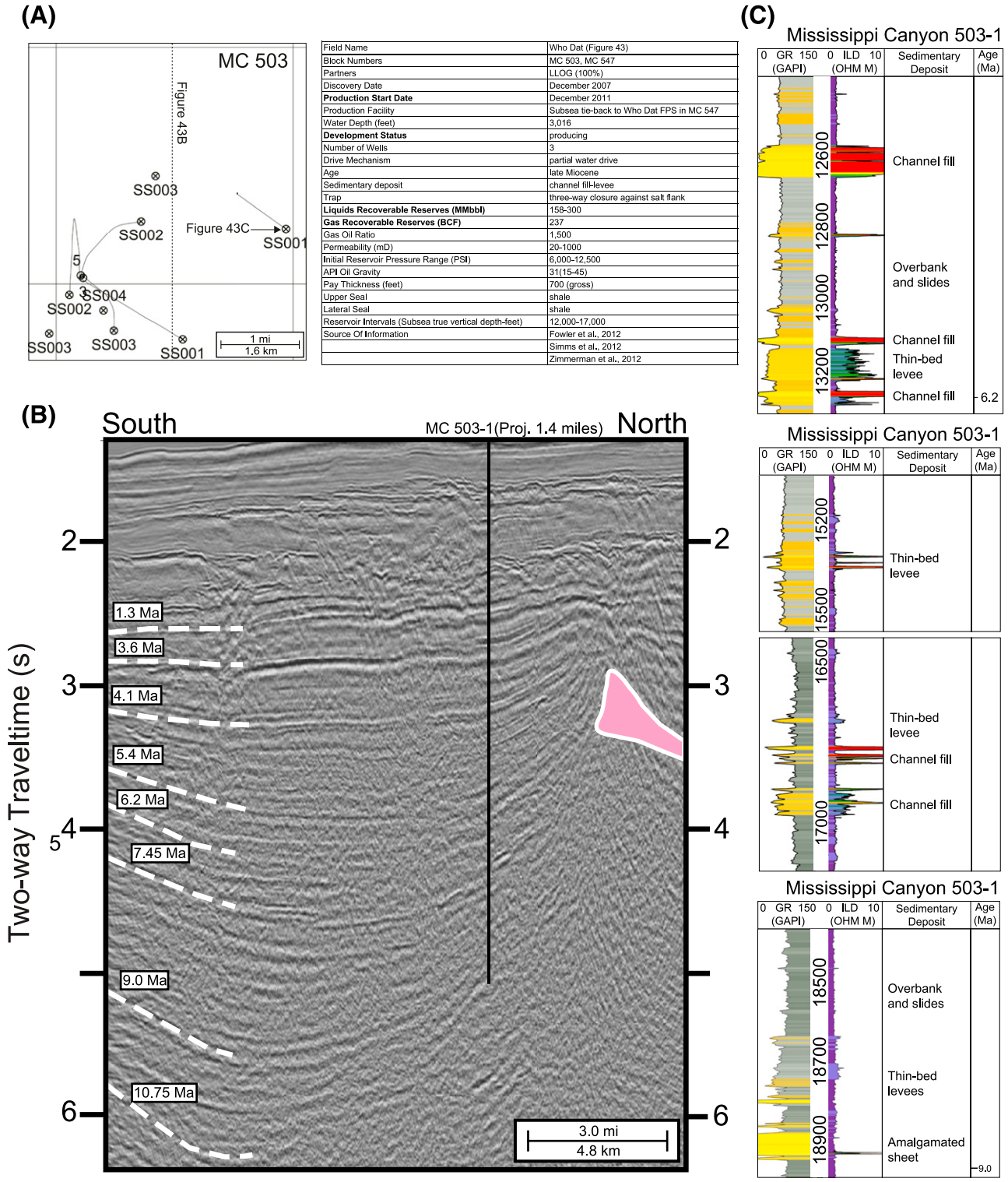

Field Name	Who Dat (Figure 43)
Block Numbers	MC 503, MC 547
Partners	LLOG (100%)
Discovery Date	December 2007
Production Start Date	December 2011
Production Facility	Subsea tie-back to Who Dat FPS in MC 547
Water Depth (feet)	3,016
Development Status	producing
Number of Wells	3
Drive Mechanism	partial water drive
Age	late Miocene
Sedimentary deposit	channel fill-levee
Trap	three-way closure against salt flank
Liquids Recoverable Reserves (MMbbl)	158-300
Gas Recoverable Reserves (BCF)	237
Gas Oil Ratio	1,500
Permeability (mD)	20-1000
Initial Reservoir Pressure Range (PSI)	6,000-12,500
API Oil Gravity	31(15-45)
Pay Thickness (feet)	700 (gross)
Upper Seal	shale
Lateral Seal	shale
Reservoir Intervals (Subsea true vertical depth-feet)	12,000-17,000
Source Of Information	Fowler et al,. 2012
	Simms et al., 2012
	Zimmerman et al., 2012

Figure 43. Mississippi Canyon (MC) 503 Who Dat field. (A) Location map. (B) Seismic profile. (C) Gamma-ray (GR) and resistivity log. Reprinted with permission of Schlumberger. See Figure 4 for the regional setting of the field. ILD = deep induction.

Wrigley Field, Figure 44

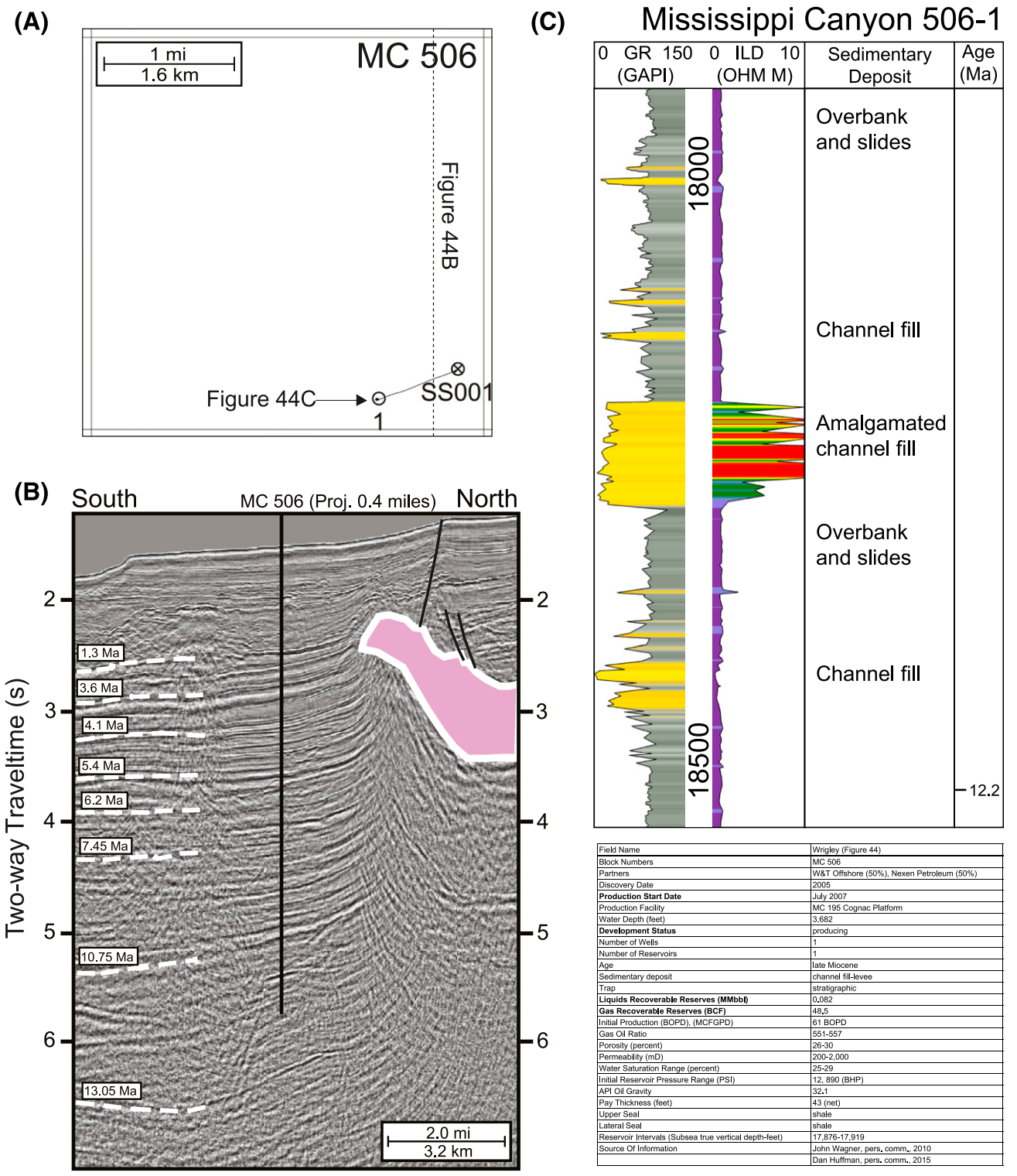

Field Name	Wrigley (Figure 44)
Block Numbers	MC 506
Partners	W&T Offshore (50%), Nexen Petroleum (50%)
Discovery Date	2005
Production Start Date	July 2007
Production Facility	MC 195 Cognac Platform
Water Depth (feet)	3,682
Development Status	producing
Number of Wells	1
Number of Reservoirs	1
Age	late Miocene
Sedimentary deposit	channel fill-levee
Trap	stratigraphic
Liquids Recoverable Reserves (MMbbl)	0,082
Gas Recoverable Reserves (BCF)	48,5
Initial Production (BOPD), (MCFGPD)	61 BOPD
Gas Oil Ratio	551-557
Porosity (percent)	26-30
Permeability (mD)	200-2,000
Water Saturation Range (percent)	25-29
Initial Reservoir Pressure Range (PSI)	12, 890 (BHP)
API Oil Gravity	32,1
Pay Thickness (feet)	43 (net)
Upper Seal	shale
Lateral Seal	shale
Reservoir Intervals (Subsea true vertical depth-feet)	17,876-17,919
Source Of Information	John Wagner, pers. comm., 2010
	Dan Huffman, pers. comm., 2015

Figure 44. Mississippi Canyon (MC) 506 Wrigley field. (A) Location map. (B) Seismic profile. Reprinted with permission of Schlumberger. (C) Gamma-ray (GR) and resistivity log. See Figure 4 for the regional setting of the field. ILD = deep induction.

Santiago-Santa Cruz Field, Figure 45

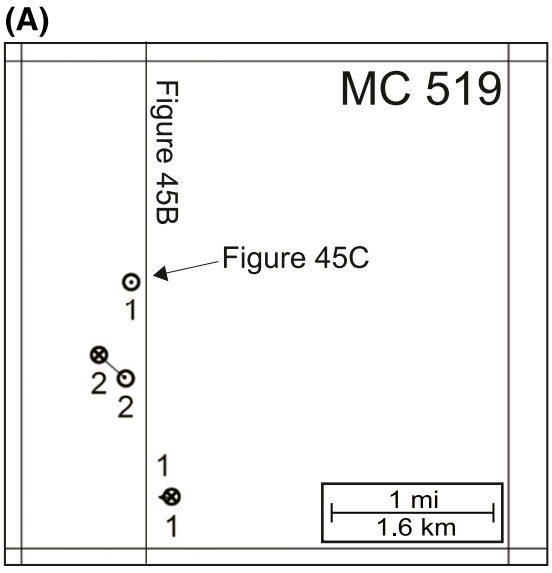

Field Name	Santiago-Santa Cruz (Figure 45)
Block Numbers	MC 519, MC 563
Partners	BP (46..50%) Noble (23.25%)
	Red Willow Production (20.25%)
	Houston Energy (10%)
	Note: these two fields are accumulations on the
	north side (Santiago), and soutside (Santa Cruz)
	of a fault,
Discovery Date	May 2011 (Santiago), March 2009 (Santa Cruz)
Production Start Date	June 2012
Production Facility	Subsea to tie-back to Na Kika in MC 474
Water Depth (feet)	6,541
Development Status	producing
Number of Wells	3
Age	middle Miocene
Sedimentary deposit	channel fill
Trap	three-way closure against fault
Liquids Recoverable Reserves (MMbbl)	65
Gas Recoverable Reserves (BCF)	46
Gas Oil Ratio	700
API Oil Gravity	28-32
Oil Column (feet)	110
Gas Column (feet)	140
Upper Seal	shale
Lateral Seal	shale

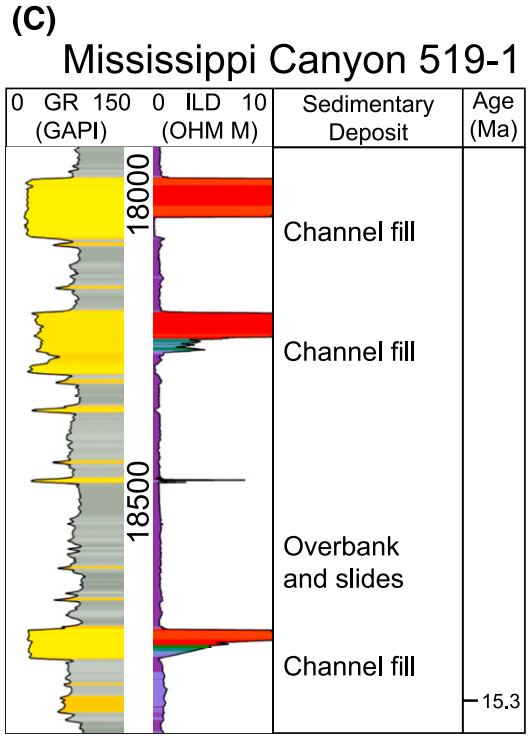

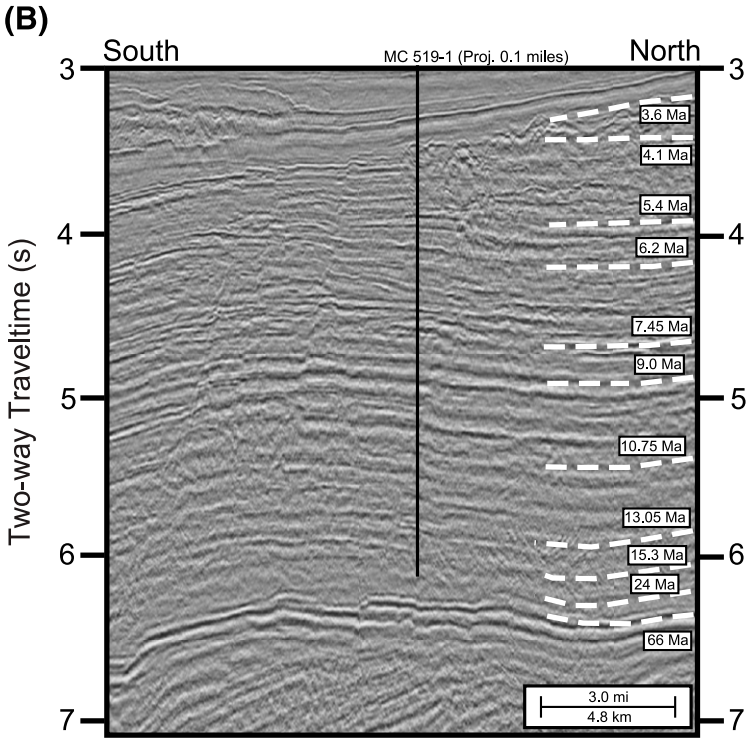

Figure 45. Mississippi Canyon (MC) 519–520 Santiago–Santa Cruz field. Note: The Santiago field was discovered in 2009. Santa Cruz is the downdip extension of the reservoir across the fault that was drilled in 2011. (A) Location map of MC 519–520 Santiago–Santa Cruz field. Also shown are the locations for (B) and (C). (B) Seismic profile across the MC 519–520 Santiago–Santa Cruz field. Reprinted with permission of Schlumberger. (C) Gamma-ray (GR) and resistivity log from the MC 519-1. See Figure 4 for the regional setting of the field. ILD = deep induction.

Herschel Field, Figure 46

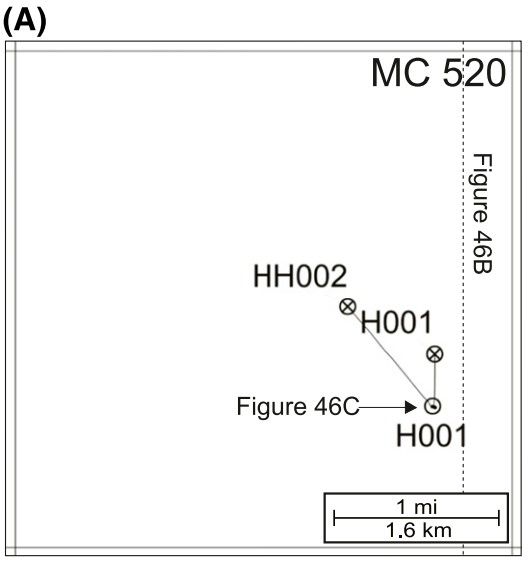

Field Name	Herschel (Figure 46)
Block Numbers	MC 520
Partners	BP (50.00%), Shell (50.00%)
Discovery Date	June 1996
Production Start Date	December 2003
Production Facility	Subsea to tie-back to Na Kika in MC 474
Water Depth (feet)	6841
Development Status	producing
Number of Wells	1
Number of Reservoirs	1
Age	middle Miocene
Sedimentary deposit	Amalgamated sheet overlying levee-thin beds
Trap	three-way closure against fault
Liquids Recoverable Reserves (MMbbl)	30
Gas Recoverable Reserves (BCF)	25
Initial Production (BOPD), (MCFGPD)	oil
Gas Oil Ratio	987
API Oil Gravity	26.7
Upper Seal	shale
Lateral Seal	shale

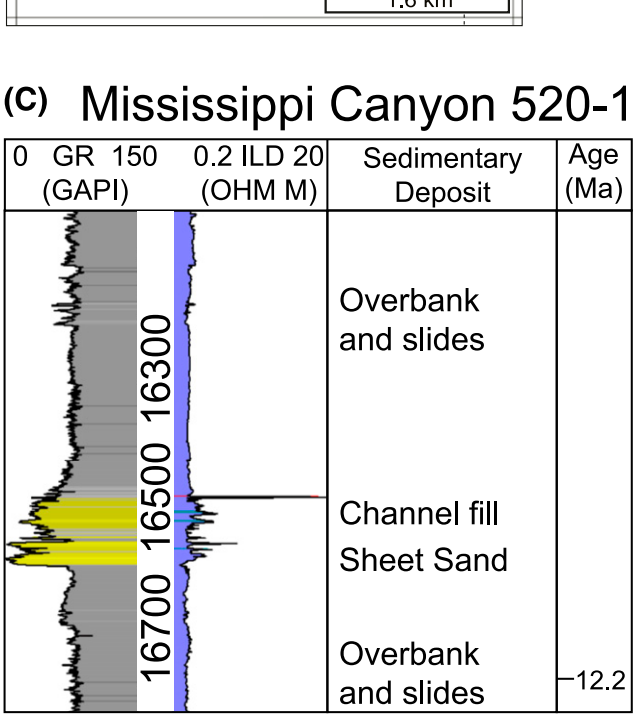

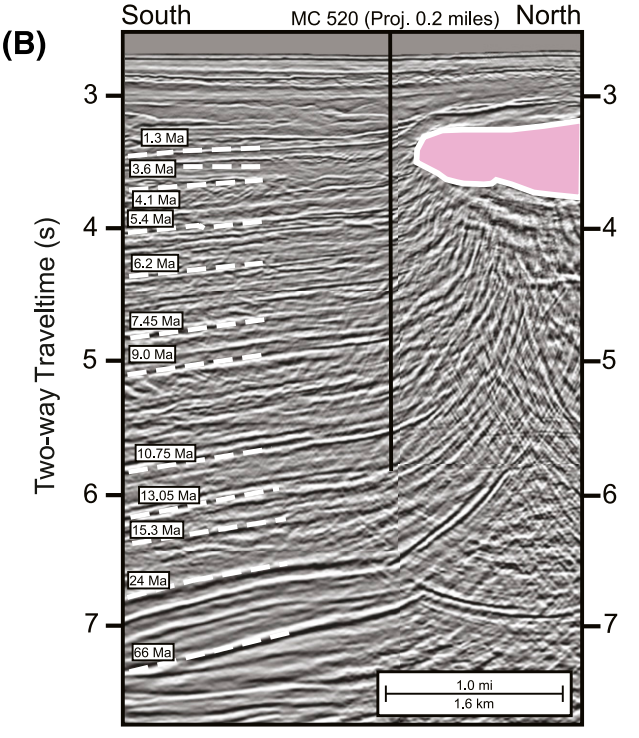

Figure 46. Mississippi Canyon (MC) 520 Herschel field. (A) Location map. (B) Seismic profile. Reprinted with permission of Schlumberger. (C) Gamma-ray (GR) and resistivity log. See Figure 4 for the regional setting of the field. ILD = deep induction.

Fourier Field, Figure 47

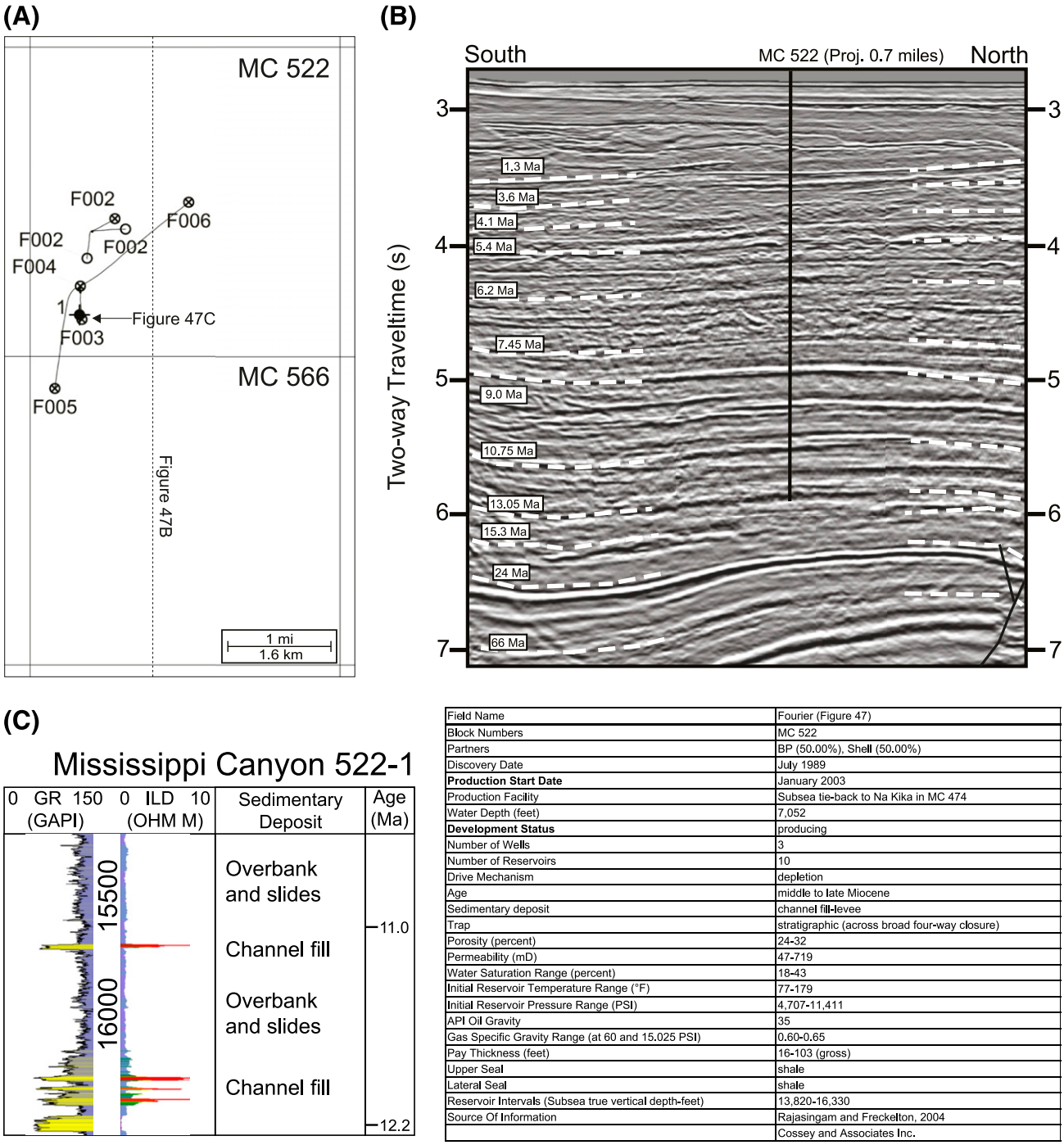

Field Name	Fourier (Figure 47)
Block Numbers	MC 522
Partners	BP (50.00%), Shell (50.00%)
Discovery Date	July 1989
Production Start Date	January 2003
Production Facility	Subsea tie-back to Na Kika in MC 474
Water Depth (feet)	7,052
Development Status	producing
Number of Wells	3
Number of Reservoirs	10
Drive Mechanism	depletion
Age	middle to late Miocene
Sedimentary deposit	channel fill-levee
Trap	stratigraphic (across broad four-way closure)
Porosity (percent)	24-32
Permeability (mD)	47-719
Water Saturation Range (percent)	18-43
Initial Reservoir Temperature Range (°F)	77-179
Initial Reservoir Pressure Range (PSI)	4,707-11,411
API Oil Gravity	35
Gas Specific Gravity Range (at 60 and 15.025 PSI)	0.60-0.65
Pay Thickness (feet)	16-103 (gross)
Upper Seal	shale
Lateral Seal	shale
Reservoir Intervals (Subsea true vertical depth-feet)	13,820-16,330
Source Of Information	Rajasingam and Freckelton, 2004
	Cossey and Associates Inc.

Figure 47. Mississippi Canyon (MC) 522 Fourier field. (A) Location map. (B) Seismic profile. Reprinted with permission of Schlumberger. (C) Gamma-ray (GR) and resistivity log. See Figure 4 for the regional setting of the field. ILD = deep induction.

Rydberg Field, Figure 48

(A)

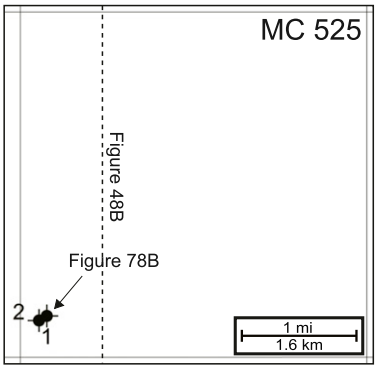

Field Name	Rydberg (Figure 48)
Block Numbers	MC 525
Partners	Shell (57.2%) , Ecopetrol (28.5%), Nexen (14.3%)
Discovery Date	August 2013
Production Start Date	2020 (projected)
Production Facility	Subsea-tieback to Appomattox Hub in MC 437
Water Depth (feet)	7,479
Development Status	under evaluation
Number of Reservoirs	1
Age	Late Jurassic
Sedimentary deposit	eolian
Trap	three-way closure against fault
Liquids Recoverable Reserves (MMbbl)	100
Pay Thickness (feet)	400 (gross)
Upper Seal	shale
Lateral Seal	shale

(C)

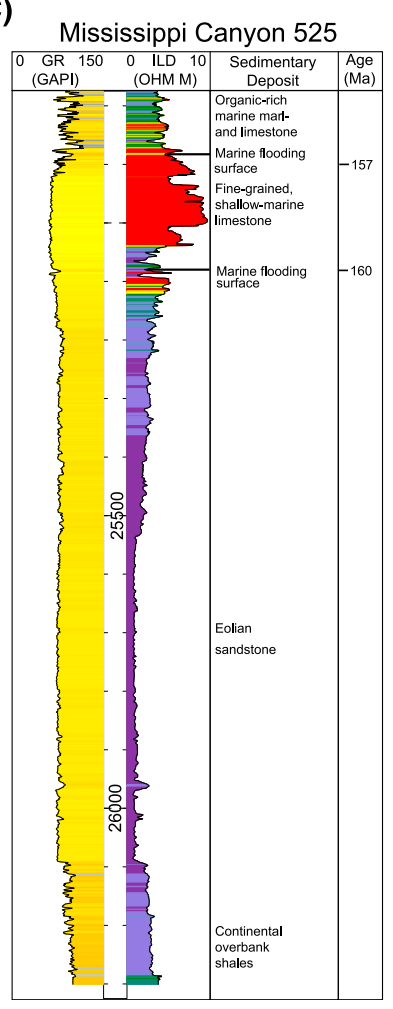

(B)

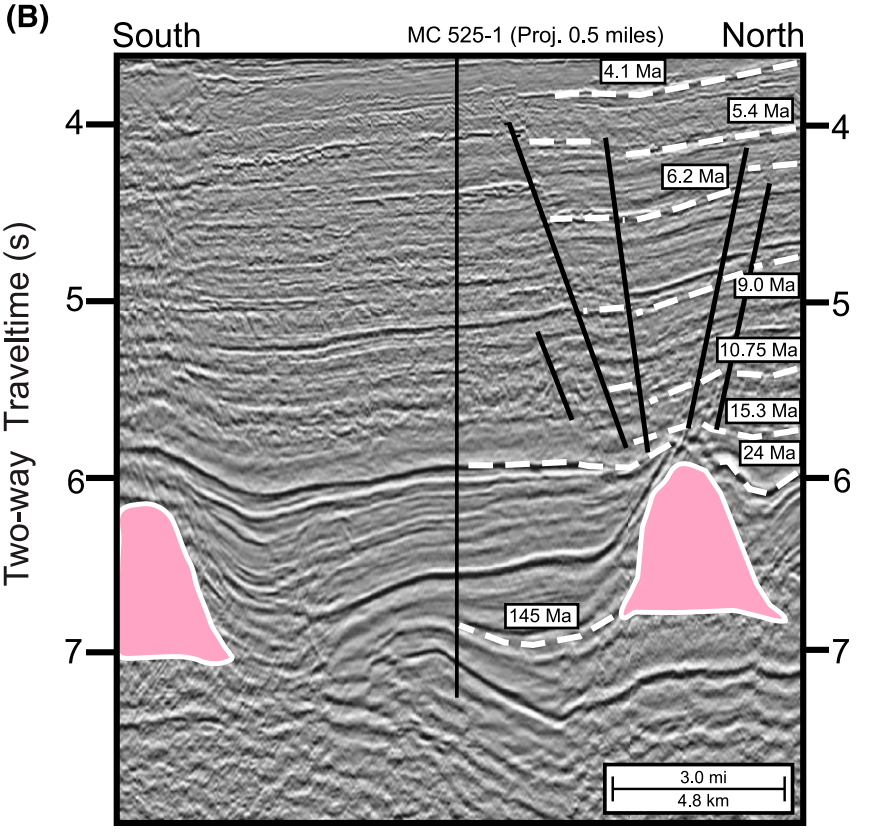

Figure 48. Mississippi Canyon (MC) 525 Rydberg field. (A) Location map. (B) Seismic profile. Reprinted with permission of Schlumberger. (C) Gamma-ray and resistivity log. See Figure 4 for the regional setting of the field.

Medusa North Field, Figure 49

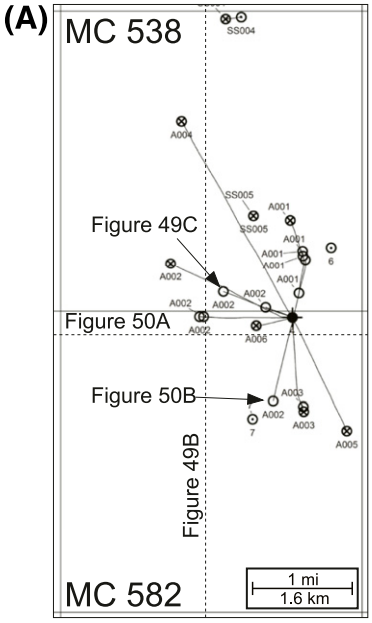

Field Name	Medusa North (Figure 49)
Block Numbers	MC 538
Partners	Murphy Oil (17.00%), Marubeni (68.00%),
	Callon Petroleum (15.00%)
Discovery Date	July 2003
Production Start Date	April 2005
Production Facility	Subsea tie-back to MC 582
Water Depth (feet)	2,237
Development Status	producing
Age	e. Pliocene
Sedimentary deposit	channel fill
Trap	three-way closure against fault
Liquids Recoverable Reserves (MMbbl)	2.66
Gas Recoverable Reserves (BCF)	1.98
API Oil Gravity	22
Upper Seal	shale
Lateral Seal	shale
Source Of Information	Chhajlani et al., 2002
	Lach et al., 2005
	Soter et al., 2005
	L. Czerniakowski, pers. comm., 2010

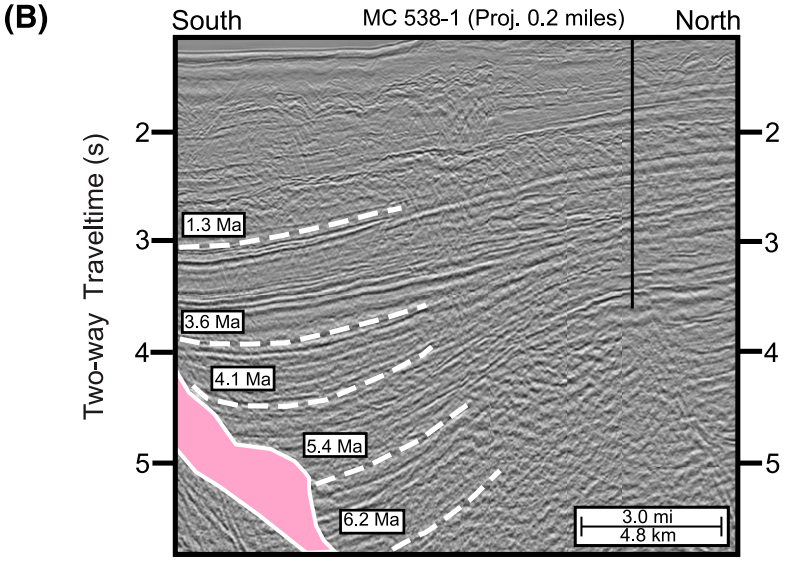

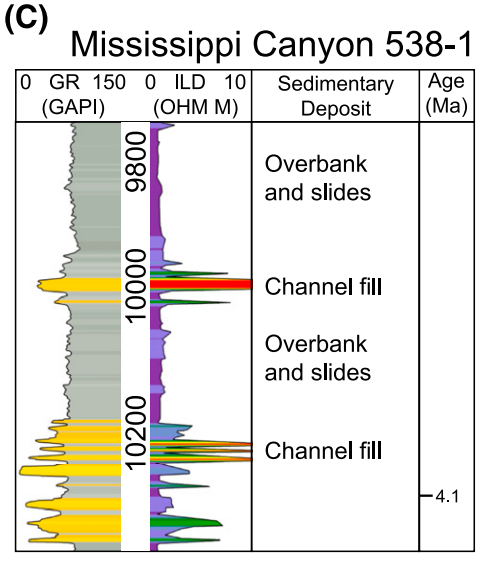

Figure 49. Mississippi Canyon (MC) 538 Medusa North field. (A) Location map of MC 538 Medusa North field and MC 582 Medusa field. (B) Seismic profile. Reprinted with permission of Schlumberger. (C) Gamma-ray (GR) and resistivity log. See Figure 4 for the regional setting of the field. ILD = deep induction.

Medusa Field, Figure 50

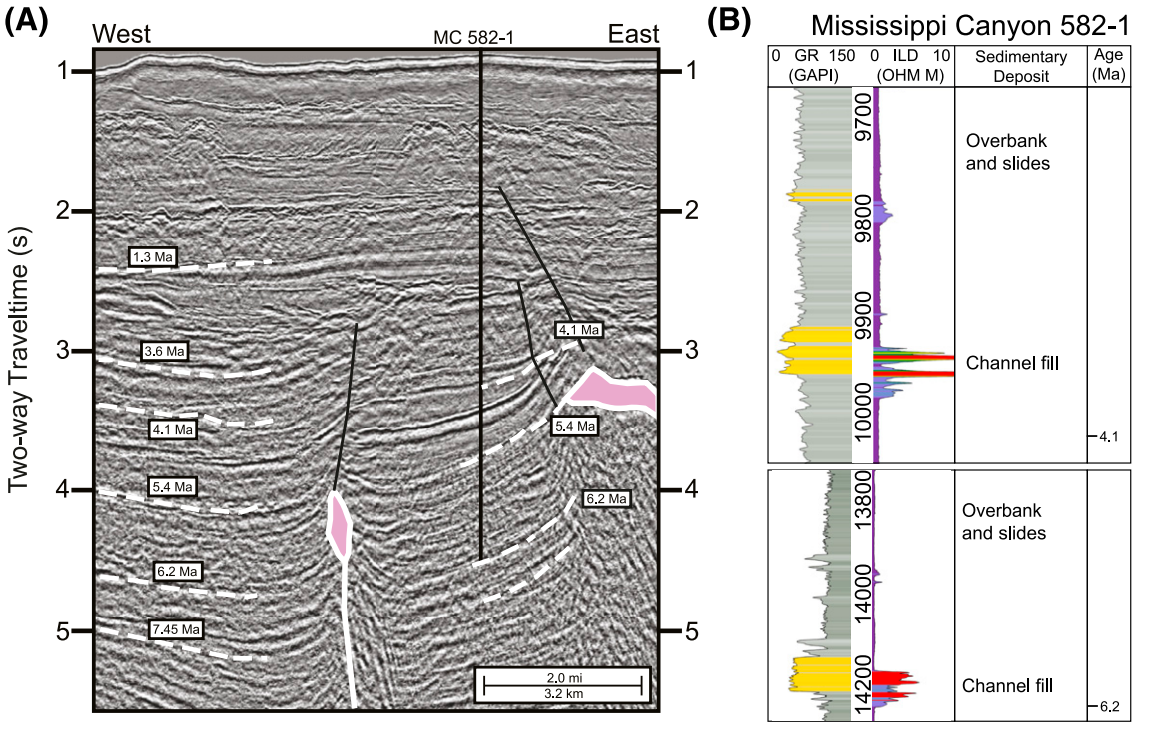

Field Name	Medusa (Figure 50)
Block Numbers	MC 582, MC 538
Partners	Murphy Oil (60.00%), Eni (25.00%),
	Callon Petroleum (15.00%)
Discovery Date	August 1998
Production Start Date	December 2003
Production Facility	Subsea tie-back to Medusa SPAR in MC 582
Water Depth (feet)	2,214
Development Status	producing
Field Size (acres)	2,200
Number of Wells	6
Number of Reservoirs	4
Drive Mechanism	aquifer
Age	late Miocene, Pliocene
Sedimentary deposit	channel fill-levee
Trap	three-way closure against fault
Liquids Recoverable Reserves (MMbbl)	76.29
Gas Recoverable Reserves (BCF)	83.11
Initial Production (BOPD), (MCFGPD)	40,000 BOPD
Gas Oil Ratio	800-1,200
Recovery Efficiency (percent)	26
Porosity (percent)	20-34
Permeability (mD)	600-1,100
Initial Reservoir Pressure Range (PSI)	5,500-7,700
API Oil Gravity	25.4
Oil Column (feet)	300
Upper Seal	shale
Lateral Seal	shale
Reservoir Intervals (Subsea true vertical depth-feet)	8,000-14,600
Source Of Information	Lach et al., 2005
	Soter et al. 2005
	Cossey and Associates Inc.
	L. Czerniakowski, pers. comm., 2010

Figure 50. Mississippi Canyon (MC) 582 Medusa field. (A) Seismic profile. Reprinted with permission of Schlumberger. (B) Gamma-ray (GR) and resistivity log. See Figure 49A for location of profile and well. See Figure 4 for the regional setting of the field. ILD = deep induction.

Isabela Field, Figure 51

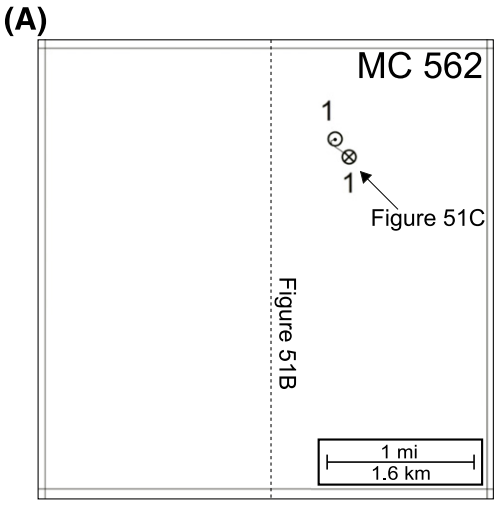

Field Name	Isabela (Figure 51)
Block Numbers	MC 562
Partners	BP (66.67%), Noble Energy (33.33%)
Discovery Date	April 2007
Production Start Date	June 2012
Production Facility	Subsea tie-back to Na Kika in MC 474
Water Depth (feet)	6,537
Development Status	producing
Number of Wells	3
Number of Reservoirs	2
Age	middle Miocene
Sedimentary deposit	sheet sands
Trap	four-way closure fault bounded
Liquids Recoverable Reserves (MMbbl)	52
Oil Column (feet)	90
Gas Column (feet)	48
Upper Seal	shale
Lateral Seal	shale
Source Of Information	Cossey and Associates Inc.

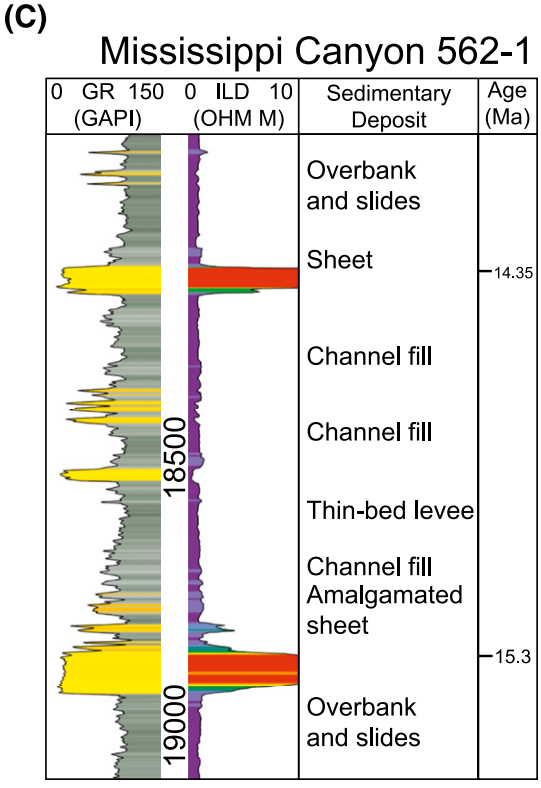

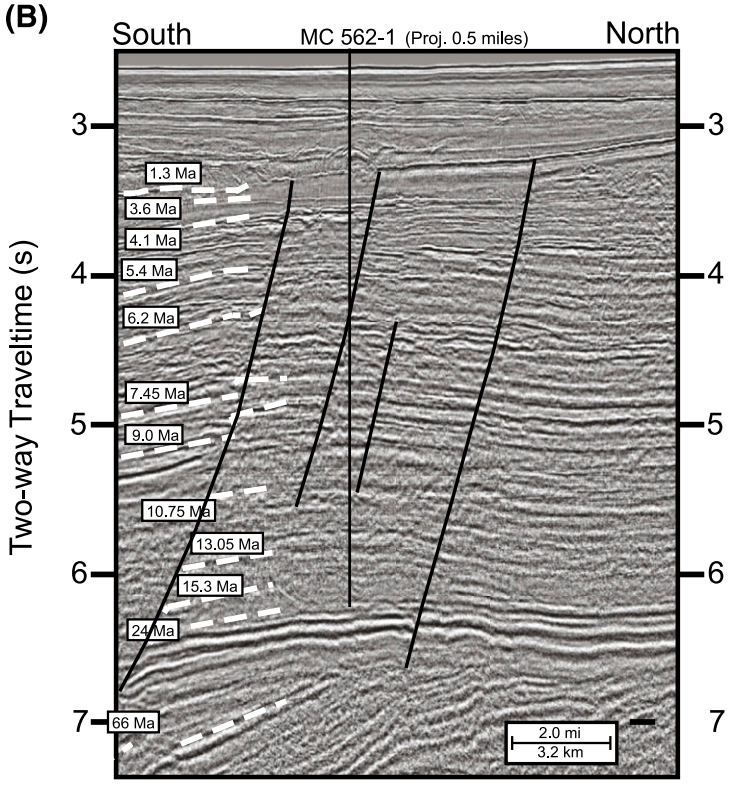

Figure 51. Mississippi Canyon (MC) 562 Isabela field. (A) Location map. (B) Seismic profile. Reprinted with permission of Schlumberger. (C) Gamma-ray (GR) and resistivity log. See Figure 4 for the regional setting of the field. ILD = deep induction.

Ulysses Field, Figure 52

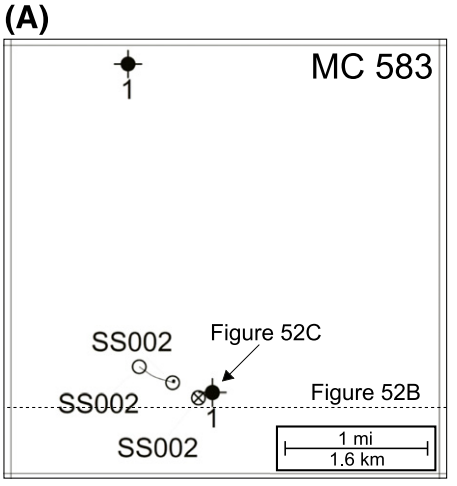

Field Name	Ulysses (Figure 52)
Block Numbers	MC 583
Partners	Walter Oil and Gas (70.63%), Eni (29.37%)
Discovery Date	2004
Production Start Date	June 2005
Production Facility	Subsea tie-back to Medusa SPAR in MC 582
Water Depth (feet)	2,487
Development Status	producing
Number of Wells	1
Age	early Pliocene
Sedimentary deposit	channel fill-levee
Trap	stratigraphic trap
Liquids Recoverable Reserves (MMbbl)	2.4
Gas Recoverable Reserves (BCF)	4.6
Upper Seal	shale
Lateral Seal	shale
Source Of Information	Cossey and Associates Inc.

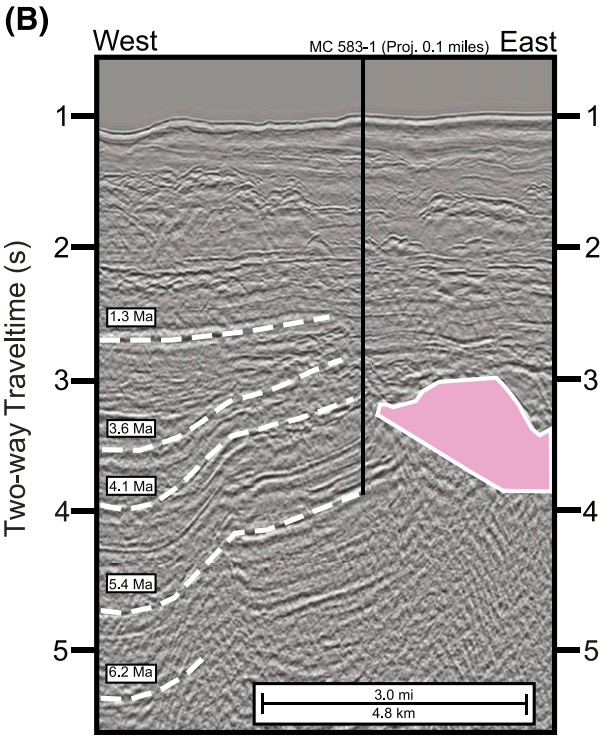

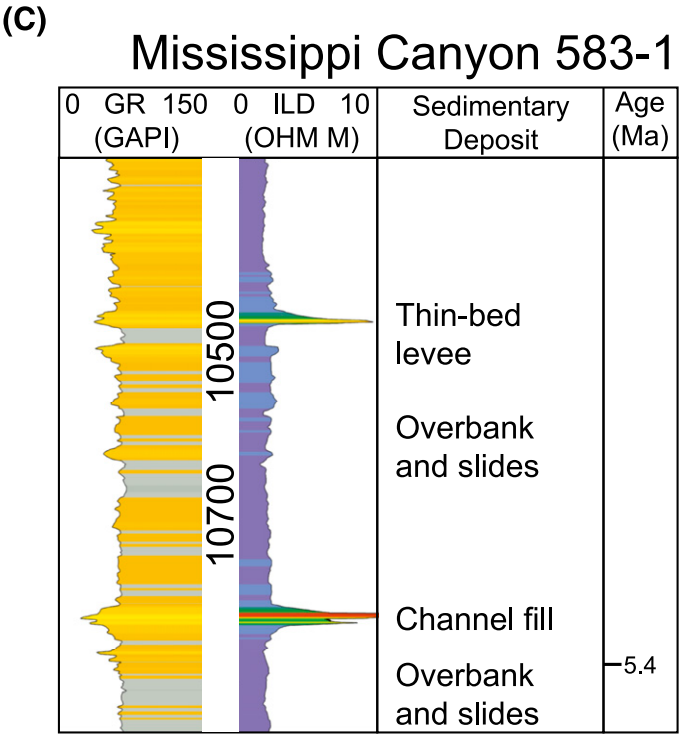

Figure 52. Mississippi Canyon (MC) 583 Ulysses field. (A) Location map. (B) Seismic profile. Reprinted with permission of Schlumberger. (C) Gamma-ray (GR) and resistivity log. See Figure 4 for the regional setting of the field. ILD = deep induction.

East Antsey Field, Figure 53

(A)

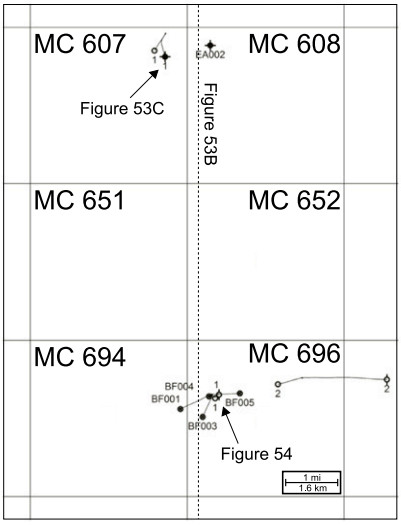

Field Name	East Antsey (Figure 53)
Block Numbers	MC 607
Partners	BP (62.50%), Shell (37.50%)
Discovery Date	December 1997
Production Start Date	December 2003
Production Facility	Subsea tie-back to Na Kika in MC 474
Water Depth (feet)	6,689
Development Status	abandoned-2010
Number of Wells	1
Age	late Miocene
Sedimentary deposit	channel fill-amalgamated sheet sand
Trap	three-way closure against fault
Liquids Recoverable Reserves (MMbbl)	30
Gas Recoverable Reserves (BCF)	170
Initial Reservoir Pressure Range (PSI)	9,500
API Oil Gravity	40
Pay Thickness (feet)	69 (net)
Upper Seal	shale
Lateral Seal	shale
Reservoir Intervals (Subsea true vertical depth-feet)	16,100-16,200
Source Of Information	Rajasingam and Freckelton, 2014
	Cossey and Associates Inc.

(B)

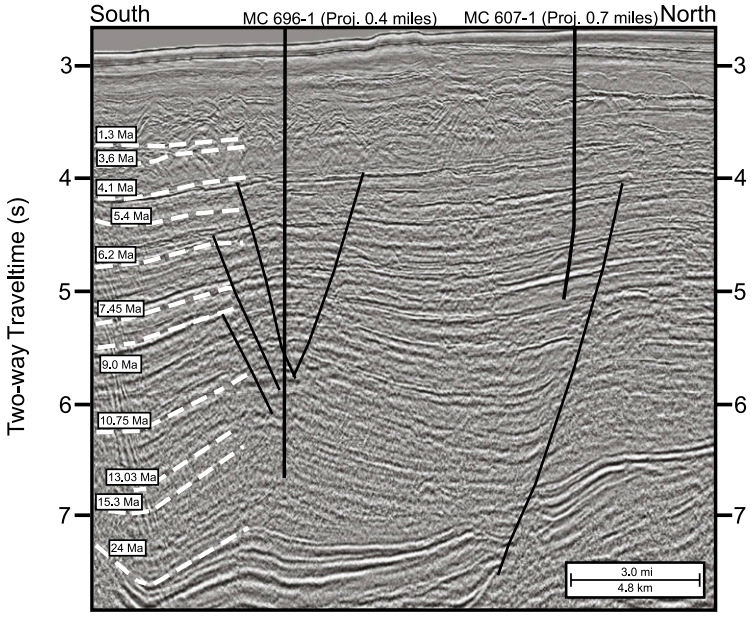

(C)

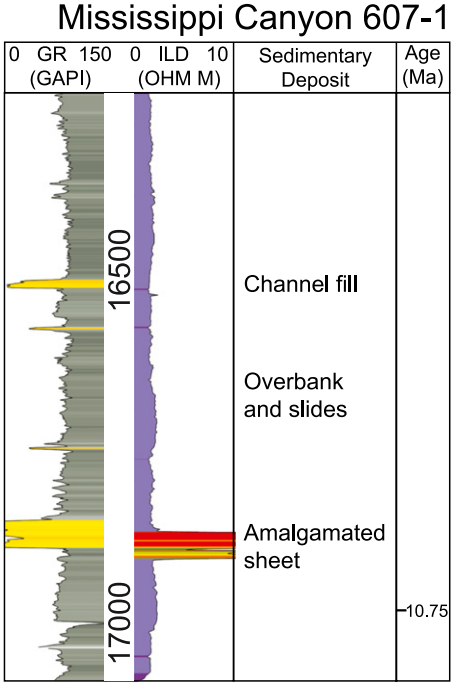

Figure 53. Mississippi Canyon (MC) 607 East Antsey field. (A) Location map of MC 607 East Antsey and MC 696 Blind Faith fields. (B) Seismic profile. Reprinted with permission of Schlumberger. (C) Gamma-ray (GR) and resistivity log. See Figure 4 for the regional setting of the field. ILD = deep induction.

Blind Faith Field, Figure 54

Field Name	Blind Faith (Figure 54)
Block Numbers	MC 696, MC 695
Partners	Chevron (75.00%), Anadarko (25.00%)
Discovery Date	September 2001
Production Start Date	November 2008
Production Facility	Subsea tie-back to Blind Faith semisubmersible platform in MC 696
Water Depth (feet)	7,042
Development Status	producing
Field Size (acres)	2,500
Number of Wells	4
Number of Reservoirs	2
Age	middle Miocene
Sedimentary deposit	channel fill-sheets
Trap	four-way closure (extensional anticline-turtle)
Liquids Recoverable Reserves (MMbbl)	85
Gas Recoverable Reserves (BCF)	76
Initial Production (BOPD), (MCFGPD)	65,000 BOPD
Gas Oil Ratio	700
Porosity (percent)	18-25
Permeability (mD)	300-2,800
Initial Reservoir Temperature Range (°F)	220-260
Initial Reservoir Pressure Range (PSI)	13,000 to 17,000
API Oil Gravity	30
Pay Thickness (feet)	500 (gross)
Oil Column (feet)	1,000
Upper Seal	shale
Lateral Seal	shale
Reservoir Intervals (Subsea true vertical depth-feet)	21,000-21,5000, 23,500-24,300
Source Of Information	Subramanian et al., 2009
	Cossey and Associates Inc.

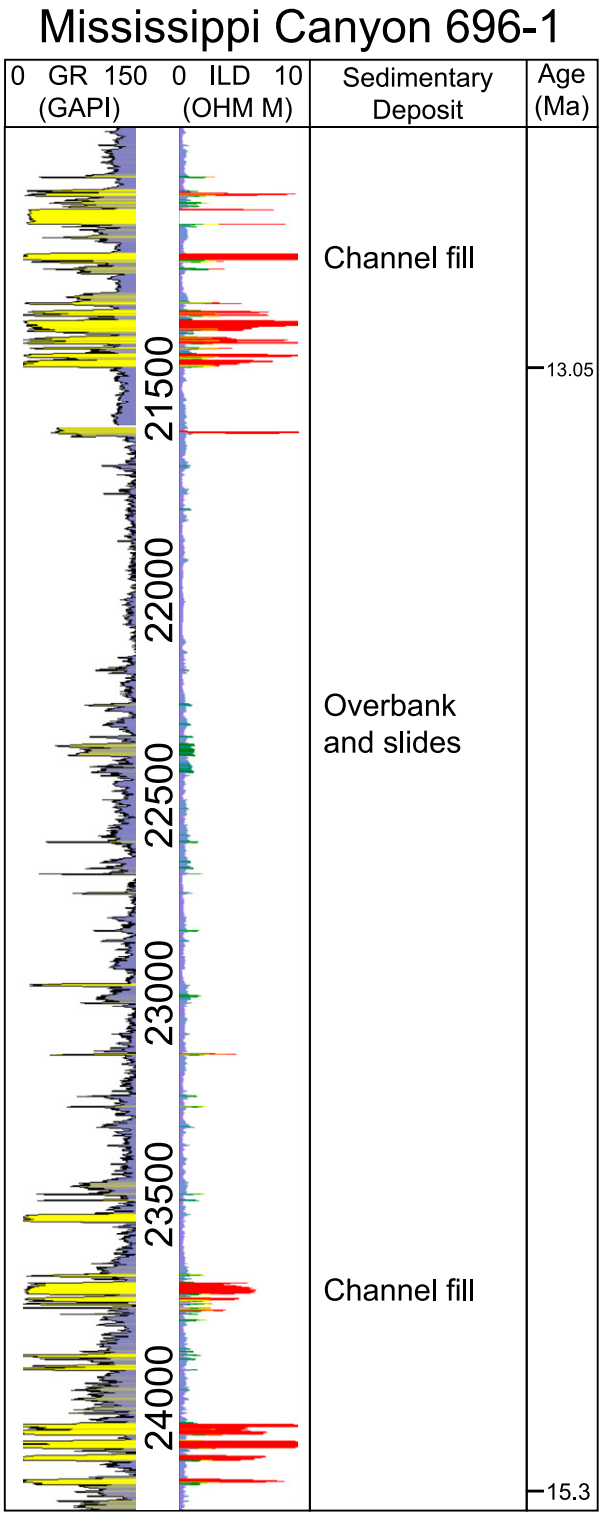

Figure 54. Mississippi Canyon 696 Blind Faith field. Gamma-ray (GR) and resistivity log. See Figure 53A for location map and Figure 53B for seismic profile. See Figure 4 for the regional setting of the field. ILD = deep induction.

Coulomb Field, Figure 55

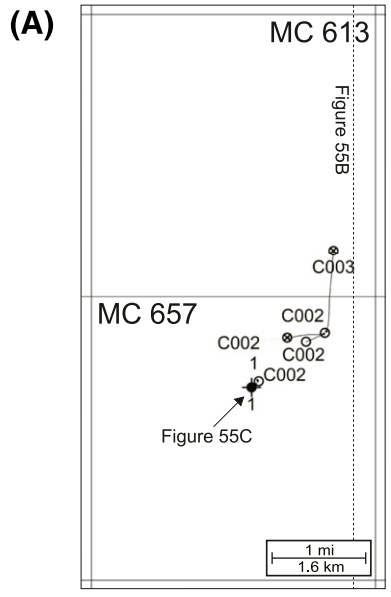

Field Name	Coulomb (Figure 55)
Block Numbers	MC 657, MC 613
Partners	Shell (100.00%)
Discovery Date	January 1988
Production Start Date	June 2004
Production Facility	Subsea tie-back to Na Kika in MC 474
Water Depth (feet)	7,795
Development Status	producing
Number of Wells	2
Number of Reservoirs	4
Drive Mechanism	partial gas
Age	middle to late Miocene
Sedimentary deposit	channel fill
Trap	three-way closure against fault
Liquids Recoverable Reserves (MMbbl)	12
Gas Recoverable Reserves (BCF)	194
Porosity (percent)	29-30
Permeability (mD)	140-1,500
Water Saturation Range (percent)	15-33
Initial Reservoir Temperature Range (°F)	111-153
Initial Reservoir Pressure Range (PSI)	7,342-10,223
API Oil Gravity	51.8
Gas Specific Gravity Range (at 60 and 15.025 PSI)	0.62
Upper Seal	shale
Lateral Seal	shale
Reservoir Intervals (Subsea true vertical depth-feet)	13,350-17,100
Source Of Information	Cossey and Associates Inc.

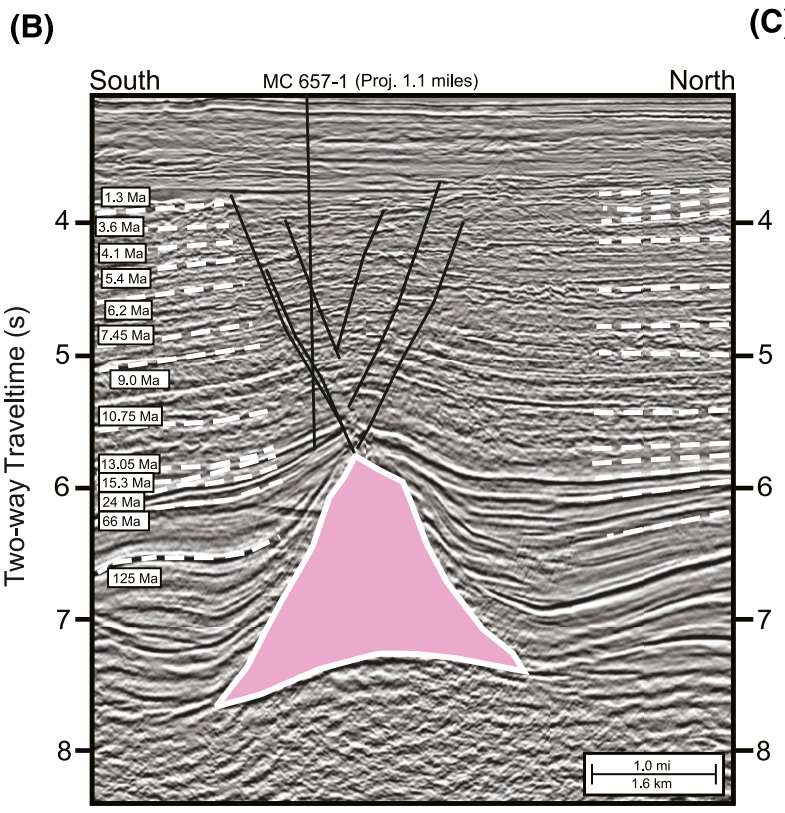

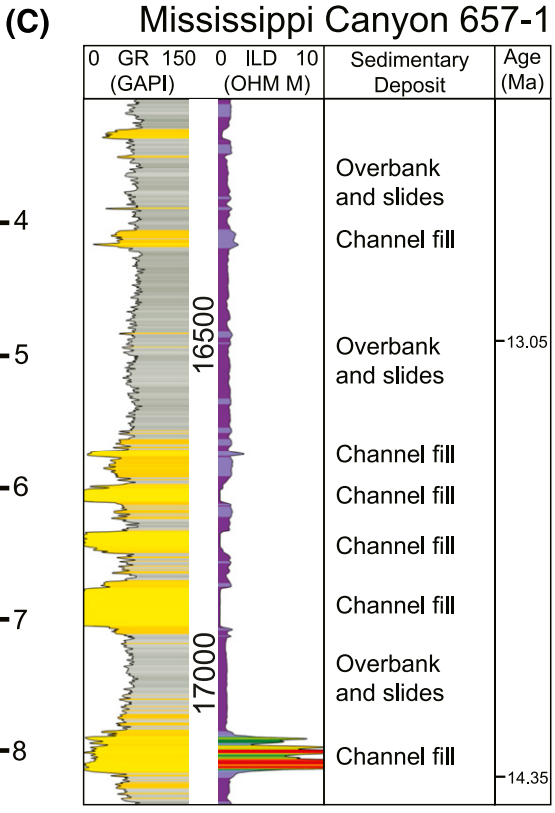

Figure 55. Mississippi Canyon (MC) 657 Coulomb field. (A) Location map. (B) Seismic profile. Reprinted with permission of Schlumberger. (C) Gamma-ray (GR) and resistivity log. See Figure 4 for the regional setting of the field. ILD = deep induction.

Big Bend Field, Figure 56

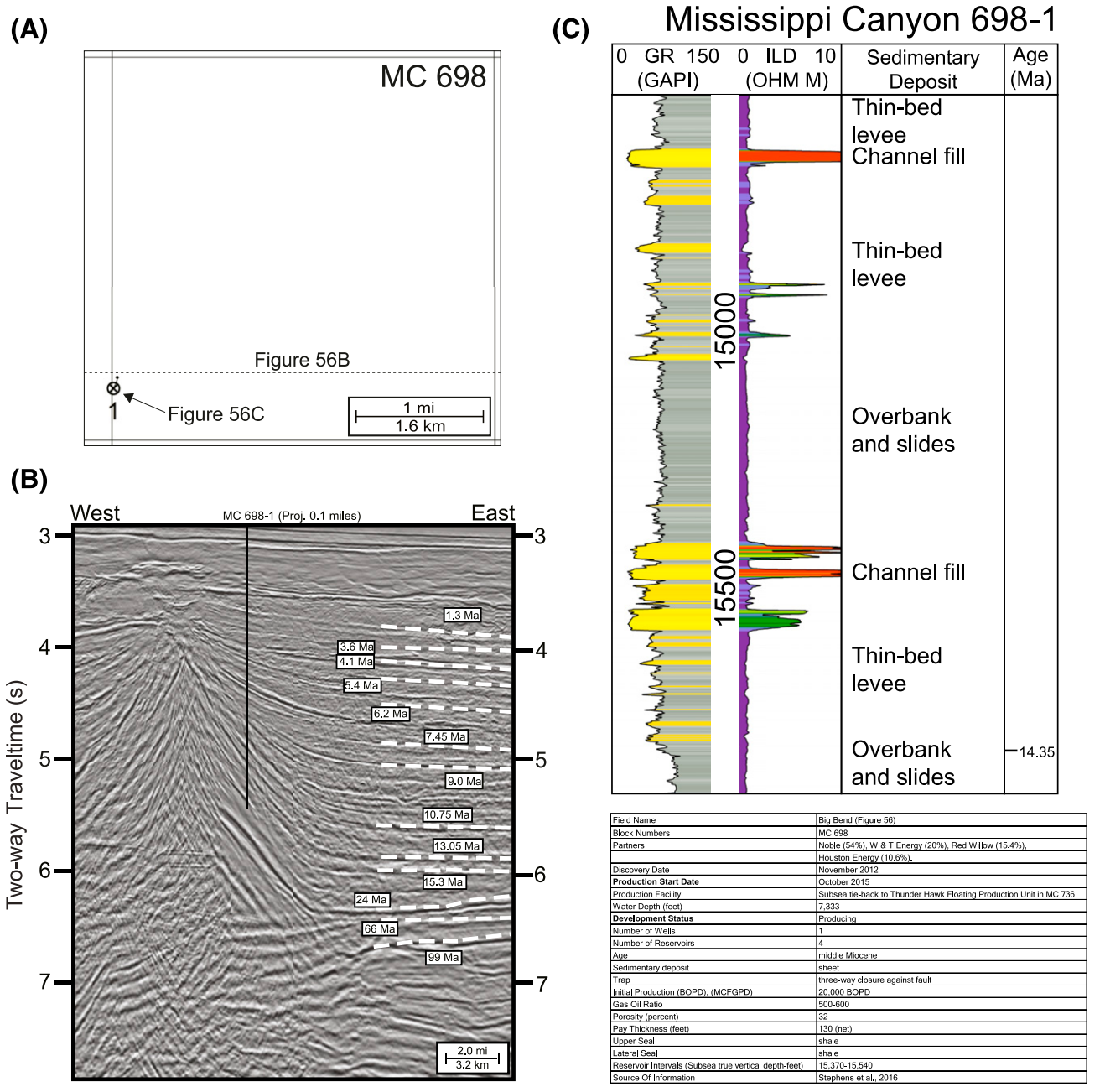

Field Name	Big Bend (Figure 56)
Block Numbers	MC 698
Partners	Noble (54%), W & T Energy (20%), Red Willow (15.4%), Houston Energy (10.6%).
Discovery Date	November 2012
Production Start Date	October 2015
Production Facility	Subsea tie-back to Thunder Hawk Floating Production Unit in MC 736
Water Depth (feet)	7,333
Development Status	Producing
Number of Wells	1
Number of Reservoirs	4
Age	middle Miocene
Sedimentary deposit	sheet
Trap	three-way closure against fault
Initial Production (BOPD), (MCFGPD)	20,000 BOPD
Gas Oil Ratio	500-600
Porosity (percent)	32
Pay Thickness (feet)	130 (net)
Upper Seal	shale
Lateral Seal	shale
Reservoir Intervals (Subsea true vertical depth-feet)	15,370-15,540
Source Of Information	Stephens et al., 2016

Figure 56. Mississippi Canyon (MC) 698 Big Bend field. (A) Location map. (B) Seismic profile. Reprinted with permission of Schlumberger. (C) Gamma-ray (GR) and resistivity log. See Figure 4 for the regional setting of the field. ILD = deep induction.

Troubadour Field, Figure 57

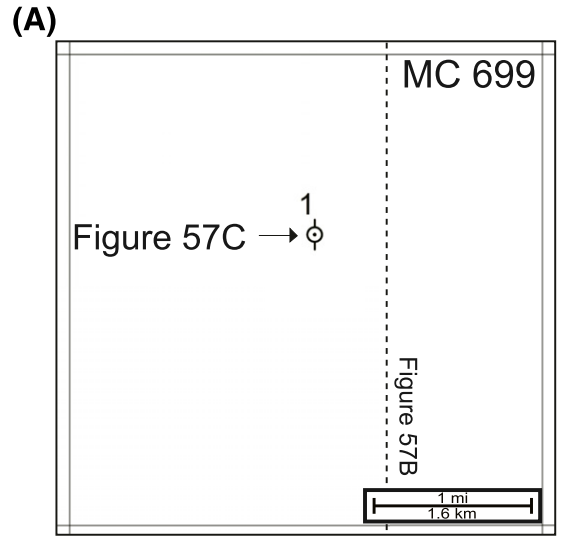

Field Name	Troubadour (Figure 57)
Block Numbers	MC 699
Partners	Noble (87.50%), Deep Gulf II (12.50%)
Discovery Date	September 2013
Production Start Date	
Water Depth (feet)	7,438
Development Status	under evaluation
Age	late Miocene
Sedimentary deposit	channel fill
Trap	stratigraphic
Liquids Recoverable Reserves (MMbbl)	50-220
Pay Thickness (feet)	50 (net)
Upper Seal	shale
Lateral Seal	shale

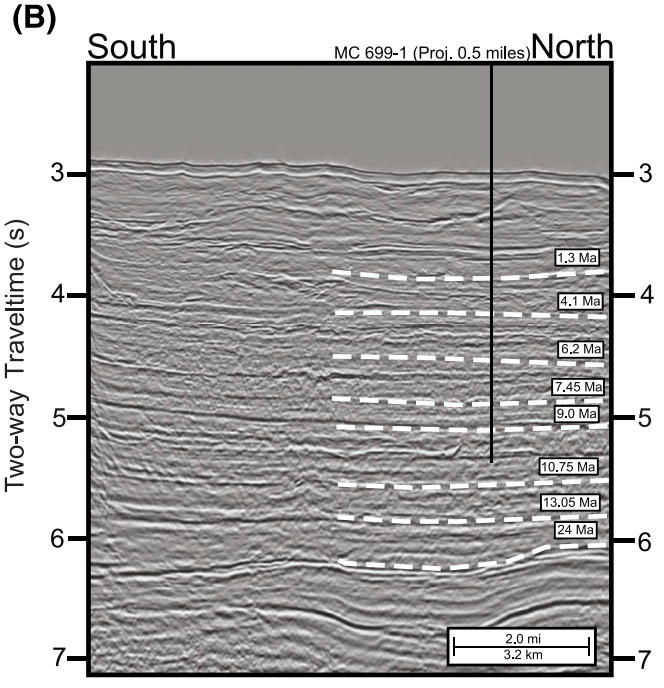

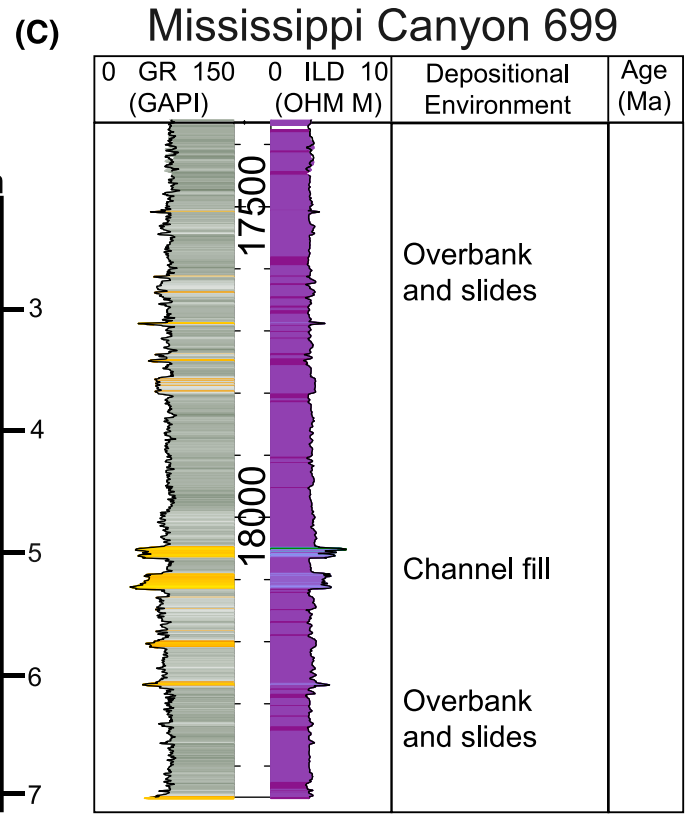

Figure 57. Mississippi Canyon (MC) 699 Troubadour field. (A) Location map. (B) Seismic profile. Reprinted with permission of Schlumberger. (C) Gamma-ray (GR) and resistivity log. See Figure 4 for the regional setting of the field.

Biddy Ball Field, Figure 58

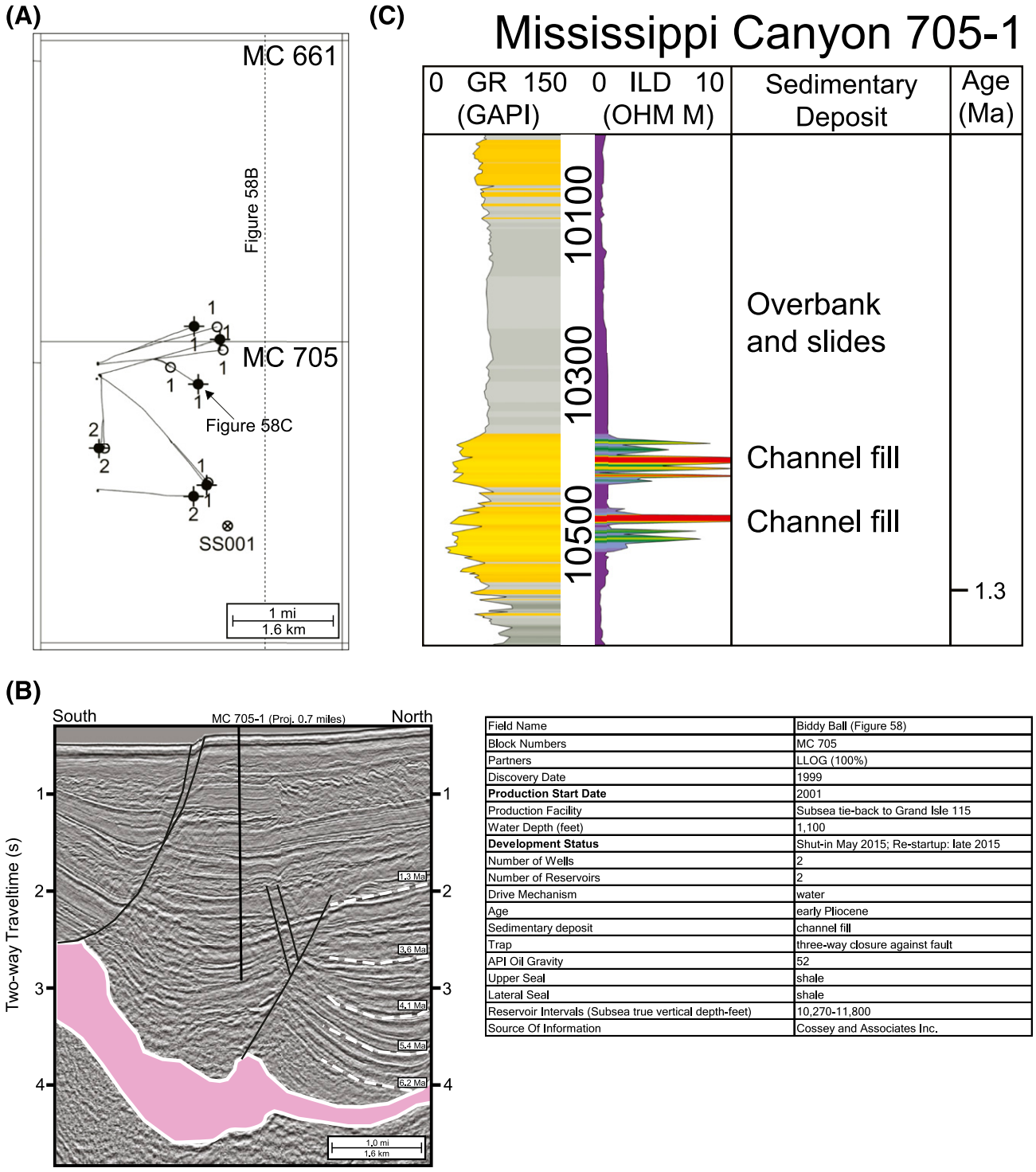

Field Name	Biddy Ball (Figure 58)
Block Numbers	MC 705
Partners	LLOG (100%)
Discovery Date	1999
Production Start Date	2001
Production Facility	Subsea tie-back to Grand Isle 115
Water Depth (feet)	1,100
Development Status	Shut-in May 2015; Re-startup: late 2015
Number of Wells	2
Number of Reservoirs	2
Drive Mechanism	water
Age	early Pliocene
Sedimentary deposit	channel fill
Trap	three-way closure against fault
API Oil Gravity	52
Upper Seal	shale
Lateral Seal	shale
Reservoir Intervals (Subsea true vertical depth-feet)	10,270-11,800
Source Of Information	Cossey and Associates Inc.

Figure 58. Mississippi Canyon (MC) 705 Biddy Ball field. (A) Location map. (B) Seismic profile. Reprinted with permission of Schlumberger. (C) Gamma-ray (GR) and resistivity log. See Figure 4 for the regional setting of the field. ILD = deep induction.

Valley Forge Field, Figure 59

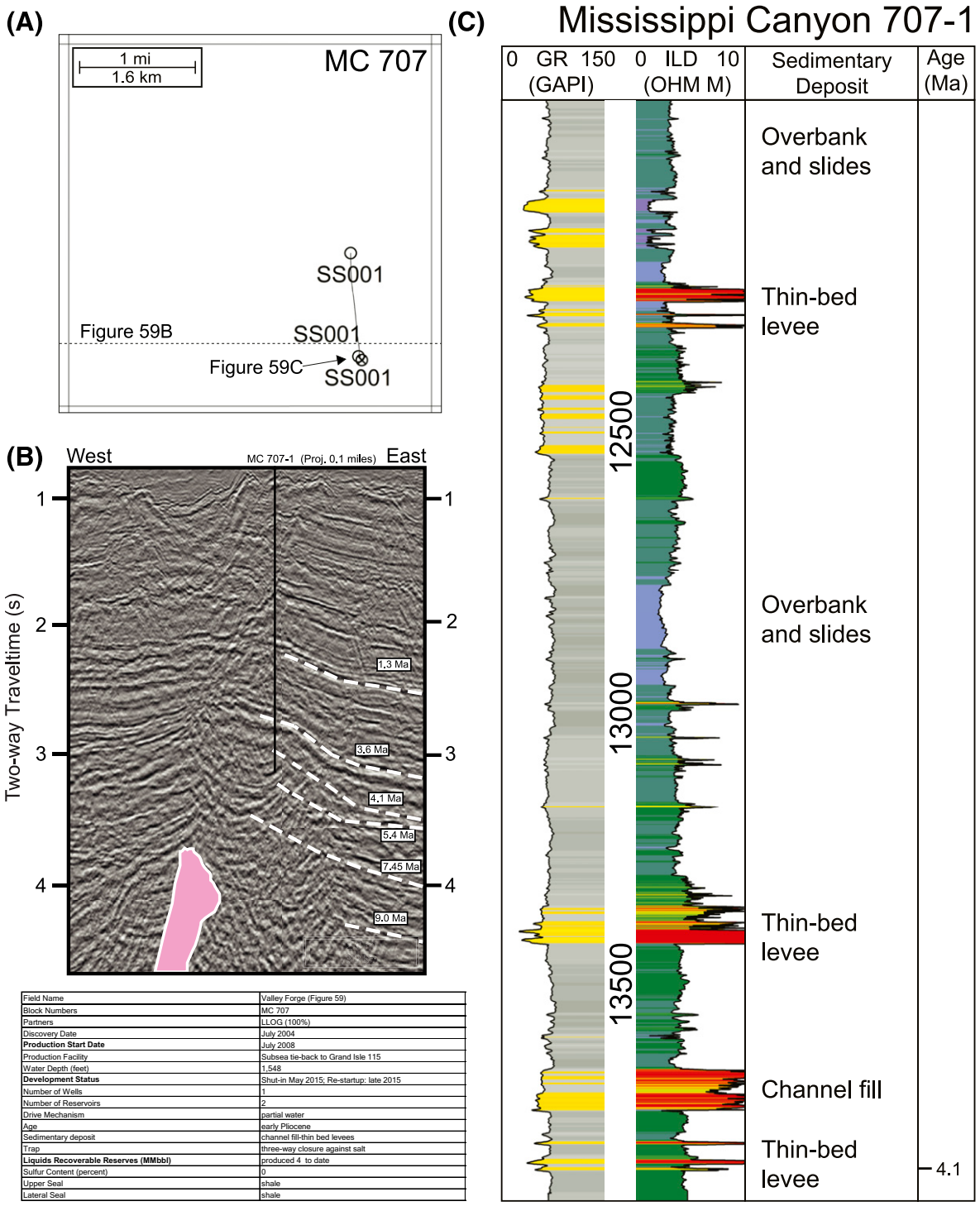

Field Name	Valley Forge (Figure 59)
Block Numbers	MC 707
Partners	LLOG (100%)
Discovery Date	July 2004
Production Start Date	July 2008
Production Facility	Subsea tie-back to Grand Isle 115
Water Depth (feet)	1,548
Development Status	Shut-in May 2015; Re-startup: late 2015
Number of Wells	1
Number of Reservoirs	2
Drive Mechanism	partial water
Age	early Pliocene
Sedimentary deposit	channel fill-thin bed levees
Trap	three-way closure against salt
Liquids Recoverable Reserves (MMbbl)	produced 4 to date
Sulfur Content (percent)	0
Upper Seal	shale
Lateral Seal	shale

Figure 59. Mississippi Canyon (MC) 707 Valley Forge field. (A) Location map. (B) Seismic profile. Reprinted with permission of Schlumberger. (C) Gamma-ray (GR) and resistivity log. See Figure 4 for the regional setting of the field. ILD = deep induction.

Gomez Field, Figure 60

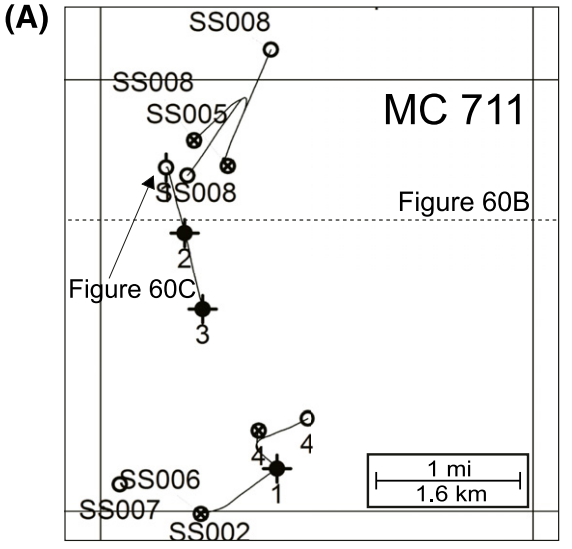

Field Name	Gomez (Figure 60)
Block Numbers	MC 711
Partners	Bennu (100.00%)
Discovery Date	December 1997
Production Start Date	March 2006
Production Facility	Gomez Hub in MC 711
Water Depth (feet)	3,016
Development Status	abandoned-2013
Number of Wells	8
Number of Reservoirs	4
Age	early Pliocene-early Pleistocene
Sedimentary deposit	thin-bed levees
Trap	three-way closure against fault
Gas Recoverable Reserves (BCF)	150
API Oil Gravity	33.7
Upper Seal	shale
Lateral Seal	shale
Reservoir Intervals (Subsea true vertical depth-feet)	11,500 to 12, 000
Source Of Information	Cossey and Associates Inc.

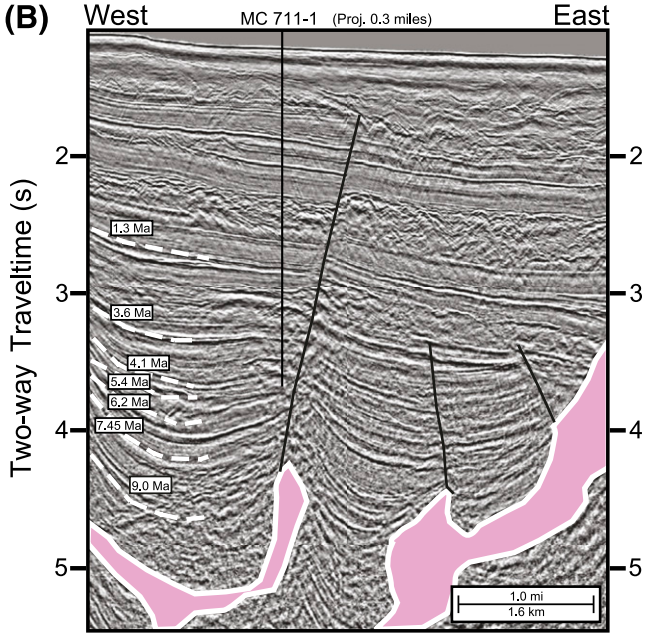

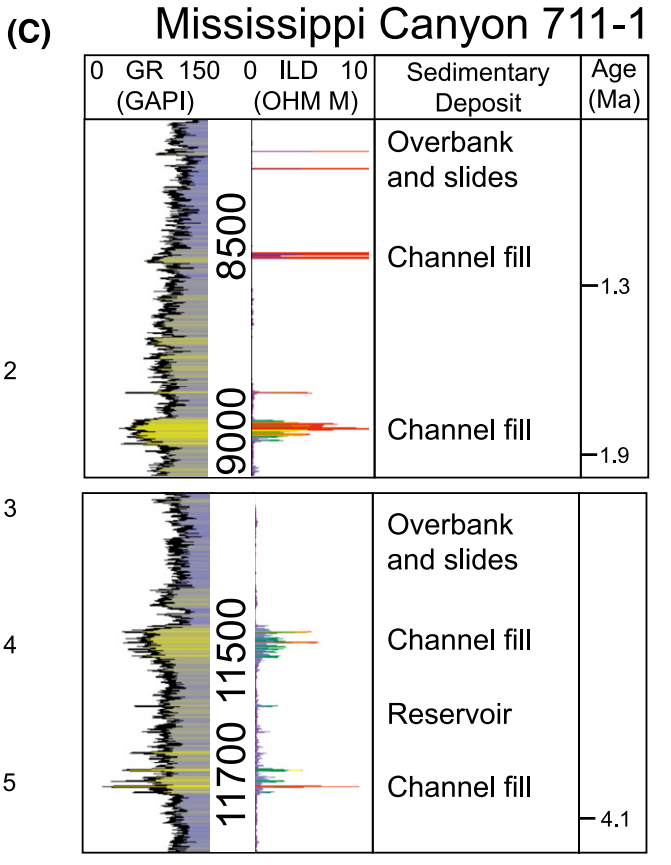

Figure 60. Mississippi Canyon (MC) 711 Gomez field. (A) Location map. (B) Seismic profile. Reprinted with permission of Schlumberger. (C) Gamma-ray (GR) and resistivity log. See Figure 4 for the regional setting of the field. ILD = deep induction.

Pluto Field, Figure 61

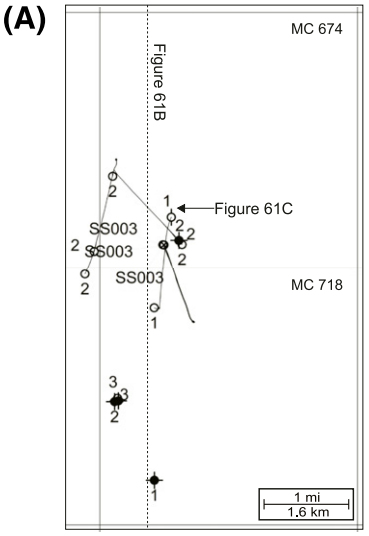

Field Name	Pluto (Figure 61)
Block Numbers	MC 718, MC 674
Partners	Mariner Energy (100.00%),
Discovery Date	1995
Production Start Date	December 1999
Production Facility	Subsea to South Pass 89
Water Depth (feet)	2,820
Development Status	abandoned-2008
Field Size (acres)	1,000
Number of Wells	2
Number of Reservoirs	2
Drive Mechanism	water
Age	late Miocene
Sedimentary deposit	channel fill-levee
Trap	three-way closure against fault
Liquids Recoverable Reserves (MMbbl)	6.4
Gas Recoverable Reserves (BCF)	42.1
Initial Production (BOPD), (MCFGPD)	13,428 BOPD, 60.35 mmcfpd
Porosity (percent)	25-30
Permeability (mD)	10-1,000
Water Saturation Range (percent)	14-35
Initial Reservoir Pressure Range (PSI)	13,350
API Oil Gravity	48
Upper Seal	shale
Lateral Seal	shale
Reservoir Intervals (Subsea true vertical depth-feet)	15,000, 18,000
Source Of Information	Cossey and Associates Inc.
	S. Burt, pers. comm., 2010

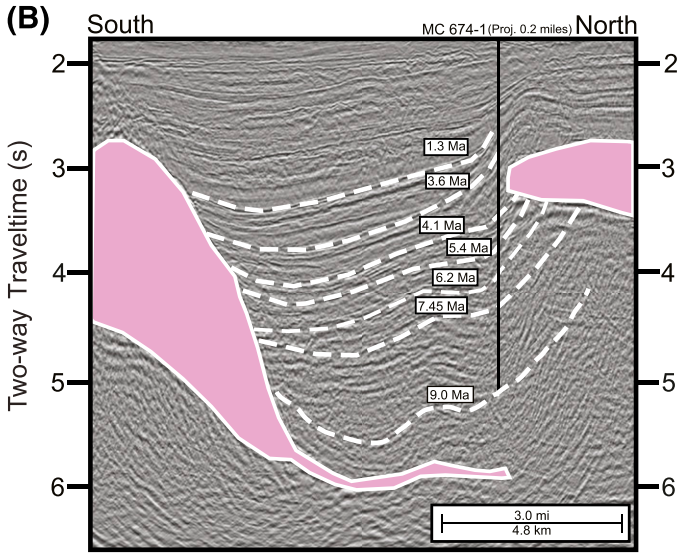

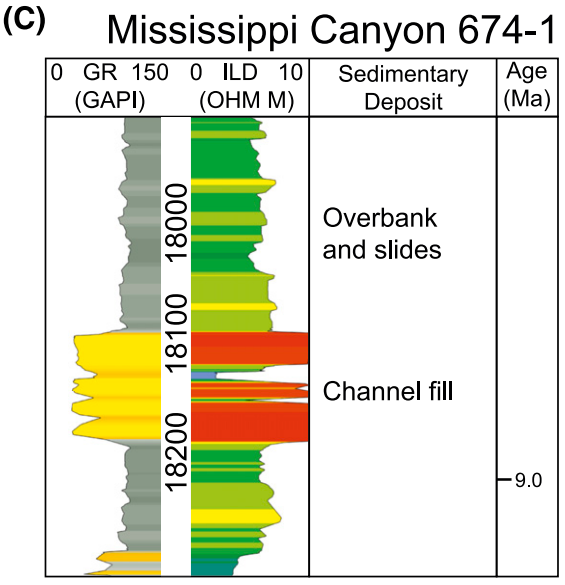

Figure 61. Mississippi Canyon (MC) 718 Pluto field. (A) Location map. (B) Seismic profile. Reprinted with permission of Schlumberger. (C) Gamma-ray (GR) and resistivity log. See Figure 4 for the regional setting of the field. ILD = deep induction.

Tubular Bells Field, Figure 62

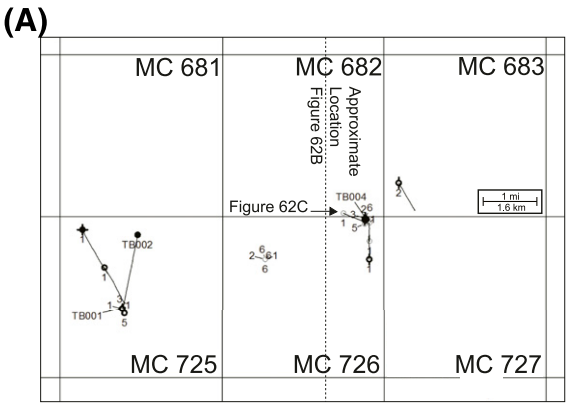

Field Name	Tubular Bells (Figure 62)
Block Numbers	MC 725, MC 682, MC 683, MC 726, MC 727
Partners	Hess (57.14%), Chevron (42.86%)
Discovery Date	November 2003
Production Start Date	November 2014
Production Facility	Subsea tie-back to Tubular Bells SPAR in MC 724
Water Depth (feet)	4326
Development Status	producing
Number of Wells	4
Number of Reservoirs	4
Drive Mechanism	water drive
Age	middle Miocene
Sedimentary deposit	channel fill
Trap	three-way closure against base of salt
Initial Production (BOPD), (MCFGPD)	50,000-60,000 BOPD
Gas Oil Ratio	2,000-5,000
Secondary Recovery	possible water injection
Porosity (percent)	17-28
Permeability (mD)	30-450
Initial Reservoir Temperature Range (°F)	250
Initial Reservoir Pressure Range (PSI)	15,000-19,000
API Oil Gravity	35
Pay Thickness (feet)	125-200 (gross)
Oil Column (feet)	>570
Upper Seal	salt
Lateral Seal	shale
Reservoir Intervals (Subsea true vertical depth-feet)	22,000-25,000
Source Of Information	Xia er al., 2009
	Greeley et al., 2013
	Cossey and Associates Inc.

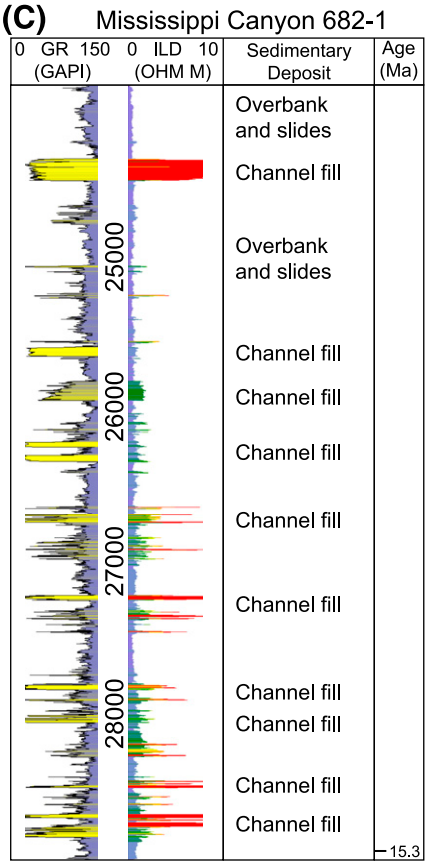

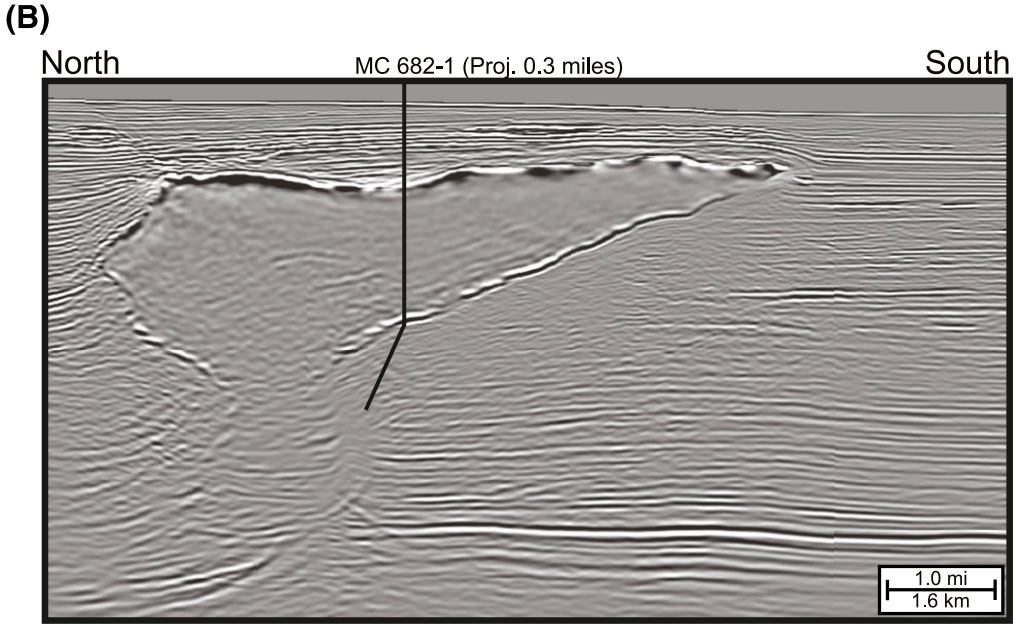

Figure 62. Mississippi Canyon (MC) 725–674 Tubular Bells field. (A) Location map. (B) Seismic profile. After Xia et al. (2009). Reprinted with permission of Society of Exploration Geophysicists. (C) Gamma-ray (GR) and resistivity log. See Figure 4 for the regional setting of the field. ILD = deep induction.

Mensa Field, Figure 63

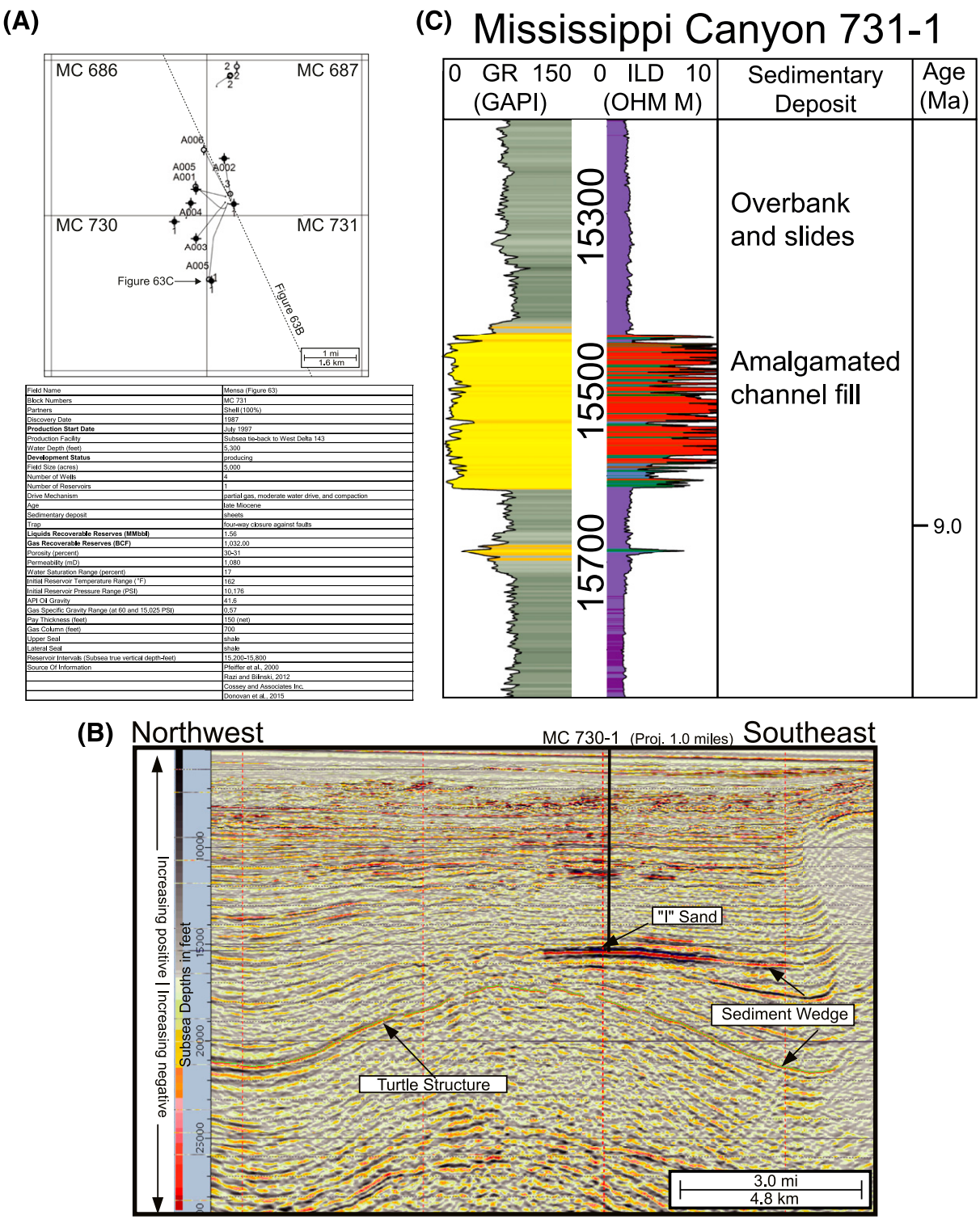

Field Name	Mensa (Figure 63)
Block Numbers	MC 731
Partners	Shell (100%)
Discovery Date	1987
Production Start Date	July 1997
Production Facility	Subsea tie-back to West Delta 143
Water Depth (feet)	5,300
Development Status	producing
Field Size (acres)	5,000
Number of Wells	4
Number of Reservoirs	1
Drive Mechanism	partial gas, moderate water drive, and compaction
Age	late Miocene
Sedimentary deposit	sheets
Trap	four-way closure against faults
Liquids Recoverable Reserves (MMbbl)	1.56
Gas Recoverable Reserves (BCF)	1,032.00
Porosity (percent)	30-31
Permeability (mD)	1,080
Water Saturation Range (percent)	17
Initial Reservoir Temperature Range (°F)	162
Initial Reservoir Pressure Range (PSI)	10,176
API Oil Gravity	41.6
Gas Specific Gravity Range (at 60 and 15,025 PSI)	0.57
Pay Thickness (feet)	150 (net)
Gas Column (feet)	700
Upper Seal	shale
Lateral Seal	shale
Reservoir Intervals (Subsea true vertical depth-feet)	15,200-15,800
Source Of Information	Pfeiffer et al., 2000
	Razi and Bilinski, 2012
	Cossey and Associates Inc.
	Donovan et al., 2015

Figure 63. Mississippi Canyon (MC) 731 Mensa field. (A) Location map. (B) Seismic profile. Reproduced with the permission of the Gulf Coast Section SEPM Foundation, and any other use requires their permission. (C) Gamma-ray (GR) and resistivity log. See Figure 4 for the regional setting of the field. ILD = deep induction.

Goose Field, Figure 64

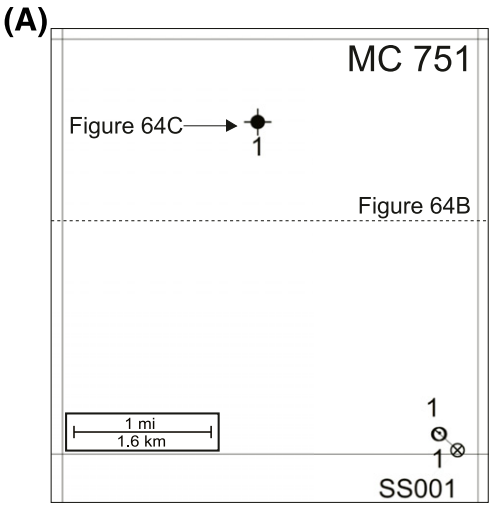

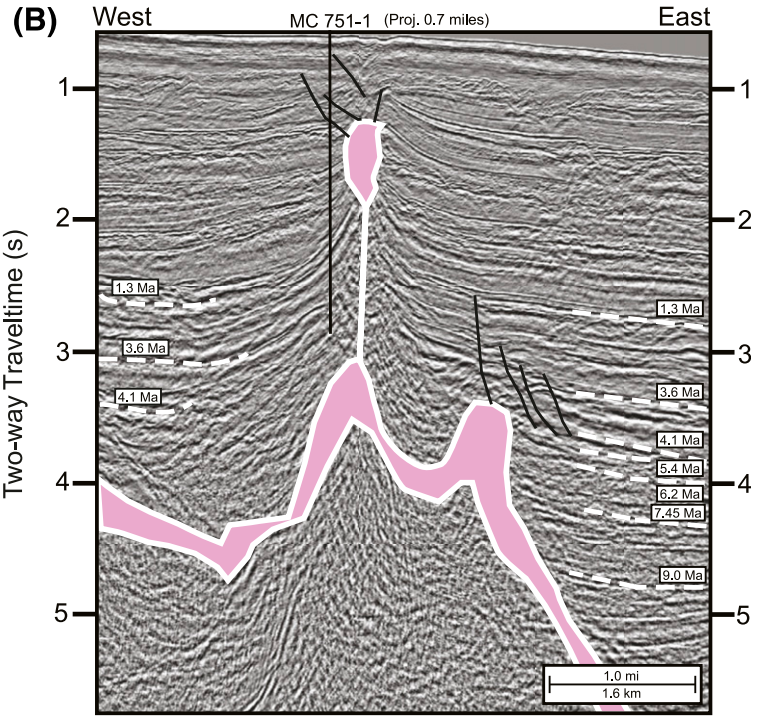

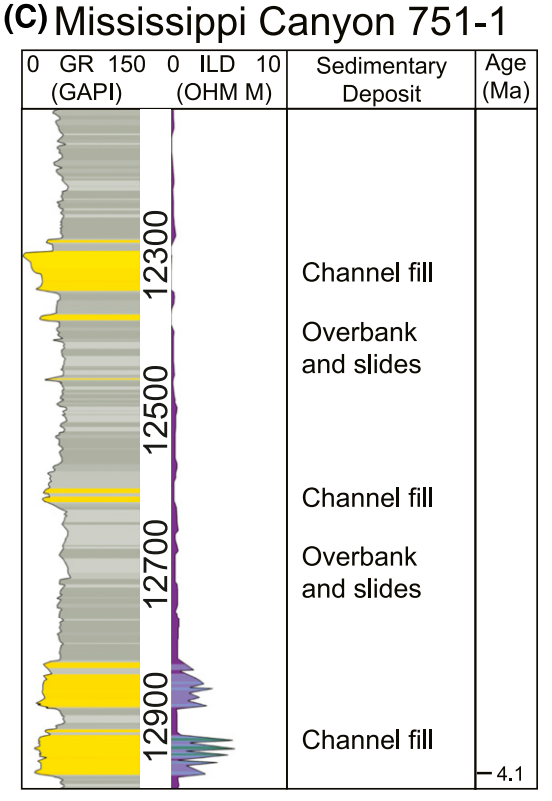

Field Name	Goose (Figure 64)
Block Numbers	MC 751
Partners	LLOG (100%)
Discovery Date	January 2003
Production Start Date	November 2012
Production Facility	Subsea tie-back to Valley Forge in MC 707
Water Depth (feet)	1634
Development Status	shut-in May 2015; re-startup: late 2015
Age	Pliocene
Sedimentary deposit	channel fill
Trap	three-way closure against salt flank
Liquids Recoverable Reserves (MMbbl)	50
Gas Recoverable Reserves (BCF)	30
Sulfur Content (percent)	0.005
Upper Seal	shale
Lateral Seal	shale

Figure 64. Mississippi Canyon (MC) 751 Goose field. (A) Location map. Also shown are the locations for (B) and (C). (B) Seismic profile across the MC 751 Goose field. Reprinted with permission of Schlumberger. (C) Gamma-ray (GR) and resistivity log from the MC 751-1 well. See Figure 4 for the regional setting of the field. ILD = deep induction.

Anduin West Field, Figure 65

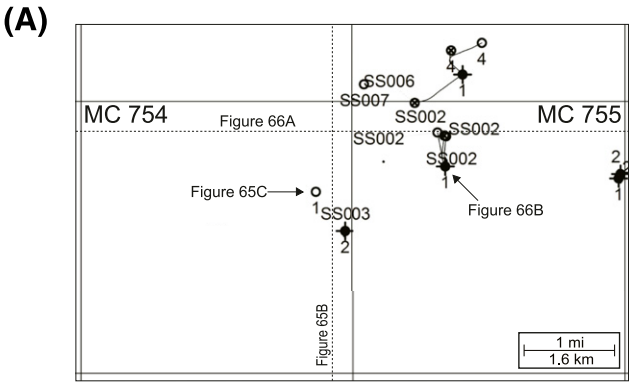

Field Name	Anduin West (Figure 65)
Block Numbers	MC 754
Partners	Bennu (75%) , LLOG (25%)
Discovery Date	April 2008
Production Start Date	February 2011
Production Facility	Gomez Hub in MC 711
Water Depth (feet)	2,713
Development Status	abandoned-2012
Age	late Miocene
Sedimentary deposit	levee
Trap	three-way closure against fault
Liquids Recoverable Reserves (MMbbl)	1
Gas Recoverable Reserves (BCF)	13
Pay Thickness (feet)	30 (net)
Gas Column (feet)	30 (gas +condensate)
Upper Seal	shale
Lateral Seal	shale

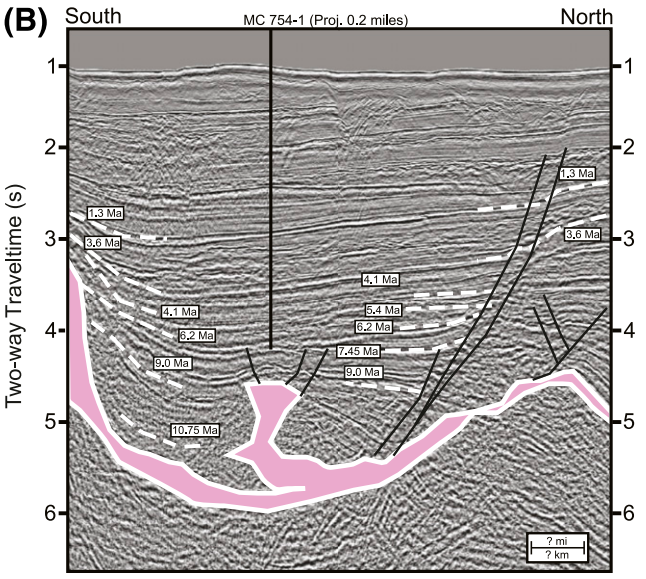

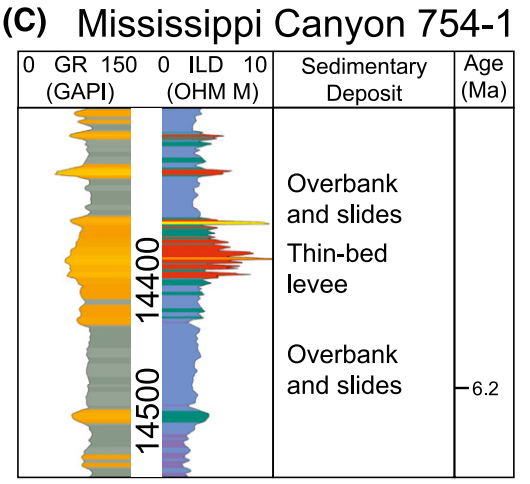

Figure 65. Mississippi Canyon (MC) 754 Anduin West field. (A) Location map of MC 754 Anduin West and 755 Anduin fields. (B) Seismic profile. Reprinted with permission of Schlumberger. (C) Gamma-ray (GR) and resistivity log. See Figure 4 for the regional setting of the field. ILD = deep induction.

Anduin Field, Figure 66

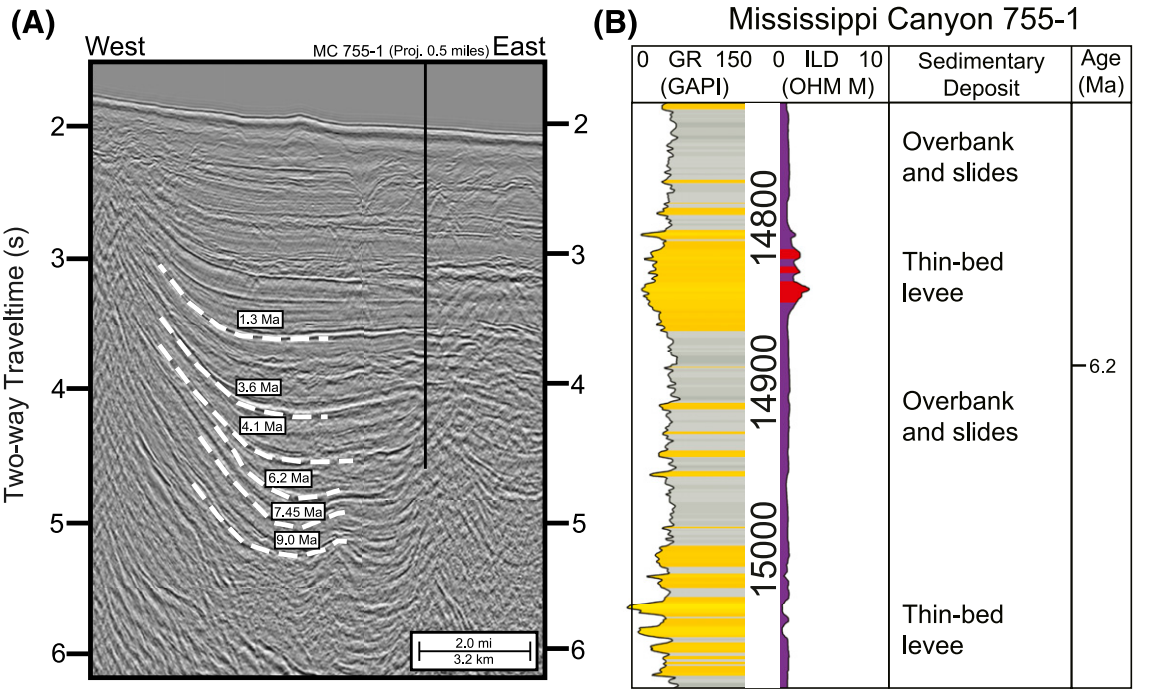

Field Name	Anduin (Figure 66)
Block Numbers	MC 755
Partners	Bennu (100%)
Discovery Date	February 2005
Production Start Date	October 2007
Production Facility	Gomez Hub in MC 711
Water Depth (feet)	2,416
Development Status	abandoned-2013
Number of Reservoirs	1
Age	late Miocene
Sedimentary deposit	channel fill
Trap	three-way closure against fault
Gas Recoverable Reserves (BCF)	47
API Oil Gravity	33.7
Pay Thickness (feet)	48 (net)
Upper Seal	shale
Lateral Seal	shale
Source Of Information	K. McCarty, pers comm., 2010

Figure 66. Mississippi Canyon (MC) 755 Anduin field. (A) Seismic profile. Reprinted with permission of Schlumberger. (B) Gamma-ray (GR) and resistivity log from the MC 755-1. See Figure 65A for location map and Figure 65B for seismic profile. See Figure 4 for the regional setting of the field. ILD = deep induction.

West Boreas Field, Figure 67

(A)

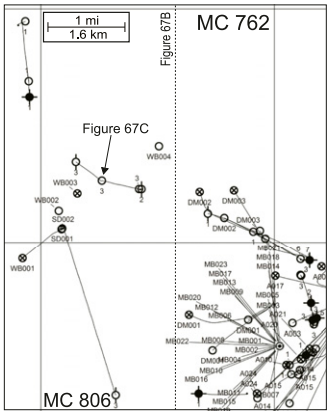

Field Name	West Boreas (Figure 67)
Block Numbers	MC 762
Partners	Shell (100.00%)
Discovery Date	March 2004
Production Start Date	February 2014
Production Facility	Subsea tie-back to Mars Olympus TLP in MC 807
Water Depth (feet)	3112
Development Status	producing
Age	late Miocene
Sedimentary deposit	channel fill-sheets
Trap	three-way closure against base of salt
Liquids Recoverable Reserves (MMbbl)	15 MMbl
Gas Recoverable Reserves (BCF)	20
Porosity (percent)	20-34
Permeability (mD)	300
Upper Seal	salt
Lateral Seal	shale
Source Of Information	Sloan and King, 2014
	T. Meckel, pers comm., 2010

(B)

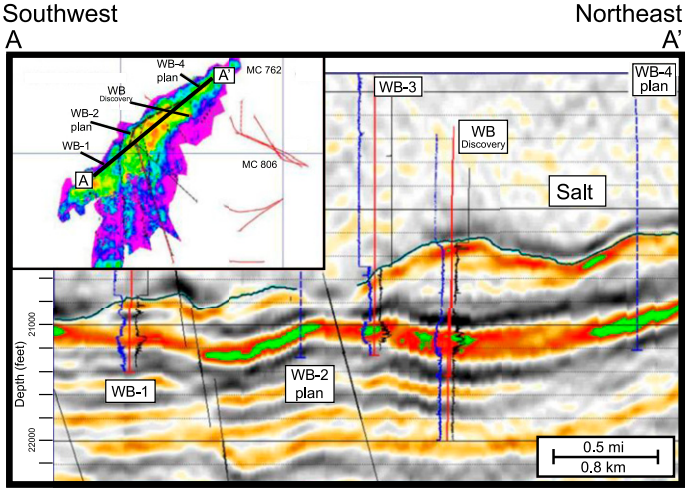

(C)

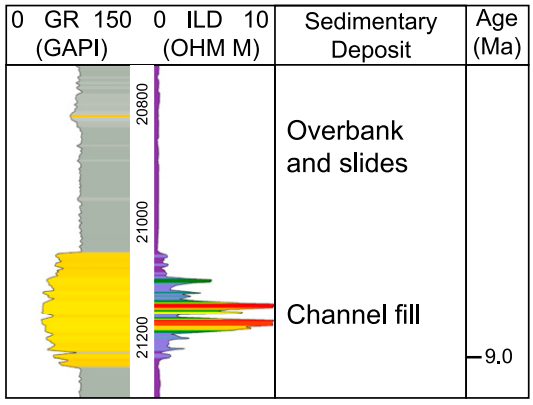

Figure 67. Mississippi Canyon (MC) 762 West Boreas field. (A) Location map for MC 762 West Boreas, MC 806 Deimos, and MC 807 Mars fields. Two different tension leg platforms (TLPs) are present in MC 807. The original TLP is located in central MC 807 and was completed in 1996. This TLP includes all wells labeled A001–A019 in blocks 807, 763, 806, 850, and 851. The Mars B (Olympus) Platform was competed in 2014 and lies along the western border of MC 807. The Mars B wells (MB001–MB024) are located in MC 806. The West Boreas subsea wells are labeled WB001–WB004 and SS001. The Deimos subsea wells are labeled DM001–DM004, and South Deimos are labeled SD001–SD002. (B) Seismic profile. After Sloan and King (2014). Inset map is an amplitude extraction from top reservoir. Locations of profile and wells are shown. Reprinted with permission of Society of Petroleum Engineers. (C) Gamma-ray (GR) and resistivity log. See Figure 4 for the regional setting of the field. ILD = deep induction.

Deimos Field, Figure 68

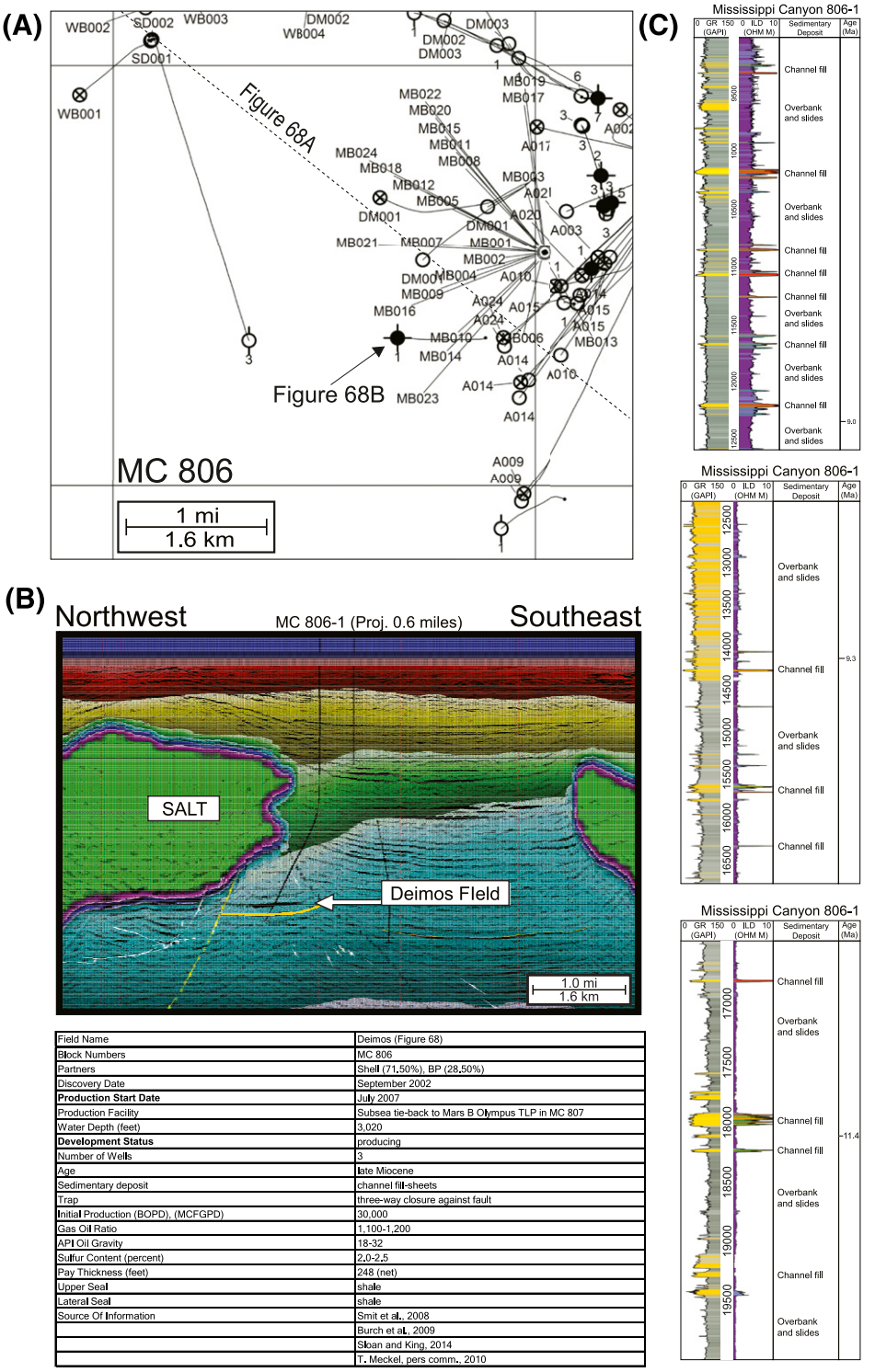

Field Name	Deimos (Figure 68)
Block Numbers	MC 806
Partners	Shell (71.50%), BP (28.50%)
Discovery Date	September 2002
Production Start Date	July 2007
Production Facility	Subsea tie-back to Mars B Olympus TLP in MC 807
Water Depth (feet)	3,020
Development Status	producing
Number of Wells	3
Age	late Miocene
Sedimentary deposit	channel fill-sheets
Trap	three-way closure against fault
Initial Production (BOPD), (MCFGPD)	30,000
Gas Oil Ratio	1,100-1,200
API Oil Gravity	18-32
Sulfur Content (percent)	2.0-2.5
Pay Thickness (feet)	248 (net)
Upper Seal	shale
Lateral Seal	shale
Source Of Information	Smit et al., 2008
	Burch et al., 2009
	Sloan and King, 2014
	T. Meckel, pers comm., 2010

Figure 68. Mississippi Canyon (MC) 806 Deimos field. (A) Location map. (B) Seismic profile. After Smit et al. (2008). Reprinted with permission of Society of Exploration Geophysicists. (C) Gamma-ray (GR) and resistivity log. See Figure 4 for the regional setting of the field. ILD = deep induction.

Mars Field, Figure 69

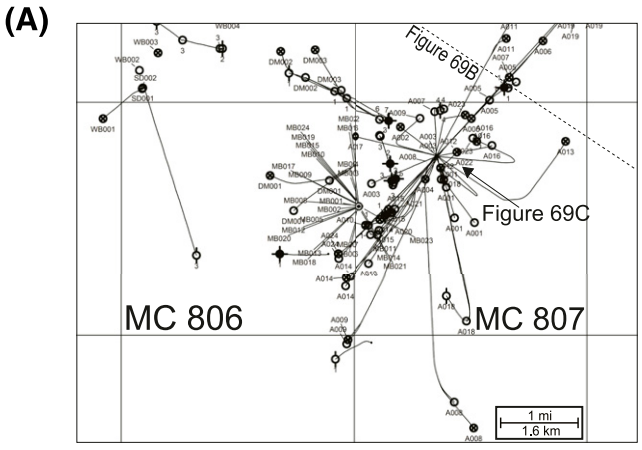

Field Name	Mars (Figure 69)
Block Numbers	MC 807, 762, 763, 806, 850, 851
Partners	Shell (71.50%), BP (28.50%)
Discovery Date	April 1989
Production Start Date	July 1996
Production Facility	Mars A TLP, Mars B Olympus TLP
Water Depth (feet)	2,957
Development Status	producing
Field Size (acres)	6,000
Number of Wells	16
Number of Reservoirs	10
Drive Mechanism	partial gas
Age	late Miocene to early Pliocene
Sedimentary deposit	channel fill-sheets
Trap	three-way closure against base of salt and faults
Liquids Recoverable Reserves (MMbbl)	660.2
Gas Recoverable Reserves (BCF)	755.88
Gas Oil Ratio	1,100-1,200
Porosity (percent)	20-31
Permeability (mD)	21-2,440
Water Saturation Range (percent)	17-40
Initial Reservoir Temperature Range (°F)	108-179
Initial Reservoir Pressure Range (PSI)	6,126-12,716
API Oil Gravity	30.5 (24-32)
Sulfur Content (percent)	1.5-2.0
Oil Column (feet)	3,000
Upper Seal	salt (deeper reservoirs), shale (shallow reservoirs)
Lateral Seal	shale
Reservoir Intervals (Subsea true vertical depth-feet)	10,500-25,000
Source Of Information	Mahaffie, 1994; Chapin et al. 1996; Reynolds, 2000;
	Cumming, 2002
	Meckel et al., 2002
	Kabir et al., 2006
	Weiland et al., 2008
	Stairr at al., 2011
	Tatanova and Hatchell, 2012
	Cossey and Associates Inc.

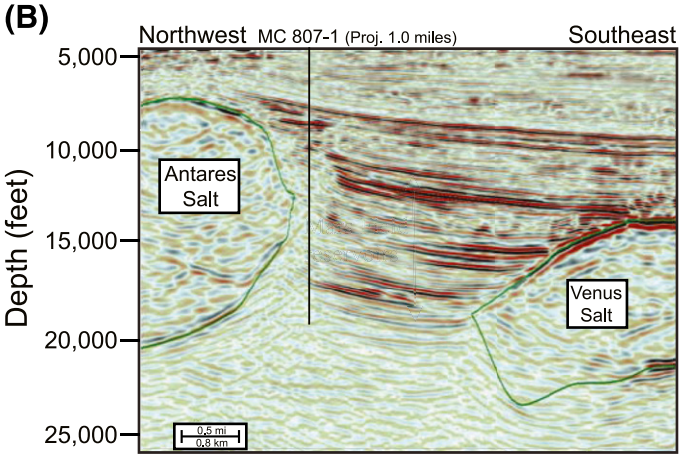

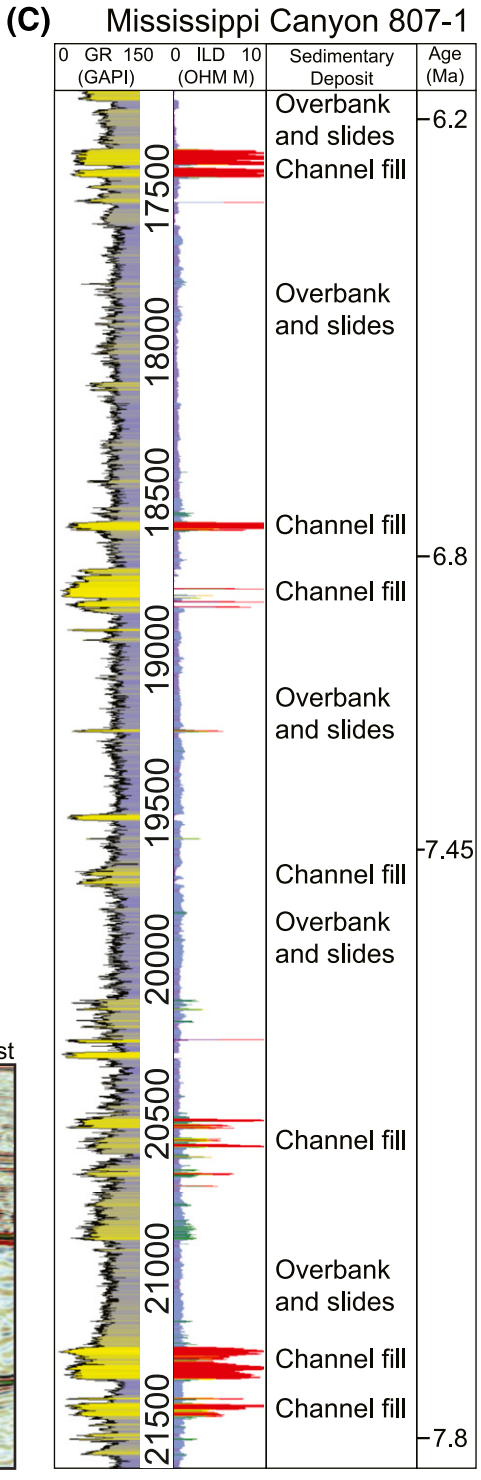

Figure 69. Mississippi Canyon (MC) 807 Mars field. (A) Location map. (B) Seismic profile. After Kabir et al. (2006). Reprinted with permission of Society of Exploration Geophysicists. (C) Gamma-ray (GR) and resistivity log. See Figure 4 for the regional setting of the field. ILD = deep induction.

King Field, Figure 70

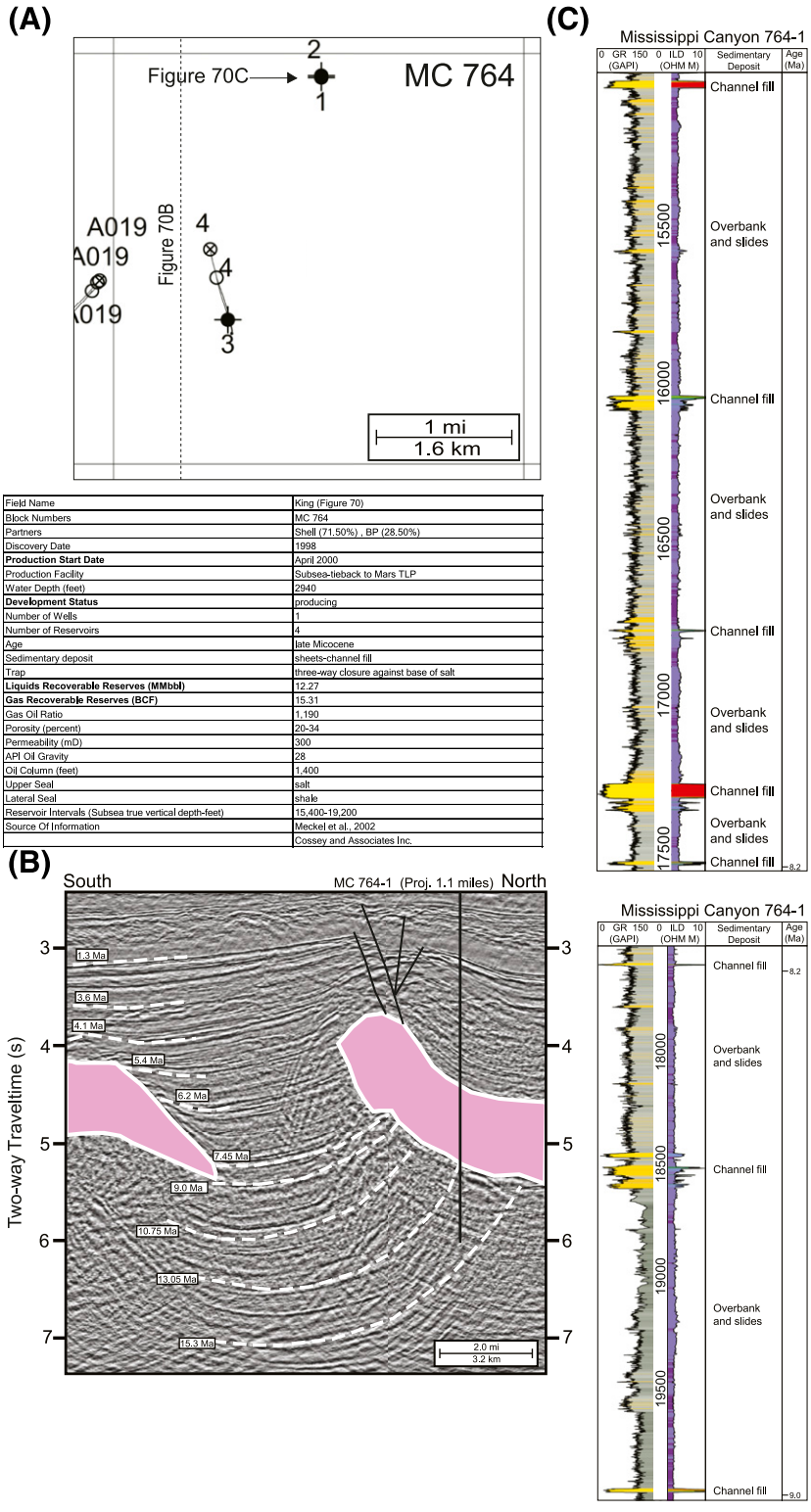

Field Name	King (Figure 70)
Block Numbers	MC 764
Partners	Shell (71.50%) , BP (28.50%)
Discovery Date	1998
Production Start Date	April 2000
Production Facility	Subsea-tieback to Mars TLP
Water Depth (feet)	2940
Development Status	producing
Number of Wells	1
Number of Reservoirs	4
Age	late Micocene
Sedimentary deposit	sheets-channel fill
Trap	three-way closure against base of salt
Liquids Recoverable Reserves (MMbbl)	12.27
Gas Recoverable Reserves (BCF)	15.31
Gas Oil Ratio	1,190
Porosity (percent)	20-34
Permeability (mD)	300
API Oil Gravity	28
Oil Column (feet)	1,400
Upper Seal	salt
Lateral Seal	shale
Reservoir Intervals (Subsea true vertical depth-feet)	15,400-19,200
Source Of Information	Meckel et al., 2002
	Cossey and Associates Inc.

Figure 70. Mississippi Canyon (MC) 764 King field. (A) Location map. (B) Seismic profile. Reprinted with permission of Schlumberger. (C) Gamma-ray (GR) and resistivity log. See Figure 4 for the regional setting of the field. ILD = deep induction.

Princess Field, Figure 71

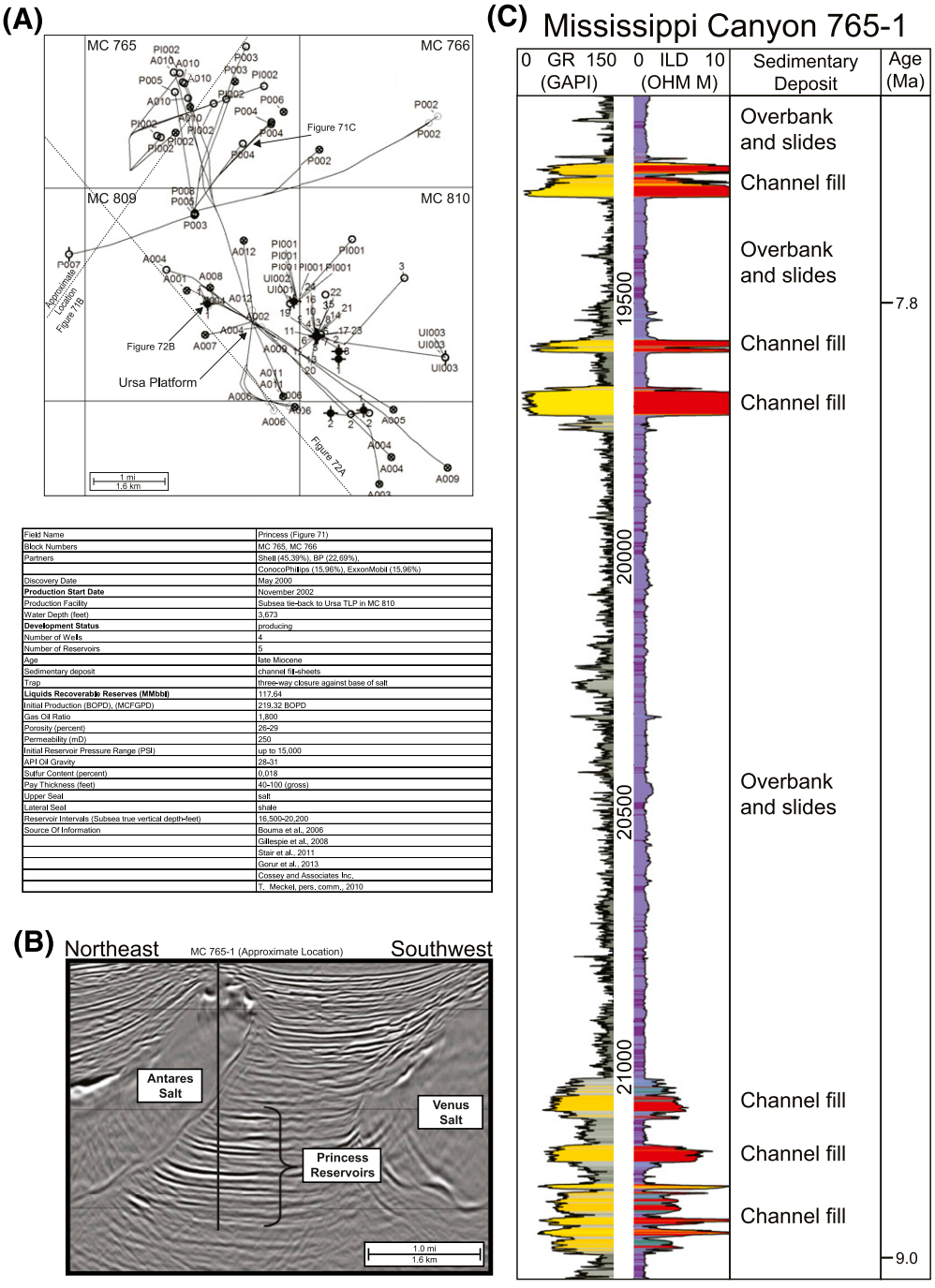

Field Name	Princess (Figure 71)
Block Numbers	MC 765, MC 766
Partners	Shell (45.39%), BP (22.69%), ConocoPhillips (15.96%), ExxonMobil (15.96%)
Discovery Date	May 2000
Production Start Date	November 2002
Production Facility	Subsea tie-back to Ursa TLP in MC 810
Water Depth (feet)	3,673
Development Status	producing
Number of Wells	4
Number of Reservoirs	5
Age	late Miocene
Sedimentary deposit	channel fill-sheets
Trap	three-way closure against base of salt
Liquids Recoverable Reserves (MMbbl)	117.64
Initial Production (BOPD), (MCFGPD)	219.32 BOPD
Gas Oil Ratio	1,800
Porosity (percent)	26-29
Permeability (mD)	250
Initial Reservoir Pressure Range (PSI)	up to 15,000
API Oil Gravity	28-31
Sulfur Content (percent)	0.018
Pay Thickness (feet)	40-100 (gross)
Upper Seal	salt
Lateral Seal	shale
Reservoir Intervals (Subsea true vertical depth-feet)	16,500-20,200
Source Of Information	Bouma et al., 2006
	Gillespie et al., 2008
	Stair et al., 2011
	Gorur et al., 2013
	Cossey and Associates Inc.,
	T. Meckel, pers. comm., 2010

Figure 71. Mississippi Canyon (MC) 765–766 Princess field. (A) Location map for MC 765–766 Princess and MC 809 Ursa fields. The tension leg platform (TLP) for Ursa field is located in the southeast quadrant of MC 809. The Princess subsea wells (P001–P008 in MC 765, 766) are tied back to a drill center in northern MC 809, which is subsequently tied back to the Ursa platform; PI001 and PI002 are injector wells. The Ursa subsea wells are A001 to A012; UI001 to UI003 are injector wells. The drilling center in the southwest quadrant of MC 810 was the original location of the Ursa TLP, before the failure of the manifolds (Winker and Stancliffe, 2007). The TLP was eventually moved to its current location in MC 809. (B) Seismic profile. After Bouma et al. (2006). Reprinted with permission of Shell Oil. (C) Gamma-ray (GR) and resistivity log. See Figure 4 for the regional setting of the field. ILD = deep induction.

Ursa Field, Figure 72

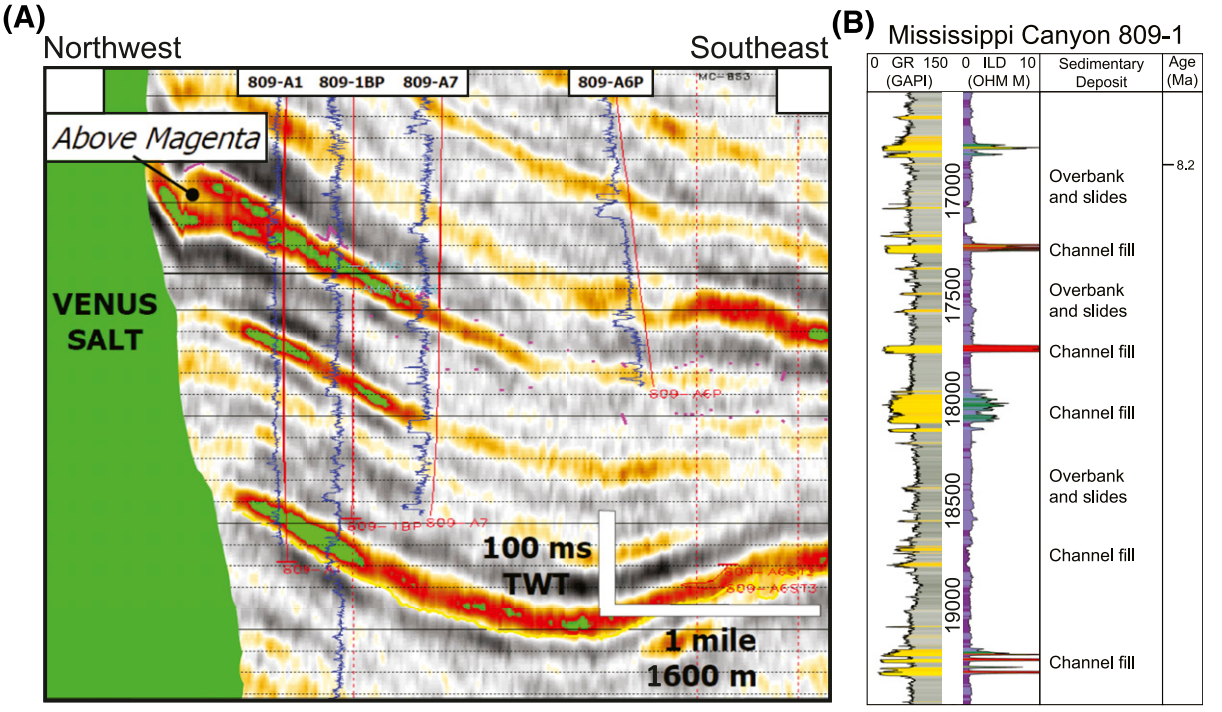

Field Name	Ursa (Figure 72)
Block Numbers	MC 809, 808, 810, 852, 854
Partners	Shell (45.39%), BP (22.69%),
	ConocoPhillips (15.96%), ExxonMobil (15.96%)
Discovery Date	January 1991
Production Start Date	April 1999
Production Facility	Subsea tie-back to Ursa TLP in MC 810
Water Depth (feet)	4,019
Development Status	producing
Number of Wells	14
Number of Reservoirs	3
Age	late Miocene to early Pliocene
Sedimentary deposit	channel fill- sheets
Trap	three-way closure against base of salt
Liquids Recoverable Reserves (MMbbl)	375
Gas Recoverable Reserves (BCF)	553
Gas Oil Ratio	1,400
Porosity (percent)	24-30
Permeability (mD)	25-625
Initial Reservoir Temperature Range (°F)	175
API Oil Gravity	27.3-30
Sulfur Content (percent)	1.5-1.9
Upper Seal	salt
Lateral Seal	shale
Reservoir Intervals (Subsea true vertical depth-feet)	12,000-19,300
Source Of Information	Meckel, 2002
	Cossey and Associates Inc.

Figure 72. Mississippi Canyon (MC) 809 Ursa field. (A) Seismic profile. After Meckel et al. (2002). Reproduced with the permission of the Gulf Coast Section SEPM Foundation, and any other use requires their permission. (B) Gamma-ray (GR) and resistivity log. See Figure 71A for location of figures. See Figure 4 for the regional setting of the field. ILD = deep induction.

Goldfinger Field, Figure 73

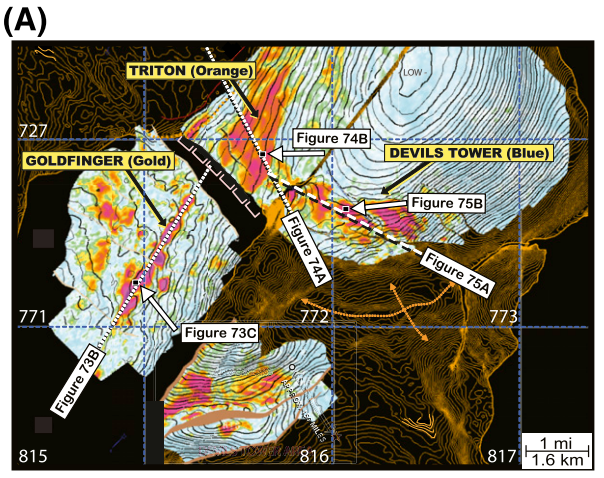

Field Name	Goldfinger (Figure 73)
Block Numbers	MC 771
Partners	Eni (75.00%), Marubeni (25.00%)
Discovery Date	May 2004
Production Start Date	December 2005
Production Facility	Subsea tie-back to Devil's Tower SPAR in MC 773
Water Depth (feet)	5,455
Development Status	producing
Number of Wells	1
Number of Reservoirs	1
Age	late Miocene
Sedimentary deposit	channel fill
Trap	stratigraphic
Liquids Recoverable Reserves (MMbbl)	39
Gas Recoverable Reserves (BCF)	28
Gas Oil Ratio	1,450
API Oil Gravity	28-32
Sulfur Content (percent)	0.012
Upper Seal	shale
Lateral Seal	shale
Source Of Information	Wieg and Fingleton, 2004

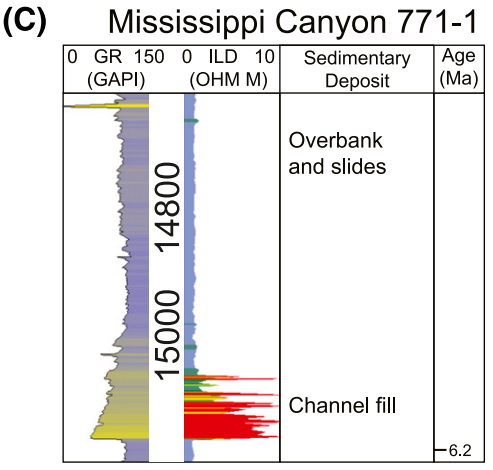

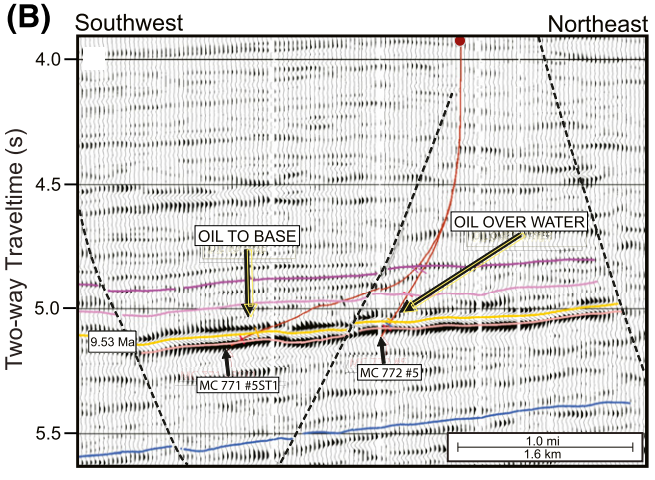

Figure 73. Mississippi Canyon (MC) 771 Goldfinger field. (A) Location map of MC 771 Goldfinger field, MC 772 Triton field, and MC 773 Devil's Tower field. Amplitude extraction of a lower Pliocene horizon is shown superposed on nonidentified structure contour (orange lines). After Wieg and Fingleton (2004). (B) Seismic profile (after Wieg and Fingleton, 2004). (C) Gamma-ray (GR) and resistivity log. Figures (A) and (B) are republished by permission of the Gulf Coast Association of Geological Societies, whose permission is required for further publication use. See Figure 4 for the regional setting of the field. ILD = deep induction.

Triton Field, Figure 74

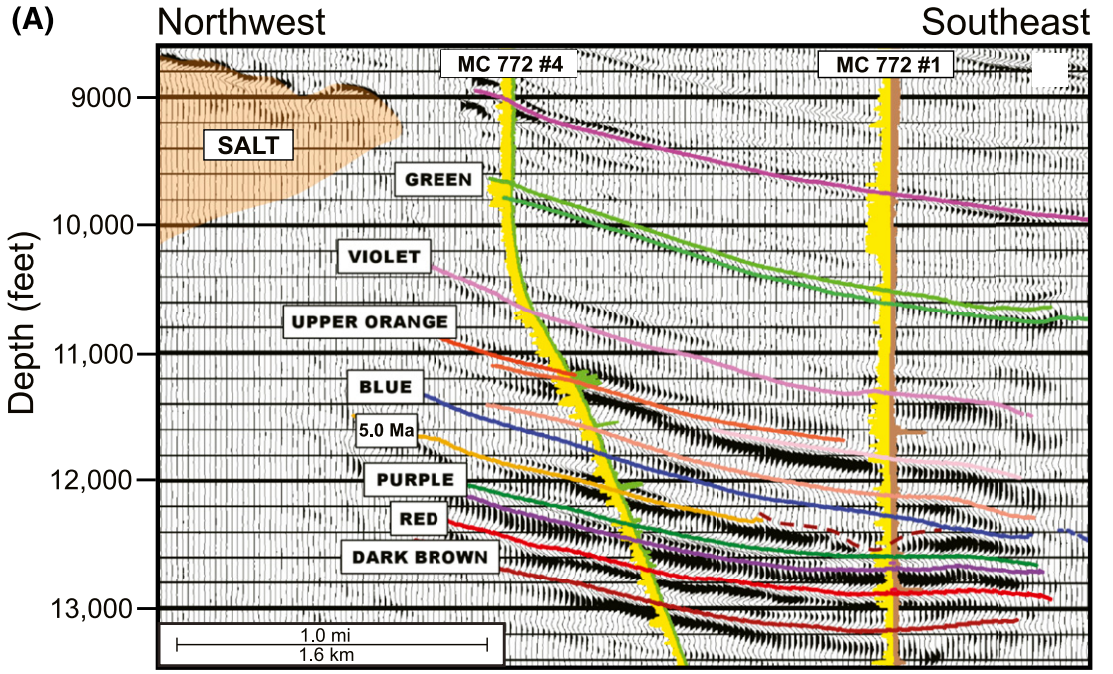

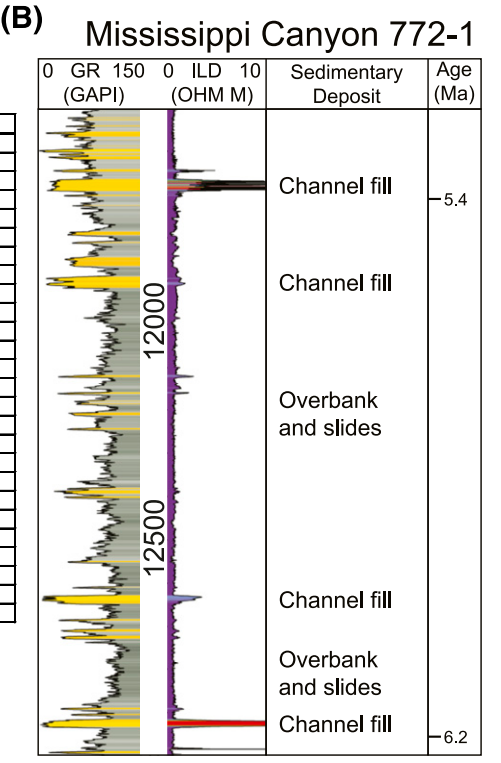

Field Name	Triton (Figure 74)
Block Numbers	MC 772
Partners	Eni (75.00%), Marubeni (25.00%)
Discovery Date	February 2004
Production Start Date	June 2005
Production Facility	Subsea tie-back to Devil's Tower SPAR in MC 773
Water Depth (feet)	5,643
Development Status	producing
Number of Wells	2
Number of Reservoirs	3
Age	late Miocene to early Pliocene
Sedimentary deposit	channel fill
Trap	three-way closure against fault
Liquids Recoverable Reserves (MMbbl)	39
Gas Recoverable Reserves (BCF)	28
Initial Production (BOPD), (MCFGPD)	13,000 BOPD
Gas Oil Ratio	675
API Oil Gravity	28-32
Sulfur Content (percent)	0.007
Upper Seal	shale
Lateral Seal	shale
Reservoir Intervals (Subsea true vertical depth-feet)	11660-11690
	12625-12645
	12910-12930
Source Of Information	Wieg and Fingleton, 2004
	Monson and Bustamante, 2005
	Cossey and Associates Inc.

Figure 74. Mississippi Canyon (MC) 772 Triton field. (A) Seismic profile across the MC 772 Triton field (after Wieg and Fingleton, 2004). Republished by permission of the Gulf Coast Association of Geological Societies, whose permission is required for further publication use. (B) Gamma-ray (GR) and resistivity log. See Figure 73A for location of seismic profile and well. See Figure 4 for the regional setting of the field. ILD = deep induction.

Devil's Tower Field, Figure 75

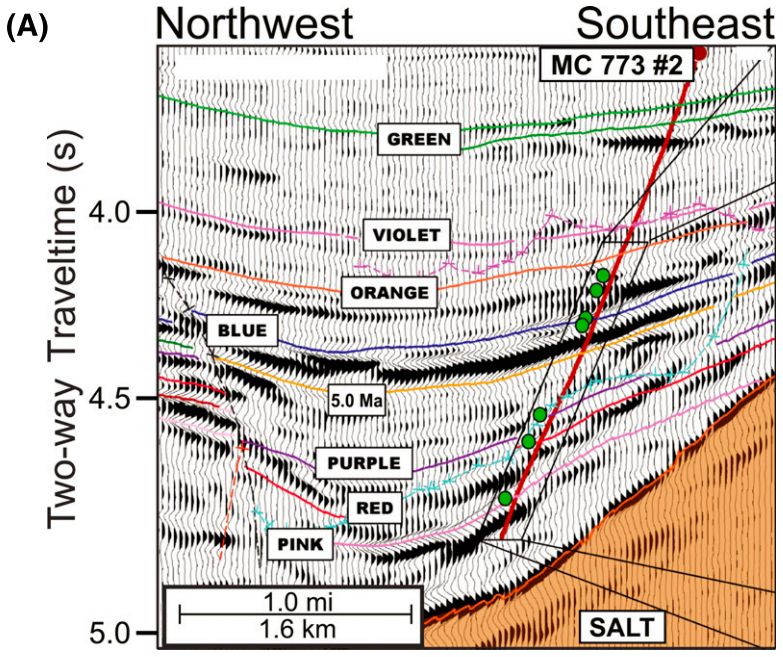

Field Name	Devil's Tower (Figure 75)
Block Numbers	MC 773
Partners	Eni (75.00%), Marubeni (25.00%)
Discovery Date	February 2000
Production Start Date	May 2004
Production Facility	Subsea tie-back to Devil's Tower SPAR in MC 773
Water Depth (feet)	5,643
Development Status	producing
Field Size (acres)	500
Number of Wells	6
Number of Reservoirs	8
Drive Mechanism	aquifer
Age	late Miocene to early Pliocene
Sedimentary deposit	channel fill
Trap	three-way closure against salt flank
Liquids Recoverable Reserves (MMbbl)	74
Gas Recoverable Reserves (BCF)	63.19
Gas Oil Ratio	1,200
Porosity (percent)	27-32
Permeability (mD)	95-2000
Initial Reservoir Temperature Range (°F)	143
Initial Reservoir Pressure Range (PSI)	8,970
API Oil Gravity	28-32%
Sulfur Content (percent)	1.5
Oil Column (feet)	1,400
Upper Seal	shale
Lateral Seal	shale
Reservoir Intervals (Subsea true vertical depth-feet)	12,200-14,200
Source Of Information	Wieg and Fingleton, 2004
	Cossey and Associates Inc.
	Fontana et al., 2015

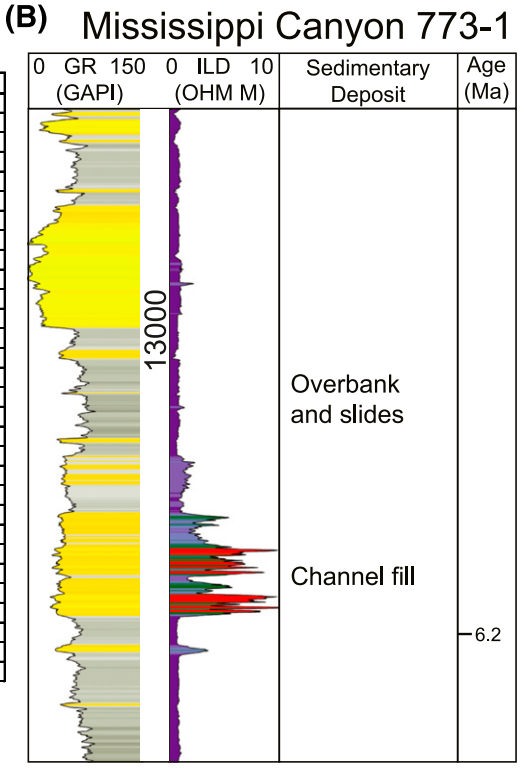

Figure 75. Mississippi Canyon (MC) 773 Devil's Tower. (A) Seismic profile (after Wieg and Fingleton, 2004). Republished by permission of the Gulf Coast Association of Geological Societies, whose permission is required for further publication use. (B) Gamma-ray (GR) and resistivity log. See Figure 73A for location of seismic profile and well. See Figure 4 for the regional setting of the field. ILD = deep induction.

Thunder Horse North Field, Figure 76

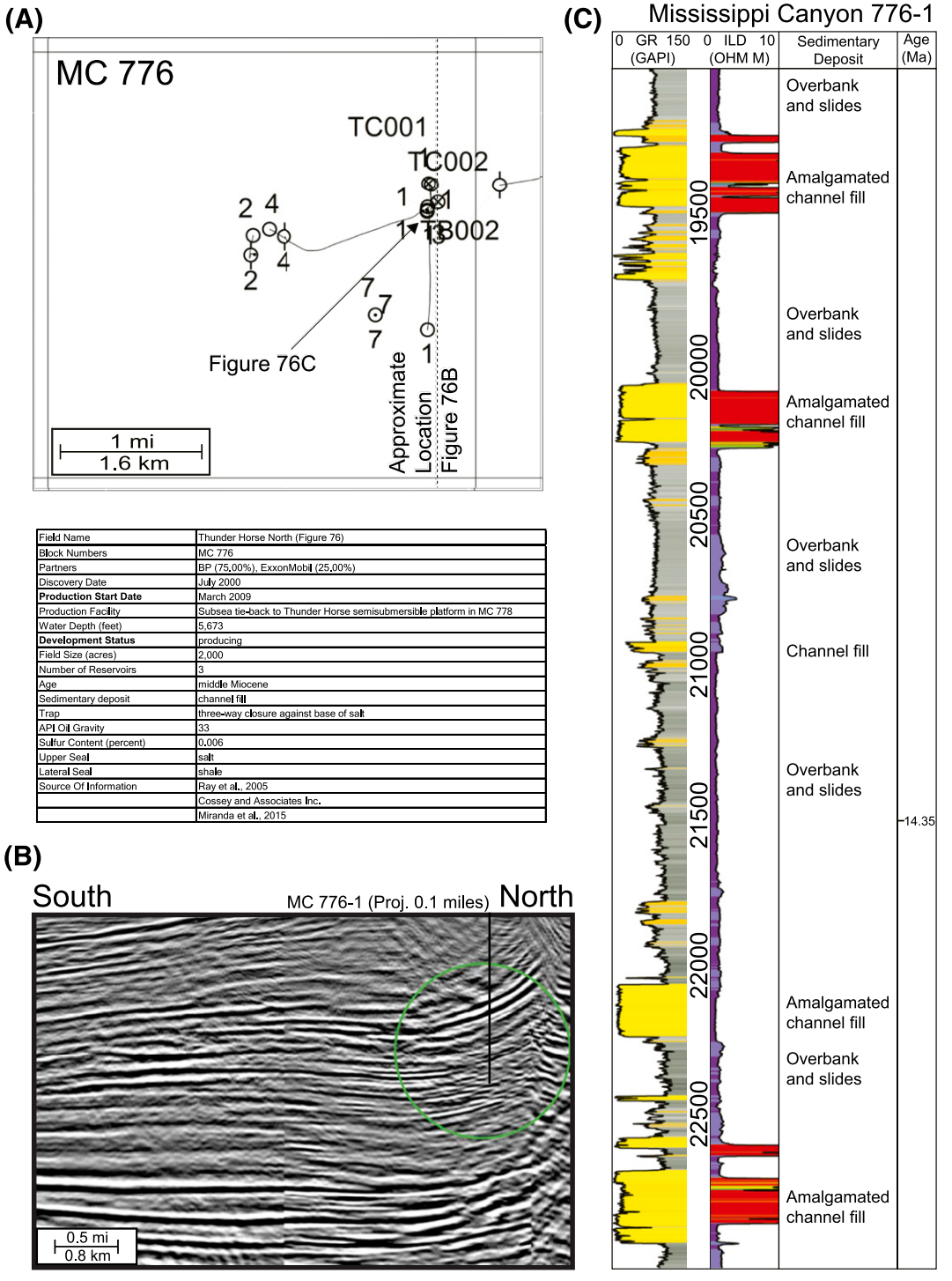

Field Name	Thunder Horse North (Figure 76)
Block Numbers	MC 776
Partners	BP (75,00%), ExxonMobil (25,00%)
Discovery Date	July 2000
Production Start Date	March 2009
Production Facility	Subsea tie-back to Thunder Horse semisubmersible platform in MC 778
Water Depth (feet)	5,673
Development Status	producing
Field Size (acres)	2,000
Number of Reservoirs	3
Age	middle Miocene
Sedimentary deposit	channel fill
Trap	three-way closure against base of salt
API Oil Gravity	33
Sulfur Content (percent)	0,006
Upper Seal	salt
Lateral Seal	shale
Source Of Information	Ray et al., 2005
	Cossey and Associates Inc.
	Miranda et al., 2015

Figure 76. Mississippi Canyon (MC) 776 Thunder Horse North field. (A) Location map. (B) Seismic profile. After Ray et al. (2005). Reprinted with permission of Society of Exploration Geophysicists. (C) Gamma-ray (GR) and resistivity log. See Figure 4 for the regional setting of the field. ILD = deep induction.

Thunder Horse Field, Figure 77

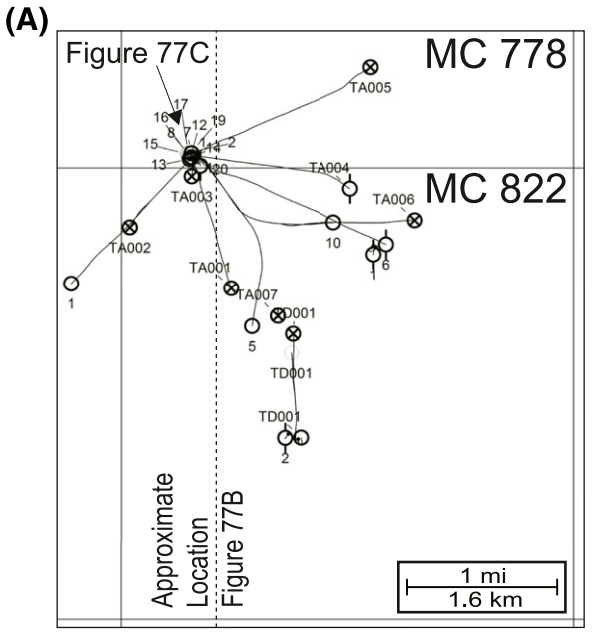

Field Name	Thunder Horse (Figure 77)
Block Numbers	MC 778, MC 822
Partners	BP (75.00%), ExxonMobil (25.00%)
Discovery Date	July 1999
Production Start Date	December 2008
Production Facility	Subsea tie-back to Thunder Horse semisubmersible platform in MC 778
Water Depth (feet)	6,036
Development Status	producing
Field Size (acres)	4,700
Number of Wells	25 scheduled
Number of Reservoirs	5
Age	middle Miocene
Sedimentary deposit	channel fills-sheets
Trap	four-way closure (extensional anticline-turtle)
Liquids Recoverable Reserves (MMbbl)	786.13
Gas Recoverable Reserves (BCF)	668,21
Initial Production (BOPD), (MCFGPD)	300,000 BOPD (from 7 wells)
Gas Oil Ratio	590
Porosity (percent)	24
Permeability (mD)	24-617
Initial Reservoir Temperature Range (°F)	275
Initial Reservoir Pressure Range (PSI)	17,404
API Oil Gravity	32.7
Upper Seal	shale
Lateral Seal	shale
Reservoir Intervals (Subsea true vertical depth-feet)	22,250-24,650
Source Of Information	Todd and Replogle, 2010
	Cossey and Associates Inc.
	Arnold et al., 2010

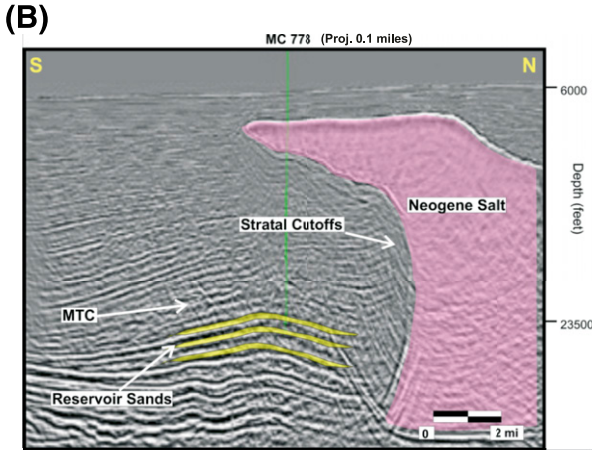

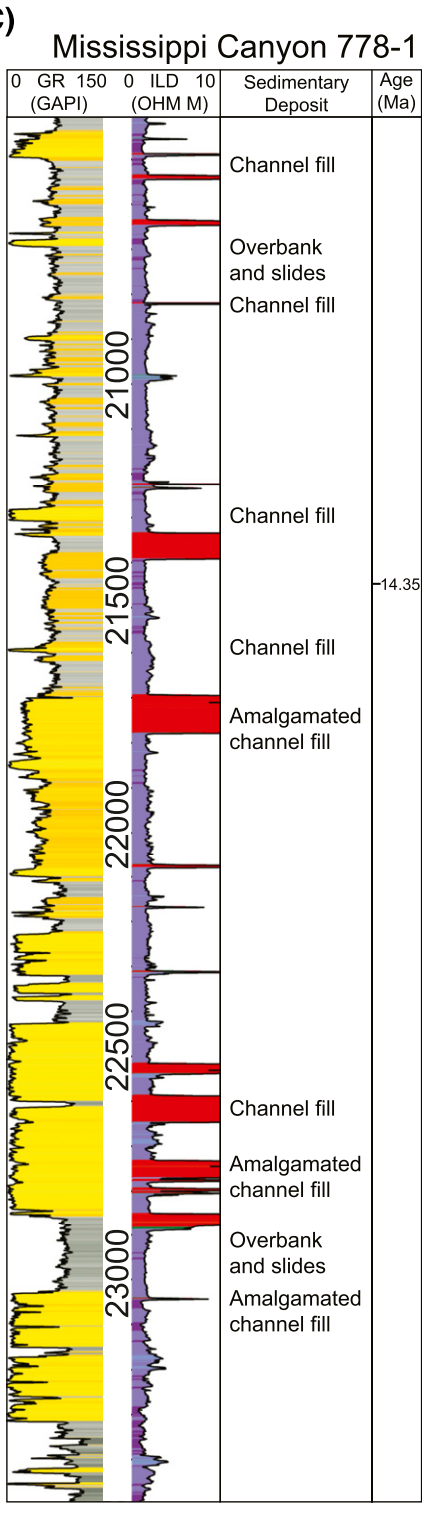

Figure 77. Mississippi Canyon (MC) 778 Thunder Horse field, (A) Location map. (B) Seismic profile. After Lapinski (2003). (C) Gamma-ray (GR) and resistivity log. See Figure 4 for the regional setting of the field. ILD = deep induction.

Dantzler Field, Figure 78

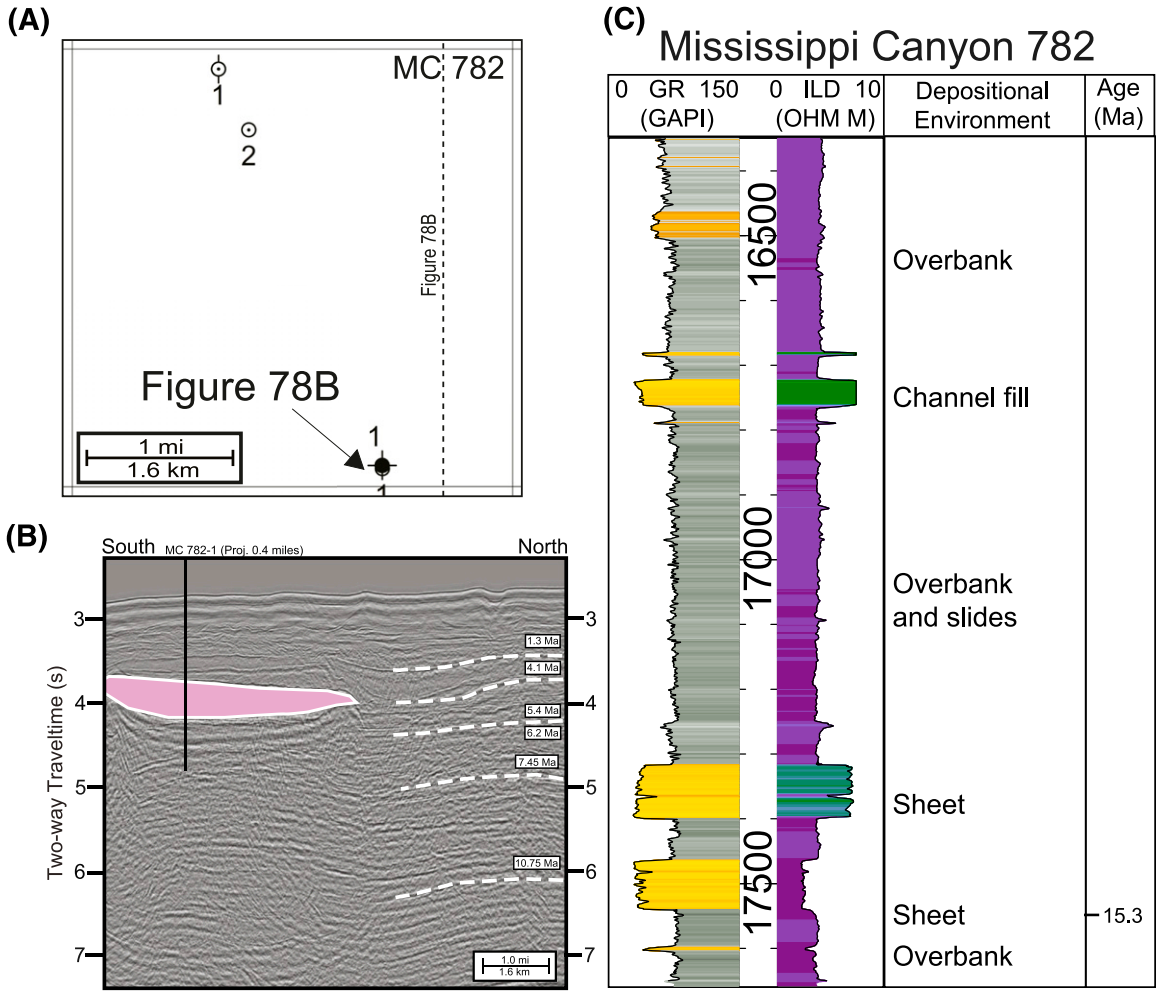

Field Name	Dantzler (Figure 78)
Block Numbers	MC 782
Partners	Noble (45%), W&T Offshore (20%), ILX Prosp (17.5%)
	Ridgewood (17.5%)
Discovery Date	December 2013
Production Start Date	November 2015
Production Facility	Subsea tie-back to Thunder Hawk Floating Produciton Unit in MC 736
Water Depth (feet)	6613
Development Status	producing
Number of Wells	2
Number of Reservoirs	2
Age	late Miocene
Sedimentary deposit	channel fill-levee
Trap	three-way closure against salt flank
Liquids Recoverable Reserves (MMbbl)	65-100
Pay Thickness (feet)	120 (gross)
Oil Column (feet)	120
Upper Seal	shale
Lateral Seal	shale
Source Of Information	D. Huffman, pers. comm., 2015

Figure 78. Mississippi Canyon (MC) 782 Dantzler field. (A) Location map. (B) Seismic profile. Reprinted with permission of Schlumberger. (C) Gamma-ray (GR) and resistivity log. See Figure 4 for the regional setting of the field.

Gladden Field, Figure 79

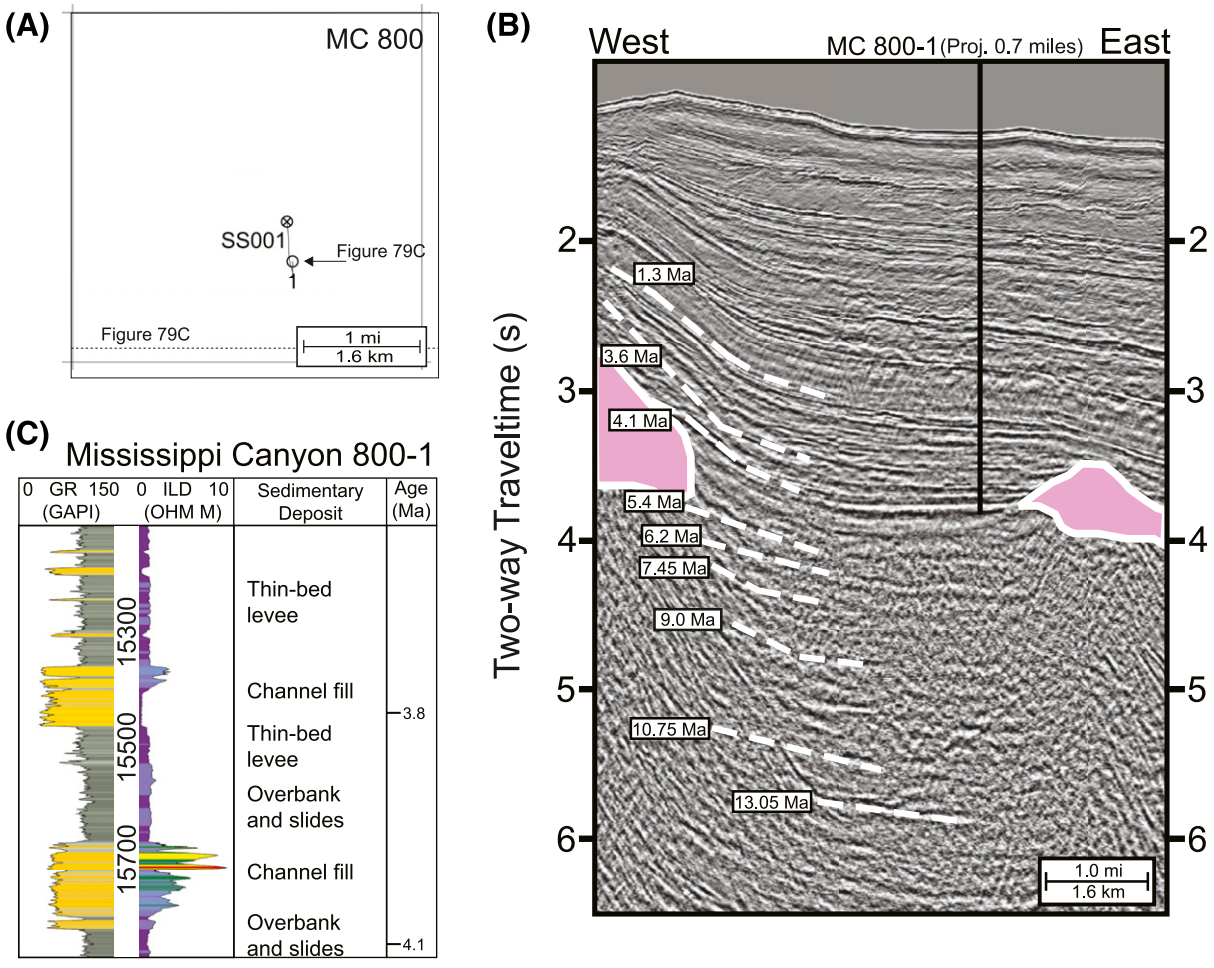

Field Name	Gladden (Figure 79)
Block Numbers	MC 800
Partners	W&T (57.50%) , Deep Gulf Energy (20%)
	Arena Energy (12.50%) , Continental Land and Fur (10%)
Discovery Date	2008
Production Start Date	February 2011
Production Facility	Subsea tie-back MC 582 Medusa
Water Depth (feet)	3,116
Development Status	producing
Number of Wells	1
Number of Reservoirs	1
Drive Mechanism	depletion
Age	early Pliocene
Sedimentary deposit	channel fill-levee
Trap	three-way closure against salt flank
Liquids Recoverable Reserves (MMbbl)	3.9
Gas Recoverable Reserves (BCF)	5.7
Initial Production (BOPD), (MCFGPD)	5,125 BOPD, 6,169 MCFGPD
Gas Oil Ratio	1,204
Porosity (percent)	30-32
Permeability (mD)	1,000
API Oil Gravity	32.5
Pay Thickness (feet)	130 (gross)
Oil Column (feet)	130
Upper Seal	shale
Lateral Seal	shale
Reservoir Intervals (Subsea true vertical depth-feet)	15,592-15,722
Source Of Information	D. Huffman, pers. comm., 2015

Figure 79. Mississippi Canyon (MC) 800 Gladden field. (A) Location map. (B) Seismic profile. Reprinted with permission of Schlumberger. (C) Gamma-ray (GR) and resistivity log. See Figure 4 for the regional setting of the field. ILD = deep induction.

MC 837 Field, Figure 80

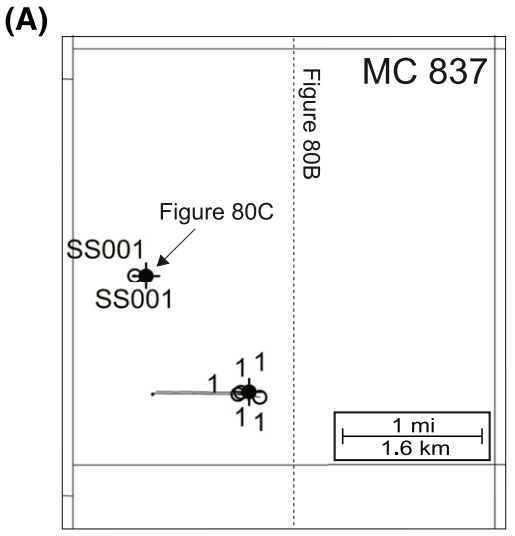

Field Name	MC 837 (Figure 80)
Block Numbers	MC 837
Partners	Walter (100%)
Discovery Date	January 2001
Production Start Date	January 2004
Production Facility	Subsea tie-back to Grand Isle 115
Water Depth (feet)	1520
Development Status	abandoned-2007
Number of Wells	2
Number of Reservoirs	2
Drive Mechanism	water
Age	Pleistocene
Sedimentary deposit	channel fill-thin bed levee
Trap	three-way closure against fault
Liquids Recoverable Reserves (MMbbl)	3,8 bcf
Gas Column (feet)	141
Upper Seal	shale
Lateral Seal	shale
Reservoir Intervals (Subsea true vertical depth-feet)	6,288-6,370
Source Of Information	M, Jobe, pers. comm,. 2015

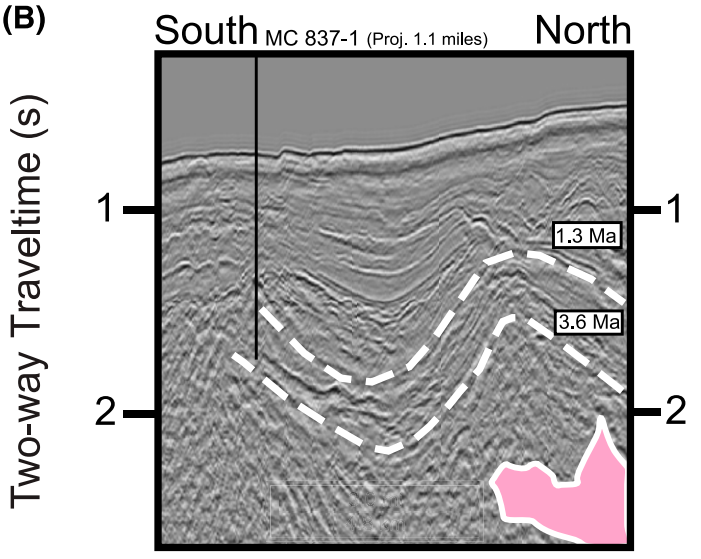

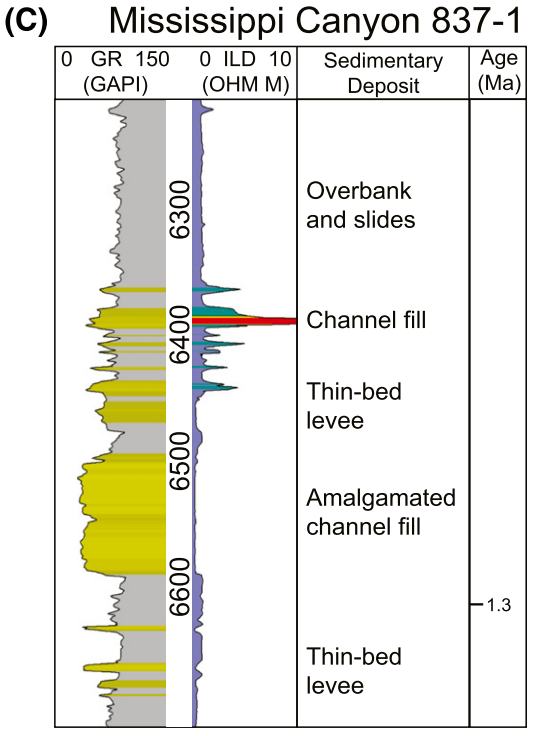

Figure 80. Mississippi Canyon (MC) 837 field. (A) Location map. (B) Seismic profile. Reprinted with permission of Schlumberger. (C) Gamma-ray (GR) and resistivity log. See Figure 4 for the regional setting of the field. ILD = deep induction.

Callisto Field, Figure 81

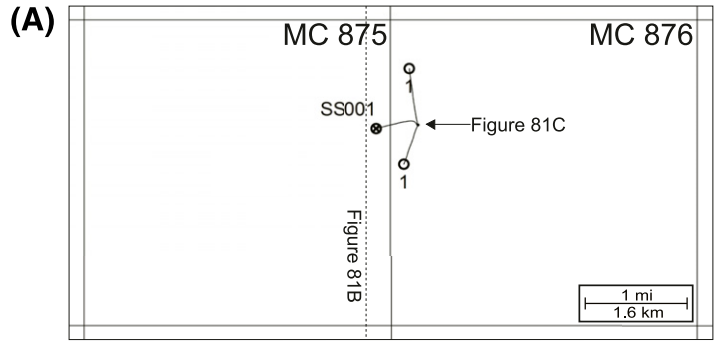

Field Name	Callisto (Figure 81)
Block Numbers	MC 876
Partners	Anadarko (100%)
Discovery Date	April 2001
Production Start Date	2011
Production Facility	Subsea tie-back to Independence Hub in MC 920
Water Depth (feet)	7940
Development Status	abandoned-2015
Number of Wells	3
Number of Reservoirs	3
Age	middle to late Miocene
Sedimentary deposit	channel fill
Trap	four-way closure against fault
Gas Recoverable Reserves (BCF)	100
Porosity (percent)	27-31
Permeability (mD)	234-1,400
Upper Seal	shale
Lateral Seal	shale
Reservoir Intervals (Subsea true vertical depth-feet)	15,600-17,500
Source Of Information	Cossey and Associates Inc.

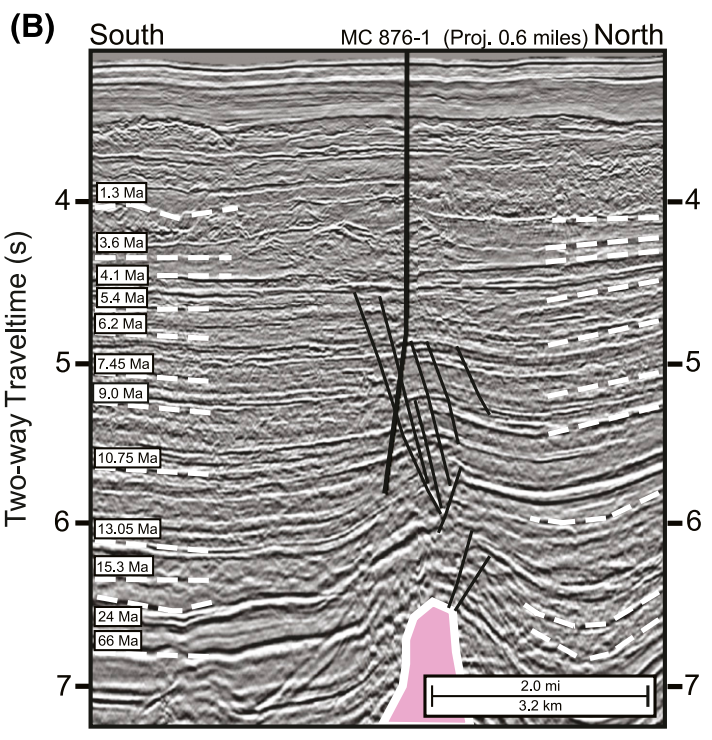

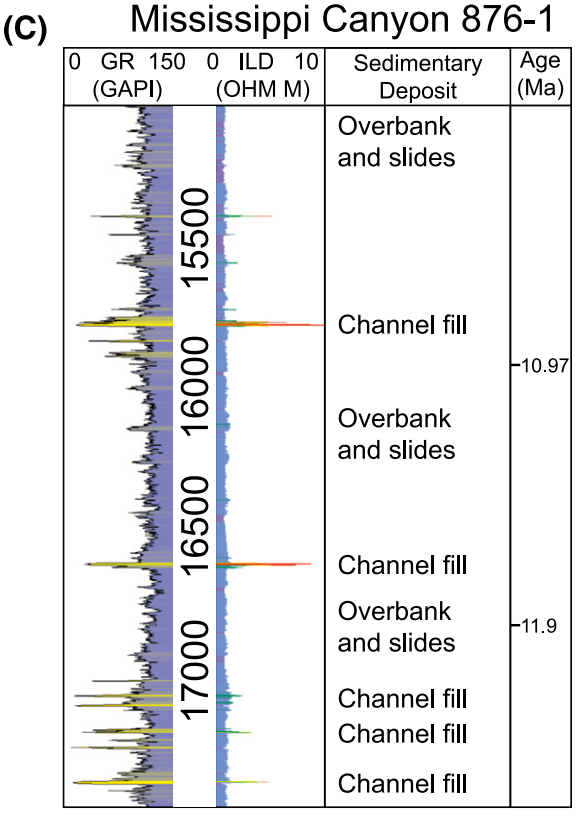

Figure 81. Mississippi Canyon (MC) 876 Callisto field. (A) Location map. (B) Seismic profile. Reprinted with permission of Schlumberger. (C) Gamma-ray (GR) and resistivity log. See Figure 4 for the regional setting of the field. ILD = deep induction.

Crosby Field, Figure 82

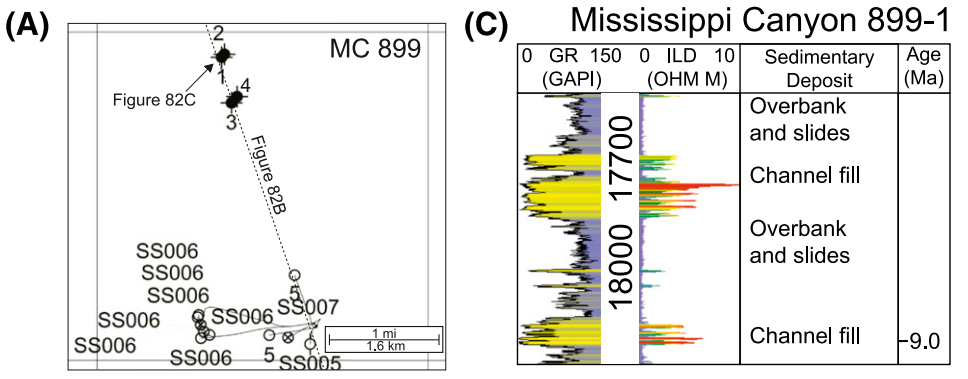

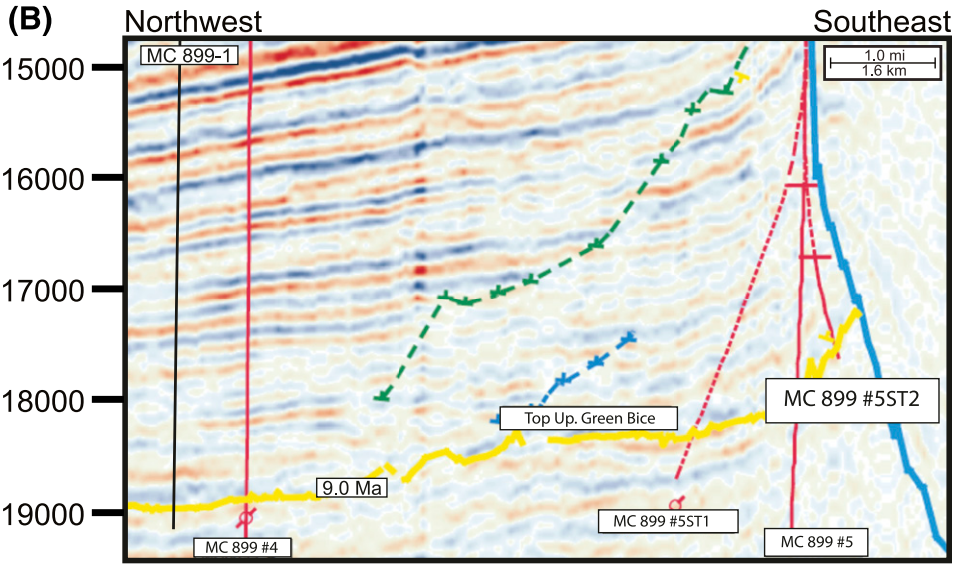

Field Name	Crosby (Figure 82)
Block Numbers	MC 899, MC 898
Partners	Shell (50.00%), BP (50.00%)
Discovery Date	December 1999
Production Start Date	December 2001
Production Facility	Subsea tie-back to Ursa in MC 810
Water Depth (feet)	4,072
Development Status	producing
Field Size (acres)	1,100
Number of Wells	3
Number of Reservoirs	3
Age	late Miocene
Sedimentary deposit	channel fill
Trap	three-way closure against base of salt
Liquids Recoverable Reserves (MMbbl)	38.16
Gas Recoverable Reserves (BCF)	51.37
Gas Oil Ratio	1,874
Porosity (percent)	22.5
Permeability (mD)	63-454
Initial Reservoir Temperature Range (°F)	178
Initial Reservoir Pressure Range (PSI)	12639
API Oil Gravity	24-30
Sulfur Content (percent)	0.02
Pay Thickness (feet)	425 (net)
Upper Seal	salt
Lateral Seal	shale
Reservoir Intervals (Subsea true vertical depth-feet)	17,000-18,000
Source Of Information	Kasten and Thompson, 2002
	Meckel, 2002
	Cossey and Associates Inc.

Figure 82. Mississippi Canyon (MC) 899 Crosby field. (A) Location map. (B) Seismic profile. After Kasten and Thompson (2002). Dashed blue lines and green lines indicate the fault traces between the number 4 and 5 wells. Green Bice horizon is 9.0 Ma (Meckel et al., 2002) Reproduced with the permission of the Gulf Coast Section SEPM Foundation, and any other use requires their permission. (C) Gamma-ray (GR) and resistivity log. See Figure 4 for the regional setting of the field. ILD = deep induction.

Europa Field, Figure 83

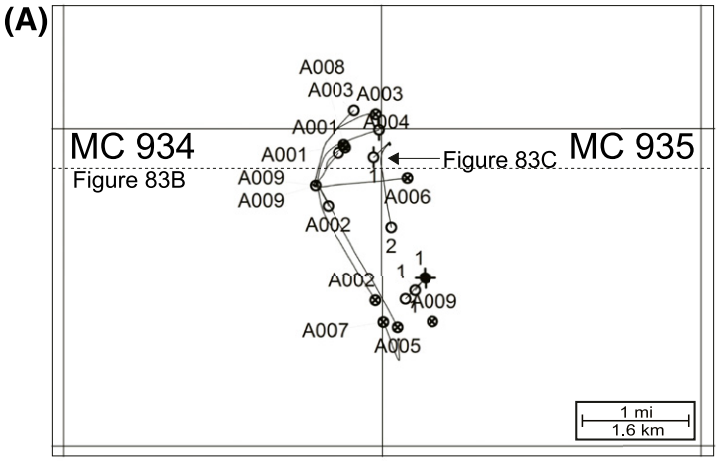

Field Name	Europa (Figure 83)
Block Numbers	MC 935, MC 890, MC 891, MC 934
Partners	Shell (33.67%), BP (33.33%),
	Eni (32.00%), ConocoPhillips (1.00%)
Discovery Date	January 1994
Production Start Date	January 2000
Production Facility	Subsea tie-back to Mars in MC 807
Water Depth (feet)	3,942
Development Status	producing
Field Size (acres)	1,600
Number of Reservoirs	4
Drive Mechanism	water
Age	late Miocene
Sedimentary deposit	channel fill
Trap	three-way closure suprasalt salt flank
Liquids Recoverable Reserves (MMbbl)	64.92
Gas Recoverable Reserves (BCF)	104.61
Gas Oil Ratio	850
Porosity (percent)	29
Permeability (mD)	69-1,308
Initial Reservoir Temperature Range (°F)	165
Initial Reservoir Pressure Range (PSI)	12,890
API Oil Gravity	24-28
Sulfur Content (percent)	0.03
Pay Thickness (feet)	125 (net)
Oil Column (feet)	600
Upper Seal	shale
Lateral Seal	shale
Reservoir Intervals (Subsea true vertical depth-feet)	16,000-19,000
Source Of Information	Tura et al., 2006
	Sharma et al., 2011
	Cossey and Associates Inc.

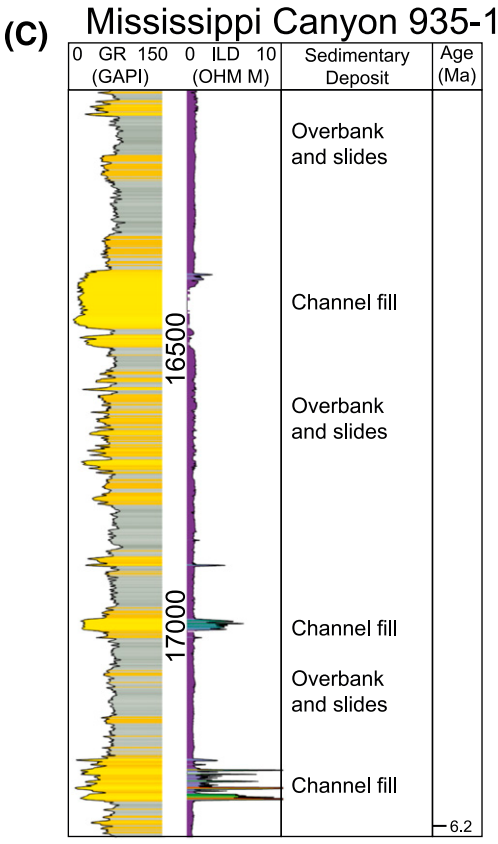

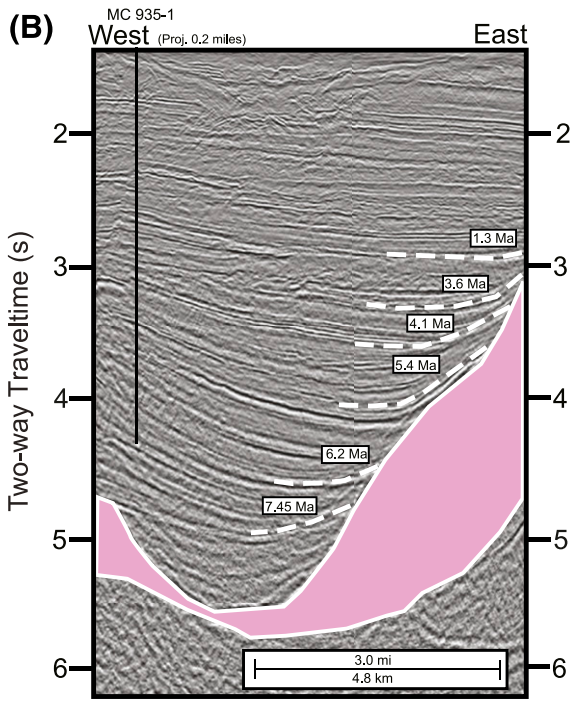

Figure 83. Mississippi Canyon (MC) 935 Europa field. (A) Location map. (B) Seismic profile. Reprinted with permission of Schlumberger. (C) Gamma-ray (GR) and resistivity log. See Figure 4 for the regional setting of the field. ILD = deep induction.

Mirage Field, Figure 84

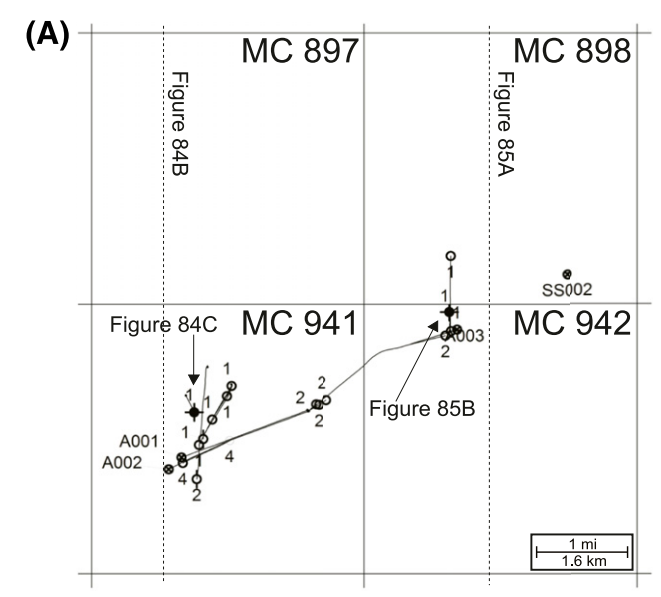

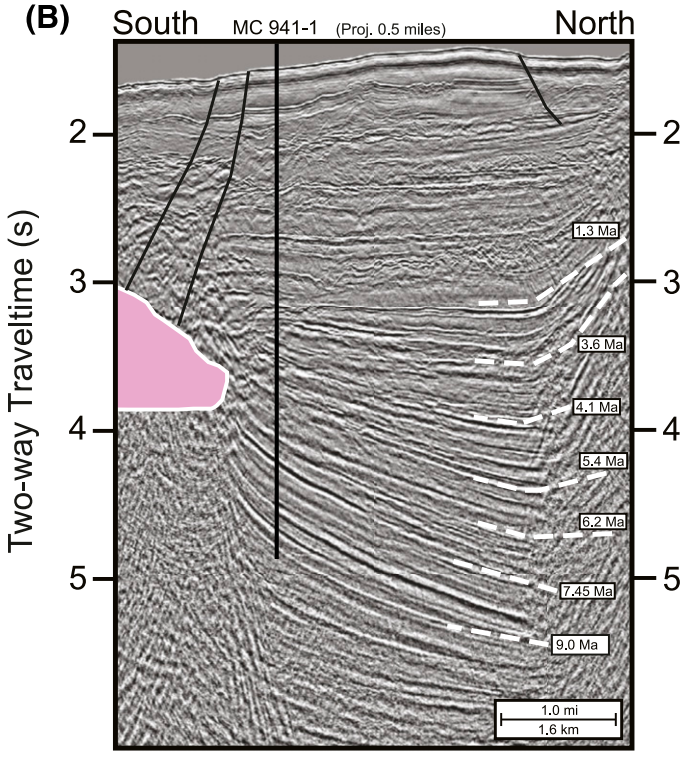

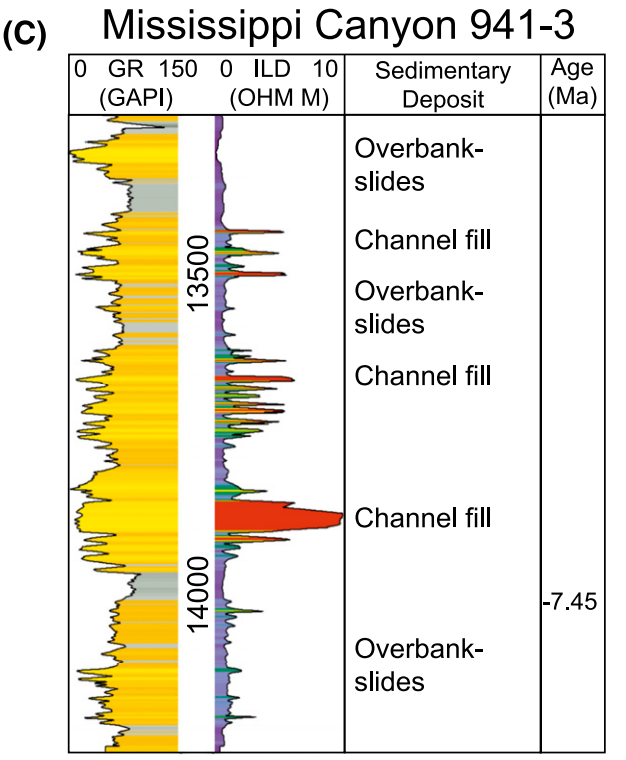

Field Name	Mirage (Figure 84)
Block Numbers	MC941
Partners	Bennu (100.00%)
Discovery Date	1998
Production Start Date	October 2010
Production Facility	Subsea tie-back to Telemark Hub in AT 63
Water Depth (feet)	3,963
Development Status	producing
Number of Wells	3
Number of Reservoirs	5
Age	late Miocene
Sedimentary deposit	channel-fill
Trap	three-way closure against base of salt
Liquids Recoverable Reserves (MMbbl)	42
Gas Recoverable Reserves (BCF)	71
Gas Oil Ratio	1,000-2,000
Porosity (percent)	32
Permeability (mD)	63-384
API Oil Gravity	22-32
Upper Seal	salt
Lateral Seal	shale
Source Of Information	Feijo et al., 2010
	Cossey and Associates Inc.

Figure 84. Mississippi Canyon (MC) 941 Mirage field. (A) Location map of MC 941 Mirage and MC 942 Morgus fields. (B) Seismic profile. Reprinted with permission of Schlumberger. (C) Gamma-ray (GR) and resistivity log. See Figure 4 for the regional setting of the field. ILD = deep induction.

Morgus Field, Figure 85

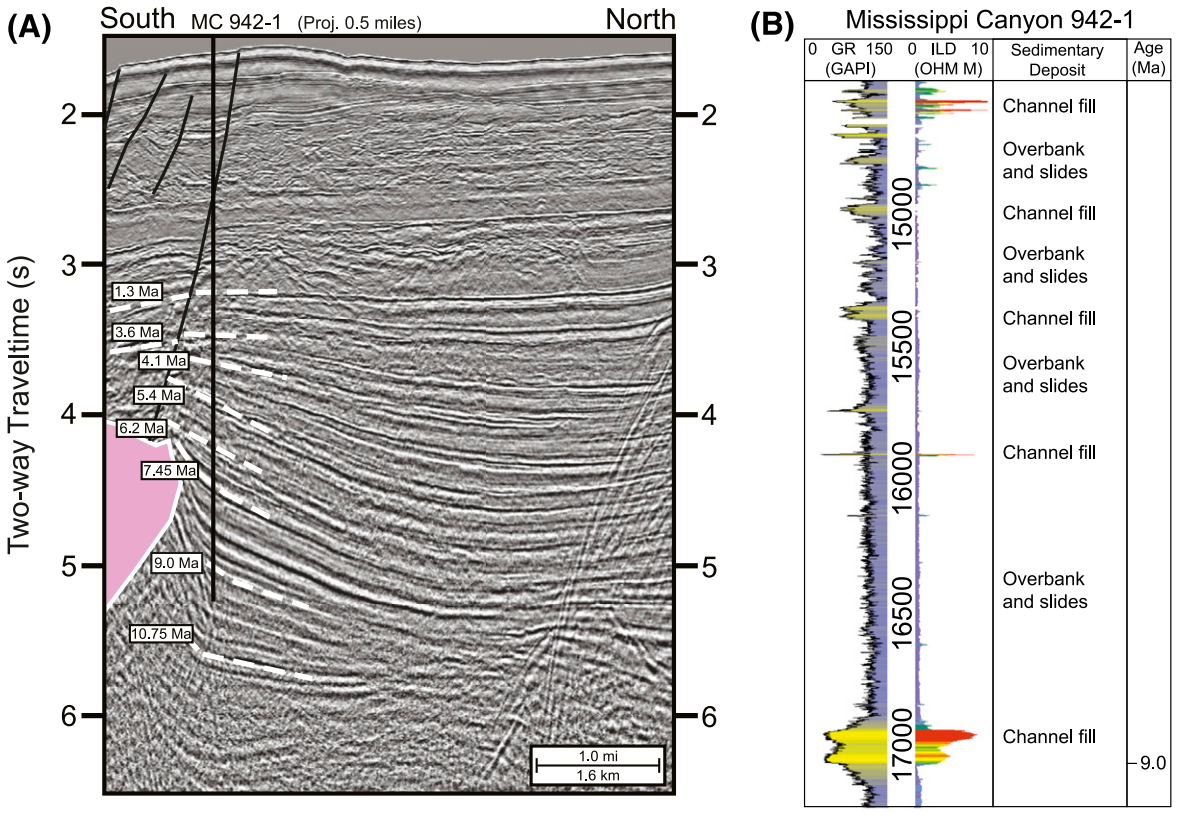

Field Name	Morgus (Figure 85)
Block Numbers	MC 942
Partners	Bennu (100.00%)
Discovery Date	March 1999
Production Start Date	February 2012
Production Facility	Subsea tie-back to Telemark Hub in AT 63
Water Depth (feet)	4,330
Development Status	producing
Number of Wells	3
Number of Reservoirs	2
Age	late Miocene
Sedimentary deposit	channel-fill
Trap	three-way closure against base of salt
Liquids Recoverable Reserves (MMbbl)	42
Gas Recoverable Reserves (BCF)	71
Gas Oil Ratio	1,000-2,000
Porosity (percent)	32
Permeability (mD)	63-384
API Oil Gravity	22-32
Upper Seal	salt
Lateral Seal	shale
Source Of Information	Cossey and Associates Inc.

Figure 85. Mississippi Canyon (MC) 942 Morgus field. (A) Seismic profile. Reprinted with permission of Schlumberger. (B) Gamma-ray (GR) and resistivity log. See Figure 84A for location map and Figure 84B for seismic profile. See Figure 4 for the regional setting of the field. ILD = deep induction.

Telemark Field, Figure 86

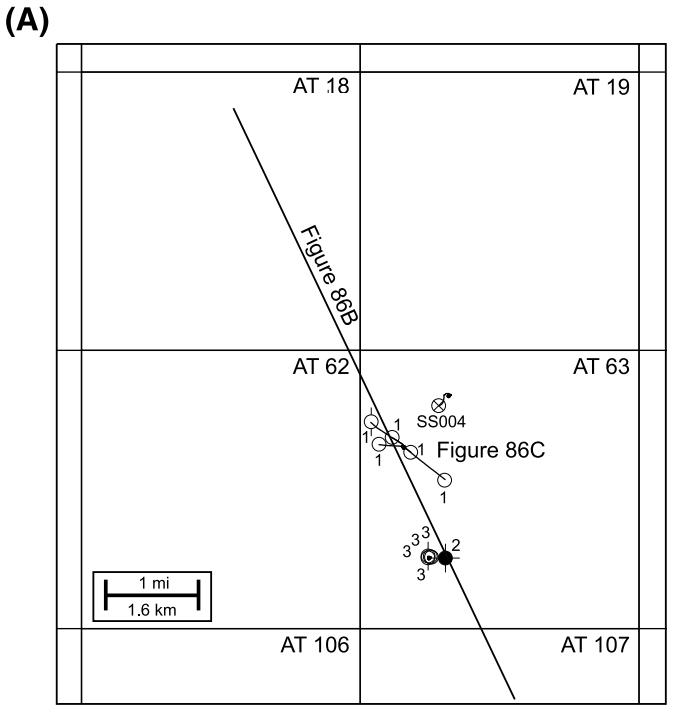

Field Name	Telemark (Figure 86)
Block Numbers	AT 063
Partners	Bennu (100.00%)
Discovery Date	February 2000
Production Start Date	March 2010
Production Facility	MiniDoc 3
Water Depth (feet)	4,412
Development Status	producing
Number of Wells	4
Number of Reservoirs	4
Age	early Miocene
Sedimentary deposit	channel fill, levee thin beds
Trap	three-way closure against base of salt
Liquids Recoverable Reserves (MMbbl)	37
Gas Recoverable Reserves (BCF)	66
Gas Oil Ratio	1,000-2,000
Porosity (percent)	32
Permeability (mD)	63-384
Initial Reservoir Pressure Range (PSI)	16,500
API Oil Gravity	22-32
Upper Seal	salt
Lateral Seal	shale
Reservoir Intervals (Subsea true vertical depth-feet)	21,000-23,000
Source Of Information	Shivers and Frazer, 2010
	Cossey and Associates Inc.
	J. Crews, pers. comm., 2010
	K. McCarty, pers. comm., 2010
	T. Meckel, pers. comm., 2010

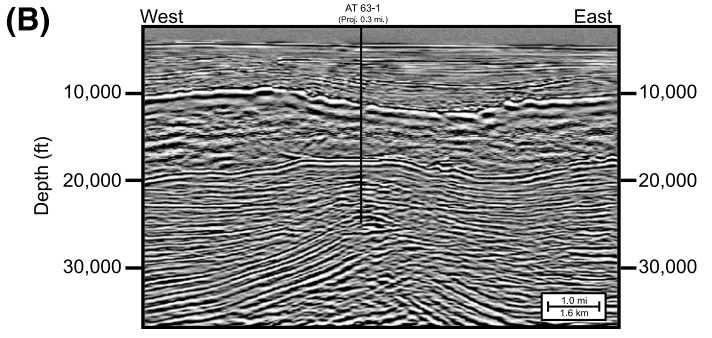

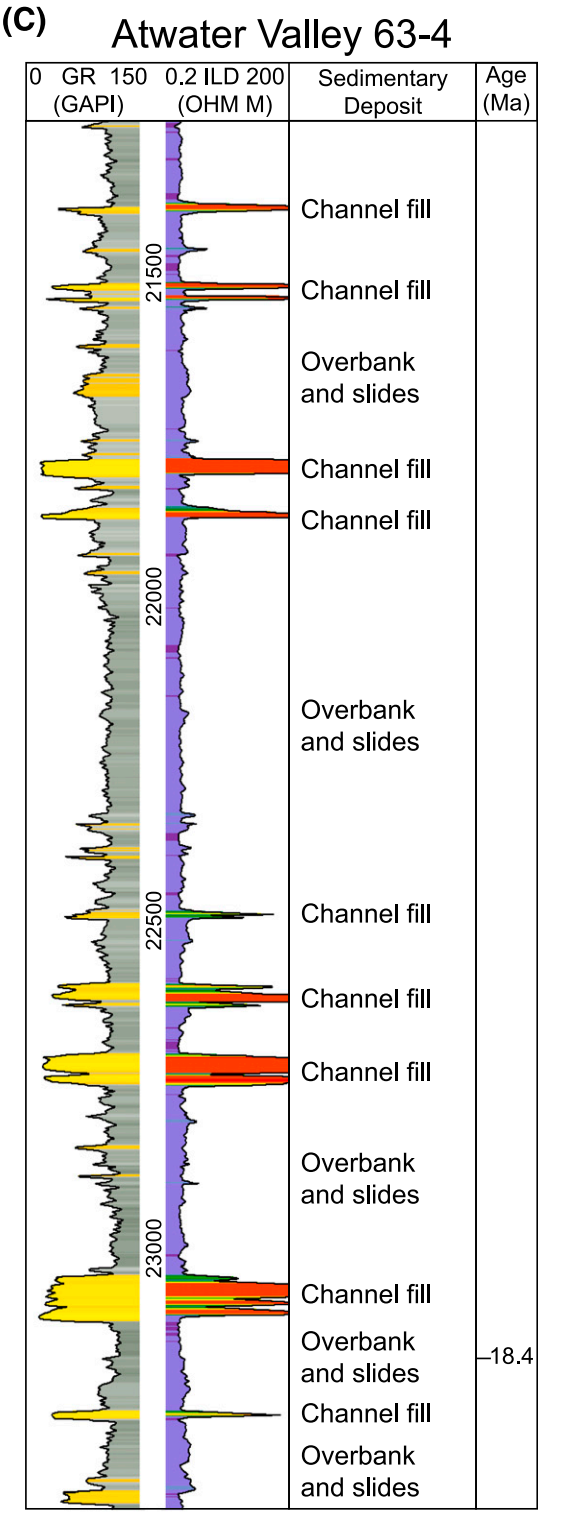

Figure 86. Atwater Valley (AT) 63 Telemark Field. (A) Location map. (B) Seismic profile. After Wilson et al. (2002). Reprinted with permission of AAPG. (C) Gamma-ray (GR) and resistivity log. See Figure 4 for the regional setting of the field. ILD = deep induction.

Thunder Hawk Field, Figure 87

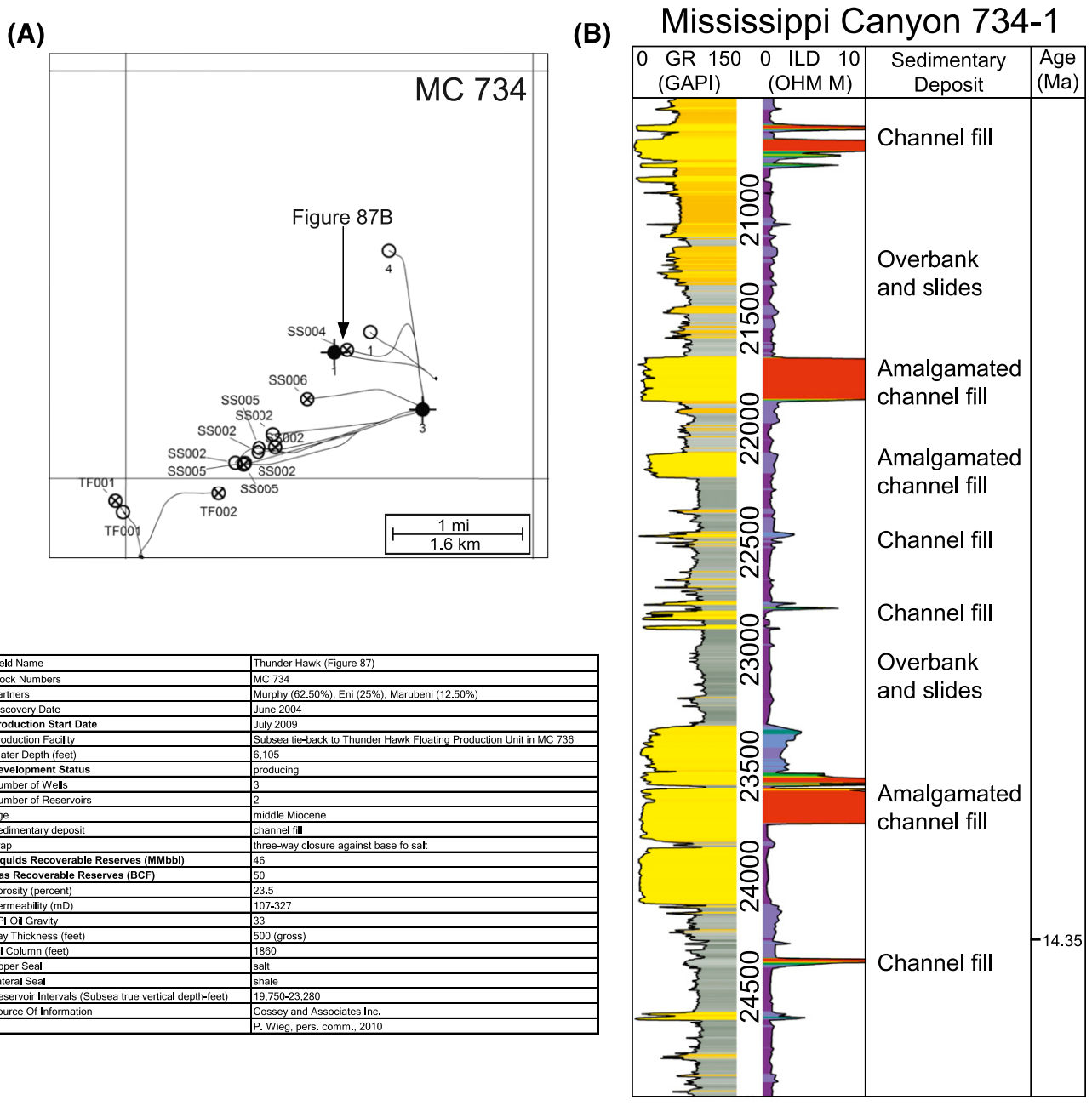

Field Name	Thunder Hawk (Figure 87)
Block Numbers	MC 734
Partners	Murphy (62.50%), Eni (25%), Marubeni (12.50%)
Discovery Date	June 2004
Production Start Date	July 2009
Production Facility	Subsea tie-back to Thunder Hawk Floating Production Unit in MC 736
Water Depth (feet)	6,105
Development Status	producing
Number of Wells	3
Number of Reservoirs	2
Age	middle Miocene
Sedimentary deposit	channel fill
Trap	three-way closure against base fo salt
Liquids Recoverable Reserves (MMbbl)	46
Gas Recoverable Reserves (BCF)	50
Porosity (percent)	23.5
Permeability (mD)	107-327
API Oil Gravity	33
Pay Thickness (feet)	500 (gross)
Oil Column (feet)	1860
Upper Seal	salt
Lateral Seal	shale
Reservoir Intervals (Subsea true vertical depth-feet)	19,750-23,280
Source Of Information	Cossey and Associates Inc.
	P. Wieg, pers. comm., 2010

Figure 87. Mississippi Canyon (MC) 734 Thunder Hawk field. (A) Location map. (B) Gamma-ray (GR) and resistivity log. See Figure 4 for the regional setting of the field. ILD = deep induction.

Kodiak Field, Figure 88

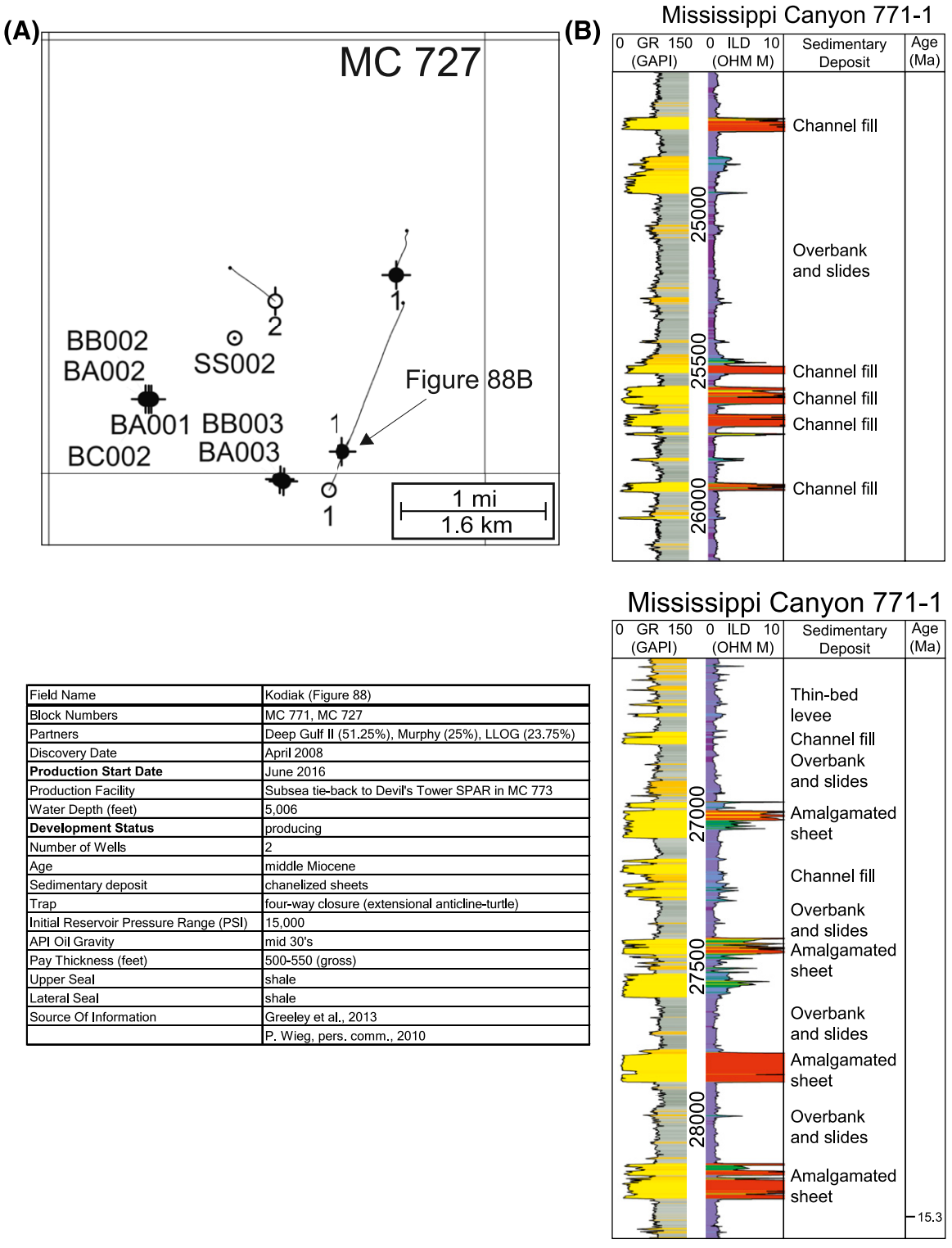

Field Name	Kodiak (Figure 88)
Block Numbers	MC 771, MC 727
Partners	Deep Gulf II (51.25%), Murphy (25%), LLOG (23.75%)
Discovery Date	April 2008
Production Start Date	June 2016
Production Facility	Subsea tie-back to Devil's Tower SPAR in MC 773
Water Depth (feet)	5,006
Development Status	producing
Number of Wells	2
Age	middle Miocene
Sedimentary deposit	chanelized sheets
Trap	four-way closure (extensional anticline-turtle)
Initial Reservoir Pressure Range (PSI)	15,000
API Oil Gravity	mid 30's
Pay Thickness (feet)	500-550 (gross)
Upper Seal	shale
Lateral Seal	shale
Source Of Information	Greeley et al., 2013
	P. Wieg, pers. comm., 2010

Figure 88. Mississippi Canyon (MC) 771 Kodiak field. (A) Location map. (B) Gamma-ray (GR) and resistivity log. See Figure 4 for the regional setting of the field. ILD = deep induction.

Gunflint Field, Figure 89

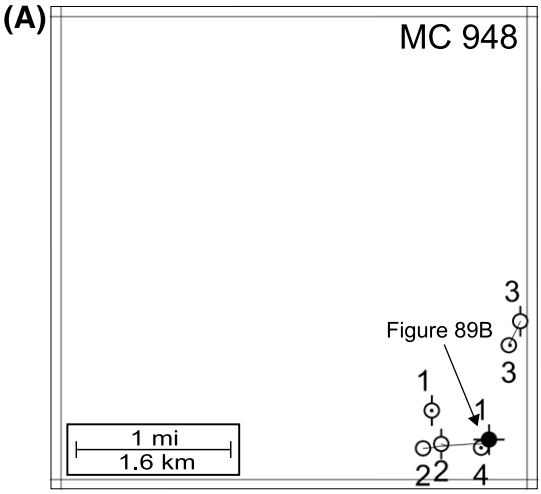

Field Name	Gunflint (Figure 89)
Block Numbers	MC 948, MC 949
Partners	Noble (31.14%), Ecopetrol (31.5%)
	Samson Offshore (19.13%) Marathon Oil (18.23%)
Discovery Date	October 2008
Production Start Date	July 2016
Production Facility	Subsea tie-back to Tubular Bells SPAR in MC 724
Water Depth (feet)	6,138
Development Status	producing
Number of Wells	2
Number of Reservoirs	7
Age	middle Miocene
Sedimentary deposit	channel fill-sheets
Trap	four-way closure (extensional anticline-turtle)
Liquids Recoverable Reserves (MMbbl)	65-90
Pay Thickness (feet)	109 (net)
Upper Seal	shale
Lateral Seal	shale
Source Of Information	Cossey and Associates Inc.
	Kuijper et al., 2016

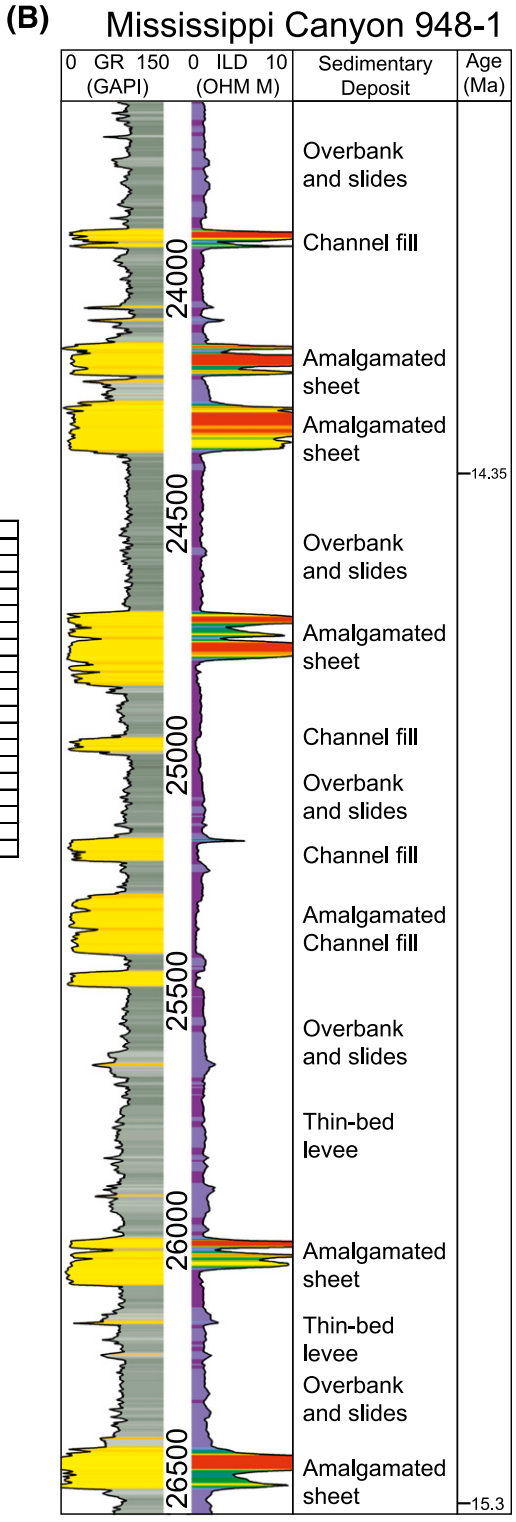

Figure 89. Mississippi Canyon (MC) 948 Gunflint field. (A) Location map. (B) Gamma-ray (GR) and resistivity log. See Figure 4 for the regional setting of the field. ILD = deep induction.

Vito Field, Figure 90

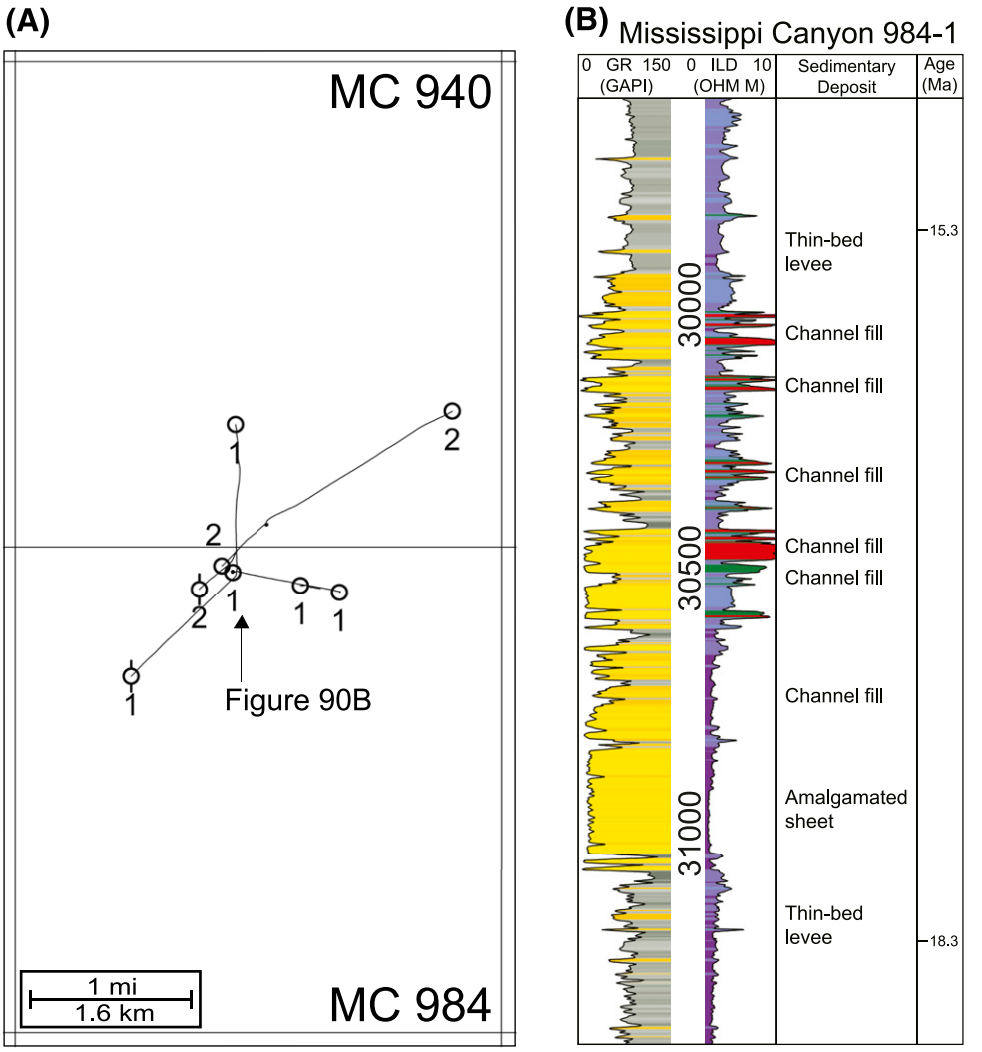

Field Name	Vito (Figure 90)
Block Numbers	MC 984, MC 940, MC 985
Partners	Shell (51.33%), Statoil (30%), Anadarko (18.67%)
Discovery Date	July 2009
Production Start Date	under evaluation
Water Depth (feet)	4,231
Development Status	discovery (appraised)
Number of Wells	2
Age	early Miocene
Sedimentary deposit	sheets- channel fill
Trap	three-way closure against base of salt
Liquids Recoverable Reserves (MMbbl)	234
Gas Recoverable Reserves (BCF)	200
Sulfur Content (percent)	0.01
Pay Thickness (feet)	300 (gross)
Upper Seal	salt
Lateral Seal	shale

Figure 90. Mississippi Canyon (MC) 984 Vito field. (A) Location map. (B) Gamma-ray (GR) and resistivity log. See Figure 4 for the regional setting of the field. ILD = deep induction.

BIOGRAPHIES

Paul Weimer holds the Bruce D. Benson Endowed Chair in the Department of Geological Sciences at the University of Colorado and serves as the director of the Energy and Minerals Applied Research Center. His recent research activities include the study of the petroleum systems of deep-water margins, creating animations for public outreach, and co-chairing the 100th AAPG Anniversary Committee.

Eric Zimmerman is the vice president of geology at LLOG Exploration, which focuses on exploration in the northern deep Gulf of Mexico. Eric has worked in industry with BP, Dominion, and now LLOG. He received his B.S. and M.S. degrees from Louisiana State University.

Steven P. J. Cossey is a geologist with over 37 years of experience with Conoco (1978 to 1983) and with Sohio/BP (1983 to 1995). From 1990 to 1992 he was at BP Research in Sunbury, United Kingdom, and helped to start their deep-water research program. In 1995, he started the consulting company Cossey and Associates, Inc., specializing in the exploration, development, and modeling of deep-water clastic reservoirs, with emphasis on the Gulf of Mexico.

Harrison Hirsh works as a consulting geologist in Boulder, Colorado. He received his B.A. degree in geology from the University of Colorado in 2015.

Brandon Snyder works as a consulting geologist in Denver, Colorado. He received his B.A. degree in geology from the University of Colorado in 2015.

Mike Leibovitz is a geologist at Caerus Oil and Gas. He received his B.A. (2005) and M.S. (2009) degrees from the University of Colorado. He has worked as an exploration and development geologist in the US Rockies, Gulf of Mexico, and Kurdistan.

Kris Schwendeman has worked as a Gulf of Mexico development geologist at Hess Corporation since 2010. He received his B.S. degree from Wright State University (2007) and M.S. degree from the University of Colorado in 2010.

Brian Hankins has worked at Weatherford Laboratories since 2010 as a geoscientist with a focus in organic and inorganic geochemistry at the well site. He received his B.A. degree in geology from the University of Colorado in 2009.

Benjamin Herber has worked as an exploration geologist at Shell since 2010, focusing on the northern Gulf of Mexico. He received his B.A. degree from The University of Texas at Austin (2005) and his M.S. degree from the University of Colorado in 2010.

Daniel Bettinger works as a consulting geologist in Denver, Colorado. He received his B.A. degree in geology from the University of Colorado in 2015.

James Adson works as a security engineer at Level 3 Communications. He received his B.A. in Asian studies from Temple University Japan in 2010. He worked as an animator and systems administrator from 2011 to 2016 for the Interactive Geology Project at the University of Colorado, Boulder.

William S. Gutterman will receive his B.A. degree in geology at the University of Colorado, Boulder in 2017.

Travis J. Payeur will receive his B.A. degree in geology at the University of Colorado, Boulder in 2016.

Renaud Bouroullec received his B.Sc. degree from the Université de Bretagne Occidentale, Brest, France (1994); his M.Sc. degree from the Université de Rennes 1, France (1996); and his Ph.D. from Imperial College, London (2001). After graduation, he conducted postdoctoral research at Energy and Minerals Applied Research Center at the University of Colorado, Boulder, and then joined the Bureau of Economic Geology at The University of Texas at Austin, where he was principal investigator of the Laser-Assisted Analogs for Siliciclastic Reservoirs Consortium. He then joined the Chevron Center of Research Excellence, Department of Geology, Colorado School of Mines, as a research assistant professor. Currently, he is a senior researcher and Basin Analysis Team coordinator at TNO, the Netherlands Organisation for Applied Scientific Research.

John G. Roesink is vice president, development planning and geoscience at Jagged Peak Energy, focusing on unconventional oil reservoirs in the Permian Basin of west Texas. He received his B.A. (1997) and M.S. (2005) degrees from the University of Colorado and has worked in the Denver oil industry in various exploration and development roles since 2005.

Joseph Nicolette works as a development geologist for Catamount Energy Partners. He received his B.A. from Western State College (Gunnison, Colorado) in 2006 and his M.S. from the University of Colorado (2012). He has worked in the Denver oil and gas industry since 2006.

Todd G. Lapinski received a B.S. from Colorado School of Mines (2000) in geophysics and an M.S. from University of Colorado (2003) in geology. For the past 13 years, he has been with BP, holding various technical and leadership positions in Gulf of Mexico, onshore Louisiana Tuscaloosa trend, Trinidad, Libya, and Egypt. He is currently a senior exploration geoscientist in Indonesia.

Aaron "Thor" A. van den Berg is a geologist with Anadarko Petroleum, where he has worked since 2004. He currently works as a reservoir modeler for Groupement Berkine, rotating out of Algeria. He received his B.S. degree from Louisiana State University in 2001 and his M.S. degree from the University of Colorado in 2004.

REFERENCES CITED

Abriel, W. L., 2008, Reservoir geophysics: Applications: Society of Exploration Geophysicists Distinguished Instructor Series 11, 137 p., doi:10.1190/1.9781560801634.

Arnold, G. A., S. R. Cavalero, P. J. Clifford, E. M. Goebel, D. A. Hutchinson, K. H. Leung, E. N. Paclibon, T. D. Weiss, and D. B. Grass, 2010, Thunder Horse takes reservoir management to the next level: Offshore Technology Conference, Houston, Texas, May 3–6, 2010, 22 p.

Ballard, A. L., 2006, Flow-assurance lessons: The Mica tieback: Offshore Technology Conference, Houston, Texas, May 1–4, 2006, p. 1–6.

Bouma, A. E., B. D. Hampton, and B. M. Hewett, 2006, The Princess discovery, sub-salt Gulf of Mexico: Challenges of sub-salt imaging in a fast-paced sub-sea development (abs.): Houston Geological Society Bulletin, v. 48, p. 35–37.

Burch, T., B. Hornby, H. Sugianto, and B. Nolte, 2010, Subsalt 3D VSP imaging at Deimos field in the deep water

Gulf of Mexico: Leading Edge, v. 29, p. 680–685, doi: 10.1190/1.3447781.

Chapin, M. A., G. M. Tiller, and M. J. Mahaffie, 1996, 3-D architecture modeling using high resolution seismic data and sparse well control: Example from the Mars "Pink" reservoir, Mississippi Canyon area, Gulf of Mexico, *in* P. Weimer and T. L. Davis, eds., Applications of 3-D seismic data to exploration and production: AAPG Studies in Geology 42/Society of Exploration Geophysicists Geophysical Developments Series 5, p. 123–132.

Chhajlani, R., Z. Zheng, D. Mayfield, and B. MacArthur, 2002, Utilization of geomechanics for Medusa field development, deepwater Gulf of Mexico: SPE Annual Technical Conference and Exhibition, San Antonio, Texas, September 29–October 2, 2002, SPE-77779-MS, p. 1–12, doi:10.2118/77779-MS.

Cumming, E. W., 2002, Core, log, and seismic characteristics of a high performance turbidite reservoir in a salt-withdrawal minibasin: The upper Miocene yellow sand, Mars field, Gulf of Mexico, *in* P. Weimer, M. R. Sweet, M. Sullivan, J. Kendrick, D. R. Pyles, and A. Donovan, eds., Gulf of Mexico deepwater reservoirs core workshop: Houston, Texas, Gulf Coast Section SEPM Foundation, p. 19–29.

Donovan, G., P. Fadesere, G. Ware, L. Daigle, F. Suparman, G. Frisch, P. Fox, M. Englar, G. Moake, and W. Guo, 2015, Behind pipe log evaluation study: Deepwater subsea abandonments in the Gulf of Mexico: SPE Annual Technical Conference and Exhibition, Houston, Texas, September 28–30, 2015, SPE-174777-MS, 23 p.

Douglas, S. W., 2010, The Jurassic Norphlet formation of the deep-water eastern Gulf of Mexico: A sedimentologic investigation of aeolian facies, their reservoir characteristics, and their depositional history, M.S. thesis, Baylor University, Waco, Texas, 59 p.

Edman, J. D., E. W. Jameson, T. M. Perkins, and G. E. Guthrie, 2001, Mississippi Canyon 348: Some reservoir engineering considerations regarding development of a deepwater biogenic gas accumulation: SPE Annual Technical Conference and Exhibition, New Orleans, Louisiana, September 30–October 3, 2001, SPE-71611-MS, p. 1–9.

Feijo, L. P., G. R. Frazer, and W. J. Parker, 2010, Development of Mirage & Telemark fields—Classification and regulatory considerations applied to an innovative concept: Offshore Technology Conference, Houston, Texas, May 3–6, 2010, 9 p.

Fontana, S., N. A. Atmajasetiadi, F. Brega, J. Villacres, K. Aliyev, and C. Catalani, 2015, Reservoir modeling of a structurally complex deepwater field: A Gulf of Mexico case history: SPE Annual Technical Conference and Exhibition, Houston, Texas, September 28–30, 2015, SPE-175045-MS, 12 p.

Fowler, R., E. Zimmermann, J. Cole, J. Doughtie, B. Cooley, C. Mullet, S. Stegeman et al., 2012, The Who Dat development: Evolution of a project from lease sale to first production: Offshore Technology Conference, Houston, Texas, April 30–May 3, 2012, 9 p.

Fowler, R. L., E. C. Zimmermann, J. M. Leimkuhler, C. Mullett, B. Cooley, B. Paternostro, and J. Boelte, 2015, Delta house project overview: Offshore Technology Conference, Houston, Texas, May 4–7, 2015, 6 p.

Geyelin, J. L., A. C. R. Bouget, and X. Manchon, 2003, Completion of Aconcagua field with a dual derrick drilling unit: SPE Annual Technical Conference and Exhibition, Denver, Colorado, October 5–8, 2003, SPE-84345-MS, 7 p., doi:10.2118/84345-MS.

Gillespie, G., C. Hinnant, C. L. Davis, J. Schober, and M. Darring, 2008, Screen development to withstand 4000-psi overbalance, subhydrostatic completion in deepwater GOM subsea waterflood injector wells: SPE Annual Technical Conference and Exhibition, Denver, Colorado, September 21–24, 2008, SPE-116091-MS, 18 p.

Godo, T. J., E. Chuparova, and D. E. McKinney, 2011, Norphlet aeolian sand fairway established in the deep water Gulf of Mexico (abs.): AAPG Annual Convention and Exhibition, Houston, Texas, April 10–13, 2011, accessed November 2, 2016, http://www.searchanddiscovery.com/abstracts/html/2011/annual/abstracts/Godo.html.

Gorur, K., R. Harris, and J. Meyers, 2013, Assessment of unlocking production from the Ursa and Princess fields using integrated production modeling: SPE Annual Technical Conference and Exhibition, September 30–October 2, 2013, New Orleans, Louisiana, SPE-166417-MS, 11 p., doi: 10.2118/166417-MS.

Greeley, D. F., P. Mitchell, P. Jeanjean, and C. Scherschel, 2013, SupraSalt 3D basin modeling and shallow borehole results: Tubular Bells, Kodiak development project in GoM Mississippi Canyon: Offshore Technology Conference, Houston, Texas, May 6–9, 2013, 30 p.

Greene, T. J., and B. E. O'Neill, 2005, Building a facies-based permeability model for deep-water Miocene reservoirs, eastern Gulf of Mexico: Gulf Coast Association of Geological Societies Transactions, v. 55, p. 268–277.

Haak, V. D., W. J. Cameron, L. S. Grant, N. J. H. Japar, and D. R. Reagins, 2014, Mars B development—Well challenges & solutions—An evolution of traditional well, rig and facility design: Offshore Technology Conference, Houston, Texas, May 5–8, 2014, 16 p.

Haddad, S., G. Simms, and C. Clerk, 2003, Using multiple reservoir measurements to improve subsurface description in deepwater Gulf of Mexico: King field: SPE Annual Technical Conference and Exhibition, Denver, Colorado, October 5–8, 2003, SPE-84380-MS, 15 p.

Hare, S., D. May, D. McCalvin, and P. Martyniak, 2003, MC305 Aconcagua SCSSV control hydraulics problems uncommanded and SCSSV closure problems: SPE Annual Technical Conference and Exhibition, Denver, Colorado, October 5–8, 2003, SPE-84347-MS, 7 p. doi: 10.2118/84347-MS

Herron, D. A., 2014, Thoughts and observation on interpreting depth-imaged data in the Jurassic Norphlet play, deepwater eastern Gulf of Mexico: AAPG Search and Discovery article 41342, accessed November 2, 2016, http://www.searchanddiscovery.com/pdfz/documents/2014/41342herron/ndx_herron.pdf.html.

Kabir, N., T. Burch, and J. Etgen, 2006, Subsalt wavefield illumination and amplitude study on Mars field in the Gulf of

Mexico: Society of Exploration Geophysicists 76th Annual International Meeting, New Orleans, Louisiana, October 1–6, 2006, p. 535–538, doi:10.1190/1.2370316.

Keller, D., 2015, davidrkeller.com/aconcagua-reservoir-model/.

Kuijper, K., O. Stephens, and K. Aleman, 2016, Deep-water depositional environments and their unique challenges within the Gunflint field: Gulf Coast Association of Geological Societies Transactions, v. 66, p. 815–818.

Lach, J., K. McMillen, R. Archer, J. Holland, R. DePauw, B. E. Ludvigsen, and P. T. Scandpower, 2005, Integration of geologic and dynamic models for history matching, Medusa field: SPE Annual Technical Conference and Exhibition, Dallas, Texas, October 9–12, 2005, SPE-95930-MS, 10 p, doi:10.2118/95930-MS.

Lapinski, T. G., 2003, 3D stratigraphic and structural evolution of the Thunder Horse mini-basin, Mississippi Canyon, northern deep-water Gulf of Mexico, Master's thesis, University of Colorado, Boulder, Colorado, 182 p.

Li, Q., J. Nahm, T. Becker, I. Ahmed, P. Foster, G. Murphy, and J. V. Gestel, 2013, Mars & Ursa OBS data joint processing: 2013 Society of Exploration Geophysicists Annual Meeting, Houston, Texas, September 22–27, 2013, 5 p.

Li, X., S. J. Tinker, M. Bruno, and S. M. Willson, 2005, Compaction considerations for the Gulf of Mexico deepwater King West field completion design: SPE/International Association of Drilling Contractors Drilling Conference, Amsterdam, February 23–25, 2005, SPE-92652-MS, 14 p.

Mahaffie, M. J., 1994, Reservoir classification for turbidite intervals at the Mars discovery, Mississippi Canyon 807, Gulf of Mexico, *in* P. Weimer, A. H. Bouma, and B. F. Perkins, eds., Submarine fans and turbidite systems: Gulf Coast Section SEPM Foundation 15th Annual Research Conference, Houston, Texas, December 4–7, 1994, p. 233–244.

Meckel, L. D. III, 2002, Core, log, and seismic characteristics of a high rate amalgamated channel reservoir in a salt-withdrawal minibasin: The upper Miocene "Above Magenta" sand, Ursa field, northern Gulf of Mexico, *in* P. Weimer, M. Sweet, M. Sullivan, J. Kendrick, D. Pyles, and A. Donovan, eds., Deep-water core workshop, northern Gulf of Mexico: Houston, Texas, Gulf Coast Section SEPM Foundation, p. 61–74.

Meckel, L. D. III, G. A. Ugueto, D. H. Lynch, B. M. Hewett, E. J. Bocage, C. D. Winker, and B. J. O'Neill, 2002, Genetic stratigraphy, stratigraphic architecture, and reservoir stacking patterns of the upper Miocene–lower Pliocene Greater Mars-Ursa intraslope basins, Mississippi Canyon, Gulf of Mexico, *in* J. M. Armentrout and N. Rosen, eds., Sequence stratigraphic models for exploration and production: Gulf Coast Section SEPM Foundation Bob F. Perkins 22nd Annual Research Conference, Houston, Texas, December 8–11, 2002, p. 113–147.

Milkov, A. V., E. Goebel, L. Dzou, D. A. Fisher, A. Kutch, N. McCaslin, and D. F. Bergman, 2007, Compartmentalization and time-lapse geochemical reservoir surveillance of the Horn Mountain oil field, deep-water Gulf of Mexico: AAPG Bulletin, v. 91, no. 6, p. 847–876, doi:10.1306/01090706091.

Miranda, J., M. Rabinovich, J. Hamman, and M. Mousavi, 2015, Reconciling log-derived water saturation and saturation-height function results through resistivity modeling, core-log integration and image log data: A case study from deepwater Gulf of Mexico: SPE Annual Technical Conference and Exhibition, Houston, Texas, September 28–30, 2015, SPE-175053-MS, 28 p.

Monson, G., and D. Bustamante, 2005, Integrated geologic model and statistical reservoir simulation: Triton field, Gulf of Mexico: Society of Exploration Geophysicists Annual Meeting, Houston, Texas, November 6–11, 2005, p. 1362–1366.

Newberry, D., 2014, 50 reservoirs, 48 well slots & two TLP's—Maximizing recovery from the deepwater prolific Mars field: Offshore Technology Conference, Houston, Texas, May 5–8, 2014, 7 p.

Nielsen, V. B. J., J. Illeman, and T. L. Guillory, 2005, Case study: Aconcagua and Camden Hills fields utilize intelligent completions to optimize production and reservoir performance: Offshore Europe Conference, Aberdeen, United Kingdom, September 6–9, 2005, 11 p.

Pfeiffer, D. S., B. T. Mitchell, and G. Y. Yevi, 2000, Mensa: Shell's Mississippi Canyon Block 731 field—An integrated field study, *in* P. Weimer, R. M. Slatt, J. L. Coleman, N. Rosen, C. H. Nelson, A. H. Bouma, M. Styzen, and D. T. Lawrence, eds., Deep-water reservoirs of the world: Gulf Coast Section SEPM Foundation 20th Annual Bob F. Perkins Research Conference, Houston, Texas, December 3–6, 2000, p. 756–775.

Purnell, N., K. Inman, T. Leary, G. Grubitz, U. Albertin, S. Kapoor, and W. Chang, 1997, Fast track 3D pre-stack depth migration of the Neptune structure, Offshore Gulf of Mexico: Society of Exploration Geophysicists Annual Meeting, Dallas, Texas, November 2–7, 1997, 5 p.

Rajasingam, D. T., and T. P. Freckelton, 2004, Subsurface development challenges in the ultra deepwater Na Kika development: Offshore Technology Conference, Houston, Texas, May 3–6, 2004, 10 p.

Ray, A., Y. Quist, Z. Yu, H. Sugianto, and B. Hornby, 2005, Acquisition of 2D walkaway VSP data to improve imaging of Thunder Horse North field, Gulf of Mexico: Leading Edge, v. 24, p. 430–432, doi:10.1190/1.1901398.

Razi, M., and P. Bilinski, 2012, Mensa field, deepwater Gulf of Mexico (GOM)—Case study: 2012 SPE Annual Technical Conference and Exhibition, San Antonio, Texas, October 8–10, 2012, SPE-159741-MS, 11 p., doi:10.2118/159741-MS.

Reynolds, T., 2000, Reservoir architecture in the Mars field, Deepwater Gulf of Mexico, USA: The implications of production, seismic, core and well log data, *in* P. Weimer, R. M. Slatt, J. L. Coleman, N. Rosen, C. H. Nelson, A. H. Bouma, M. Styzen, and D. T. Lawrence, eds., Deep-water reservoirs of the world: Gulf Coast Section SEPM Foundation 20th Annual Bob F. Perkins Research

Conference, Houston, Texas, December 3–6, 2000, p. 877–892, doi:10.5724/gcs.00.15.0877.

Salunk, S., and J. Hamman, 2015, Applying a consistent evaluation approach to thin bedded sands in a Gulf of Mexico deepwater field: Society of Petrophysicists and Well Log Analysts 56th Annual Logging Symposium, Long Beach, California, July 18–22, 2015, 9 p.

Schofield, K., and J. Serbeck, 2000, The "Above Magenta" reservoir at Ursa field: A process-response model to explain a classic wireline log signature, *in* P. Weimer, R. M. Slatt, J. L. Coleman, N. Rosen, C. H. Nelson, A. H. Bouma, M. Styzen, and D. T. Lawrence, eds., Deep-water reservoirs of the world: Gulf Coast Section SEPM Foundation 20th Annual Bob F. Perkins Research Conference, Houston, Texas, December 3–6, 2000, p. 894–910, doi: 10.5724/gcs.00.15.0894.

Schott, D. W., N. Bassett, and P. G. Belvedere, 2007, The impact of exceeding predicted performance in Kepler field, deepwater Gulf of Mexico—A multi-discipline approach to understanding a turbidite reservoir: International Petroleum Technology Conference, Dubai, United Arab Emirates, December 4–6, 2007, 11 p, doi: 10.2523/IPTC-11475-MS.

Sharma, A., T. Burch, and G. Murphy, 2011, Low cost 4D using NATS and WATS at Europa: Society of Exploration Geophysicists Annual Meeting, San Antonio, Texas, September 18–23, 2011, p. 4185–4189.

Shivers, R., and G. R. Frazer, 2010, Considerations for standalone development of small deepwater fields: 2010 Offshore Technology Conference, Houston, Texas, May 3–6, 2010, 10 p.

Simms, G. J., B. Cooley, R. Fowler, K. J. Leontaritis, and K. Krishnathasan, 2012, Subsea Who Dat project—Producing light and heavy oil in a deepwater subsea development: Offshore Technology Conference, Houston, Texas, April 30–May 3, 2012, 13 p.

Singh, A., N. Zambare, and M. Brostrøm, 2007, Development of a pipeline management system for an ultradeepwater long-distance subsea tieback in the Gulf of Mexico: Offshore Technology Conference, Houston, Texas, April 30–May 3, 2007, 9 p.

Sloan, R. F., and K. M. King, 2014, Cutting edge seismic technology boosts Mars B project by delivering exploration, maturation and development of two subsea fields tied back to New Olympus TLP at a top quartile pace: Offshore Technology Conference, Houston, Texas, May 5–8, 2014, 7 p.

Smit, F., C. Perkins, L. Lepre, K. Craft, and R. Woodard, 2008, Seismic data acquisition using ocean bottom seismic notes at the Deimos field, Gulf of Mexico: Society of Exploration Geophysicists 78th Annual International Meeting, Las Vegas, Nevada, November 9–14, 2008, p. 998–1002, doi:10.1190/1.3063805.

Soter, K., J. Malbrough, D. Mayfield, and J. Holland, 2005, Medusa Project: Integrated planning for successful deepwater Gulf of Mexico completions: SPE Annual Technical Conference and Exhibition, Dallas, Texas, October 9–12, 2005, SPE-97144-MS, 16 p., doi: 10.2118/97144-MS.

Stair, C. D., C. H. Hinnant, N. O. Hines, J. M. Schober, C. L. Davis, K. F. Lizak, and B. A. Pugh, 2011, Planning and execution of highly overbalanced completions from a floating rig: The Ursa-Princess waterflood project: SPE Drilling & Completion, v. 26, p. 396–407, doi:10.2118/134254-PA.

Stephens, O., R. Pinto, B. Maxey, and K. Gray, 2016, Big Bend: Gulf of Mexico success, from prospect to production through geoscience integration: Gulf Coast Association of Geological Societies Transactions, v. 66, p. 887–889.

Subramanian, S., M. P. Price, and R. A. Pinnick, 2009, Flow assurance design and initial operating experience from Blind Faith in Deepwater Gulf of Mexico: SPE Annual Technical Conference and Exhibition, New Orleans, Louisiana, October 4–7, 2009, SPE-124535-MS, 14 p.

Tatanova, M., and P. Hatchell, 2012, Time-Lapse AVO on deepwater OBN seismic at the Mars field: 2012 Society of Exploration Geophysicists Annual Meeting, Las Vegas, Nevada, November 4–9, 2012, 5 p.

Todd, S., and D. Replogle, 2010, Thunder Horse and Atlantis: The development and operation of twin giants in the deepwater Gulf of Mexico: Offshore Technology Conference, Houston, Texas, May 3–6, 2010, 18 p.

Tura, A., T. Barker, P. Cattemole, C. Collins, J. Davis, P. Hatchell, K. Moster, P. Schutjens, and P. Wills, 2006, Monitoring primary-depletion reservoirs with seismic amplitudes and time shifts: Offshore Technology Conference, Houston, Texas, May 1–4, 2006, 7 p.

van Gestel, J. P. C., S. Chakraborty, P. O. Ariston, G. Murphy, and K. Tollestrup, 2012, WATS on NATS time-lapse: Gulf of Mexico case study, King and Horn Mountain fields: Society of Exploration Geophysicists Annual Meeting, Las Vegas, Nevada, November 4–9, 2012, 5 p.

Vercher, C. M., and D. Blakeley, 2007, Codevelopment of Spiderman and San Jacinto fields: Offshore Technology Conference, Houston, Texas, April 30–May 3, 2007, 7 p.

Wagner, B. E., Z. Sofer, and B. L. Claxton, 1994, Source rock in the lower Tertiary and Cretaceous, deep-water Gulf of Mexico: Gulf Coast Association of Geological Societies Transactions, v. 44, p. 729–736.

Weiland, J., D. Mikulencak, P. E. Fox, G. J. Frisch, and M. Azari, 2008, Water flood surveillance in the Mars field deepwater GOM: Mississippi Canyon Block 807: SPE Annual Technical Conference and Exhibition, Denver, Colorado, September 21–24, 2008, SPE-115365-MS, 17 p.

Wells, J., and N. Zambare, 2011, Late-life field optimization, canyon express—A case study: Offshore Technology Conference, Houston, Texas, May 2–5, 2011, 11 p.

Wieg, P. K., and G. W. Fingleton, 2004, Devils Tower area: Rationalization of geophysical subtleties with geologic concepts provides basis for successful drilling program: Gulf Coast Association of Geological Societies Transactions, v. 54, p. 743–760.

Winker, C. D., and R. J. Stancliffe, 2007, Geology of shallow-water flow at Ursa: 1. Setting and causes: Offshore Technology Conference, Houston, Texas, April 30–May 3, 2007, 14 p.

Xia, G., F. Rollins, S. LaDart, J. Etgen, L. Sirgue, B. Nolte, and J. Kaldy, 2009, Wide azimuth anisotropic imaging at Tubular Bells field in the Gulf of Mexico: Society of Exploration Geophysicists 79th Annual International Meeting, Houston, Texas, October 26–30, 2009, p. 1187–1191, doi:10.1190/1.3255064.

Zimmermann, E., J. Cole, and J. Doughtie, 2012, Subsurface review of Who Dat field: Offshore Technology Conference, Houston, Texas, April 30–May 3, 2012, 7 p.

Zimmermann, E., C. Guzman, S. Hewitt, A. Kumar, M. Mahnke, V. K. Mishra, E. Ruiz, and N. Charmelo, 2015, Geological interpretation of mass transport complexes in the Gulf of Mexico: The benefits of integrating borehole geology, borehole geophysics, and reservoir engineering: Offshore Technology Conference, Houston, Texas, May 4–7, 2015, 9 p.